Synthesis and structure-activity relationships of *α*,*β*-methylene-ADP derivatives: potent and selective *ecto*-5′-nucleotidase inhibitors

Dissertation

zur

Erlangung des Doktorgrades (Dr. rer. nat.)

der

Mathematisch-Naturwissenschaftlichen Fakultät

der

Rheinischen Friedrich-Wilhelms-Universität Bonn

vorgelegt von

Sanjay Bhattarai

aus

Gauradaha (Nepal)

Bonn 2015

Angefertigt mit Genehmigung der Mathematisch-Naturwissenschaftlichen Fakultät der Rheinischen Friedrich-Wilhelms-Universität Bonn

1. Referent: Prof. Dr. Christa E. Müller
2. Referent: Prof. Dr. Michael Gütschow

Tag der Promotion: 21.07.2015

Erscheinungsjahr: 2015

Die vorliegende Arbeit wurde in der Zeit von September 2010 bis Dezember 2014 am Pharmazeutischen Institut der Rheinischen Friedrich-Wilhelms-Universität Bonn Unter der Leitung von Frau Prof. Dr. Christa E. Müller durchgeführt.

Mein besonderer Dank gilt Frau Prof. Dr. Christa E. Müller für ihre Unterstützung, ihre Diskussionsbereitschaft und ihre Anregungen, die zum Gelingen dieser Arbeit beigetragen haben.

Ebenso bedanke ich mich an dieser Stelle bei Prof. Dr. Michael Gütschow für die freundliche Übernahme des Korreferates.

Abstract

Ecto-5′-nucleotidase (*ecto*-5′-NT, *e*N, CD73, EC 3.1.3.5) is a member of the group of *ecto*-nucleotidases which dephosphorylate extracellular nucleotides. *e*N catalyzes the dephosphorylation of nucleoside monophosphates and its main substrate is AMP. Further members of the membrane-bound group of *ecto*-nucleotidases include nucleoside triphosphate diphosphohydrolases (NTPDases; subtypes 1, 2, 3 and 8), nucleotide pyrophosphatase/phosphodiesterases (NPPs 1-4) and alkaline phosphatases (APs; tissue non-specific, intestinal, placental and germ cell APs). NTPDase and NPPs are ATP- and ADP-hydrolyzing *ecto*-nucleotidases, which prevent ATP, ADP and other nucleotides from acting on purinergic P2X and P2Y receptors. They produce AMP which is further hydrolyzed by *e*N thereby elevating extracellular concentrations of adenosine which activates adenosine receptors.

Recently it was shown that inhibition of *e*N with monoclonal antibodies, siRNA, or drug-like inhibitors delays tumor growth and metastasis. Thus, *e*N inhibitors have potential as novel therapeutics, e.g. for melanomas, lung, prostate and breast cancers. Only very few, moderately potent *e*N inhibitors are currently known. In the present study we used the ADP analog *α*,*β*-methylene-ADP (AOPCP, adenosine-5′-*O*-[(phosphonomethyl)phosphonic acid]) as a lead structure for the development of potent, selective and metabolically stable *e*N inhibitors. Derivatives substituted at the N^6-, C-8- or C-2-positions and/or at the methylene diphosphonate-side chain were synthesized to improve potency and metabolic stability. All new compounds were tested for inhibition of rat recombinant *e*N.

For the preparation of the target compounds with 2-, 6- or 8-substitution and for 2,6-disubstituted derivatives, a convergent synthetic strategy was applied which involves the initial preparation of the intermediate nucleosides followed by phosphorylation with methylenebis(phosphonic dichloride) to provide the desired AOPCP derivatives. For side-chain-modified analogs of

Abstract

AOPCP commercially available substituted bis(phosphonic acid) derivatives were employed for 5′-phosphorylation. Altogether 60 AOPCP derivatives and analogs were obtained in good yields and high purity by an optimized method for their preparation. 6-(Ar)alkylamino-substitution, 2-amino-, 2-halo-, and 2-thioalkyl-substitution significantly improved potency. The most potent nucleotides were 2-chloro-N^6-(2-chlorobenzyl)purine riboside-5′-*O*-[(phosphonomethyl)-phosphonic acid] (**144**, K_i= 0.34 nM), and 2-chloro-N^6-benzyl-N^6-methylpurine riboside-5′-*O*-[(phosphonomethyl)phosphonic acid] (**149,** K_i= 0.88 nM). The compounds displayed high selectivity versus other *ecto*-nucleotidases and ADP-activated P2Y receptors. They also showed high metabolic stability upon incubation with liver microsomes and blood plasma. These compounds are the most potent *e*N inhibitors known to date and may serve as valuable pharmacological tools to further elucidate the enzyme's (patho)physiological roles.

Table of contents:

I. Introduction 1
1.1. Purinergic Signalling 1
1.2. Synthesis and storage of ATP 2
1.3. Purinergic receptor family 4
1.3.1. P0 receptors 4
1.3.2. P1 receptor 5
1.3.3. P2 receptors 6
1.4. Nucleotides and adenosine releasing pathways 7
1.5. Purinergic signalling pathways and *e*cto-nucleotidases 9
1.6. *E*cto-nucleotidases 10
1.6.1. *E*cto-nucleoside triphosphate diphosphohydrolases 11
1.6.2. *E*cto-nucleotide pyrophosphatase/phosphodiesterases 15
1.6.3. Alkaline phosphatases 16
1.6.4. Additional nucleotide-metabolizing enzymes 17
2. *E*cto-5′-nucleotidase 18
2.1. General properties of *e*cto-5'-nucleotidase 19
2.2. Protein and crystal structure of *e*cto-5'-nucleotidase 19
2.3. Active site and catalytic mechanism of *e*cto-5'-nucleotidase 20
2.4. Physiological functions of the *e*cto-5'-nucleotidase 22
2.4.1. Ischemic-reperfusion injury of the lungs and hypoxia 22
2.4.2. Inflammation 23
2.4.3. Antinociceptive effects 24
2.4.4. Platelet function 25
2.4.5. Renal function 25
2.4.6. Cancer 25
II. Literature review 27
3. Medicinal Chemistry of *e*cto-5'-nucleotidase inhibitors 27
3.1. Adenine nucleotide derivatives as *e*cto-5'-nucleotidase inhibitors 27

3.2. Uridine nucleotide mimetics as *e*cto-5'-nucleotidase inhibitors 29
3.3. Anthraquinone derivatives as *e*cto-5'-nucleotidase inhibitors 30
3.4. Sulfonamide derivatives as *e*cto-5'-nucleotidase inhibitors 31
3.5. Sulfonic acid derivatives as *e*cto-5'-nucleotidase inhibitors 32
3.6. Various *e*cto-5'-nucleotidase inhibitors 33
4. Assays of *e*cto-5'-nucleotidase 34
4.1. Malachite green assay 34
4.2. Capillary electrophoresis assay 35
4.3. Luciferase-based assay 35
4.4. Radiometric assay 36
III. Aim of the project 37
5.1. Design and synthesis of adenine-base modified analogues of AOPCP 37
5.2. Design and synthesis of side-chain-modified analogues of AOPCP 38
5.3. Metabolic stability studies of selected potent AOPCP derivatives and analogues 39
IV. Results and discussion 40
6. Results and discussion - part I: chemical synthesis 40
6.1. N^6-Mono- and dialkyl-or aryl-substituted adenosine-5′-*O*-[(phosphonomethyl)phosphonic acid] derivatives (**53-76**) 40
6.1.1. Synthesis of (intermediate) 6-substituted nucleosides (**29-48**) 40
6.1.2. Phosphoprylation of 6-substituted nucleosides (**29-48**) 44
6.2. 6-Ethoxy-, 6-benzyloxy-, and 6-benzylthio-purine riboside-5′-*O*-[(phosphonomethyl)phosphonic acid] (**81-83**) 53
6.2.1. Synthesis of O^6-ethyl, O^6-benzyl, and S^6-benzyl-purine riboside derivatives (**77-80**) 53
6.2.2. Phosphorylation of 6-ethoxy-, 6-benzyloxy-, and 6-benzylthiopurine riboside (**77**, **78**, **80**) 55
6.3. 8-substituted adenosine-5′-methylenebisphosphonic acid derivatives (**89-92**) 56
6.3.1. Synthesis of 8-substituted adenosine derivatives (**84**, **86-88**) 56
6.3.2. Phosphoprylation of 8-substituted adenosine derivatives (**84**, **86-88**) 58
6.4. 2-Substituted adenosine-5′-*O*-[(phosphonomethyl)phosphonic acid] derivatives (**109-114**) 59
6.4.1. Synthesis of intermediate 2-substituted-adenosine derivatives (**98-108**) 59
6.4.2. Phosphorylation of 2-substituted-nucleosides 64

6.5. 2-Amino-, 2-choro- and 2-iodo-N^6-mono-/dialkyl-or aryl-substituted adenosine-5′-*O*-[(phosphonomethyl)phosphonic acid] derivatives (**139-150**) 65
6.5.1. Synthesis of 2,6-disubstituted nucleosides (**127-138**) 65
6.5.2. Phosphorylation of 2,6-disubstituted purine ribosides (**127-138**) 66
6.6. Phosphorylation of further nucleosides 67
6.7. Synthesis of methylene diphosphonate-side chain-modified analogues of AOPCP (**161**, **162**) 70
6.7.1. Synthesis of adenosine-5′-dichloromethylenediphosphonic acid (**161**) 70
6.7.2. Synthesis of adenosine-5′-(1-hydroxy)ethane-1,1-diphosphonic acid (**162**) 72
7. Results and discussion - part II: Pharmacological Evaluation 78
7.1. Pharmacological Evaluation at rat *e*N 78
7.1.1. Structure-activity relationships of 6-substituted AOPCP derivatives at rat *ecto*-5′-nucleotidase 79
7.1.2. Structure-activity relationships of 8-substituted AOPCP derivative at rat *ecto*-5′-nucleotidase 84
7.1.3. Structure-activity relationships of 2-substituted AOPCP derivative at rat *ecto*-5′-nucleotidase 85
7.1.4. Structure-activity relationships of 2,6-disubstituted AOPCP derivative at rat *ecto*-5′-nucleotidase 88
7.1.5. Structure-activity relationships of AOPCP derivatives with modification of the methylene bis-phosphonate partial structure at rat *ecto*-5′-nucleotidase 90
7.2. Selectivity studies 92
7.2.1. Activity at nucleoside triphosphate diphosphohydrolases and nucleotide phosphodiesterases 92
7.2.2. Selectivity versus ADP-activated P2Y receptors 94
8. Results and discussion - part II: Metabolic stability studies 95
8.1. Stability of inhibitors in liver microsomes 95
8.1.1. Metabolism/ biotransformation 96
8.1.2. Invitro-metabolic study models 97
8.1.3. Metabolic stability results 98
8.2. Plasma stability 108
8.2.1. Plasma stability results 109
V. Experimental 114

9. Chemical synthesis 114
9.1. General remarks 114
9.2. Preparation of triethylammonium hydrogen carbonate buffer (TEAC) 115
9.3. Ion Exchange Chromatography 115
9.4. Preparative HPLC 116
10.1. 2′,3′,5′-Tri-*O*-acetylinosine (**26**) 116
10.2. 6-Chloro-2′,3′,5′-tri-*O*-acetylinosine (**27**) 116
10.3. 6-Chloropurine riboside (**28**) 116
11.1 General procedure for the synthesis of N^6-substituted-purine ribosides (**29**, **30**, **33**-**48**) 116
11.2. Procedure for the synthesis of N^6-substituted-purine ribosides (**31**-**32**) 116
11.3. N^6-Methylpurine riboside (**29**) 116
11.4. N^6-Ethylpurine riboside (**30**) 121
11.5. N^6-Dimethylpurine riboside (**31**) 116
11.6. N^6-Diethylpurine riboside (**32**) 116
11.7. N^6-Ethyl-N^6-methyl-purine riboside (**33**) 116
11.8. N^6-Phenylpurine riboside (**34**) 116
11.9. N^6-Benzylpurine riboside (**35**) 125
11.10. N^6-(2-Phenylethyl)purine riboside (**36**) 126
11.11. N^6-Benzyl-N^6-methyl-purine riboside (**37**) 127
11.12. N^6-Benzyl-N^6-ethyl-purine riboside (**38**) 128
11.13. N^6-Dibenzylpurine riboside (**39**) 129
11.14. N^6-(4-Aminobenzyl)purine riboside (**40**) 130
11.15. N^6-(4-Chlorobenzyl)-purine riboside (**41**) 131
11.16. N^6-(3-Chlorobenzyl)-purine riboside (**42**) 132
11.17. N^6-(2-Chlorobenzyl)-purine riboside (**43**) 133
11.18. N^6-(4-Hydroxybenzyl)-purine riboside (**44**) 134
11.19. N^6-(4-Methoxybenzyl)-purine riboside (**45**) 135
11.20. N^6-(1-Phenylethyl)-purine riboside (**46**) 116
11.21. N^6-(4-Nitrobenzyl)purine riboside (**47**) 137
11.22. N^6-(4-Sulfamoylbenzyl)adenosine (**48**) 138

12.1. Procedure for the synthesis of N^6-substituted 2′,3′-*O*-isopropylidene-purine ribosides **49-52** 139
12.2. 2′,3′-*O*-Isopropylidene-N^6-methyl-purine riboside (**49**) 139
12.3. 2′,3′-Isopropylidiene-N^6-ethyl-purine riboside (**50**)..... 140
12.4. 2′,3′-Isopropylidiene-N^6-dimethyl-purine riboside (**51**) 141
12.5. 2′,3′-Isopropylidene-N^6-diethylpurine riboside (**52**)..... 142
13.1. General procedure for the synthesis of nucleotides (**53-56**) 142
13.2. 2′,3′-*O*-Isopropylidene-N^6-methylpurine riboside-5′-*O*-[(phosphonomethyl)phosphonic acid] (**53**)..... 143
13.3. 2′,3′-*O*-Isopropylidene-N^6-ethylpurine riboside-5′-*O*-[(phosphonomethyl)phosphonic acid] (**54**)..... 144
13.4. 2′,3′-*O*-Isopropylidene-N^6-dimethylpurine riboside-5′-*O*-[(phosphonomethyl)phosphonic acid] (**55**)..... 145
13.5. 2′,3′-*O*-Isopropylidene-N^6-diethylpurine riboside-5′-*O*-[(phosphonomethyl)phosphonic acid] (**56**)..... 145
13.6. General procedure for the synthesis of nucleotides (**57-60**) 145
13.7. N^6-Methylpurine riboside-5′-*O*-[(phosphonomethyl)phosphonic acid] (**57**)..... 147
13.8. N^6-Ethylpurine riboside-5′-*O*-[(phosphonomethyl)phosphonic acid] (**58**)..... 147
13.9. N^6-Dimethylpurine riboside-5′-*O*-[(phosphonomethyl)phosphonic acid] (**59**) 148
13.10. N^6-Diethylpurine riboside-5′-*O*-[(phosphonomethyl)phosphonic acid] (**60**)..... 149
13.11. General procedure for the synthesis of nucleotides (**61-76**) 149
13.12. N^6-Ethyl-N^6-methylpurine riboside-5′-*O*-[(phosphonomethyl)phosphonic acid] (**61**) 150
13.13. N^6-Phenylpurine riboside-5′-*O*-[(phosphonomethyl)phosphonic acid] (**62**) 151
13.14. N^6-Benzylpurine riboside-5′-*O*-[(phosphonomethyl)phosphonic acid] (**63**) 151
13.15. N^6-(2-Phenylethyl)purine riboside-5′-*O*-[(phosphonomethyl)phosphonic acid] (**64**) 152
13.16. N^6-Benzyl-N^6-methylpurine riboside-5′-*O*-[(phosphonomethyl)phosphonic acid] (**65**) . 153
13.17. N^6-Benzyl-N^6-ethylpurine riboside-5′-*O*-[(phosphonomethyl)phosphonic acid] (**66**)..... 154
13.18. N^6-Dibenzylpurine riboside-5′-*O*-[(phosphonomethyl)phosphonic acid] (**67**)..... 154
13.19. N^6-(4-Aminobenzyl)purine riboside-5′-*O*-[(phosphonomethyl)phosphonic acid] (**68**)... 155
13.20. N^6-(4-Chlorobenzyl)purine riboside-5′-*O*-[(phosphonomethyl)phosphonic acid] (**69**)... 156
13.21. N^6-(3-Chlorobenzyl)purine riboside-5′-*O*-[(phosphonomethyl)phosphonic acid] (**70**)... 157
13.22. N^6-(2-Chlorobenzyl)purine riboside-5′-*O*-[(phosphonomethyl)phosphonic acid] (**71**)... 157

13.23. N^6-(4-Hydroxybenzyl)purine riboside-5′-*O*-[(phosphonomethyl)phosphonic acid] (**72**) 158
13.24. N^6-(4-Methoxybenzyl)purine riboside-5′-*O*-[(phosphonomethyl)phosphonic acid] (**73**) 159
13.25. N^6-(1-Phenylethyl)purine riboside-5′-*O*-[(phosphonomethyl)phosphonic acid] (**74**) 160
13.26. N^6-(4-Nitrobenzyl)purine riboside-5′-*O*-[(phosphonomethyl)phosphonic acid] (**75**) 161
13.27. N^6-(4-Sulfamoylbenzyl)purine riboside-5′-*O*-[(phosphonomethyl)phosphonic acid] (**76**) 161
14.1. General procedure for the synthesis O^6-alkylpurine riboside (**77**, **78**) 161
14.2. 6-Ethoxypurine riboside (**77**) 161
14.3. 6-Benzyloxypurine riboside (**78**) 161
14.4. 6-Benzylthiopurine riboside (**80**) 161
15.1. General procedure for the synthesis of nucleotides (**81-83**) 161
15.2. 6-Ethoxypurine riboside-5′-*O*-[(phosphonomethyl)phosphonic acid] (**81**) 166
15. 3. 6-Benzyloxypurine riboside-5′-*O*-[(phosphonomethyl)phosphonic acid] (**82**) 167
15.4. 6-Benzylthiopurine riboside-5′-*O*-[(phosphonomethyl)phosphonic acid] (**83**) 167
16.1. 8-Bromoadenosine (**84**) 167
16.2. 8-Chloroadenosine (**86**) 167
16.3. 8-Ethylthioadenosine (**87**) 167
16.4. 8-Aminomethyl-adenosine (**88**) 167
17.1. General procedure for the synthesis of nucleotides (**89-92**) 167
17.2. 8-Bromoadenosine-5′-*O*-[(phosphonomethyl)phosphonic acid] (**89**) 173
17.3. 8-Chloroadenosine-5′-*O*-[(phosphonomethyl)phosphonic acid] (**90**) 173
17.4. 8-Ethylthioadenosine-5′-*O*-[(phosphonomethyl)phosphonic acid] (**91**) 174
17.5. 8-Aminomethyladenosine-5′-*O*-[(phosphonomethyl)phosphonic acid] (**92**) 175
18.1. 2-Amino-2′,3′,5′-tri-*O*-acetylinosine (**94**) 175
18.2. 2-Amino-6-chloro-2′,3′,5′-tri-*O*-acetylinosine (**95**) 175
18.3. 2-Amino-6-chloropurine riboside (**96**) 175
18.4. 2,6-dichloro-2',3', 5'-triacetyl-purine riboside (**97**) 175
18.5. 2-Chloroadenosine (**98**) 175
18.6. 6-Chloro-2-iodo-2',3',5'-triacetyl-purine riboside (**99**) 175
18.7. 2-Iodoadenosine (**100**) 181
18.8. 2-Hydrazinyladenosine (**101**) 175

18.9. 2-Boc-piperazinyladenosine (**102**)..... 175
18.10. 2-piperazinyladenosine (**103**)..... 175
18.11. Synthesis of 2-allylthio- and 2-cyclohexylethylthio-adenosine (**107**, **108**)..... 175
18.12. 2-Allylthioadenosine (**107**) 175
18.13. 2-Cyclohexylethylthio-adenosine (**108**)..... 175
19.1. General procedure for the synthesis of nucleotides (**109-114**)..... 175
19.2. 2-Chloroadenosine-5′-*O*-[(phosphonomethyl)phosphonic acid] (**109**)..... 187
19.3. 2-Iodoadenosine-5′-*O*-[(phosphonomethyl)phosphonic acid] (**110**) 188
19.4. 2-Hydrazinyladenosine-5′-*O*-[(phosphonomethyl)phosphonic acid] (**111**)..... 189
19.5. 2-Piperazinyladenosine-5′-*O*-[(phosphonomethyl)phosphonic acid] (**112**) 189
19.6. 2-Allylthioadenosine-5′-*O*-[(phosphonomethyl)phosphonic acid] (**113**) 190
19.7. 2-Cyclohexylethylthioadenosine-5′-*O*-[(phosphonomethyl)phosphonic acid] (**114**)..... 191
20.1. General Procedure for the synthesis of nucleoside derivatives (**115-126** and **127-138**) .. 191
20.2. N^6-Dimethyl-2-aminopurine riboside (**127**)..... 191
20.3. N^6-Diethyl-2-aminopurine riboside (**128**)..... 191
20.4. N^6-Benzyl-2-aminopurine riboside (**129**) 194
20.5. N^6-Benzyl-2-chloropurine riboside (**130**) 195
20.6. N^6-Benzyl-2-iodopurine riboside (**131**) 196
20.7. N^6-(2-Chlorobenzyl)-2-chloropurine riboside (**132**)..... 197
20.8. N^6-(1-Phenylethylamine)-2-chloropurine riboside (**133**)..... 198
20.9. N^6-((*S*)-1-Phenylethylamine)-2-chloropurine riboside (**134**)..... 199
20.10. N^6-((*R*)-1-Phenylethylamine)-2-chloropurine riboside (**135**) 200
20.11. 2-Iodo-N^6-methyl-N^6-benzyl-purine riboside (**136**)..... 201
20.12. 2-Chloro-N^6-methyl-N^6-benzylpurine riboside (**137**) 202
20.13. 2-Iodo-N^6-Benzyl-N^6-methyl-purine riboside (**138**)..... 203
21.1. General procedure for the synthesis of nucleotides (**139-150**)..... 204
21.2. 2-Amino-N^6-dimethylpurine riboside-5′-*O*-[(phosphonomethyl)phosphonic acid] (**139**). 204
21.3. 2-Amino-N^6-diethylpurine riboside-5′-*O*-[(phosphonomethyl)phosphonic acid] (**140**).... 205
21.4. 2-Amino-N^6-benzylpurine riboside-5′-*O*-[(phosphonomethyl)phosphonic acid] (**141**) 206
21.5. N^6-Benzyl-2-chloropurine riboside-5′-*O*-[(phosphonomethyl)phosphonic acid] (**142**) 206
21.6. N^6-Benzyl-2-iodopurine riboside-5′-*O*-[(phosphonomethyl)phosphonic acid] (**143**) 207

21.7. N^6-(2-Chlorobenzyl)-2-chloropurine riboside-5′-*O*-[(phosphonomethyl)phosphonic acid] (**144**). 208

21.8. 2-Chloro-N^6-(1-phenylethyl)- purine riboside-5′-*O*-[(phosphonomethyl)phosphonic acid] (**145**) 209

21.9. 2-Chloro-N^6-((*S*)- 1-phenylethyl)-purine riboside-5′-*O*-[(phosphonomethyl)phosphonic acid] (**146**) 210

21.10. 2-Chloro-N^6-((*R*) -1-phenylethyl)- purine riboside-5′-*O*-[(phosphonomethyl)phosphonic acid] (**147**) 211

21.11. 2-Amino-N^6-benzyl-N^6-methylpurine riboside-5′-*O*-[(phosphonomethyl)phosphonic acid] (**148**) 211

21.12. N^6-Benzyl-N^6-methyl-2-chloropurine riboside-5′-*O*-[(phosphonomethyl)phosphonic acid] (**149**) 212

21.14. N^6-Benzyl-N^6-methyl-2-iodopurine riboside-5′-*O*-[(phosphonomethyl)phosphonic acid] (**150**) 213

22.1. 2,6-Diaminoadenosine (**156**) 213

22.2. Isoguanosine (**157**) 213

23.1. General procedure for the synthesis of nucleotides (**151**-**154**, **156** and **158**) 213

23.2. Inosine-5′-*O*-[(phosphonomethyl)phosphonic acid] (**151**) 216

23.3. 6-Chloropurine riboside-5′-*O*-[(phosphonomethyl)phosphonic acid] (**152**) 217

23.4. Guanosine-5′-*O*-[(phosphonomethyl)phosphonic acid] (**153**) 218

23.5. 2-Amino-6-chloroadenosine-5′-*O*-[(phosphonomethyl)phosphonic acid] (**154**) 218

23.6. 2,6-Diaminoadenosine-5′-*O*-[(phosphonomethyl)phosphonic acid] (**156**) 219

23.7. Isoguanosine-5′-*O*-[(phosphonomethyl)phosphonic acid] (**158**) 220

24.1. 2′,3′-*O*-Isoproylidene-adenosine (**159**) 223

24.2. 2′,3′-*O*-Isopropylidene-5′-tosyladenosine (**160**) 223

24.3. Procedure for the synthesis of nucleotides (**161**, **162**) 223

24.4. Adenosine-5′-dichloromethylenediphosphonic acid (**161**) 223

24.5. Adenosine-5′-(1-hydroxy)ethane-1,1-diphosphonic acid (**162**) 224

25.1. Biological experiments 224

25.1.1. Radiometric *e*N assay 224

25.1.2. NPP 1-3 colorimetric assay 225

25.1.2.1. Assay condition for NPP 1 and NPP 3 226

25.1.2.2. Assay condition for NPP 2 226

25.1.3. Human NTPDases 1-3 malachite green assay 226
25.1.4. $P2Y_1$ Calcium assay 227
25.1.5. $P2Y_{12}$ β-arrestin assay 228
25.2. Metabolic stability studies on rat liver 228
25.2.1. Preparation of Rat Liver Microsomes 228
25.2.2. LC-MS Analyses 229
25.2.3. Metabolism by rat Liver Microsomes 229
25.2.4. Plasma stability studies 229
VI. Summary 231
VII. References 239
VIII. Abbreviations 239

List of figures

1. Extracellular purine and pyrimidine signalling molecules 2
2. The purinergic neuromuscular transmission hypothesis 3
3. The purinergic receptor family, with their physiological agonists 5
4. Nucleotides and adenosine releasing pathways 8
5. Purinergic signalling pathways 9
6. Schematic diagram of *ecto*-nucleotidases 50
7. Schematic representation of the ecto-domain of rat NTPDase 1 14
8. Domain movements of human *e*N 20
9. Binding of AOPCP to human *e*N in the closed form 21
10. Immunomodualation by NTPDase 1 and *e*N in tandem 24
11. Structures of base-modified target compounds 38
12. Structures of side chain-modified target compounds 39
13. Possible products of the phosphorylation of nucleoside using methylenebis(phosphonic dichloride) 47
14. ^{31}P NMR spectra (202 MHz, D_2O) δ ppm: purity control of compound **110** and **148** respectively 73

15. ^{31}P NMR spectra (202 MHz, D_2O) δ ppm: purity control of compound **149** and **112** respectively 74

16. LC/ESI-MS spectra of the synthesized nucleotide **63** 75

17. LC/ESI-MS spectra of the synthesized nucleotide **71** 76

18. LC/ESI-MS spectra of the synthesized nucleotide **82** 77

19. Radiometric assays at rat *e*N 91

20. Compounds used in the liver microsomal metabolic study 99

21. Metabolic stability studies of **ADP**, **AOPCP**, **diazepam** and AOPCP derivatives **71**, **74**, **149** and **150** in rat liver microsomes 101

22. Phase 1 metabolic products of **ADP**, **AOPCP** and inhibitor **149** after incubation with rat liver microsomes 102

23. Representative HPLC chromatogram and corresponding MS spectra of compound **149** after 4 h incubation 104

24. Representative HPLC chromatogram and corresponding MS spectra of compound **149** 105

25. Representative HPLC chromatogram and corresponding MS spectra of **ADP** after incubation 106

26. Representative HPLC chromatogram and corresponding MS spectra of **AOPCP** after incubation 107

27. Stability studies of ADP, AOPCP and AOPCP derivatives **149**, **150 and 71** in human blood. 109

28. Representative HPLC chromatogram and corresponding MS spectra of **149** in human blood 111

29. Representative HPLC chromatogram and corresponding MS spectra of **ADP** after incubation with human blood 112

30. Representative HPLC chromatogram and corresponding MS spectra of **AOPCP** after incubation with human blood 113

31. Structure of the most potent *e*N inhibitors 234

32. Structure-activity relationships of 6-and 8-substituted AOPCP derivatives and analogs..... 235

33. Structure-activity relationships of 2-mono-, 2,6-disubstituted and methylene bis(phosphate) side chain-modified AOPCP 237

34.Compounds investigated in metabolic studies 237

List of tables

1. Locolization and physiological effects of *e*NTPDase subtypes 11

2. Members of the *e*NPP family with their cellular expression pattern and functions 15

3. Member of APs with their expression pattern and physiological role 17

4. Additional nucleotide-metabolizing enzymes with substrate and physiological effect 17

5. Activity of adenine nucleotide derivatives at rat *e*N 28

6. Potency of uridine derivatives at rat *e*N 29

7. Potency of anthraquinone derivative at rat *e*N 30

8. Potency of sulfonamide derivatives as inhibitors of rat *e*N 31

9. Activity of sulfonic acid derivatives at rat *e*N 32

10. Optimization of reaction condition for the synthesis of N^6-dimethyl-2′,3′-*O*-isopropylidine-purine riboside methylenebis(phosphonic acid)] 49

11. Optimization of reaction conditions for the synthesis of N^6-dimethylpurine riboside 5′-*O*-[(phosphonomethyl)phosphonic acid] 50

12. Inhibitory potency of N^6-substituted-purine riboside-5′-*O*-[(phosphonomethyl)phosphonic acid] derivatives at rat *ecto*-5′-nucleotidase 80

13. Potency of inosine-5′-*O*-[(phosphonomethyl)phosphonic acid], 6-chloro-purine riboside-5′-*O*-[(phosphonomethyl)phosphonic acid], and O^6- and S^6-substituted-purine riboside-5′-*O*-[(phosphonomethyl)phosphonic acid] at rat *ecto*-5′-nucleotidase 82

14. Potency of 8-substituted-adenosine-5′-*O*-[(phosphonomethyl)phosphonic acid] derivatives at rat *ecto*-5′-nucleotidase 85

15. Potency of 2-substituted-adenosine-5′-*O*-[(phosphonomethyl)phosphonic acid] derivatives at rat *ecto*-5′-nucleotidase 87

16. Potency of 2-amino, 2-chloro or 2-iodo-N^6-mono-/dialkyl- or aryl-adenosine-5′-*O*-[(phosphonomethyl)phosphonic acid] derivatives at rat *ecto*-5′-nucleotidase 89

17. Potency of adenosine-5′-dichloromethylenediphosphonic acid and adenosine-5′-(1-hydroxy)ethane-1,1-diphosphonic acid 90

18. Potency of selected derivatives at human NTPDase 1-3 and NPP 1-3 93

19. Potency of selected derivatives at ADP-activated P2Y receptor subtypes 94

20. Percentage remaining of **AOPCP** and **ADP** at different time intervals (min) 100

21. Percentage remaining of diazepam, **71**, **74**, **149** and **150** at different time intervals (hour). 100

22. Percentage remaining of **74** and **149** at different time intervals (hour) under incubation with liver microsomes after adding NADPH regenerating system 103

23. Percentage remaining of **ADP**, **AOPCP**, diazepam, **71**, **149** and **150** at different time intervals (min) 110

List of schemes

1. Synthesis of 2′,3′,5′-tri-*O*-acetylinosine (**26**) 41

2. Synthesis of 6-chloro-2′,3′,5′-tri-*O*-acetylinosine (**27**) 42

3. Synthesis of 6-chloropurine riboside (**28**) 43

4. Synthesis of N^6-substituted-purine ribosides (**29-48**) 44

5. Synthesis of N^6-substituted-2′,3′-*O*-isopropylidene purine ribosides (**49-52**) 45

6. Electrophic adduct formed by the reaction of trimethyl phosphate and methylenebis (phosphonic dichloride) 47

7. Intermediate formed during phosphoryaltion reaction by methylenebis(phosphonic dichloride) 48

8. Synthesis of target nucleotides **53-60** 51

9. Synthesis of target derivatives **61-76** 52

10. Synthesis of 6-ethoxy- and 6-benzyloxypurine riboside (**77**, **78**) 54

11. Synthesis of 6-benzylthiopurine riboside (**80**) 55

12. Synthesis of target nucleotides **81-83** 56

13. Synthesis of 8-bromoadenosine (**84**) 57

14. Synthesis of 8-chloroadenosine (**86**) 57

15. Synthesis of 8-ethylthioadenosine (**87**) 58

16. Synthesis of 8-methylaminoadenosine (**88**) 58

17. Synthesis of nucleotides **89-92** 59

18. Synthesis of 2-amino-2′,3′,5′-tri-*O*-acetylinosine (**94**) 60

19. Synthesis of 2-amino-6-chloro-2′,3′,5′-tri-*O*-acetylinosine (**95**). 60

20. Synthesis of 2-amino-6-chloropurine riboside (**96**) 61

21. Synthesis of 2-chloroadenosine (**98**) 61

22. Synthesis of 2-iodoadenosine (**100**) 62

23. Synthesis of 2-hydrazinyladenosine (**101**) 63

24. Synthesis of 2-piperazinyladenosine (**103**) 63

25 Synthesis of 2-cyclohexylethylthio- and 2-allythioadenosine (**107**, **108**) 64

26. Synthesis of target nucleotides **109-114** 65
27. Synthesis of 2-amino, 2-choro or 2-iodo-N^6-mono/dialkyl or aryl-purine ribosides (**127-138**) 66
28. Synthesis of target nucleotides **139-150** 67
29. Synthesis of inosine-5′-*O*-[(phosphonomethyl)phosphonic acid] (**151**)..... 67
30. 6-chloropurine riboside-5′-*O*-[(phosphonomethyl)phosphonic acid] (**152**) 68
31. Synthesis of guanosine-5′-*O*-[(phosphonomethyl)phosphonic acid] (**153**) 68
32. Synthesis of 2-amino-6-chloropurine riboside-5′-*O*-[(phosphonomethyl)phosphonic acid] (**154**)..... 69
33. Synthesis of 2,6-diaminopurine riboside-5′-*O*-[(phosphonomethyl)phosphonic acid] (**156**). 69
34.Synthesis of isoguanosine-5′-*O*-[(phosphonomethyl)phosphonic acid] (**158**) 70
35. Synthesis of adenosine-5′-dichloromethylenediphosphonic acid (**161**) 72
36. Synthesis of adenosine-5′-(1-hydroxy)ethane-1,1-diphosphonic acid **(162)**..... 72

I. Introduction

1.1. Purinergic Signalling

Extracellular signalling purine and pyrimidine derivatives like ATP (**1**), ADP (**2**), UTP (**3**), UDP (**4**) and adenosine (**5**) regulate various functions in living organisms. These molecules are present in the extracellular space by release from cells or by metabolic formation from precursors. Until the 1970s studies on the physiological functions of these nucleotides and nucleosides were limited.[1] The research focus was restricted to the cell metabolism of ATP and its function as an energy source. Then, in 1970, Burnstock and coworkers presented evidence for ATP as a neurotransmitter in nonadrenergic, noncholinergic nerves (NANC) supplying the gut.[2-4] Two years later they coined the word "purinergic" and also proposed a purinergic neurotransmission hypothesis.[4] After that, there has been continuous growth in the field of extracellular purinergic signalling. Few years later, in 1978, they proposed specific membrane-bound, so-called purinergic receptors, to be activated by nucleosides and nucleotides. The receptors were initially divided into two families: the P1 receptors, activated by nucleosides and the P2 receptors, activated by nucleotides.[1] Apart from the involvement of these nucleotides and nucleosides in differentiation and development, they have wide physiological involvement mediated by purinergic signaling. The alterations in the physiology of purinergic signalling may result in the development of various pathological conditions. Due to the involvement of these molecules in pathological conditions, there has been long standing interest in purinergic signalling from a medicinal chemistry point of view.[4] Some therapeutics targeting purine receptors are already marketed and many are evaluated in clinical studies. The anti-platelet drug Clopidogrel which was later found to be an irreversible allosteric inhibitor of the $P2Y_{12}$ receptor after formation of a reactive metabolite. It is one of the blockbuster drugs with billion dollar sales. Regadenoson, an

adenosine A_{2A} receptor agonist was approved by the FDA (USA) in 2008 as a coronary vasodilator and is currently widely used in cardiac imaging. Diquafosol, an agonist of $P2Y_2$ receptors, was approved by some countries for the treatment of dry eye disease. Istradeylline, a selective antagonist of A_{2A} receptors was approved for the treatment of Parkinson's disease in combination with *L*-3,4-dihydroxyphenylalanine (*L*-DOPA) in Japan.

The study of purinergic signalling has also helped to understand the potential side-effects of some already commercialized drugs: e.g. the non-selective adenosine receptor antagonist theophylline which was previously used as a bronchodilator was restricted from its usage due to potential side-effects such as seizures and cardiac arrhythmias caused by adenosine A_1 receptor antagonism.

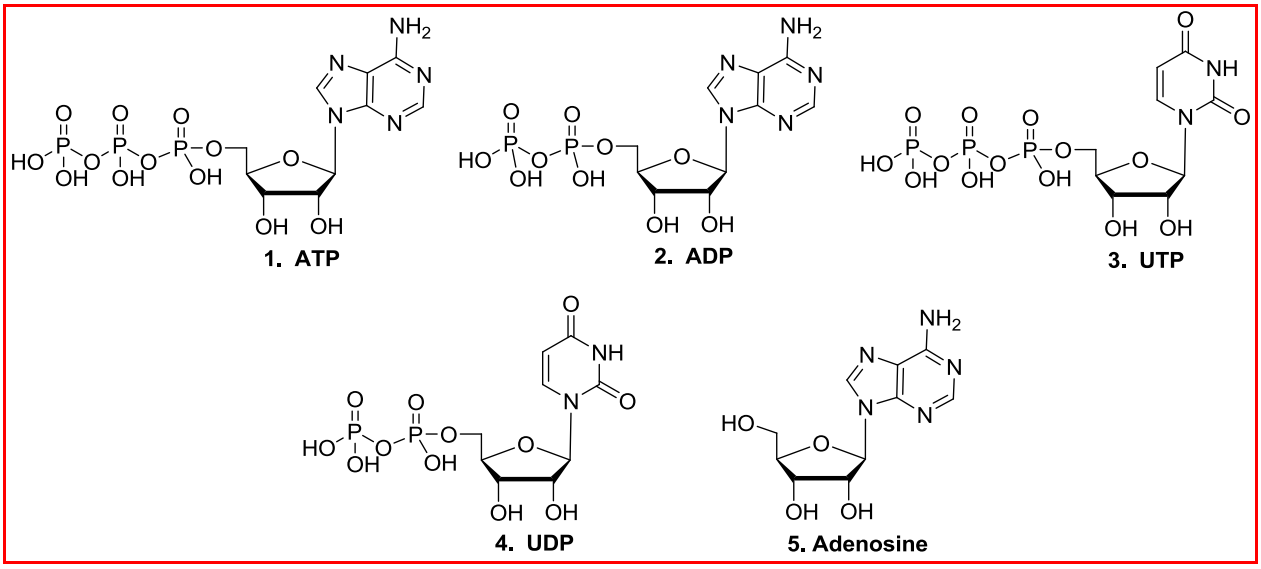

Figure 1. Extracellular purine and pyrimidine signalling molecules.
(ATP: adenosine triphosphate; ADP: adenosine diphosphate; UTP: uridine triphosphate; UDP: uridine diphosphate)

1.2. Synthesis and storage of ATP

The schematic representation of synthesis, storage, release and inactivation of ATP in purinergic nerves as proposed by Burnstock[2-4] is shown in Figure 2. He proposed that ATP is broken down

extracellularly by enzymes, namely ATPases and 5'-nucleotidases. ATPases convert ATP into AMP (via ADP) and 5'-nucleotidases converts AMP to adenosine. Adenosine may also be broken down further by adenosine deaminase to inosine, and removed by the circulation. Adenosine can be taken up by the vessels to resynthesise ATP for usage in mitochondria or stored in vesicles at the nerve endings. ATP can be released by exocytosis to act on P2 receptors of smooth muscle.

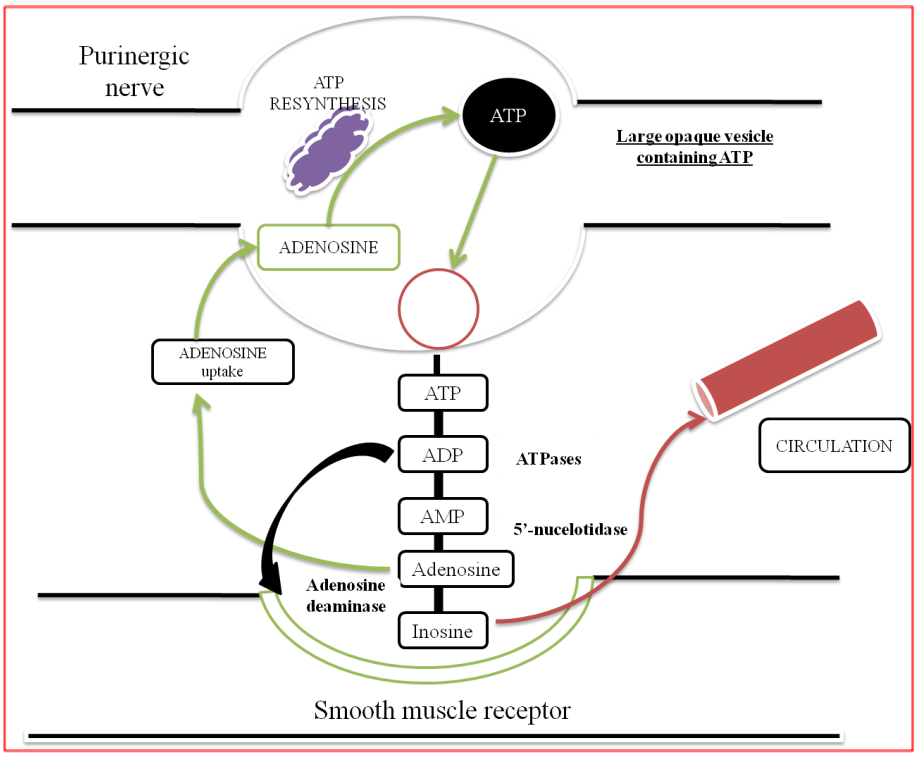

Figure 2. The purinergic neuromuscular transmission hypothesis.[3]
(AMP: adenosine monophosphate; Mitochondria is represented by purple color; ATP storing nerve vesicles are represented by brown circle; blood vessel is depicited by brown cylinder)

Nucleotides and nucleosides in the extracellular space are subjected to metabolism by different enzymes. These extracellular enzymes have potential as drug targets. ATPases cleave phosphoric acid-anhydride bonds, whereas 5'-nucleotidase hydrolyzes nucleoside 5'-phosphoric acid ester bonds.[5] These enzymes which metabolize nucleotides are collectively called *ecto*-nucleotidases.[6] *Ecto*-nucleotidases have important roles in purinergic signal transmission by decreasing the

nucleotides acting at purinergic P2 receptors.[7, 8] The hydrolytic product generated, nucleosides in turn activate P1 receptors or can be taken up via nucleoside transporters for re-phosphorylation.[8] The hydrolytic by product is inorganic pyrophosphate (PP_i) and inorganic phosphate (P_i), which controls bone mineralization and muscle calcification.

1.3. Purinergic receptor family

Presently the purinergic receptor family consists of three subfamilies: P0, P1 and P2 purinergic receptors.[9]

1.3.1. P0 receptors

P0 receptors, which are also called adenine receptors, are G-protein-coupled receptors for which the endogenous ligand is adenine. This receptor is expressed in the small neurons of dorsal root ganglia, ovaries, kidney and small intestine in rat. The detailed physiological roles of adenine receptors is not well known but it may play an important role in nociception. Studies have also shown the involvement of adenine in human renal dysfunction which can be correlated to the significance of adenine receptors in maintaining proper renal function.[10]

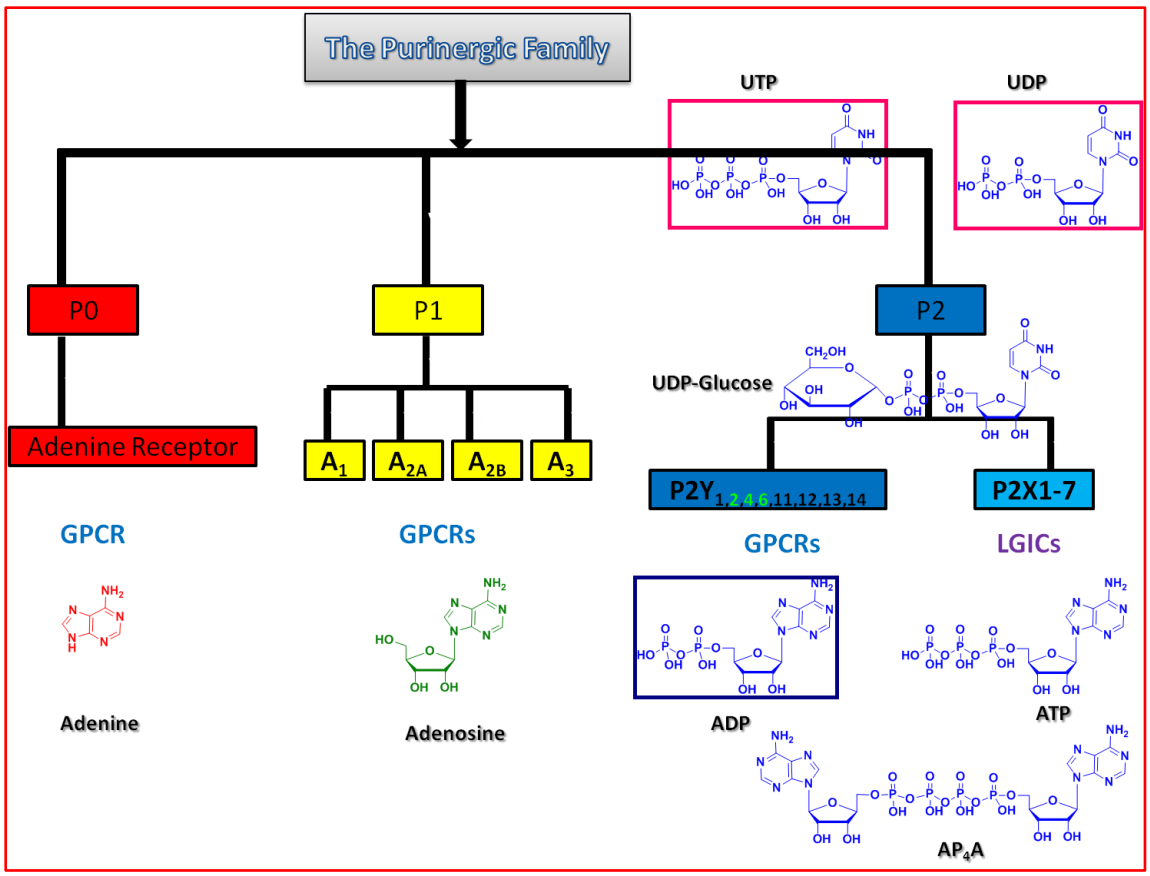

Figure 3. The purinergic receptor family, with their physiological agonists.[8, 9]
(AP_4P: Diadenosine 5',5'''-P^1,P^4-tetraphosphate; GPCR: G protein-coupled receptor; LGIC: Ligand-gated ion channel)

1.3.2. P1 receptor

P1 receptors, or adenosine receptors (AR or A), are receptor proteins belonging to the family of membrane-bound G protein-coupled receptors (GPCRs). On the basis of their distribution pattern, molecular structure and physiological effects adenosine receptors are further subdivided into four subtypes, A_1, A_{2A}, A_{2B} and A_3.[11-13] For human ARs, the most similar ones are the A_1 and A_3 which share 49% sequence similarity and the A_{2A} and A_{2B} with 59% similarity. The A_1 receptor is highly expressed in brain, spinal cord, heart, stomach, eye and adrenal gland. A_{2A} is expressed in brain, heart, spleen, lungs, immune cells and blood vessels. The A_{2B} receptor is prominently expressed in cecum, colon and bladder whereas A_3 is highly expressed in lungs and

liver. A_1 and A_3 receptors interact with $G_{i/o}$ proteins of G-protein family where as A_{2A} and A_{2B} interact with members of the G_s family. A_1 and A_3 receptors couple to adenylate cyclase in an inhibitory manner, whereas A_{2A} and A_{2B} receptor stimulate the enzyme. Adenosine activates adenosine receptors to produces many important effects, e.g., anti-inflammatory, antilipolytic, anticonvulsive, sedative, vasodilatory, immunosuppressive, antidiuretic, and negative inotropic effects. Both, activators and inhibitors of ARs, are investigated as potential drugs in many therapeutic areas like the respiratory and the cardiovascular systems, neuroprotection, pain processes and inflammatory responses.[14]

1.3.3. P2 receptors

P2 receptors are divided into two major families: ionotropic (P2X) and G protein-coupled (P2Y) receptors.[7] Nucleotides are agonist at both, P2X and P2Y receptor subtypes. P2X receptors (seven subtypes, P2X1 to P2X7), are homo- or hetero-trimeric and are activated by ATP. They represent Na^+-, K^+-, and Ca^{2+}-permeable ion channels and their activation results an increase in intracellular cations and depolarization. P2X1 and P2X3, desensitize rapidly (within 100-300 milliseconds), and P2X2, P2X4, P2X5, P2X6 and P2X7, do not desentize at all or desensitize very slowly. P2X receptors are distributed on heart muscle, smooth muscle cells (vas deferens and urinary bladder) and neurons (nerve terminals), glial cell and leukocytes.[7, 9, 15] The important physiological role of P2X receptors are modulation of vascular tone, cardiac rhythm and contractility, contraction of urinary bladder and vas deferens, apoptosis, platelet aggregation and macrophage activation. P2Y receptors are subdivided into eight types: $P2Y_1$ (agonist ADP), $P2Y_2$ (agonists UTP and ATP), $P2Y_4$ (agonist UTP), $P2Y_6$ (agonist UDP), $P2Y_{11}$ (agonists ATP and NAD^+), $P2Y_{12}$ (agonist ADP), $P2Y_{13}$ (agonist ADP), and $P2Y_{14}$ (agonists UDP, UDP-glucose and other nucleotide sugars). Based on the structural similarities, P2Y receptor can be

divided into two groups: $P2Y_{12,13,14}$ receptors whose coupling leads to the inhibition of adenylate cyclase and $P2Y_{1,2,4,6,11}$ receptors whose coupling results in the activation of phospholipase C. P2Y receptors are distributed in brain, heart, kidney, liver, lung, pancreas, prostate and thymus, bone and haematopoietic cells. P2Y receptors are involved in many important physiological processes and pathological conditions like reducing the risks of strokes and heart attacks ($P2Y_{12}$), platelet aggregration ($P2Y_1$ and $P2Y_{12}$),[16] treatment of hypertension ($P2Y_2$, $P2Y_6$ and $P2Y_{11}$), insulin release, T-cell mediated inflammation ($P2Y_6$), inflammation and immunomodulation ($P2Y_1$, $P2Y_2$ and $P2Y_{11}$), neuroprotection in brain and treatment of neurodegenerative diseases such as Alzheimer's, Parkinson's and lateral sclerosis, target for tumor proliferation ($P2Y_1$ and $P2Y_2$), pain, cystic fibrosis ($P2Y_2$), chronic bronchitis and chronic obstructive pulmonary disease (COPD).[15]

1.4. Nucleotides and adenosine releasing pathways

The purinergic signalling chain is initiated by the release of endogenous nucleotides to the extracellular spaces.[17] The nucleotides are released by cell lysis in various pathological conditions like injury, shock and inflammatory conditions, and/or by non-lytic mechanisms by nucleotide effluxes. Nucleotides are released from various excitatory tissues such as nerve terminals, chromaffin cells, pancreatic acinar cells and platelets via exocytosis. Moreover, nucleotide are released from various non-excitatory tissues, like astrocytes, fibroblasts, glial cells, bone cells, hepatocytes, keratinocytes, cardiomyocytes, epithelial and endothelial cells, erythrocytes, macrophages, neutrophils, and other hematopoietic cells by various mechanical stimuli.

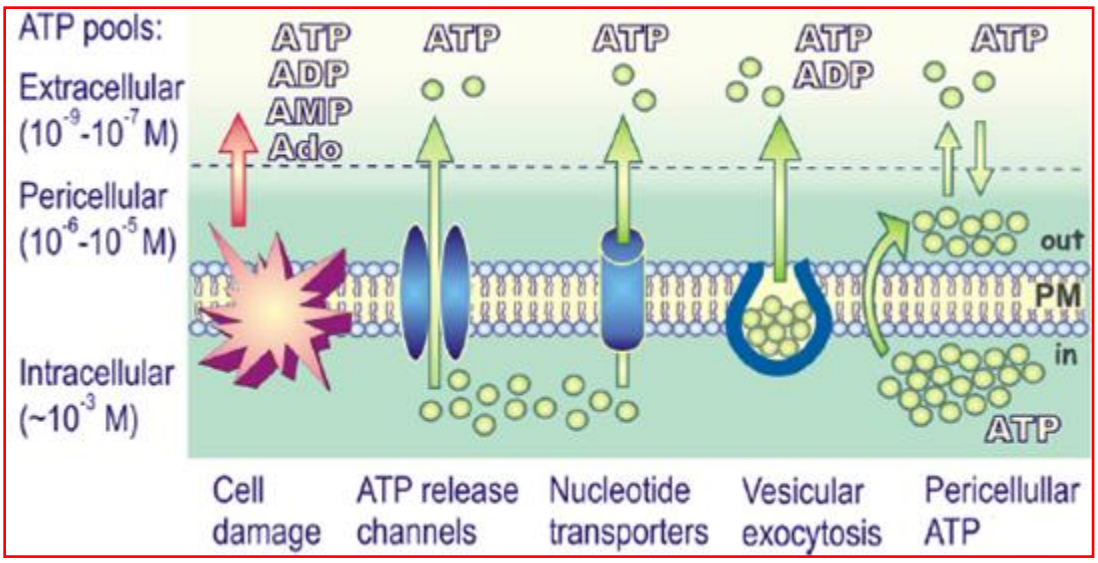

Figure 4. Nucleotides and adenosine releasing pathways[17]
(Ado: adenosine)

The cellular mechanism of nucleotide release includes:

- electrodiffusional movement
- facilitated diffusion
- cargo-vesicle trafficking and exocytotic granule secretion.

The electrodiffusional movement is through membrane ion channels e.g. connexin hemichannels, stretch- and voltage-activated channels. The facilitated diffusion is mediated by nucleotide-specific ATP-binding cassette (ABC) transporters, e.g. cystic fibrosis transmembrane conductance regulator (CFTR), multiple organic anion transporters, and multidrug resistance proteins. UTP, UDP and UDP-glucose are also released as a response to stress and injury. Dinucleoside polyphosphates are released upon cell damage.[17, 18]

1.5. Purinergic signalling pathways and *ecto*-nucleotidases

The purinergic signalling chain consists of both purinergic receptors and *ecto*-enzymes. [19, 20] These *ecto*-enzyme can hydrolyzes both nucleotides and nucleosides. The major *ecto*-enzymes involved in nucleotide hydrolysis in the purinergic signaling cascade comprises *ecto*-nucleotide pyrophosphatases/ phosphodiesterases (*e*NPPs, **1**), *ecto*-nucleoside triphosphate diphosphohydrolases (*e*NTPDase, **2**) and *ecto*-5'-nucleotidase (*e*N, **3**). The resulting adenosine (Ado) can be further deaminated via inosine (Ino) into hypoxanthine (Hyp) by other *ecto*-enzymes such as *ecto*-adenosine deaminase (ADA, **4**) and purine nucleoside phosphorylase (PNP, **5**) reactions.[17, 21] The inactivating mechanisms for adenine nucleotides and adenosine are highlighted below in Figure 5.

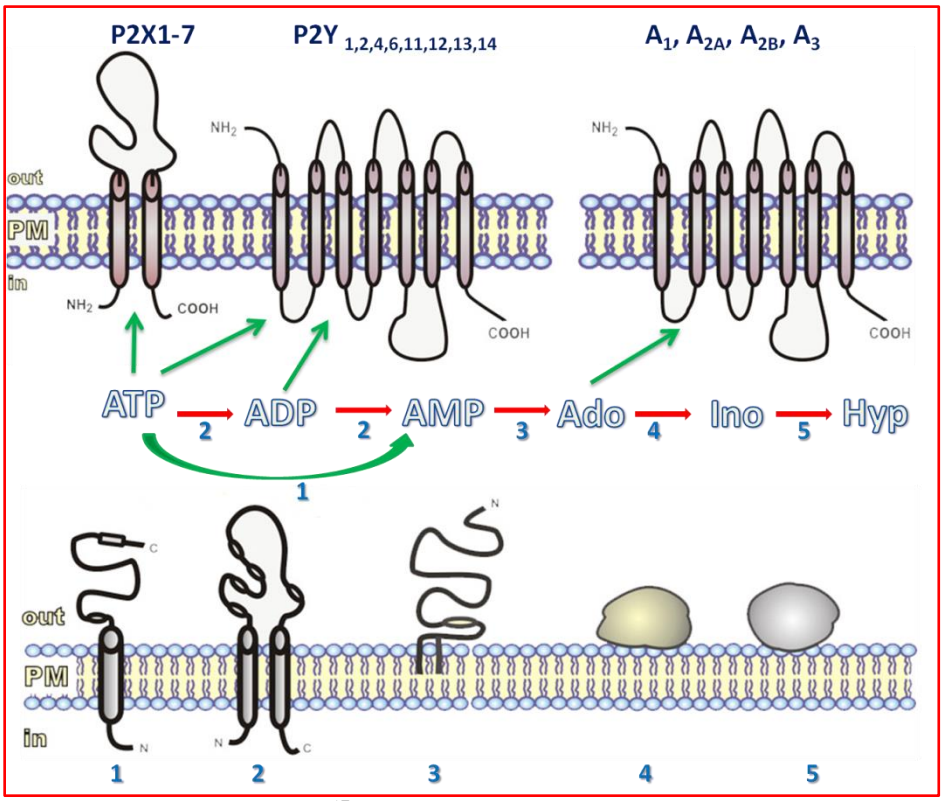

Figure 5. Purinergic signalling pathways[17]
(Ino: inosine; Hyp: hypoxanthine; 1: eNPPs, ecto-nucleotide pyrophosphatase/ phosphodiesterases; 2: eNTPDases, ecto-nucleoside triphosphate diphosphohydrolases; 3: eN, ecto-5'-nucleotidase; 4: ADA, ecto-adenosine deaminase; 5: PNP, purine nucleoside phosphorylase; PM: plasma membrane)

1.6. *Ecto*-nucleotidases

The four major *ecto*-nucleotidases include the *ecto*-nucleoside triphosphate diphosphohydrolases (*e*NTPDases), *ecto*-5′-nucleotidase (*e*N), *ecto*-nucleotide pyrophosphatases/ phosphodiesterases (*e*NPPs), and alkaline phosphatases (APs).[22, 23] *E*-NTPDases and *e*NPPs are ATP- and ADP-hydrolyzing *ecto*-nucleotidases, while *e*N catalyzes the final step, the hydrolysis of AMP to adenosine. APs are the only *ecto*-nucleotidases which can hydrolyze ATP, ADP and AMP.[23, 24]

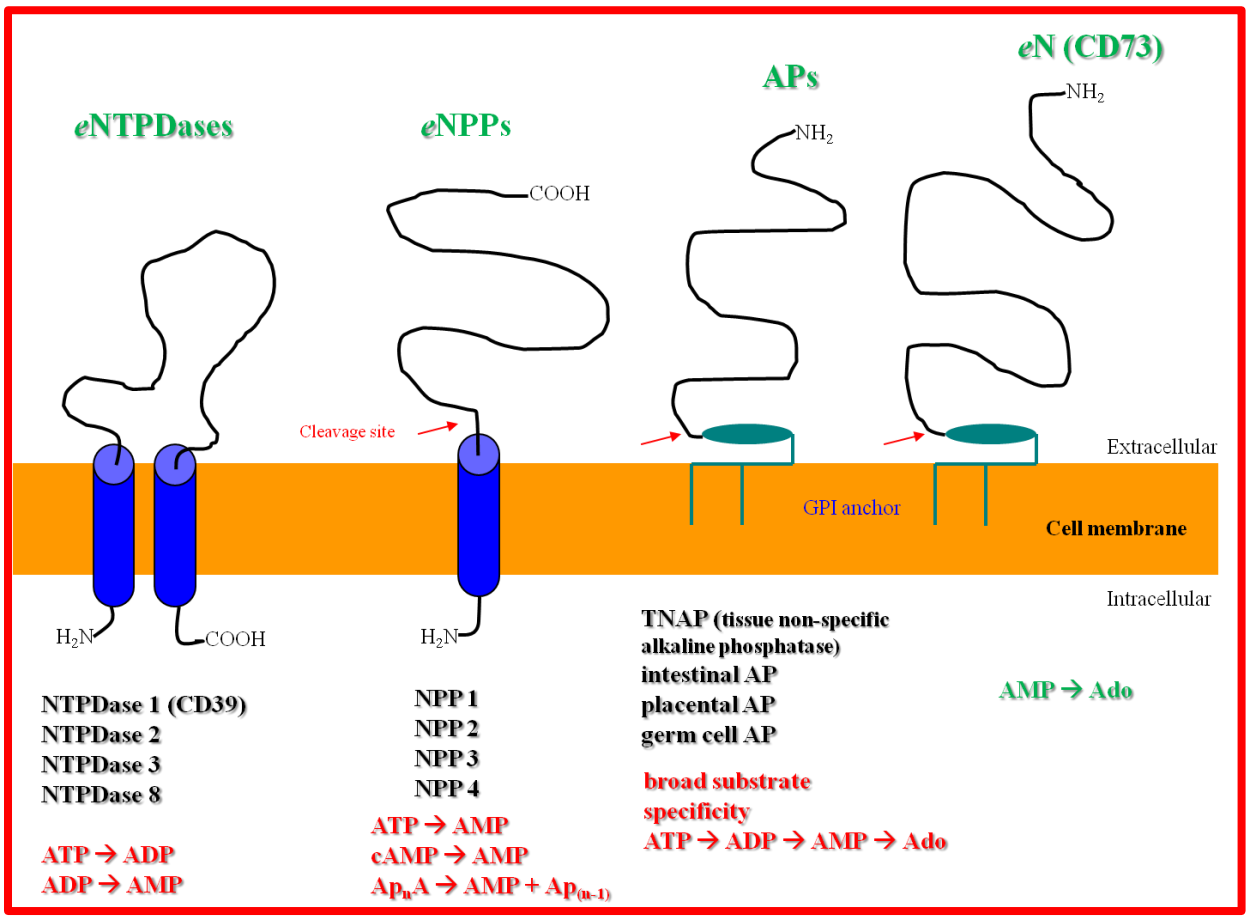

Figure 6. Schematic diagram of *ecto*-nucleotidases.[6]
(AP: alkaline phosphatase; GPI: glycosylphosphatidylinositol; cAMP: cyclic AMP)

1.6.1. *Ecto*-nucleoside triphosphate diphosphohydrolases

Ecto-nucleoside triphosphate diphosphohydrolases which are also called *e*NTPDases are major nucleotide-metabolizing enzymes. They hydrolyze extracellular nucleotide tri- and diphosphates in the presence of millimolar concentrations of Ca^{2+} or Mg^{2+} at physiological extracellular pH values between 7 and 8 and nucleoside monophosphates are their final hydrolysis product. Out of the eight subtypes identified in human, four of these (NTPDase 1 or CD39, NTPDase 2 or CD39L1, NTPDase 3 or CD39L3, and NTPDase 8) are cell surface-located enzymes which function as *ecto*-nucleotidases. NTPDase 4–7 have intracellular organellar localization, whereas NTPDase 5 and NTPDase 6 are also intracellularly located but are present in secreted forms. NTPDases vary from each other in terms of substrate specificity and preference for particular kind of substrates.[23-25]

Human NTPDase 1 and 2 have a preference for adenine over uracil nucleotides i.e more preferences for ATP and ADP. The K_m values for ATP of human NTPDase 1, NTPDase 2, and NTPDase 3 were determined 17, 70, and 75 μM, respectively, so NTPDase 1 is the enzyme with the highest preferences for ATP.[26] NTPDase 2, NTPDase 3, and NTPDase 8 hydrolyze ATP to ADP then further hydrolyzed to AMP after releasing from the enzyme. NTPDase 2 hydrolyzes ATP to ADP thus accumulating ADP before further hydrolyzing to AMP.[27-29] But NTPDase 1 hydrolyzed ATP directly to AMP, without accumulation of ADP. NTPDases have broad tissue distribution.[30-36]

Table 1. Locolization and physiological effects of *e*NTPDase subtypes[23, 24, 33, 34, 36]

Organs/ Organells/ Tissue/ or System	**NTPDases sub-type**	**Locolization**	**Physiological effect**
Vasculature	NTPDase 1	endothelial cells, vascular smooth muscle	-thrombroregulatory effect - cerebroprotection - cardioprotection

	NTPDase 2	Advential surface of vessels	-vascular hemostasis
Liver	NTPDase 2	portal fibroblasts	-regulation of bile ductular signaling and secretion - regulates epithelial cell Proliferation
	NTPDase 8	hepatic canalicule	- regulate the concentration of nucleotides, plays important role in purine salvage in the liver
	NTPDase 1	more on vessels and less on sinusoids and Kupffer cells	-regulate glycogenolysis
Pancreas	NTPDase 1	Luminal membranes and basolateral membranes of larger ducts	-regulats paracrine mediator function between pancreatic acini and ducts
	NTPDase 2	epithelial cells, myoepithelial cells, the basolateral membrane of acini	-regulates paracrine mediator function between pancreatic acini and ducts
Salivary glands	NTPDase 1	Vascular cells	-regulates transport of electrolytes by modulating the extracellular ATP concentration
	NTPDase 2	Myoepithelial cells and nerves	-regulates transport of Electrolytes
Kidney	NTPDase 1	vascular structures, including blood vessels of glomerular and peritubular capillaries	-vascular perfusion
	NTPDase 2	Bowman's Capsules	-vascular perfusion
	NTPDase 3	cortical and outer medullary collecting ducts	-vascular perfusion
	NTPDase 8	luminal side of porcine renal tubules	-vascular perfusion
Astrocytes	NTPDase 2	subventricular zone of the lateral ventricles and the dentate gyrus of the hippocampus	-alter their protein expression Profile

Stem cells in brain	NTPDase 2	subventricular zone	augment cell proliferation and control neurogenesis
Taste buds	NTPDase 2	Schwann cells	Regulator of taste Transmission
Immune system	NTPDase 1	natural killer cells, monocytes, dendritic cells, and activated T cells	-control of the cellular immune response -lymphocyte activation Marker

NTPDase 1 which is a well studied NTPDase, has a important role in the angiogenesis, vascular relaxation and permeability, macrophage function, thrombosis and tumor growth.[37-39] Apart from those mentioned in Table 1, NTPDase 3 is found in brain neurons, kidney, airways, reproductive and digestive systems, and pancreas.[40] NTPDase 8 has a limited tissue distribution and is expressed in the liver, kidney, and intestine.[38, 41]

The closely related NTPDase 1, NTPDase 2, NTPDase 3, and NTPDase 8 contain about 500 amino acid residues, and the molecular mass of the glycosylated monomers is about 70 to 80 kDa sharing approximately 40 % amino acid identity. They all contain two transmembrane domains (TMDs), and an extracellular loop containing the catalytic domain. The extracellular loop contains five apyrase-conserved regions (ACRs) and ten conserved cysteine residues. TMDs maintain catalytic activity, substrate specificity and anchor the protein to the membrane. Members of the *e*NTPDase family form oligomeric complexes and are N-glycosylated.[27, 42]

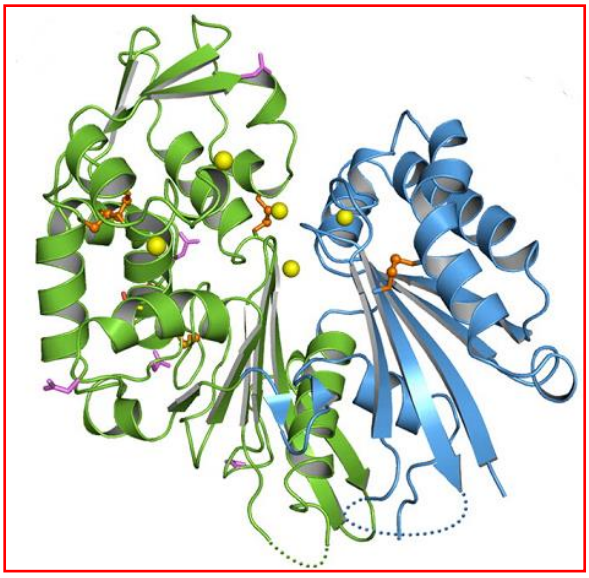

Figure 7. Schematic representation of the ecto-domain of rat NTPDase 1[27, 28]
(Domain I and domain II are represented in blue and green respectively; Disulfide bridges are shown in orange; N-glycosylation sites are shown in purple; five chloride ions are depicited in yellow; dotted lines represent unmodeled region)

Among the 5 ACRs, ACR1 and ACR4, and ACR3 and ACR5 form symmetry axis and connects the two domains (domain I and II). As per the published crystal structures,[27,28] the residues involved in water-mediated coordination of the metal ion are aspartic acid-45 and aspartic acid-201, binding of the substrate's phosphate tail are serine-48 to histidine-50, glycine-204 to serine-206, and positioning of the nucleophilic water is serine-206. ACR3 provides the catalytic base glutamic acid-165 which along with tryptophan-436 from ACR5 are involved in water-mediated metal ion binding.[43] ACR2 provides threonine-122, alanine-123, and arginine-126 for the substrate as well as cofactor binding and positioning of the nucleophile water.

Hydrolysis proceeds via an attack of a nucleophilic water on the terminal phosphate resulting in the increase in partial positive charge of the phosphorus by coordination of the metal ion. Upon nucleophilic attack, a trigonal planar transition state is formed. The two phosphate-binding loops (i.e. ACR1 and 4) provide proton-donating hydrogen bonds to stabilize the negative charge of the transition state.[38]

1.6.2. *Ecto*-nucleotide pyrophosphatase/phosphodiesterases

To date, seven *ecto*-nucleotide pyrophosphatase/phosphodiesterase subtypes (*e*NPP 1-7) were found to be expressed in vertebrates.[44] NPP 1–NPP 4 are classified as alkaline nucleotide pyrophosphatase (EC 3.6.1.9) and phosphodiesterase I (EC 3.1.4.1), and can only hydrolyze nucleotides.[45] They hydrolyze nucleoside triphosphates and diphosphates, NAD^+, FAD, UDP sugars, dinucleoside polyphosphates and synthetic substrates such as *p*-nitrophenyl thymidine monophosphate.[46, 47] NPP 2 hydrolyzes phospholipids and sphingosylphosphorylcholine but has low affinity for ATP which is an exception among the NPPs.[48, 49] *e*NPPs are the major enzymes responsible for the extracellular hydrolysis of dinucleoside polyphosphates.[50] They can also produce nucleotides as additional agonists of P2X and P2Y receptors as a result of hydrolysis of dinucleoside polyphosphates.[51] Nucleoside monophosphates such as AMP or UMP are not hydrolyzed. NPP 1–NPP 4 have a wide tissue distribution.[52] According to the different literatures the K_m values of *e*NPPs for ATP range between 17 and 300 μM.[23, 53]

Table 2. Members of the *e*NPP family with their cellular expression pattern and functions[53,54]

NPP type	Expressing cell type	Physiological function	Pathological function
NPP 1	Synoviocytes Chondrocytes Hepatocytes Plasmacytoma Osteoblasts	Nucleotide recycling, calcification	Ossification of posterior longitudinal ligament (OPLL), Calcium pyrophosphate dihydrate disease (CPPD disease), type 2 diabetes[55]
NPP 2	Osteosarcoma Synoviocytes Epithelial cells Neuroblastoma Mesenchymal progenitor cells Endothelial and smooth muscle cells	Calcification, regulation of cell motility	Increased tumor motility and invasion, angiogenesis
NPP 3	Vascular smooth muscle cells and Chondrocytes	Nucleotide recycling	Increased tumor invasion

NPP 4	Brain vascular endothelium	Inducing platelet aggregation	Stroke

Human NPP 1–NPP 3 contain 863–925 amino acid residues with a molecular mass of 115 to 125 kDa and shares 40–50 % identity. NPP 1 and NPP 3 contain a N-terminal transmembrane helix, a cytoplasmic domain, and a extracellular domain where as NPP 2 is a secreted protein and synthesized as a pre-pro-enzyme and contains C-terminal transmembrane helix.[48] NPP 1 and NPP 3 are homodimeric whereas NPP 2 is monomeric. The ecto-domains of NPP 1–3 consist of two short somatomedin B-like repeats of 40 to 50 amino acids, a central catalytic domain of approximately 400 amino acids, and a C-terminal nuclease like domain (NLD) of approximately 250 residues. The "EF hand" which is the Ca^{2+}-binding motif is essential for the catalytic activity in NPP 1 and NPP 3 but has less effect on the NPP 2. NPP 1–NPP 3 also contain two cysteine-rich tandem structures which is the protein interaction domains.[56]

1.6.3. Alkaline phosphatases

Alkaline phosphatases (APs) can hydrolyze extracellular ATP via ADP and AMP to adenosine sequentially so are included under *ecto*-nucleotidases.[57] APs are widely expressed in prokaryotes and eukaryotes and are found in every mammalian tissue as well as serum. They are located on endothelium, enterocytes, kidney tubules, biliary epithelium, mucosal surface of airways, embryonic stem cells, primordial stem cells, neural stem cells, and hair follicles.[58] APs are expressed in variety of tumors. APs have optimum activity at alkaline pH values of 9-10. All mammalian APs reveal broad substrate specificity and they can also catalyze the hydrolysis of phosphoric acid monoesters e.g. mineralization inhibitor PP_i and pyridoxal 5'-phosphate (PLP).[59]

Table 3. Member of APs with their expression pattern and physiological role[57-59]

APs subtype	**Human genes**	**Expression**	**Physiological role**
Tissue-nonspecific AP (TNAP)[60]	ALPL	Liver bone kidney	bone mineralization
Placental AP (PLAP)	ALPP	Syncytiotrophoblast tumor-cells	Unknown
Germ cell AP (GCAP)	ALPP2	Testis malignant trophoblasts testicular cancer	Unknown
Intestinal AP (IAP)	ALPI	Gut (microvillus membranes of enterocytes)	-intestinal absorption -preventing inflammation -homeostasis

APs are homodimeric proteins with a MW of about 80 kDa and behave as non-cooperative allosteric enzymes. The stability and catalytic properties of each monomer are controlled by the conformation of the second subunit. The catalytic site contains three metal ions, two Zn^{2+}, and one Mg^{2+}.[56] The activation takes place in two steps. First, the transporters stabilize the apoform of the enzyme then in a second step, Zn^{2+} is loaded onto the protein, converting it from the apo- to the holo-form and finally carried to the plasma membrane. All APs contain a signalling sequence of 17 to 21 amino acid residues, a glycosylphosphatidylinositol (GPI)-anchor, and five cysteine residues, of which four are involved in disulfide bonds formation.[61]

1.6.4. Additional nucleotide-metabolizing enzymes

Apart from these enzymes, there are some other enzymes that can also hydrolyze certain nucleotides.

Table 4. Additional nucleotide-metabolizing enzymes with substrate and physiological effect[23]

Enzymes	**Subsrate**	**Expression**	**Physiological effect**
Mammalian prostatic acid phosphatase	AMP ADP(minor extent)	dorsal spinal cord	antinociceptive effects (A_1-adenosine

(PAP)[62]			receptor activation)
Mammalian tartrate resistant acid phosphatase (TRAP)[63, 64]	Phosphate monoesters, nucleotides (ATP and ADP)	osteoclasts, osteoblasts	bone remodeling
Soluble calcium-activated nucleotidase (CAN)[65]	NDPs mainly UDP	testis, smooth muscle in stomach and small intestine, platelets, lungs, placenta	Hemostasis
Neural cell adhesion molecule (NCAM)	ATP	Glia, neurons, skeletal muscle, natural killer cells	Cell-cell adhesion, synaptic plasticity, neurite outgrowth, development of gut

2. *Ecto*-5′-nucleotidase

CD73 or *ecto*-5'-nucleotidase (*e*N, EC 3.1.3.5) is a Zn^{2+}-binding glycosylphosphatidylinositol (GPI)-anchored homodimeric protein, with its catalytic domain facing the extracellular medium. Therefore it belongs to the group of *ecto*-nucleotidases.[23] It is found both in membrane-anchored and soluble forms. *e*N hydrolyzes ribo- and deoxyribonucleoside 5′-monophosphates but the ribonucleotide AMP, the principal substrate of *e*N, is the most effectively hydrolyzed one.[66] K_m values for AMP range between 1-50 μM.[67] Human *e*N is encoded by the NT5E gene and can hydrolyze nicotinamide mononucleotide and NAD^+ to a minor extent. *e*N has been described to exist in both, catalytically active and inactive forms. *e*N is the major AMP hydrolyzing *ecto*-nucleotidase and the production of extracellular adenosine from extracellular AMP is its major function. *e*N activity is also controlled by a feedback mechanism depending on the extracellular level of nucleotides and adenosine. The adenosine formed activates specific G protein-coupled adenosine (P1) receptors (A_1, A_{2A}, A_{2B}, A_3).[23]*e*N is involved in cellular reuptake and purine salvage of adenosine. *e*N has a broad tissue distribution, and it is expressed by subpopulations of human T and B lymphocytes and also by a variety of tumor cells.[68, 69] ATP and ADP are

competitive inhibitors of *e*N with K_i values in the low micromolar range. ATP and ADP, despite being nucleotides, bind to the catalytic site of the enzyme without being hydrolyzed.[23]

2.1. General properties of *ecto*-5'-nucleotidase

Ecto-5'-nucleotidase is a well studied *ecto*-nucleotidase. It was first cloned from rat, human placenta, and the electric ray (Torpedo electric organ), and the *c*DNA sequence of a different mammalian species has also been identified.[70] The mouse *e*N cDNA is 86 and 92 % identical to the human and rat *c*DNAs, respectively. The apparent molecular mass of mammalian *e*N is 60–80 kDa for the monomer and 160 kDa for the dimer. A glycosylphosphatidylinositol (GPI) anchor is attached to the hydrophobic C-terminal fragment and is linked to the serine-523 residue which is conserved in all species. GPI anchors impart a variety of functional properties including lateral motility, lipid clustering, transmembrane signaling and cellular sorting. Phylogenetically, *e*N is grouped into the calcineurin superfamily of dinuclear metallophosphatases with plenty members in prokaryotes and eukaryotes. The bacterial *e*N reveals a broader spectrum of substrate specificity as compared to the murine and human orthologs.[67]

2.2. Protein and crystal structure of *ecto*-5'-nucleotidase

Ecto-5'-nucleotidase consists of two domains (N-terminal domain and C-terminal domain), which are linked by a long α-helix. The N-terminal domain (residues 25 to 342) binds two metal ions and also confers the phosphohydrolase activity. The C-terminal domain (residues 362 to 550) has a GPI-anchor. This domain is responsible for the substrate specificity and also provides sites for binding the nucleotide substrates. The active site is located in a space between the two domains.[71]

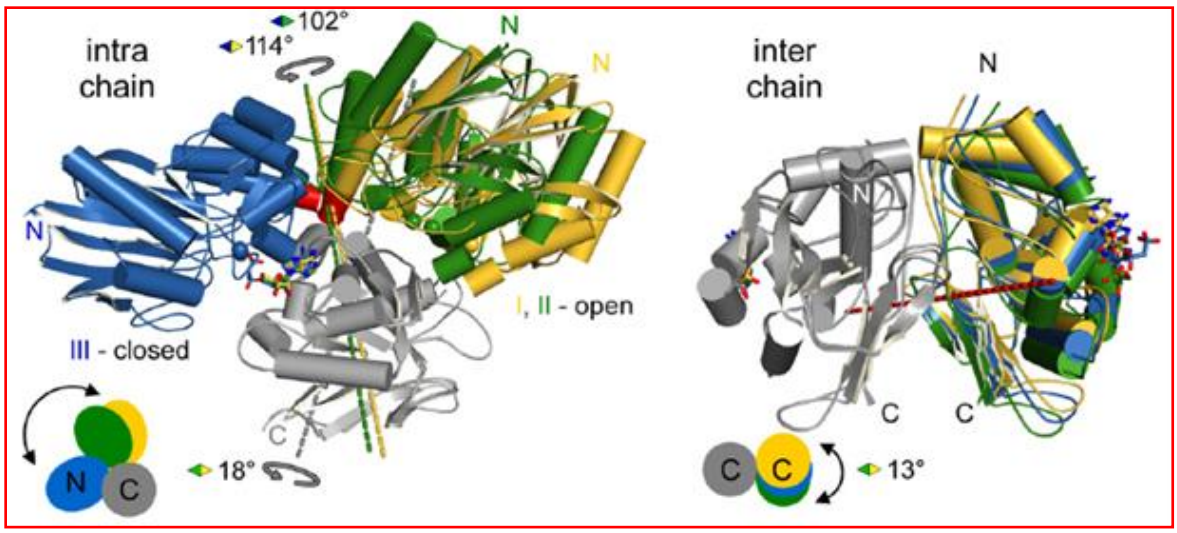

Figure 8. Domain movements of human *e*N[71]
(Figure on the left shows active site closure movement of *e*N and figure on the right shows dimerization interface. C-terminal domain are shown in grey; two open conformations are shown by yellow and green in the left figure; closed conformation is shown in blue; respective colored dashed line along with dashed red line represents rotation axis; hinge residue are represented by red color)

Ecto-5'-nucleotidase has been crystallized in both open and closed form and undergoes a large and unique domain motion. In the open form, the nucleotide binding pocket is accessible for substrate binding and product leaving and the substrate AMP binds at a distance of about 25 Å away from the di-metal site. In the closed conformation, the ADP analogue α,β-methylene-ADP (AOPCP) which is also the inhibitor of *e*N, binds as shown in Figure 8. In both open and closed form, the adenosine moiety of the substrate binds to the same binding site of the C-terminal domain. *e*N shows a hinge-bending domain movement which resembles a ball- and-socket motion in catalysis. The C-terminal domain mimics the ball rotating around its center, supported by bending residues 352–364, and resulting in conformational switch between the open and closed forms.[72]

2.3. Active site and catalytic mechanism of *ecto*-5'-nucleotidase

The crystal structure of AOPCP (*α,β*-methylene-ADP) with *e*N in the closed form provides details of substrate binding and catalysis mechanism. *e*N is a divalent enzyme and contains two

metal ions (viz. 1 and 2) in the active site approximately 3.3 Å apart from each other. Unlike metal ion 2, residues of the coordination sphere of the metal ion 1 are not conserved in *E. coli* and human, whereas Q254 (glutamine-254) of the *E. coli* enzyme is replaced by an asparagine residue (N245) in the human enzyme. The asparagine-254 residue in the human *e*N is shorter, therefore it binds to a water molecule which in turn is coordinated to the metal ion.[73]

AOPCP binds to the active site between both domains, and the adenosine moiety is bound by the C-terminal domain, whereas the terminal part of the methylene(bisphosphonic acid) is bounded to the N-terminal domain. The adenine-base formed hydrophobic stacking interaction between two phenylalanine residues. The N1 nitrogen of the adenine ring formed a hydrogen bond to the asparagine-431 in the *E. coli* which is replaced by glycine-419 in the human. The ribose group is coordinated by aspartic acid-504, glycine-458, and arginine-410. Arginine-375 and arginine-379 bind the α-phosphate group of AOPCP. The *β*-phosphate group of AOPCP binds to arginine-410 of C-terminal domain as well as to asparagine-116 and histidine-117 of N-terminal domain.[71]

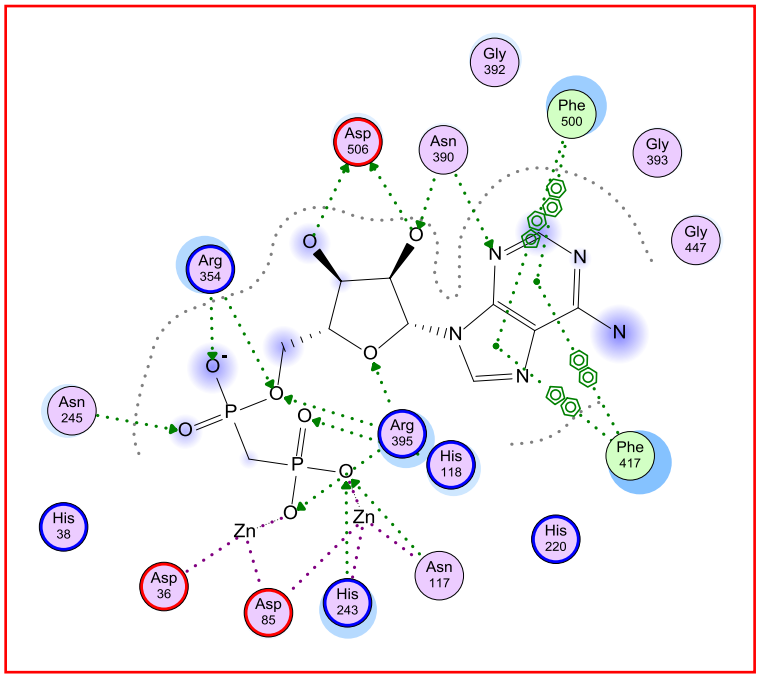

Figure 9. Binding of AOPCP to human *e*N in the closed form.[71]

The terminal phosphate group (β) of AOPCP is bound to the amino acids of N-terminal domain via hydrogen bonds to and is bridged to the metal ion 1 by a water molecule. One oxygen atom of the terminal phosphate group (β) is directly coordinated to the metal ion 2 because of which phosphate group is polarized for nucleophilic attack, with the neucleophile being the water molecule terminally coordinated to the metal ion 1. Coordination to the metal ion lowers the pK_a value of the water molecule resulting its deprotonation to a hydroxide ion even at neutral pH. The coordination results in the transition state stabilized by the two metal ions, as well as by histidine-117 and arginine-410. For catalysis of AMP hydrolysis protonation of the alkoxide leaving group is facilitated by a water molecule resulting the direct transfer of the phosphoryl group to the water nucleophile without the formation of a covalent intermediate.[23, 71, 74]

2.4. Physiological functions of the *ecto*-5'-nucleotidase

The broad tissue distribution of *e*N contributes to its involvement in various physiological and pathological functions. The physiology of *e*N in various pathological conditions is related to the formation of extracellular adenosine. *e*N is overexpressed in inflammation. The phosphorylated A_{2A} receptor agonist 2-cyclohexylethylthio-AMP is a potent prodrug for treating inflammation where *e*N expression is preferentially activated.[66, 75] *e*N is involved in many patho-physiological roles like endothelial barrier function and fluid transport, hypoxia and the airways, ischemia, the cardiovascular system (CVS), lung, liver, and kidney function, immunity and inflammation, leucocyte trafficking, the nervous system, nociception and cancer immunity and metastasis.[76-78]

2.4.1. Ischemic-reperfusion injury of the lungs and hypoxia

Ischemic-reperfusion injury is common in the lung transplanted patient. Ischemic-reperfusion injury is the tissue damage caused by returning blood supply to the tissue after a brief period of ischemia or lack of oxygen. CD73 (*e*N) is expressed on endothelial cells and lymphocytes of the

lungs.[79] *e*N decreases proinflammatory adenine nucleotides and generates anti-inflammatory and immunosuppressive adenosine. Thus *e*N plays an important role as an immunoregulator. The stimulation of A_{2A} receptors by adenosine released from *e*N activity decreases the adhesion of leukocytes and reduces of endothelial-leukocyte interaction, thus decreasing the generation of injurious free radical like superoxides and subsequently reducing ischemia.[80]

Hypoxia is the condition where there is lack of adequate oxygen supply in the whole body or a part of the body. Anoxia is a more severe hypoxic condition where there is complete deprivation of oxygen. Adenosine generated by *e*N plays an important role in decreasing hypoxia by increasing cerebral blood flow and cerebrovascular resistance. Hypoxia damages the blood brain barrier (BBB) leading to vasogenic brain edema. In the central nervous system (CNS) the adenosine concentration is dramatically increased up to 100-fold because of *e*N upregulation. During brain ischemia adenosine produced by *e*N in brain microvessel endothelial cells exerts neuroprotective effect in the brain maintained by A_1 receptors. Stimulation of A_1 receptors also prevents brain edema by releasing glutamate (excitatory neurotransmitter) and increases neuronal activity. [81, 82]

2.4.2. Inflammation

Inflammation is a protective phenomena on the vascular tissue in response to a harmful stimulus, such as pathogens, irritants or damaged cells. *e*N is expressed widely in immune cells and produces inflammation in several disease models. The role of *e*N in several inflammation models has been studied e.g. in chronic vascular inflammation disease atherosclorosis.[83] This is an inflammatory disease produced by intense immunological activity resulting in the formation of atherosclerotic plaques which contain mainly neutrophil and T-cells.[84] During inflammation there is massive accumulation of ATP which trigger pro-inflammatory responses. There is

negative feedback inhibition by over expression of NTPDase 1 and *e*N in neutrophil and T-cells. Over expression of NTPDase 1 converts ATP to AMP, and over expression of *e*N in T regulatory (Treg) cells and uncommitted primed precursors Th (Thpp) cells generates adenosine. Thus generated adenosine inhibits proliferation and cytokine secretion of Th1 effector cells resulting in the suppression of interferon gamma (INF-γ) and tumor necrosis factor alpha (TFN-α) production through A_{2A} receptors thereby depressing the immune cell activity and promoting inflammation.[85-89]

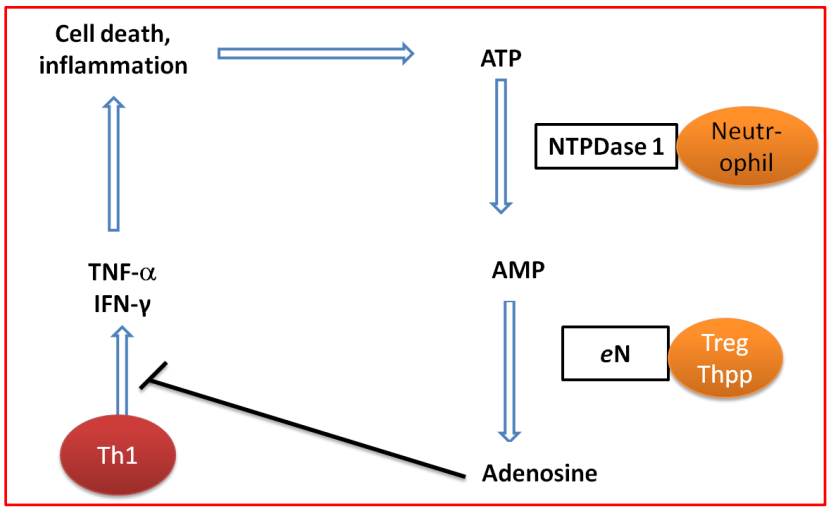

Figure 10. Immunomodualation by NTPDase 1 and *e*N in tandem[90]
(Thpp: uncommitted primed precursors Th; Treg: T regulatory cells; IFN-γ: interferon gamma; TFN-α: tumor necrosis factor alpha)

2.4.3. Antinociceptive effects

Nociception is the ability of the body to sense potential harm. Nociceptors or pain receptors can sense pain as a result of tissue damage. *e*N is expressed in peptidergic and non-peptidergic nociception (pain sensing) neurons and their axon terminals in spinal cord and spine. *e*N can be used for the treatment of chronic pain involving A_1-receptors. *e*N generates adenosine, which might have A_1-receptor dependent antinociception effects.[91]

2.4.4. Platelet function

Nucleotides metabolism are important in proper maintaining of platelet function. Certain degree of platelet dysfunction resulting from reduction of bleeding time has been observed in *e*N-deficient mice. In *e*N-deficient mice it has also been observed that platelet cAMP was reduced because of decrease in the circulating adenosine.[78]

2.4.5. Renal function

Adenosine is important for the maintaining of proper glomerular filtration involving tubuloglomerular feedback mechanism. In *e*N-deficient mice tubuloglomerular feedback mechanism was found to be very low with reduced nephron glomerular filteration rates as compared to wild types. It was also found that the decrease was due to the reduction in extracellular adenosine concentration not due to the defects in adenosine receptor activation.[78]

2.4.6. Cancer

Cancer, also known as malignant tumor, comprises diseases with abnormal cell growth with its potential to invade or spread to other parts of the body. *e*N is involved in metastasis of tumor as well as immunity. Extracellular adenosine induces potent immunosuppressive effect via adenosine receptors. [92] Several studies in cancer models have indicated that an increase in expression of *e*N is associated with tumor invasiveness and metastasis.[93] *e*N activity is increased in human colon adenocarcinoma, breast cancer, gastric cancer, pancrese cancer and lymphoma.[95] Studies have shown that *e*N is increased in many breast cancers, promotes tumor growth and also serve as a marker of breast cancer progression.[96] As progression of tumor depends on vasodilatation, angiogenesis, cytoprotective and immunosuppressive activities, *e*N promotes cancer progression via activation of A_{2B} adenosine receptor. In breast cancer, at early stage extradiol down regulates the expression of *e*N through estrogen receptor. But in advance stage

there is loss of estrogen receptor (ER) expression because of increase in *e*N expression and resulting in increase in extracellular adenosine concentration which can promotes tumor directly. Targeted blockade of *e*N using monoclonal antibody, siRNA[102] and *e*N inhibitors inhibit the metastatic potential of tumor cell. To evaluate the therapeutic potential of *e*N inhibitors, studies are also focused on *e*N knockout mice. Tumor growth is retarded in *e*N knockout mice. *e*N deficiency also suppresses prostate tumorigenesis in TRAMP transgenic mice (transgenic adenocarcinoma of the mouse prostate). High *e*N expression has been reported in triple-negative breast cancers (TNBC), and it has also been demonstrated that targeted blockade of CD73 significantly prolonged the survival in anthracycline-resistant animal models of cancer.[97]

II. Literature review

3. Medicinal Chemistry of *ecto*-5'-nucleotidase inhibitors

Ecto-5'-nucleotidase inhibitors have potential as novel drugs, e.g. for cancer therapy.[97-104] *e*N inhibitors reduce extracellular adenosine levels, resulting in an indirect blockade of adenosine (P1) receptor activation. In contrast to direct receptor ligand interaction, enzyme inhibitors are indirect antagonists, which will exhibit site- and event-specific effects since they are only active in the presence of enzyme, substrate, and receptor. ADP and ATP are competitive inhibitors of *e*N. However these inhibitors are not suitable as drugs, since they themselves are subjected to enzymatic degradation by *e*NTPDase, *e*NPPs and/or non-specific alkaline phosphatases. [{5-(6-aminopurin-9-yl)-3,4-dihydroxyoxolan-2-yl}methoxy-hydroxyphosphoryl]methylphosphonic acid (α,β-Methylene-ADP, AOPCP), an analog of ADP, is one of the more potent, competitive inhibitors of *e*N. In addition to nucleotide analogues, only anthraquinones, sulfonamides, sulfonic acid derivatives, some polyoxometalates (POMs) and some natural polyphenol derivatives are currently known to potently inhibit *e*N. Among them the most potent inhibitors are anthraquinone derivatives, but their selectivity versus NTPDases as well as P2Y receptor subtype is limited.[38, 105-115]

3.1. Adenine nucleotide derivatives as *ecto*-5'-nucleotidase inhibitors

Adenine nucleotide derivatives were the first *e*N inhibitors to be discovered. ATP (**1**) and ADP (**2**) despite being the inhibitors of *e*N are physiological nucleotides.[105] AOPCP (**6**) has a K_i value of 850 and 870 nM for Torpedo marmorata and, rat *e*N, respectively. The inhibitors ATP, ADP and AOPCP are not highly selective. ATP and ADP are activators of various P2 purinergic receptors. Moreover NTPDases, NPPs and APs can hydrolyse ATP and ADP. AOPCP has been

reported to also block NPP 1 with a K_i value of **16.5** ± 3.2 µM.[106] $P2Y_1$ and $P2Y_{12}$ are ADP-activated P2Y receptors. ADP has EC_{50} values of 289 and 133 nM at $P2Y_1$ and $P2Y_{12}$ respectively.[107] Various ATP derivatives (**7-9**) have moderate activity as *e*N inhibitors (see Table 5).[108-110]

Table 5. Activity of adenine nucleotide derivatives at rat *e*N[109-110]

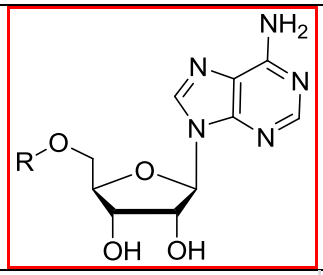

Compd.	R	rat *e*N K_i ± SEM (µM)
1 **ATP**	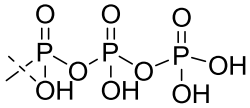	**8.90** ± 0.36 (pH 7.4)[a] **10.6** ± 4.0 (pH 5.6)[b] **70.8** ± 8.7 (pH 7.4)[b]
2 **ADP**	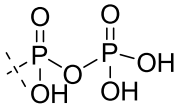	**0.91** ± 0.01 (pH 7.4)[a] **0.51** ± 0.06 (pH 5.6)[b] **1.20** ± 0.01 (pH 7.4)[b]
6 **AOPCP**	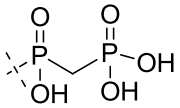	**0.87** ± 0.02 (pH 7.4)[a] **0.073** ± 0.0014 (pH 5.6)[b] **0.028** ± 0.0057 (pH 7.4)[b]
7 **APPNHP**	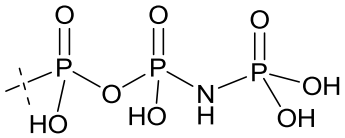	54 (pH 7.4)[a] > 20
8 **β, γ-Me-ATP**	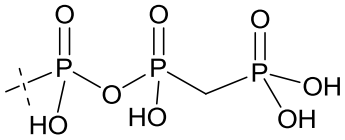	56 (pH 7.4)[a] > 20
9 **α, β-Me-ATP**	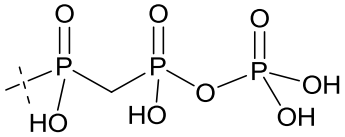	73 (pH 7.4)[a] > 20

Capillary electrophoresis assay: [a]substrate concentration 0.5 mM AMP, K_m of AMP = 25 µM, inhibitor concentration is 100 µM. [b]substrate concentration 0.4 mM AMP, K_m of AMP = 45.9 µM at pH 5.6 and 45.2 at pH 7.4.

3.2. Uridine nucleotide mimetics as *ecto*-5'-nucleotidase inhibitors

Brunschweiger *et al.* described uracil and 5,6-dihydrouracil nucleotide mimetics as potent inhibitors of *e*N.[109] These molecules were uracil derivatives which contain terminal dicarboxylate groups were linked via alkyl linkers and amide bonds to the 5'-position of the nucleoside. 5,6-Dihydrouracil derivatives were more potent as compared to uracil and adenosine derivatives. Among them the most potent was compound **11** with a IC_{50} value of 1340 nM at pH 5.6. The compound exhibits a non-competitive mechanism of inhibition.[110] Compound **11** was an activator of *e*N at physiological pH. This property of compound **11** may be used for the development of pH-dependent therapeutics as many tumor cells have lower pH values than normal cells, where **11** may act as inhibitor. Acid ester derivatives were inactive at *e*N indicating the free carboxylate groups were required. Inhibitor **10** and **11** were selective against NTPDase 1, $hP2Y_4$, $rP2Y_6$, and $hP2Y_{12}$.[109]

Table 6. Potency of uridine derivatives at rat *e*N[110]

Compd.	**Structure**	**rat *e*N** IC_{50} ± SEM (µM)
10	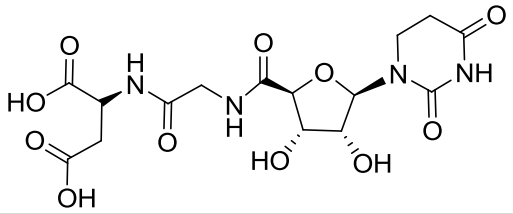	**81.40** ± 20.7 (pH 5.6)[a] >> 25 (-10.0 ± 4.2) (pH 7.4)[a]
11 PSB-11532	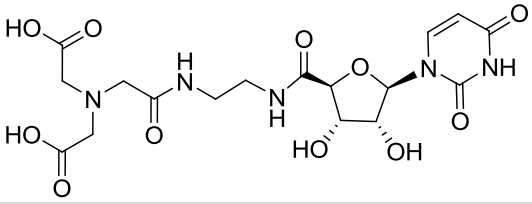	**13.4** ± 1.90 (pH 5.6)[a] > 25 (-66.2 ± 6.0) (pH 7.4)[a] inhibitor at pH 5.6 and activator at pH 7.4
12	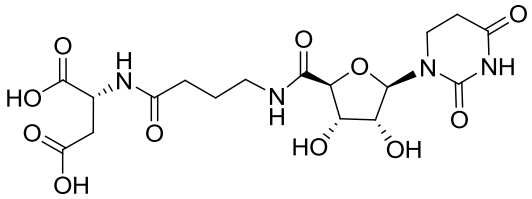	**72.5** ± 10.3 (pH 5.6)[a] >> 25 (11.5 ± 7.5) (pH 7.4)[a]

[a]Capillary electrophoreisis assay: substrate concentration 0.4 mM AMP, K_m of AMP = 45.9 µM. Effects were normalized to the signal induced by AMP.[110]

3.3. Anthraquinone derivatives as *ecto*-5'-nucleotidase inhibitors

Baqi *et al.* discovered anilinoanthraquinone derivatives related to the dye Reactive Blue-2 as a new class of *e*N inhibitors.[111] These compounds exhibit a competitive mechanism of inhibition. The most potent compound was **13** with activity in the nano-molar range. These compounds were optimized to obtain more potent and selective *e*N inhibitors. Compound **13** had a selectivity of about 150-fold versus NTPDases as well as P2Y ($P2Y_2$, $P2Y_4$, $P2Y_6$, $P2Y_{12}$) receptor subtypes. During the structure-activity relationship study it was found that a sulfonate group at position/2 of the anthraquinone scaffold appeared to be essential for *e*N inhibitory activity. The amino group at the 4-position of anthraquinone was substituted by various lipophilic groups like benzyl, phenyl, substituted phenyl, cycloalkyl residues etc. Among them anthracenyl substitution was the best, since anthracene derivatives probably fit best into the hydrophobic pocket of *e*N and forms aromatic stacking interactions with aromatic protein residues.[111]

Table 7. Potency of anthraquinone derivative at rat *e*N[111]

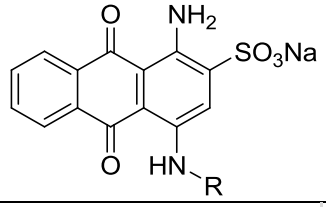

Compd.	R	rat *e*N K_i ± SEM (nM)
13	2-anthracenyl	**150** ± 0.20[a]
14	2-carboxy-5-flourophenyl	**260** ± 0.10[a]
15	4-aminophenyl	**297** ± 0.90[a]

16	4-hydroxyphenyl	**620** ± 1.50[a]

[a]Capillary electrophoreisis assay: substrate concentration 0.5 mM AMP, K_m of AMP = 25 µM. Effects were normalized to the signal induced by AMP, corresponding to a maximal response at the enzyme.[111]

3.4. Sulfonamide derivatives as *ecto*-5'-nucleotidase inhibitors

Ripphausen, Freundlieb *et al.* performed docking analysis (structure-based virtual screening approach augmented by chemical similarity searching) of 372 compounds selected from the ZINC-8 database, and a subset of 128 compounds was selected based on certain criteria.[112] Out of these compounds 51 commercially available compound were procured and tested in *e*N assays. Among them 13 compounds were found with *e*N inhibition activity. Compound **17 (**6-chloro-2-oxo-*N*-(4-sulfamoylphenyl)-2*H*-chromene-3-carboxylic acid amide), showed an IC_{50} value of 1.90 µM and was the most potent inhibitor of the series. These compounds exhibit a competitive inhibition mechanism. Moreover, these structurally diverse compounds show drug-like property. The structure of these compounds was mapped with other nucleotide-based inhibitors and observed to contain two moieties, first a nucleoside-mimicking heterocycle or a substituted benzene ring and second a sulfonamide group that very likely interacts with an active site zinc cation, like phosphate, phosphonate or sulfonate groups in other *e*N inhibitors. An amide, a hydrazone, or a urea linker connected the both moieties.[112]

Table 8. Potency of sulfonamide derivatives as inhibitors of rat *e*N[112]

Compd.	**Structure**	**rat *e*N** IC_{50} ± SEM (nM)
17	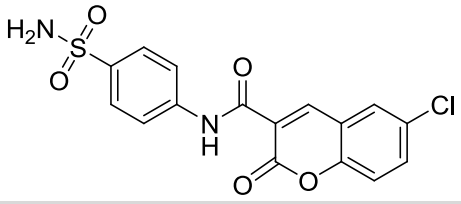	**1900** ± 2.10[a]

18	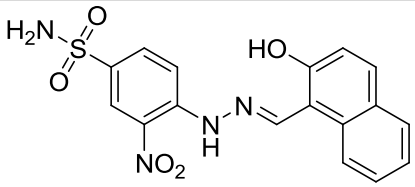	**6540** ± 2.60[a]
19	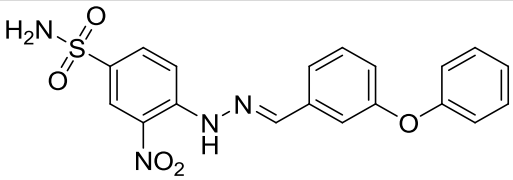	**3900** ± 1.46[a]
20	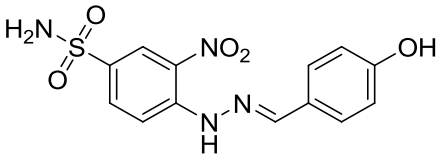	**8030** ± 6.10[a]

[a]Radiometric assay: Effects were normalized to the signal induced by 5 µM [^{3}H]AMP, corresponding to a maximal response at the enzyme.

3.5. Sulfonic acid derivatives as *ecto*-5'-nucleotidase inhibitors

Iqbal *et al.* discovered a series of simple sulfonic acid derivatives as moderately potent *e*N inhibitors.[113] About thirteen molecules were tested to evaluate their inhibitory potency against both rat and human enzyme. Some compounds were found to be moderately potent inhibitors of both, rat and human enzyme. All compound showed higher activity in human as compared to the rat enzyme. Compound **21** was the most potent inhibitor for both the rat and human enzyme. The structure-activity analysis suggests that amino, hydroxyl and sulfonic acid groups are important for the activity. Compound **21** contains all three groups attached to the naphthalene ring system.[113]

Table 9. Activity of sulfonic acid derivatives at rat *e*N[113]

Compd.	**Structure**	***e*N** K_i ± SEM (nM)
21	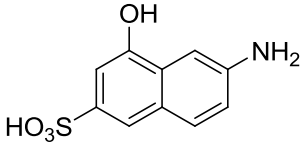	**1320** ± 0.90 (human)[a] **10400** ± 33 (rat)[a]

22	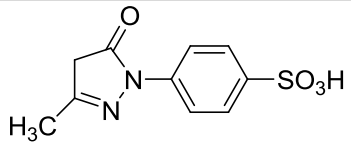	**6100** ± 3.00 (human)[a] **44300** ± 10.0 (rat)[a]
23	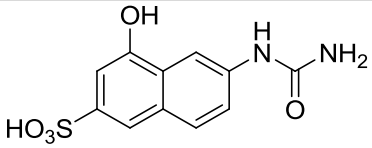	**30500** ± 21.0 (human)[a] > 25000 (rat)[a]
24	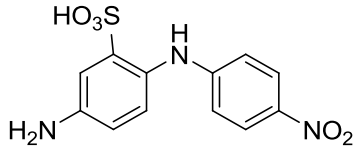	**47600** ± 16.0 (human)[a] **72900** ± 13.0 (rat)[a]

[a]Capillary electrophoreisis assay: Substrate concentration 0.5 mM AMP, K_m of AMP = 25 µM, inhibitor concentration is 100 µM.

3.6. Various *ecto*-5'-nucleotidase inhibitors

Various polyphenols isolated from the seed of the betel palm (*Areca catechu*) showed some *e*N inhibition activity. A small series of polyphenolic compounds were tested, including NPF-86IA, NPF-86IB, NPF-86IIA and NPF-86IIB. They were found to be the non-competitive inhibitors in the low micro-molar range.[114] The flavonoid quercetin was found to be an inhibitor of *e*N expressed on the human U138MG glioma cell line.[115] Its IC_{50} was determined to be 45300 nM. Similarly concanavalin A (ConA), a lectin from jack-bean (*Canavalia ensiformis*) also inhibited *e*N of intact C6 glioma cells. An IC_{50} was obtained of 20 µg of ConA/mL. But complete inhibition was not observed even at high concentrations. Recently Lee, Fiene *et al.* had identified rhenium and tungsten-based POMs as inhibitors of *e*N. $K_6H_2[TiW_{11}CoO_{40}]\cdot 13H_2O$, $K_4[(Re_6S_8)(OH)_6]\cdot 8H_2O$ and $K_4[(Re_6S_8)(HCOO)_6]$ had IC_{50} values of 14.1, 11.8, 4.57 µM respectively at rat *e*N. These POMs inhibitors had non-competitive inhibition mechanism.[116]

4. Assays of *ecto*-5'-nucleotidase

There are several methods to assay 5'-nucleotidase, involving luminescent, spectroscopic and radiometric techniques. But some of these methodologies have drawbacks. These methods are time-consuming, possess low sensitivity, and require high substrate concentration. Some methods are only suitable for water-soluble inhibitors. [117-121] The conventional methods to assay *e*N include

- measurement of free phosphate by using a dye such as malachite green
- measurement and quantification of adenosine produced by chromatographic techniques such as high performance liquid chromatography (HPLC) or by capillary electrophoresis.

Phosphate-containing and colored compounds cannot be detected in the malachite green assay. HPLC and capillary electrophoresis techniques are relatively time-consuming.[118]

4.1. Malachite green assay

It is the most widely used colorimetric method for *e*N assays. Malachite green is the basic dye and its reaction with inorganic phosphate released from the substrate (AMP) hydrolysis because of *e*N activity formed the malachite green-phosphomolybdate complex in presence of sodium molybdate. This complex has strong absorbance band and can be measured at 620-650 nM.[120] This assay procedure ensured a color change (yellow to greenish blue) during the course of the reaction which can be visible even through naked eye. This assay is generally performed according to the method developed by Baykov *et al.* for orthophosphate determination.[121] Since the molar absorption coefficient of the malachite green-phosphomolybdate complex is higher, the absorbance can be measured more conveniently as compared to other colorimetric methods.

By this method non-coloring substances can be efficiently measured. This method is simple and highly sensitive and even can detect 10^{-5} IU of the enzyme.[120, 121]

4.2. Capillary electrophoresis assay

Iqbal *et al.* developed a capillary electrophoresis (CE)-based electrophoretically mediated microanalysis assay method.[108] In this method, enzyme and substrate with or without inhibitor are incubated, followed by electrophoretic separation of products formed. For determing K_m and V_{max}, 500 µM of AMP as substrate was dissolved in the reaction mixture and the reaction was initiated by adding 10 µL of enzyme at 37^{o}C for 15 min. After stopping the reaction, 50 µL of reaction mixture was transferred to a capillary electrophoresis vial in the off-line capillary method, or in the online method the whole reaction was carried out in the capillary along with quantification. The K_m value determined for the online and offline methods were similar, 25 µM and 23 µM, respectively, for AMP using recombinant rat *e*N. This CE-based assay is a powerful method for screening *e*N inhibitors as it could test one compound in only 6 minutes. This method could also be performed in the 96-well plate format making it suitable for high-through put screening of inhibitors.[108]

4.3. Luciferase-based assay

Sachsenmeier *et al.* developed a method which indirectly measures AMP metabolism in a luciferase-based system.[122] This method has the advantage, that it can also be used for inhibitors containing phosphate in contrast to the malachite green assay. The assay uses a luciferase-based assay reagent, the Promega CellTiter-Glo (CTG) kit. The kit converts ATP to AMP and diphosphate. But the presence of AMP in the reaction mixture inhibits luciferase reaction and it is indicated by the emission of little or no light. Addition of soluble recombinant *e*N to a reaction mixture of ATP and AMP in the buffer, resulted the conversion of AMP to adenosine. The

hydrolysis of AMP leads to the whole or partial rescue of AMP-mediated inhibition of the ATP reaction. The *e*N enzyme activity is measured as the resultant increase in ATP detection which is directly proportional to light detected in the CTG assay. The standardized parmeters for the assay includes 100 µM ATP, 30 min of incubation time, and 300 ng/mL of enzyme for the recombinant human *e*N. This assay is high-throughput compatible and was validated with anti-*e*N antibody.[122]

4.4. Radiometric assay

Freundlieb *et al.* developed a new, highly sensitive *e*N assay method that uses [^{3}H]adenosine-5'-monophosphate (AMP) as a substrate.[118] The reaction product [^{3}H]adenosine was separated from [^{3}H]AMP by precipitation of the latter with lanthanum chloride. The filtrate was collected by filtration through glass fiber filters. It was further quantified in the scintillation counting by adding scintillation cocktail. Series of experiments were done to optimize various assay parameters for recombinant rat *e*N. The optimized parameters were 5 µM AMP as a substrate, 0.3 µg/mL enzyme, and 25 min of incubation time. The determined K_m value was 59 µM for AMP. For further validation of the assay, the inhibitory effects of known competitive inhibitors, AOPCP and ADP, were determined. The assay validation demonstrated its suitability for high-throughput screening. Advantages of the new assay include a very low limit of detection (LOD) of 0.03 µM for adenosine, which was much lower than that of all other assay methods. Moreover, this assay does not interfere with colored compounds or inorganic phosphate.[118]

5. Aim of the project

A major drawback of *e*N inhibitors discovered till now is their moderate potency and selectivity and/or the fact that they are highly polar since they contain acidic residues. Some of them, e.g. nucloeotides, are presumably not highly stable, susceptible to being hydrolyzed by physiological enzymes such as *ecto*-nucleotidases and phosphatases. The number of studies on structure-activity relationships (SARs) of *e*N inhibitors is very limited. AOPCP has relatively high chemical and metabolic stability as compared to ADP. The newly synthesized *e*N inhibitors should have selectivity vs. P1 and P2 receptors, high potency, selectivity, suitable pharmacokinetic properties and high chemical and enzymatic stability. AOPCP is one of the most potent *e*N inhibitors so far with K_i value of 0.87 μM.[108] Our goal is to synthesize selective *e*N inhibitors derived from AOPCP, which are more potent and more stable *in-vivo* in comparison to the lead structure.

5.1. Design and synthesis of adenine-base modified analogues of AOPCP

In the present study we designed and synthesized variety of base-modified analogues of AOPCP by introducing substituent at the 2-, 6- and 8-position of AOPCP. Furthermore, we planned to combine the best functionalities in order to obtain more potent derivatives. Simultaneously, we planned to enhance the metabolic stability and selectivity by synthesizing N^6-disubstituted analogues as well as 6-O- or 6-S-analogues. The structures of the target compounds are depicted in Figure 11.

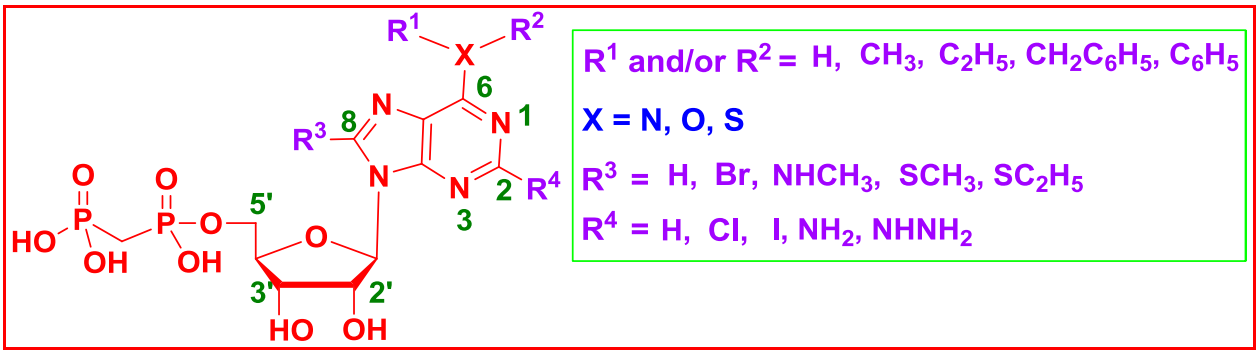

Figure 11. Structures of base-modified target compounds

For these newly synthesized analogues we used the radiometric *e*N assay at rat *e*N to pharmacologically characterize and to improve the potency of newly synthesized analogues. AOPCP analogues appear to have advantages: though having ADP-mimetic functional groups they do not potently activate any of the P2 receptor subtypes, as well as AOPCP also has at least some selectivity versus other *ecto*-nucleotidases.

5.2. Design and synthesis of side-chain-modified analogues of AOPCP

As a further part of this project we planned to modify the methylenebis(phosphonic acid) side chain of AOPCP in order to obtain more potent and selective analogues. Several substituted bis(phosphonic acid) derivatives are commercially available or can be synthesized, and we planned to combine those with adenosine at the 5'-position. Target structures are depicted in Figure 12.

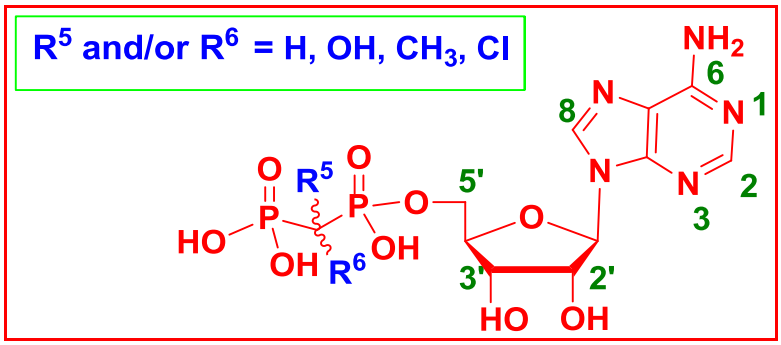

Figure 12. Structures of side chain-modified target compounds

5.3. Metabolic stability studies of selected potent AOPCP derivatives and analogues

Selected potent AOPCP derivatives and analogues were to be further investigated for their stability, (i) in rat liver microsomes and (ii) human blood, in order to investigate potential metabolic degradation by liver enzymes and plasma, respectively.

6. Results and discussion - part I: chemical synthesis

For the preparation of the target compounds, a convergent synthetic strategy was applied which involves first the synthesis of the intermediate nucleosides followed by their phosphorylation to give the desired nucelotides. Different purine nucleosides were synthesized with substituents in the 2-, 6- and 8-position of the purine ring. Progressive structural modification of the compounds was based on the biological screening results so as to synthesize more potent and selective derivatives with improved pharmacokinetic properties.

6.1. N^6-Mono- and dialkyl-or aryl-substituted adenosine-5′-O-[(phosphonomethyl)phosphonic acid] derivatives (53-76)

N^6-Mono- and dialkyl- or aryl-substituted adenosine-5′-*O*-[(phosphonomethyl)phosphonic acid]s were prepared by phosphorylation of 6-substituted purine nucleosides (**29-48**).

6.1.1. Synthesis of (intermediate) 6-substituted nucleosides (29-48)

There are different methods for the synthesis of N^6-mono- and dialkyl- or aryl-substituted adenosine derivatives (**29-48**).[123] The most common method is the substitution of 6-halopurine ribosides with amines. Some 6-halopurine ribosides like 6-chloropurine riboside (**28**) are commercially available, but expensive. So, the reaction was started from commercially available inosine (**25**). The method for the synthesis of 6-substituted purine-nucleosides[124] involves four steps:

- synthesis of 2′, 3′,5′-tri-*O*-acetylinosine (**26**)
- synthesis of 6-chloro-2′, 3′,5′-tri-*O*-acetylinosine (**27**)
- synthesis of 6-chloropurine riboside (**28**)
- synthesis of N^6-substituted purine riboside derivatives (**29-48**)

6.1.1.1. Synthesis of 2′,3′,5′-tri-*O*-acetylinosine

6-Chloroadenosine was synthesized from inosine according to a reported procedure with little modification (Schemes 1-3).[124-125] The chlorination of the keto-functional group at the 6-position of inosine requires protection at the 2′-, 3′- and 5′-hydroxyl groups as they are all susceptible for chlorination. There are several reported protecting groups such as (2′,3′,5′-*O*-acetyl), (2′,3′,5′-*O*-phenyl), (2′,3′,5′-*O*-benzyl), (2′,3′-acetonide), (2′,3′-dibenzyloxycarbonylester) etc. Since nucleosides are unstable in highly acidic medium, acetyl as a protecting group was used as it can be conveniently removed under mild alkaline condition. Protection of the 2′-, 3′- and 5′-hydroxyl groups of inosine was carried out using acetic anhydride and pyridine by refluxing at 80 ^{o}C (Scheme 1). The forward reaction was favored by adding an excess amount of acetic anhydride. The excess of acetic anhydride was quenched after the completion of the reaction by adding ice and stirring for additional 30 min. The resulting product **26** was obtained by extraction with dichloromethane in high yield and purity.

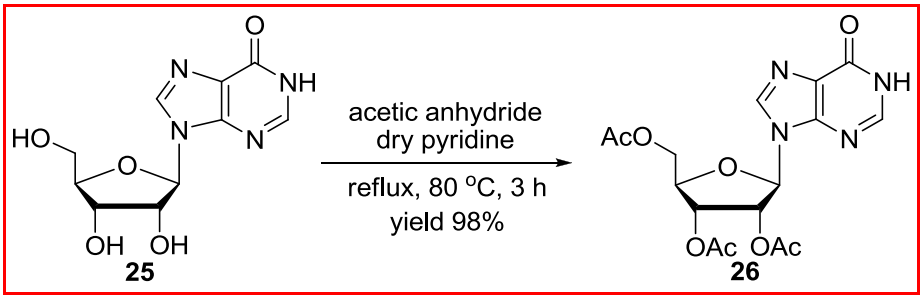

Scheme 1. Synthesis of 2′,3′,5′-tri-*O*-acetylinosine (**26**)

6.1.1.2. Synthesis of 6-chloro-2′,3′,5′-tri-*O*-acetylinosine (27)

Various chlorine-containing compounds are used for chlorination like carbon tetrachloride, phosphorus oxychloride, phosphorus pentachloride, phosphorus trichloride, sulfuryl chloride, thionyl chloride, *N*-chlorosuccinimide etc. There are reported methods of chlorination of **26** with

thionyl chloride.[126-127] Chlorination using thionyl chloride is generally preferred because it generates gaseous side-product which would simplify the purification process. However, these by-products are themselves highly reactive and may generate a large number of side-products. During the chlorination of **26** with thionyl chloride, many side-products were observed. So the chlorination of **26** was carried out with phosphorus oxychloride (Scheme 2). The hydrogen chloride generated as a by-product in this reaction might cleave the glycosidic bond between ribose and purine. In order to diminish side-product formation, the chlorination was carried out with phosphorus oxychloride in the presence of *N*,*N*-dimethylaniline. *N*,*N*-Dimethylaniline is a tertiary amine and can neutralize the hydrogen chloride generated in the reaction. Optimization of the reaction showed that stirring it for only 20 min resulted in the desired product with high yield. Excessive phosphorus oxychloride in the reaction was neutralized by adding ice. Crude **27** was extracted by dichloromethane and purified by silica gel column chromatography.

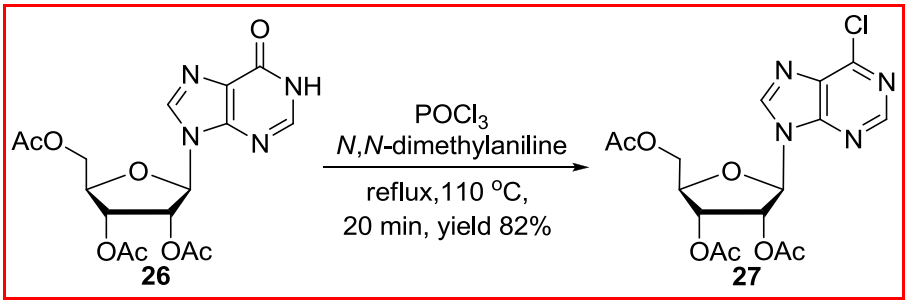

Scheme 2. Synthesis of 6-chloro-2′,3′,5′-tri-*O*-acetylinosine (**27**)

6.1.1.3. Synthesis of 6-chloropurine riboside (28)

The deprotection of acetyl groups at the 2′-, 3′- and 5′-positions is the crucial reaction step for the synthesis of 6-chloropurine riboside.[128] The acetyl groups can be removed by both, acids and bases. As explained earlier, acidic medium can cleave glycosidic bond between the purine and ribose. However some bases can also react with the chloro-functional group at 6-position and

again result in the amino group at the 6-position. For preliminary trials various bases like ammonia in water, sodium methoxide, ammonia in methanol and ethanol were used. Complete deprotection was achieved using ammonia 7N solution in methanol, and adenosine as a side-product was not observed under these conditions (Scheme 3)**.** The desired product **28** was precipitated during the course of the reaction and was collected by filtration. It was then dissolved in methanol and purified by silica gel column chromatography.

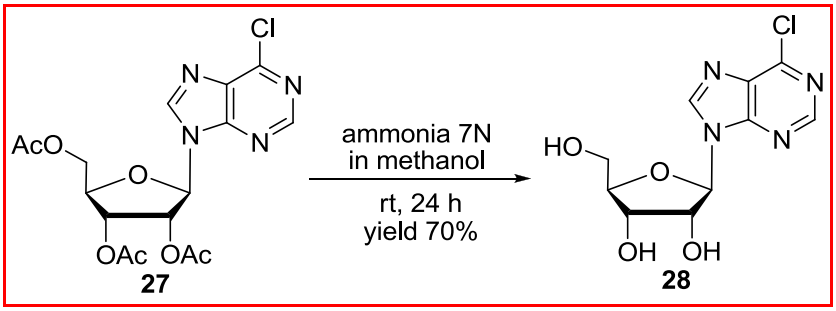

Scheme 3. Synthesis of 6-chloropurine riboside (**28**)

6.1.1.4. Synthesis of N^6-substituted purine ribosides (29-48)

For the synthesis of the intermediate N^6-substituted purine ribosides, 6-chloropurine riboside (**28**) was reacted with *N*-mono- or *N,N*-dialkylamine.HCl, and *N*-mono- or *N,N*-dialkyl- or arylamine.[129-132] Since diethyl and dimethylamine are commercially available as hydrochloride salts, the *N,N*-dialkylamine.HCl salt was reacted with **28** in DMF at low temperature (0 ^{o}C) followed by addition of triethylamine resulting in the corresponding free amine, which would alkylate **28**. The completion of the reaction was monitored by TLC with a solvent system of dichloromethane: methanol (3: 1) mixture. After completion of the reaction the triethylammonium hydrochloride precipitate was filtered off and DMF was evaporated *in vacuo*. The crude mixture was then purified by silica gel column chromatography to give derivatives **31** and **32**. For the synthesis of other intermediate nucleoside derivatives **29**, **30** and **33-48**, 6-

chloropurine riboside dissolved in ethanol was refluxed with those amines that were commercially available as free amines, in the presence of triethylamine (Scheme 4).[127]

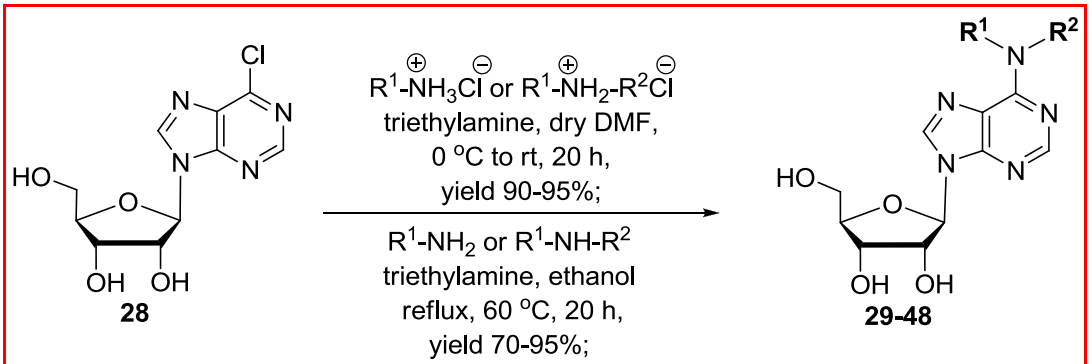

Compd	R^1	R^2	Compd	R^1	R^2
29	methyl	H	**39**	benzyl	benzyl
30	ethyl	H	**40**	4-aminobenzyl	H
31	methyl	methyl	**41**	4-chlorobenzyl	H
32	ethyl	ethyl	**42**	3-chlorobenzyl	H
33	ethyl	methyl	**43**	2-chlorobenzyl	H
34	phenyl	H	**44**	4-hydroxybenzyl	H
35	benzyl	H	**45**	4-methoxylbenzyl	H
36	2-phenylethyl	H	**46**	1-phenylethyl	H
37	benzyl	methyl	**47**	4-nitrobenzyl	H
38	benzyl	ethyl	**48**	4-sulfamoylbenzyl	H

Scheme 4. Synthesis of N^6-substituted-purine ribosides (**29-48**)

6.1.2. Phosphoprylation of 6-substituted nucleosides (29-48)

Selective phosphorylation of nucleosides in the 5′-position occasionally requires protection of the 2′- and 3′-hydroxyl groups as they are all liable for phosphorylation. Protection will result in the formation of less number side-products and increase the yield of nucleotide.

6.1.2.1. Synthesis of N^6-substituted-2′,3′-*O*-isopropylidene-purine ribosides (49-52)

Frequently, nucleosides are treated with benzyldehyde or *p*-methoxybenzyldehyde and zinc chloride in THF to give acetal-protected compounds.[133] But 2′,3′-*O*-acetyl protection with

benzyldehyde did not work out with the N^6-substituted nucleosides. Therefore 2′,3′-*O*-isopropylidene protection was carried out using acetone and 2,2-dimethoxypropane under strongly acidic conditions to give protected nucleosides (Scheme 5).[135] 2,2-Dimethoxypropane is an alkylating agent which can also be used as a water scavenger in water-sensitive reactions. Strong acids like *p*-toluenesulfonic acid (tosylic acid), nitric acid and sulphonic acid are frequently used to give 2′,3′-*O*-isopropylidene protection. In our reaction we used conc. sulfuric acid, which has the additional property of being a dehydrating agent and at the same time being very strong acid. The yield with sulfuric acid was higher than with other acids. During the optimization of the reaction with sulfuric acid, we obtained the same yield with or without the use of 2,2-dimethoxypropane. The use of 2,2-dimethoxypropane decreases the reaction time and simplify the purification steps. The amount of sulfuric acid used during the reaction was less than 1%. After completion of the reaction the solvents were evaporated *in vacuo* and the desired product was purified by silica gel column chromatography.

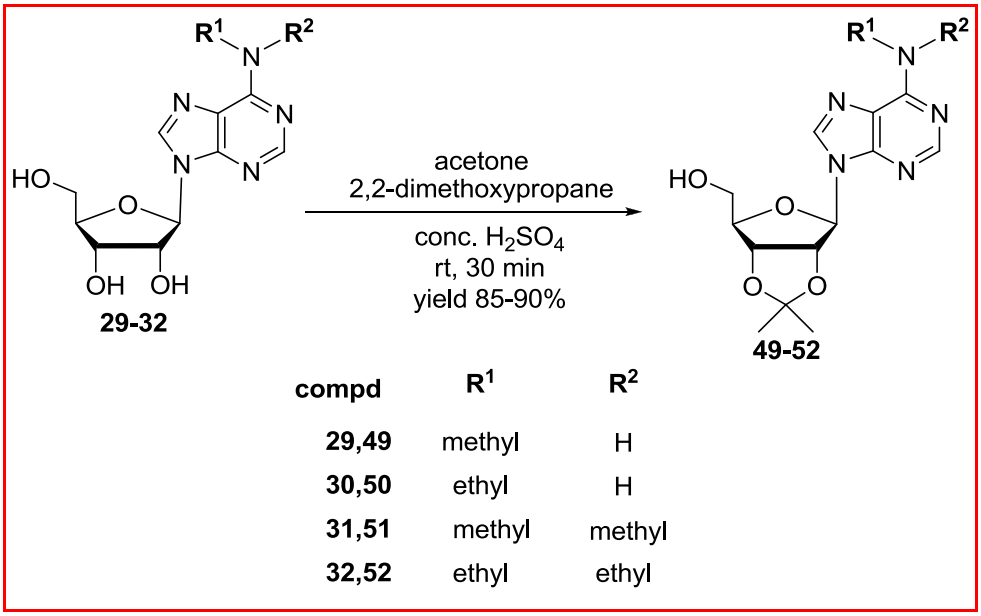

compd	R^1	R^2
29,49	methyl	H
30,50	ethyl	H
31,51	methyl	methyl
32,52	ethyl	ethyl

Scheme 5. Synthesis of N^6-substituted-2′,3′-*O*-isopropylidene purine ribosides (**49-52**)

6.1.2.2. Optimization of the phosphoprylation reaction

For the preparation of nucleoside-5′-*O*-[(phosphonomethyl)phosphonic acid] derivatives there are several commonly used multi-step methods, such as:

- protected nucleoside reacting with strongly activated bisphosphonates like (4-nitrophenyl)ethyl phosphonates[135]
- Mitsunobu reaction of phosphonates with protected nucleosides[136]
- Esterification of phosphonic acid with protected nucleosides by trichloroacetonitrile and dicyclohexylcarbodiimide
- Preparation of a protected nucleoside-5′-sulfonyl ester followed by its nucleophilic substitution with alkylammonium salts of bisphosphonic acid.[137-139]

All of these methods utilize protected nucleosides and give products in low yields. However in the early 2000s, two separate groups reported on the preparation of nucleoside-5′-*O*-[(phosphonomethyl)phosphonic acid] derivatives by phosphorylation of nucleosides with methylenebis(phosphonic dichloride) followed by hydrolysis with TEAC (triethyl ammonium bicarbonate buffer, pH 7.4-7.6).[140,141] Methylenebis(phosphonic dichloride) is a similar reagent to phosphorus oxychloride which is used for the 5′-phosphorylation of nucleosides. But it is more bulky and reactive than phosphorus oxychloride. We also observed that all of the products were formed faster with higher yields as compared with phosphorus oxychloride. The lack of electron back-donation from the central methylene group in methylenebis(phosphonic dichloride) makes phosphorus centre more electrophilic.[140] During phosphorylation of nucleosides in addition to the 5′-phosphorylation there is a risk of 2′- and 3′-phosphorylation (**III** and **IV**). Apart from that, there is also a high risk of the formation of the nucleoside-5′,3′-cyclomethylenebis(phosphonic acid) (**V**) and dinucleoside-bisphosphonic acid (**II**). The formation of many products will hinder and complicate the purification process. So the use of

2′,3′-*O*-isopropylidene protection can be justified as it limits 2′- and 3′-phosphorylation and the formation of 5′,3′-cyclomethylenebis(phosphonic acid).

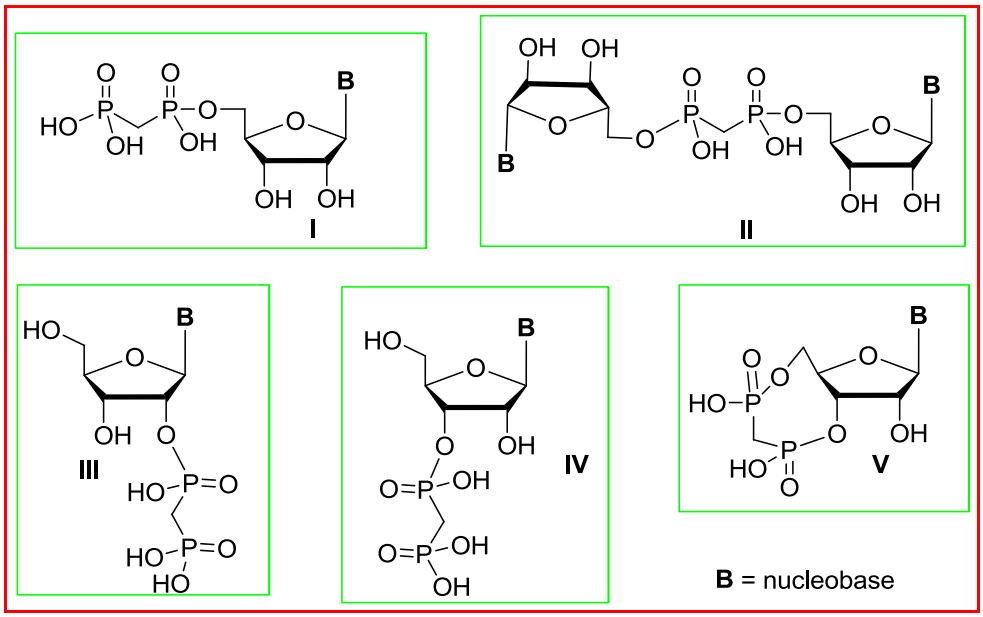

Figure 133. Possible products of the phosphorylation of nucleoside using methylenebis(phosphonic dichloride)

The phosporylation reaction is generally carried in various dry solvents like acetonitrile, DMF or DMSO. Yoshikawa *et al.* introduced the phosphorylation of nucleosides in trimethyl phosphate.[142] The inertness of trimethyl phosphate improves the selectivity and efficiency of product formation. Trimethyl phosphate itself can participate in producing an electrophilic adduct for initiating the reaction.[143]

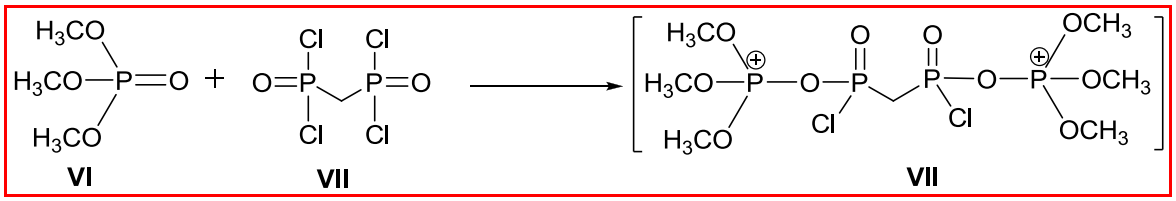

Scheme 6. Electrophic adduct formed by the reaction of trimethyl phosphate and methylenebis (phosphonic dichloride)

The phosporylation reaction was carried in two steps. First nucleosides or protected nucleosides are phosphorylated using methylenebis(phosphonic dichloride) leading to the formation of intermediate **X**. The second step involved hydrolysis of the highly unstable intermediate **X** with TEAC (Scheme 7).[140]

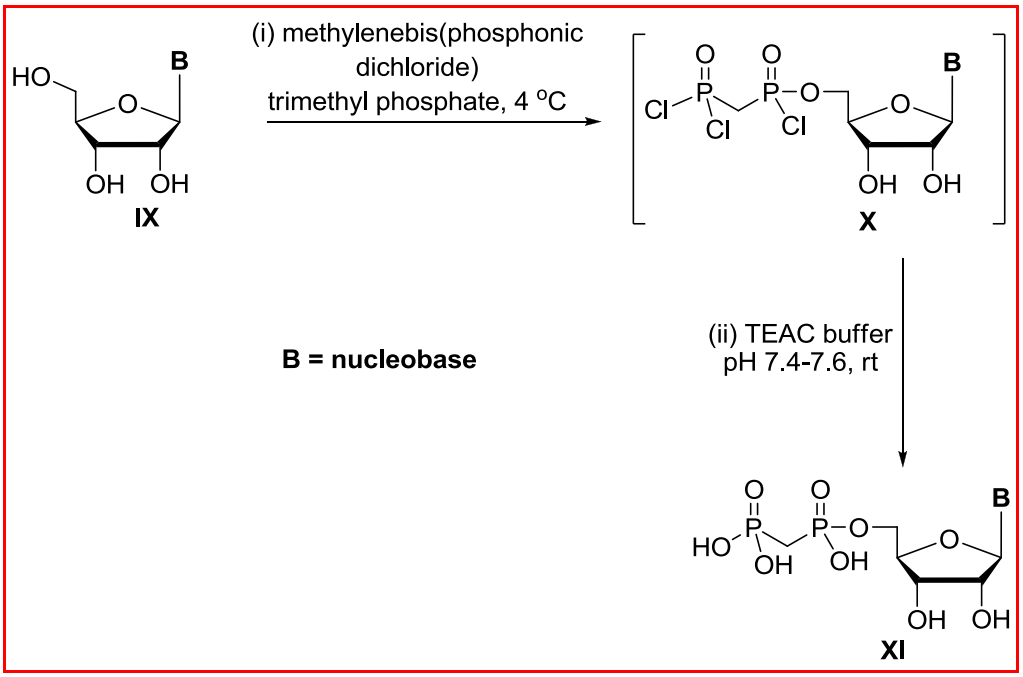

Scheme 7. Intermediate formed during phosphoryaltion reaction by methylenebis(phosphonic dichloride)

Since the phosphorylation reaction yields a number of side-products, it is always desirable to increase the yield of product formation. In-order to increase the yield of products using protected and unprotected nucleosides two different strategies were used:

- increasing the amount of methylenebis(phosphonic dichloride) used during the reaction
- decreasing the reaction time.

For optimization reaction, both protected and unprotected nucleosides [2′,3′-*O*-isopropylidene-N^6-dimethyladenosine (**51**) and N^6-dimethyladenosine (**35**)] were used. Compounds **35** and **51** were separately reacted with various equivalents of methylenebis(phosphonic dichloride) and the

reaction was quenched at different time intervals. The products formed were analyzed by LC-MS. Detailed LC-MS study results are summarized in Table 10 and 11.

Table 100. Optimization of reaction condition for the synthesis of N^6-dimethyl-2′,3′-*O*-isopropylidine-purine riboside methylenebis(phosphonic acid)]

Equivalent of methylenebis(phosphonic dichloride)	Time of reaction	Products formed
2 eq.	4 h	Only dinucleotide-methylenebis(phosphonic acid)
3 eq.	2 h	Only dinucleotide-methylenebis(phosphonic acid)
4 eq.	2 h	Mixture of dinucleotide methylenebis(phosphonic acid) and nucleoside -5′-*O*-[(phosphonomethyl)phosphonic acid]
5 eq.	1 h	Only nucleoside-5′-*O*-[(phosphonomethyl)phosphonic acid]

The reaction of **51** was started with the method reported for adenosine (using 2 equivalents of methylenebis(phosphonic dichloride) and stirring for 4 h,[140] but only dinucleotide-methylenebis(phosphonic acid) was obtained. Then simultaneously the reaction time was decreased thereby increasing the amount of methylenebis(phosphonic dichloride) used in the reaction. Using 5 equivalents of methylenebis(phosphonic acid) and stirring for only 1 hour gave only the desired product. The optimization of the reaction of **35** was also started from the same method as described for adenosine.[140] However, we obtained a complex mixture of side-products. By using the method optimized for protected nucleoside we obtained mainly 5′-phosphorylated product and a very low amount of side-products. So we decreased the reaction time to 30 min keeping the same amount of methylenebis(phosphonic acid). Under these conditions we got only 5′-phosphorylated product. In addition to that we observed that a small amount of unreacted nucleoside remained, this can be easily removed by HPLC as nucleoside and nucleotide have very different retention times.

Table 11. Optimization of reaction conditions for the synthesis of N^6-dimethylpurine riboside 5′-*O*-[(phosphonomethyl)phosphonic acid]

Equivalent of methylenebis(phosphonic dichloride)	Time of reaction	Products formed
2 eq.	4 h	complex mixture of dinucleotide-methylenebis(phosphonic acid) and 2′- and 3′-phosphorylated product
4 eq.	3 h	mixture of dinucleotide-methylenebis(phosphonic acid) and 2′- and 3′-phosphorylated product
4 eq.	2 h	2′-, 3′-and 5′-phosphorylated product and dinucleotide-methylenebis(phosphonic acid)
5 eq.	1 h	5′-phosphorylated product and very low amount of side-products
5 eq.	30 min	Only 5′-phosphorylated product and a small amount of unreacted nucleoside

6.1.2.3. Phosphorylation reaction with protected nucleosides (49-52) and deprotection

The initial phosphoryation reactions were performed using protected nucleosides (**49-52**). Only after complete optimization of the reactions, they were carried out using un-protected nucleosides, since the optimization led to the sole formation of nucleoside-5′-*O*-[(phosphonomethyl)phosphonic acid] derivatives. Reaction using 5 equivalents of methylenebis(phosphonic dichloride) for 1 hour followed by hydrolysis with TEAC produced only 2′,3′-*O*-isopropylidene-nucleoside-5′-*O*-[(phosphonomethyl)phosphonic acid] as the final product (Scheme 8). The advantage of the synthesis of some 2′,3′-*O*-isopropylidene-nucleoside-5′-*O*-[(phosphonomethyl)phosphonic acid] derivatives were also to elaborate the role of free and protected 2′,3′-hydroxyl groups in relation to the compounds' enzyme inhibition potency.

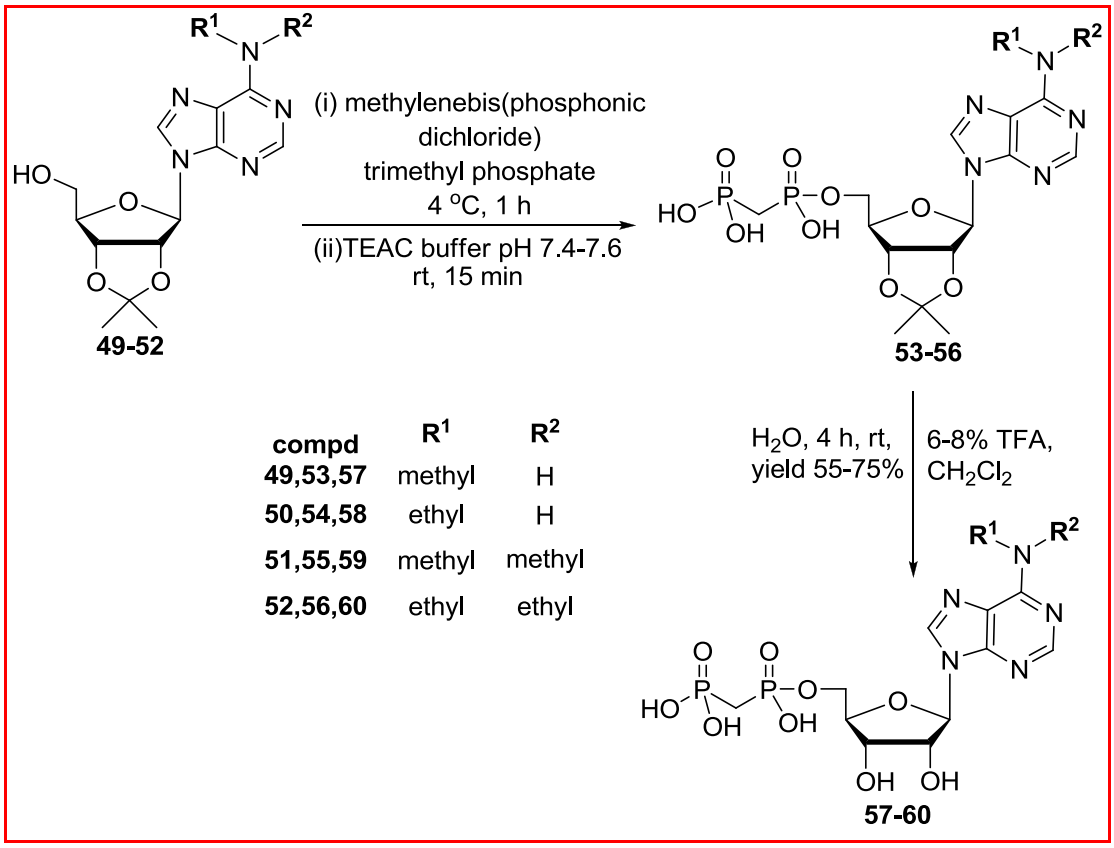

Scheme 8. Synthesis of target nucleotides **53-60**

The isopropylidene-protecting group at the 2′,3′-position of ribose is frequently deprotected by acids. Compounds **53-56** have two groups which are liable to be degraded by acid, i.e. the glycosidic bond between purine and ribose, and the 5′-oxygen-phosphorus bond. So, we optimized this deprotection by using various acids, including HCl, acetic acid and trifluoroacetic acid (TFA) at different concentrations. We found that 6-8% TFA can effectively deprotect the ribose in 4 hours without cleaving any other bonds. Compounds **53-56** and **57-60** were purified by ion exchange chromatography followed by HPLC.

6.1.2.4. Phosphorylation reactions of un-protected nucleosides (33-48)

Reaction using 5 equivalents of methylenebis(phosphonic dichloride) for 30 min, followed by hydrolysis with TEAC produced only nucleoside-5′-*O*-[(phosphonomethyl)phosphonic acid]

derivatives as the final product (Scheme 9). The nucleotides were purified by HPLC using various gradients of 50 mM ammonium bicarbonate buffer solution and acetonitrile.

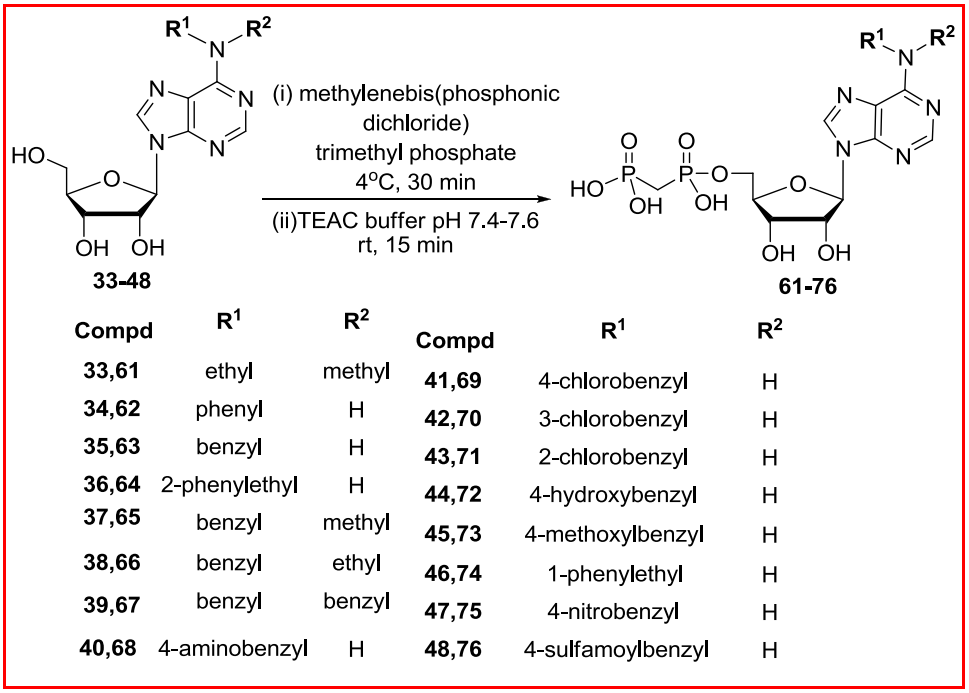

Compd	R^1	R^2	Compd	R^1	R^2
33,61	ethyl	methyl	**41,69**	4-chlorobenzyl	H
34,62	phenyl	H	**42,70**	3-chlorobenzyl	H
35,63	benzyl	H	**43,71**	2-chlorobenzyl	H
36,64	2-phenylethyl	H	**44,72**	4-hydroxybenzyl	H
37,65	benzyl	methyl	**45,73**	4-methoxylbenzyl	H
38,66	benzyl	ethyl	**46,74**	1-phenylethyl	H
39,67	benzyl	benzyl	**47,75**	4-nitrobenzyl	H
40,68	4-aminobenzyl	H	**48,76**	4-sulfamoylbenzyl	H

Scheme 9. Synthesis of target derivatives **61-76**

6.1.2.5. Purification of nucleotides

The phosphorylation reaction yields a number of side products. The most crucial step is the purification and separation of side-products. The purification of nucleotide derivatives is critical for biological evaluation, as the side-products also being the nucleotides can influence biological assay readings. So, our goal was to obtain high purity products. Depending on the type of side-product formed during the reaction, the separation process also varies. The compounds were generally purified by using ion-exchange chromatography followed by HPLC.[66]

The synthesized nucleotides were initially purified by anion exchange chromatography on Sephadex diethylaminoethyl (DEAE) A-25 gel using a fast protein liquid chromatography (FPLC) instrument. The negatively charged nucleotides are eluted after interaction with the

positively charged gel by applying a linear gradient of a 0-900 mM TEAC according to the number of charges. Uncharged molecules and compounds with a lower number of charges are eluted first. In addition to nucleotide side-products the reaction mixture also contains a large number of inorganic salts, such as phosphates, bisphosphates and its decomposed products as well as buffer components. So the products were further purified by HPLC on reverse phase C18 material. Some inorganic phosphates may be coeluted with the nucleotides.[66] The structures of the isolated compound were elucidated by mass spectroscopy as well as ^{31}P-NMR for purity determination. Our synthesized biphosphate derivatives should have two peaks in the ^{31}P-NMR spectra and compounds having more than two peaks were not subjected to biological evaluation though, having more than 95% LC-MS purity. Those compounds were subjected to multiple purification processes to achieve sufficient purity. The final purity of all compounds was above 98% as confirmed by LC-MS and NMR analyses. The structures of the synthesized compounds were confirmed by ^{1}H-, ^{13}C-NMR, DEPT-135 and ^{31}P-NMR spectroscopy, in addition to LC/ESI-MS in positive and negative mode.

6.2. 6-Ethoxy-, 6-benzyloxy-, and 6-benzylthio-purine riboside-5'-O-[(phosphonomethyl)phosphonic acid] (81-83)

The synthesis strategy to obtain the target nucleotides involved the synthesis of the corresponding nucleosides followed by phosphorylation.

6.2.1. Synthesis of O^6-ethyl, O^6-benzyl, and S^6-benzyl-purine riboside derivatives (77-80)

Nucleoside 6-ethoxy-, 6-benzyloxy-, and 6-benzylthio-purine ribosides were synthesized from 6-chloroadenosine (**28**).

6.2.1.1. Synthesis of 6-ethoxy- and 6-benzyloxypurine riboside (77, 78)

For synthesis of 6-(aryl)alkoxy-substituted purine nucleoside derivatives, 6-chloro-purine riboside (**28**) was reacted with sodium (aryl)alkoxide in the corresponding (aryl)alkyl alcohol (Scheme 10).[124, 144] For the synthesis of 6-ethoxy-substituted derivative **77**, sodium ethoxide in ethanol and for the 6-benzyloxy-substituted derivative **78**, sodium benzyloxide in benzyl alcohol was used. Both, benzyloxide and ethoxide are commercially available. The reaction of 6-chloropurine riboside with sodium (aryl)alkoxide is characterized as a salt metathesis reaction where there is an exchange of bonds between the two reacting chemical species. The reaction was performed by refluxing the reaction mixture at 100 ^{o}C, and the progress of reaction was monitored by TLC in a DCM : methanol (9 : 1) mixture. After the reaction was completed the volatiles were removed *in vacuo* and the products were separated by silica gel column chromatography.

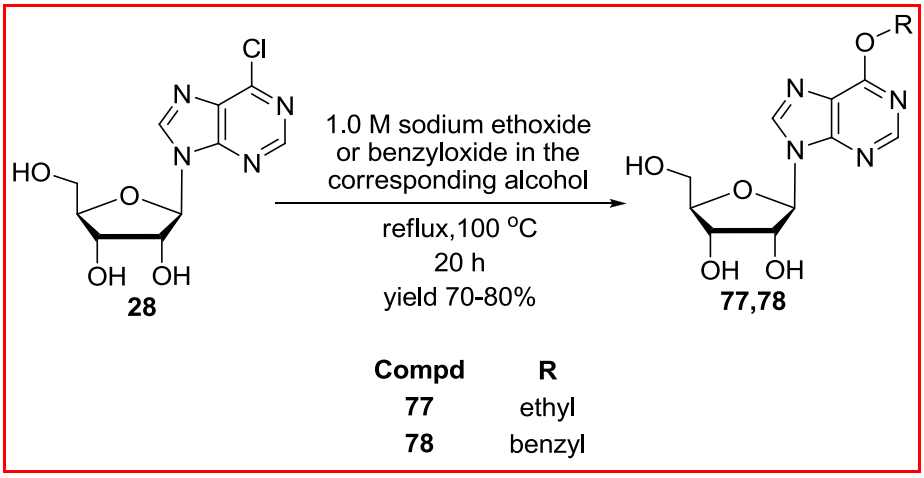

Scheme 10. Synthesis of 6-ethoxy- and 6-benzyloxypurine riboside (**77**, **78**)

6.2.1.2. Synthesis of 6-benzylthiopurine riboside (80)

6-Benzylthio-substituted derivative was also synthesized from 6-chloropurine riboside (**28**), in a two step reaction: first 6-chloropurine riboside was converted to the 6-thiopurine riboside (**79**).

The next step was the alkylation of the thiol.[145] Hydrogen sulfide, sodium hydrogensulfide and thiourea are common thiolating agents. In our case we used thiourea. The reaction of thiourea with 6-chloropurine riboside is a multistep, one pot process where isothiouronium salt is the intermediate which is then hydrolyzed to give 6-thiopurine riboside (**79**) in the presence of base sodium hydroxide. The product formed was separated from the formed urea by washing with water, followed by filtration and evaporation of the filtrate to give **79**. Thiols readily undergo *S*-alkylation reaction with various alkyl halides to yield thioethers.[146] Therefore, 6-thiopurine riboside was reacted with benzyl chloride under microwave conditions in the presence of base to give 6-benzylthiopurine riboside product **80**, which was then purified by silica gel column chromatography (Scheme 11).

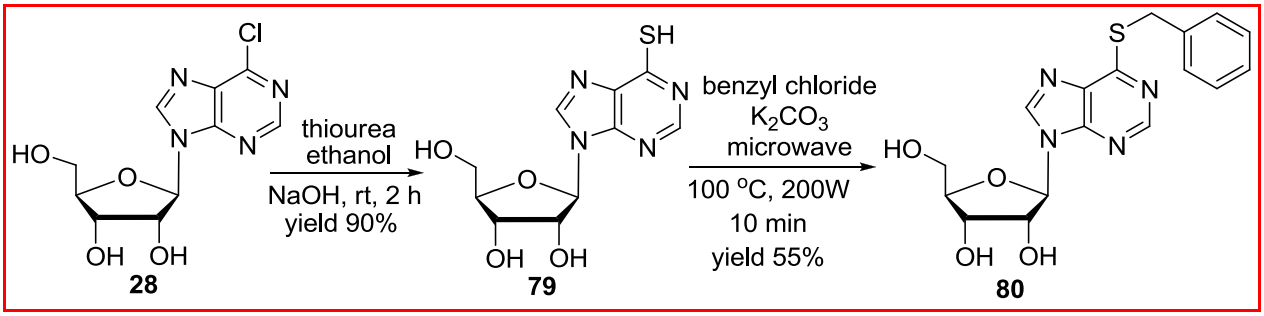

Scheme 11. Synthesis of 6-benzylthiopurine riboside (**80**)

6.2.2. Phosphorylation of 6-ethoxy-, 6-benzyloxy-, and 6-benzylthiopurine riboside (77, 78, 80)

Both 6-O-alkyl/aryl-purine riboside (**77**, **78**) and 6-S-benzyl-purine riboside (**80**) were phosphorylated applying the earlier explained method using methylenebis(phosphonic dichloride) followed by hydrolysis with TEAC buffer solution (Scheme 12).

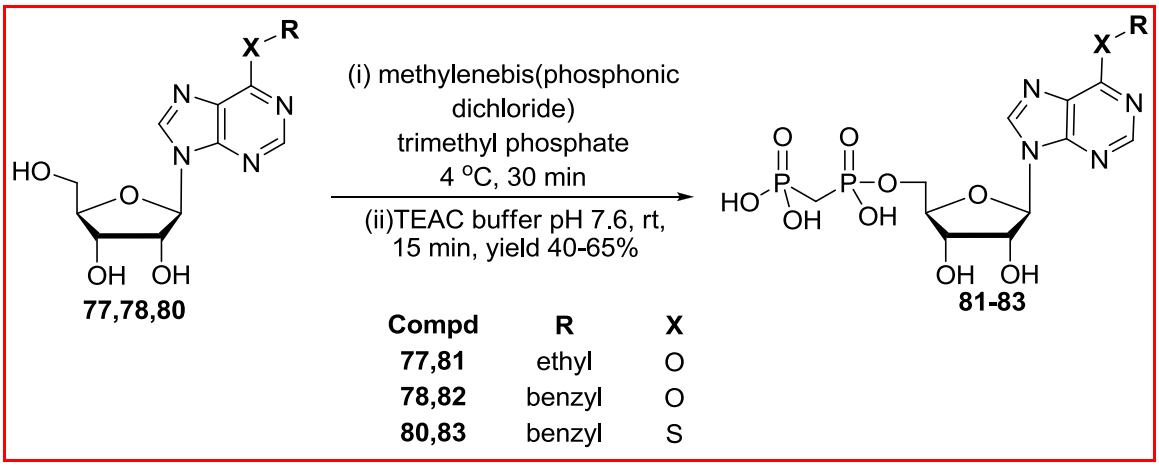

Scheme 12. Synthesis of target nucleotides **81-83**

6.3. 8-substituted adenosine-5′-methylenebisphosphonic acid derivatives (89-92)

The synthetic strategy involved first the synthesis of the 8-substituted-nucleosides followed by phosphorylation.

6.3.1. Synthesis of 8-substituted adenosine derivatives (84, 86-88)

For the synthesis of 8-substituted nucleoside derivatives, a commercially available adenosine was used as a starting compound. Four different 8-substituted derivatives were synthesized, that are 8-bromo- (**84**), 8-chloro- (**86**), 8-thioethyl- (**87**) and 8-aminomethyl-substituted adenosine derivatives (**88**).

6.3.1.1. Synthesis of 8-bromoadenosine (84)

Unlike for chlorination reactions, the most popular bromination reagent is bromine itself. Adenosine was brominated using bromine-water at room temperature in sodium-acetate buffer to give 8-bromoadenosine (**84**).[147] The carbon-carbon double bond in the 8-position of adenosine is selective for bromination versus that at the 2-position of the adenine ring. It is a typical case of a halogen addition reaction to the double bond system, where the bromine atom approaching for

the attack at the 8-position behaves as an electrophile due to electron repulsion by the double bond. The other bromine atom is released as hydrogen bromide thereby increasing the pH values of reaction mixture, which was balanced by a sodium-acetate buffer solution. After completion of the reaction, the mixture was decolorized by $NaHSO_3$ (Scheme 13). The pH was adjusted to 7 and left overnight for crystallization of 8-bromoadenosine at 4 ^{o}C.

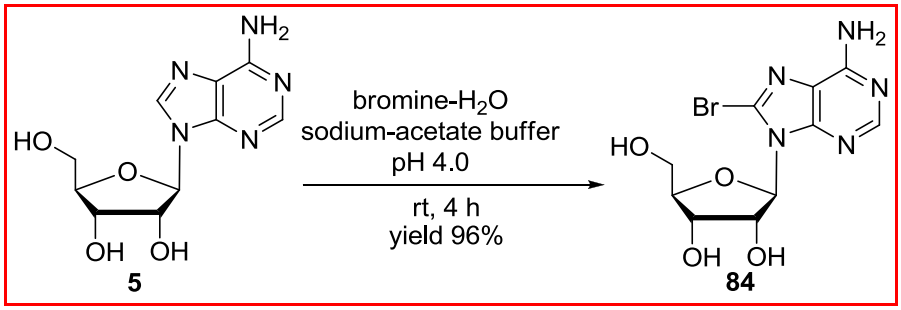

Scheme 13. Synthesis of 8-bromoadenosine (**84**)

6.3.1.2. Synthesis of 8-chloroadenosine (86)

8-Chloroadenosine (**86**) was synthesized from 8-thioadenosine (**85**) by reacting it with *N*-chlorosuccinimide for 4 h at room temperature. 8-Thioadenosine was synthesized as previously explained by thiolation of 8-bromoadenosine (**86**) using thiourea (Scheme 14).[148] Stirring of the **85** with *N*-chlorosuccinimide in methanol gave 8-chloradenosine. The solution was evaporated *in vacuo* and the product was purified by HPLC.

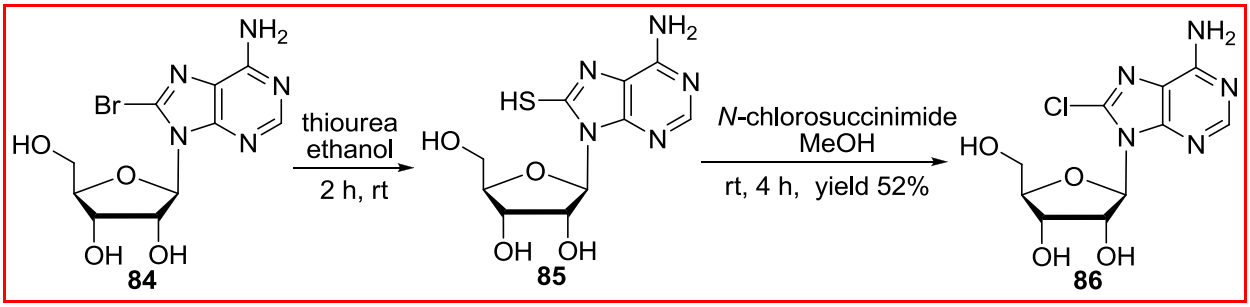

Scheme 14. Synthesis of 8-chloroadenosine (**86**)

6.3.1.3. Synthesis of 8-ethylthioadenosine (87)

8-Thioadenosine (**85**) was reacted with ethyl iodide yielding 8-ethylthioadenosine (**87**). Iodide is a good leaving group and ethyl iodide is a powerful ethylating agent.

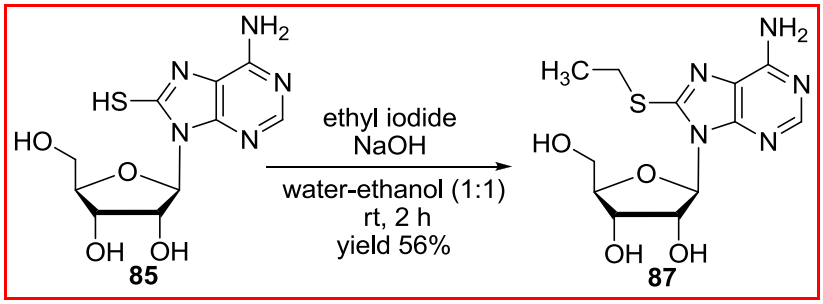

Scheme 15. Synthesis of 8-ethylthioadenosine (**87**)

6.3.1.4. Synthesis of 8-aminomethyladenosine (88)

8-Aminomethyladenosine (**88**) was directly synthesized from 8-chloradenosine (**86**) by reacting it with methylamine in the presence of triethylamine.[149] Methylamine dissolved in methanol is a good nucleophile as it is basic and unhindered.

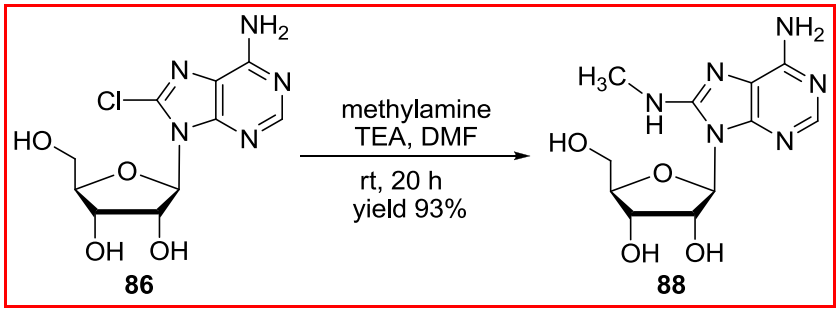

Scheme 16. Synthesis of 8-methylaminoadenosine (**88**)

6.3.2. Phosphoprylation of 8-substituted adenosine derivatives (84, 86-88)

8-Substituted adenosine derivatives were subsequently reacted with 5 equivalents of methylenebis(phosphonic dichloride) to give the corresponding nucleoside 5′-*O*-[(phosphonomethyl)phosphonic acid] derivatives as final products. Reactions of these derivatives

for 30 min under the optimized conditions resulted in very low yields. Therefore, the reaction mixtures were stirred for 1 h (Scheme 17). The yields for 8-substituted derivative were lower than those of the 6-substituted derivatives as the larger substituents at 8-position can induce a conformational change from the *anti*- to the *syn*-conformation around the nucleosidic bond.[150, 151]

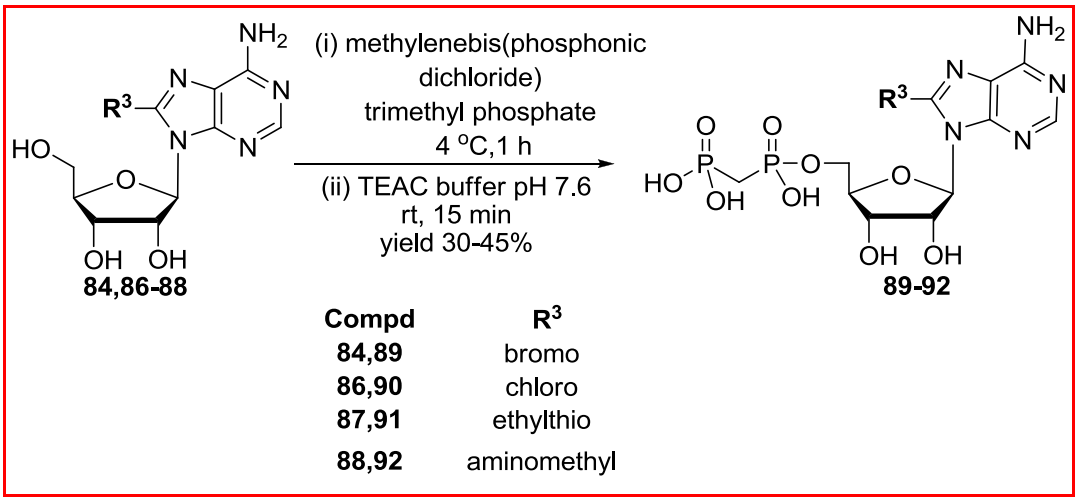

Scheme 17. Synthesis of nucleotides **89-92**

6.4. 2-Substituted adenosine-5′-O-[(phosphonomethyl)phosphonic acid] derivatives (109-114)

The synthesis strategy involved first the synthesis of the 2-substituted-nucleosides followed by phosphorylation.

6.4.1. Synthesis of intermediate 2-substituted-adenosine derivatives (98-108)

The 2-substituted adenosine derivatives were synthesized from the commercially available guanosine (**93**).

6.4.1.1. Synthesis of 2′,3′,5′-tri-*O*-acetylguanosine (94)

Guanosine (**93**) was acylated by a similar procedure as described for inosine (**25**), but by using acetic anhydride, 4-dimethylaminopyridine (DMAP) and *N*-ethyldimethylamine (EDMA) at 40

^{o}C for 1 h to achieve **94** (Scheme 18). Acetic anhydride is a versatile reagent for acylation. Bases such as DMAP and pyridine function as catalysts in the acylation reaction.

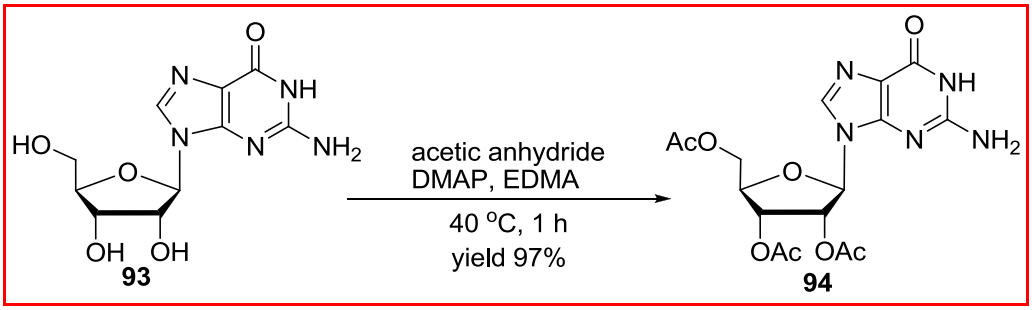

Scheme 18. Synthesis of 2-amino-2′,3′,5′-tri-*O*-acetylinosine (**94**)

6.4.1.2. Synthesis of 2-amino-6-chloro-2′,3′,5′-tri-*O*-acetylinosine (95)

2′,3′,5′-Tri-*O*-acetylguanosine (**94**) was then chlorinated at the 6-position to give 2-amino-6-chloro-2′,3′,5′-*O*-acetyl-purine riboside (**95**) using phosphorus oxychloride, *N*,*N*-dimethylaniline and tetraethylammonium chloride.[125, 152] The use of tetraethylammonium chloride in the chlorination reaction of guanosine increases the yield of **95** to 75%.

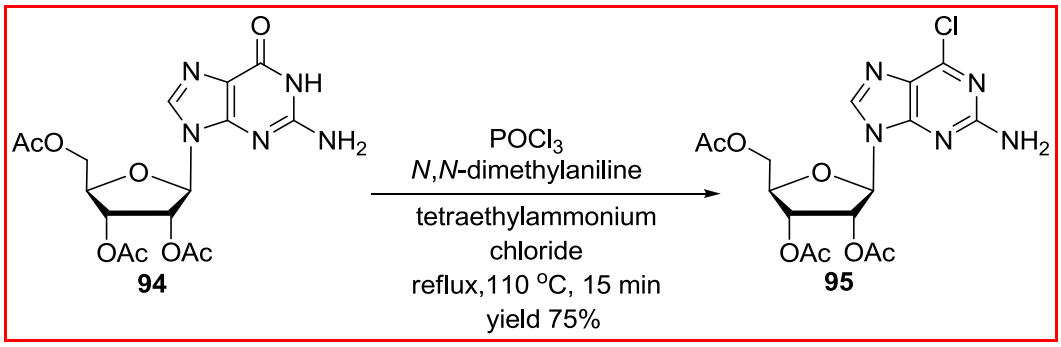

Scheme 19. Synthesis of 2-amino-6-chloro-2′,3′,5′-tri-*O*-acetylinosine (**95**)

6.4.1.3. Synthesis of 2-amino-6-chloropurine riboside (96)

The next step was the removal of the acetyl groups from 2-amino-6-chloro-2′,3′,5′-tri-*O*-acetylinosine (**95**). Deprotection of acetyl groups is normally carried out using bases, e.g. NH_3 or sodium methoxide. We used the method as for inosine (**25**) but the yield was very low. So, we

tested various concentrations of sodium methoxide solutions. The best result was obtained with 2% NaOMe in methanol. NaOMe has the property of methylating the 6-position, resulting in the formation of O^6-methyl derivatives. However, 2% NaOMe in methanol is not sufficient to methylate the 6-position. A small amount of starting material was remaining after stirring the mixture for several days. So the reaction was stopped after 24 h and the desired product 2-amino-6-chloropurine riboside (**96**) was purified by the silica gel column chromatography.

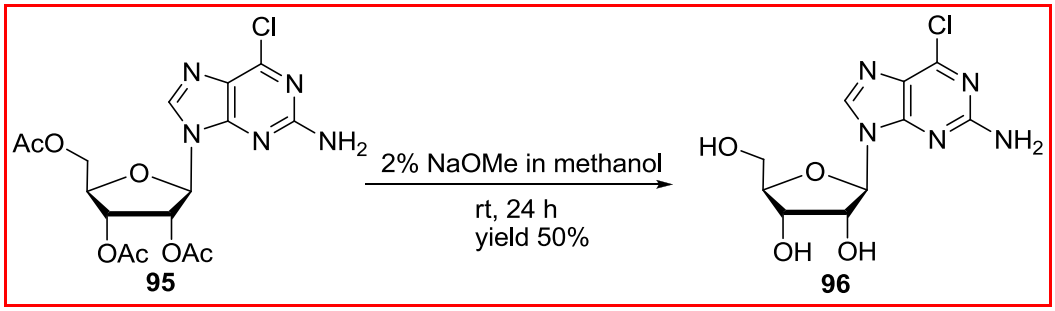

Scheme 20. Synthesis of 2-amino-6-chloropurine riboside (**96**)

6.4.1.4. Synthesis of 2′,3′,5′-tri-*O*-acetyl-2,6-dichloropurine riboside (97)

2-Amino-6-chloro-2′,3′,5′-tri-*O*-acetylinosine (**95**) was diazotized with benzyltriethylammonium nitrite (BETA-NO_2) in the presence of acetyl chloride to give 2,6-dichloro-substituted nucleoside **97**, which on reacting with ammonia in ethanol, 2-chloroadenosine (**98**) was obtained (Scheme 21).[153] The employed Sandmeyer reaction utilizes aryl diazonium salts to convert anilines to aryl chlorides. Mechanistically aromatic amino group is converted to a diazonium salt followed by its displacement with a nucleophile resulting in the formation of halides. BETA-NO_2 is not commercially available so it is prepared from the benzyltriethylammonium chloride (BETA-chloride) by replacing chloride with nitrate using ion-exchanger. 2,6-Dichloro-2′,3′,5′-tri-*O*-acetylinosine (**97**) was obtained in good yield.[153, 154] Deprotection of **97** with sodium methoxide and 7N ammonia solution in methanol resulted 2,6-dichloropurine riboside with a low yield.[154]

In contrast deprotection with ammonia in ethanol appeared more beneficial as ammonia promotes nucleophilic attack on the acetyl-protecting groups resulting in 2-chloroadenosine. 2-Chloroadenosine (**98**) was purified by silica gel column chromatography.[155]

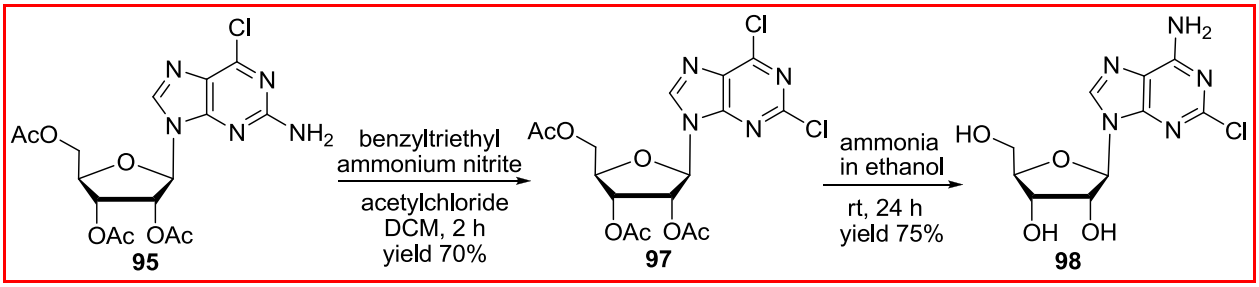

Scheme 21. Synthesis of 2-chloroadenosine (**98**)

6.4.1.5. Synthesis of 2′,3′,5′-tri-*O*-acetyl-6-chloro-2-iodopurine riboside (99)

Intermediate **95** was also diazotized with isoamyl nitrate in the presence of cuprous(I) iodide and diiodomethane to give the 2-iodo-6-chloro nucleoside **99** which on readily reacting with ammonia in ethanol afforded 2-iodoadenosine (**100**). This is the direct diazotization-iodination reaction, where isoamyl nitrate acts as a diazotizing agent.[156]

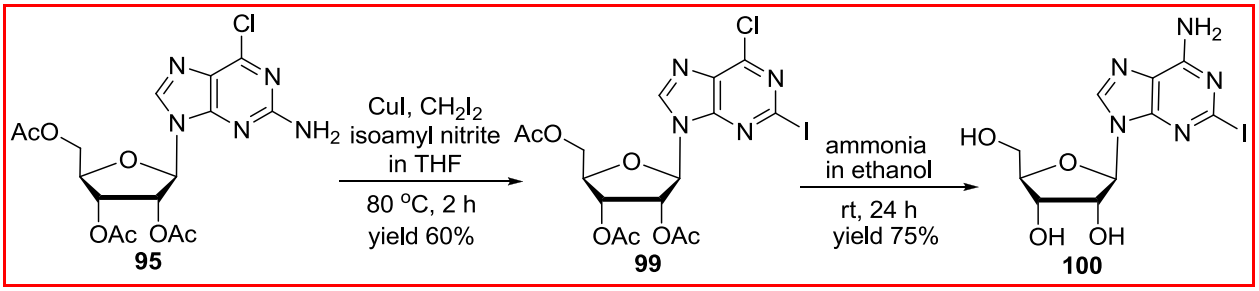

Scheme 22. Synthesis of 2-iodoadenosine (**100**)

6.4.1.6. Synthesis of 2-hydrazinyladenosine (101)

In general, hydrazine hydrate is a good nucleophile which can readily replace the halogens. 2-Chloroadenosine (**98**) was reacted with hydrazine hydrate to give 2-hydrazinyl derivative **101**. It

was also prepared by the same process as reported by El-Tayeb *et al.*[157] The progress of reaction was determined by TLC (CH_2Cl_2:MeOH = 3:1).[158]

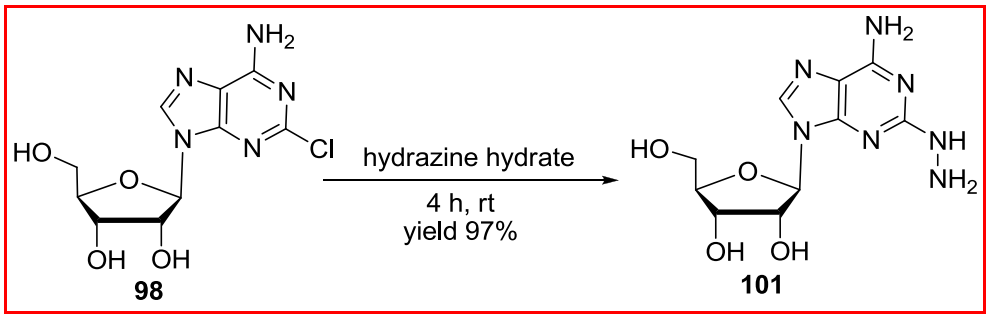

Scheme 23. Synthesis of 2-hydrazinyladenosine (**101**)

6.4.1.7. Synthesis of 2-piperazinyladenosine (103)

1-Boc-piperazine is basic and can be *N*-alkylated by halides. However, 2-chloroadenosine (**98**) is less reactive than 6-chloropurine riboside (**28**). Alkylation requires an excess of both, 1-boc-piperazine as well as triethylamine.[159] 2-Chloroadenosine (**98**) was reacted with 1-boc-piperazine to give intermediate **102**, which was purified by column chromatography after evaporating the volatiles *in vacuo*. The *tert*-butyloxycarbonyl protecting group (boc group) was removed by 8% triflouroacetic acid in $CHCl_3$: water (9 : 1) to give 2-piperazinyladenosine (**103**), which was subsequently purified by HPLC (Scheme 24).

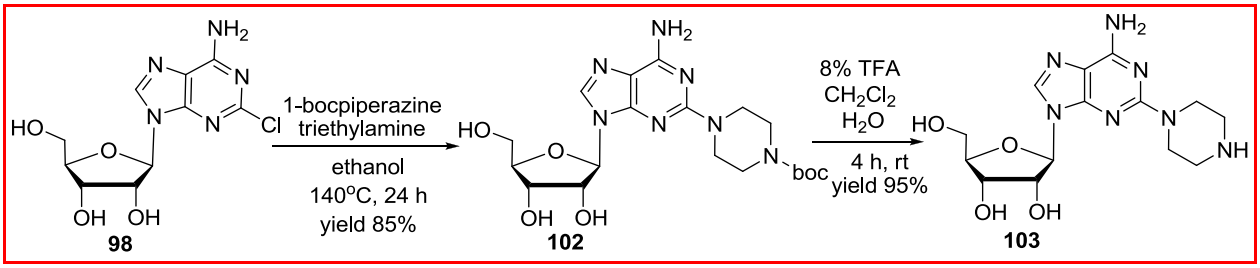

Scheme 24. Synthesis of 2-piperazinyladenosine (**103**)

6.4.1.8. Synthesis of 2-alkylthio-adenosine derivatives (107, 108)

2-Thioadenosine (**106**) was obtained by oxidation of adenosine using a previously reported method.[66, 160, 161] Adenosine was oxidized with hydrogen peroxide in the presence of acetic acid to give adenosine N^1-oxide (**104**). Subsequent ring opening with sodium hydroxide afforded the carboximidoxime intermediate **105**, which was then thiolated with carbon disulfide in an autoclave to give 2-thioadenoisine (**106**). Compound **106** was subsequently alkylated with allyl bromide, and 2-cyclohexylethyl bromide respectively, to give 2-allythio- and 2-cyclohexylethylthioadenosine (**107** and **108**).

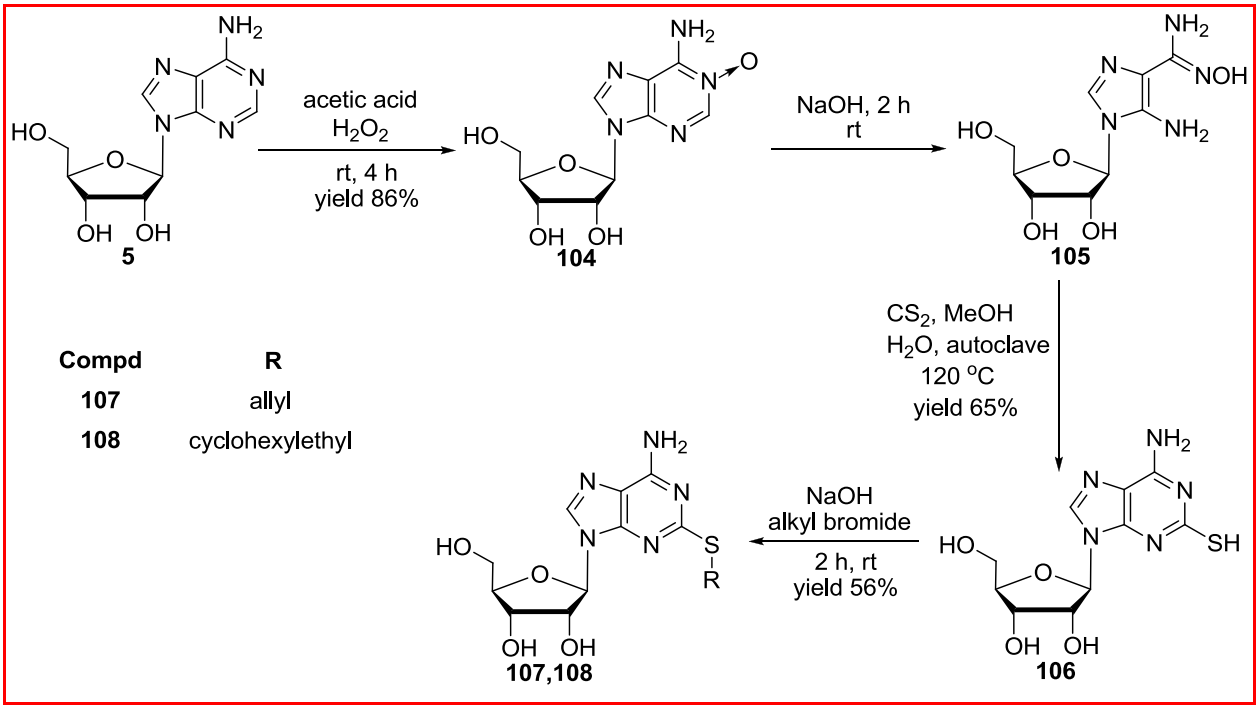

Scheme 25. Synthesis of 2-cyclohexylethylthio- and 2-allythioadenosine (**107**, **108**)

6.4.2. Phosphorylation of 2-substituted-nucleosides

All 2-substituted adenosine derivatives (**98-102, 107** and **108**) were phosphorylated using earlier optimized method of phosphorylation. The reaction was carried out using 5 equivalents of methylenebis(phosphonic dichloride) for 30 minutes (Scheme 26). The target compounds were

obtained in good yields and purified by HPLC using a gradient of ammonium bicarbonate buffer and acetonitrile.

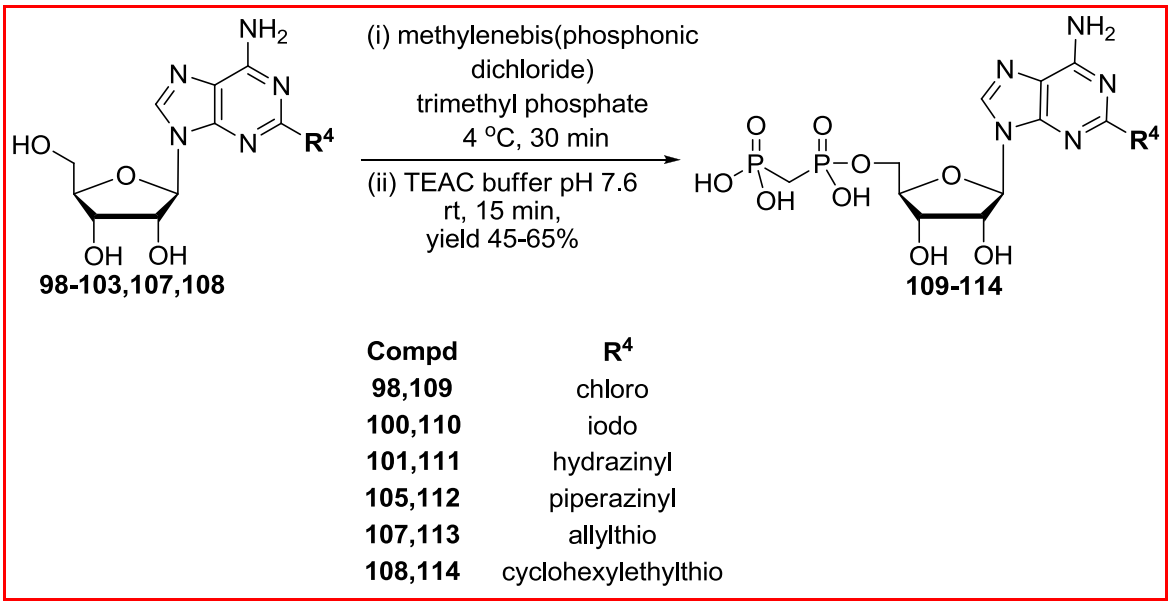

Scheme 26. Synthesis of target nucleotides **109-114**

6.5. 2-Amino-, 2-choro- and 2-iodo-N^6-mono-/dialkyl-or aryl-substituted adenosine-5′-O-[(phosphonomethyl)phosphonic acid] derivatives (139-150)

The synthetic strategy involved first the synthesis of the corresponding 2-amino-, 2-choro- and 2-iodo-N^6-mono-/dialkyl-and aryl-substituted purine ribosides followed by phosphorylation.

6.5.1. Synthesis of 2,6-disubstituted nucleosides (127-138)

For the synthesis of the intermediate nucleosides, the 2-amino-6-chloro-substituted compound **95**, the 2,6-dichloro-substituted compound **97**, and 6-chloro-2-iodo-substituted compound **99** were refluxed with the appropriate amines in the presence of triethylamine to give the corresponding N^6-substituted nucleoside derivatives (**115-126**), using the same methods as used for 2-unsubstituted-6-substituted nucleosides (Scheme 27). For *N*-alkylation of 2-unsubstituted nucleosides 6-chloropurine riboside (**28**) had been used. For the 2,6-dihalo-subsubstituted

derivatives **97** and **99**, the reaction was selective for the 6-position. The progress of the reaction could be monitored by TLC and the reaction was stopped before 2-alkylation started. Deprotection of the intermediates **115-126** was achieved in a solution of 2% NaOMe in methanol to provide **127-138**. All compounds, intermediate and final products were purified by column chromatography.

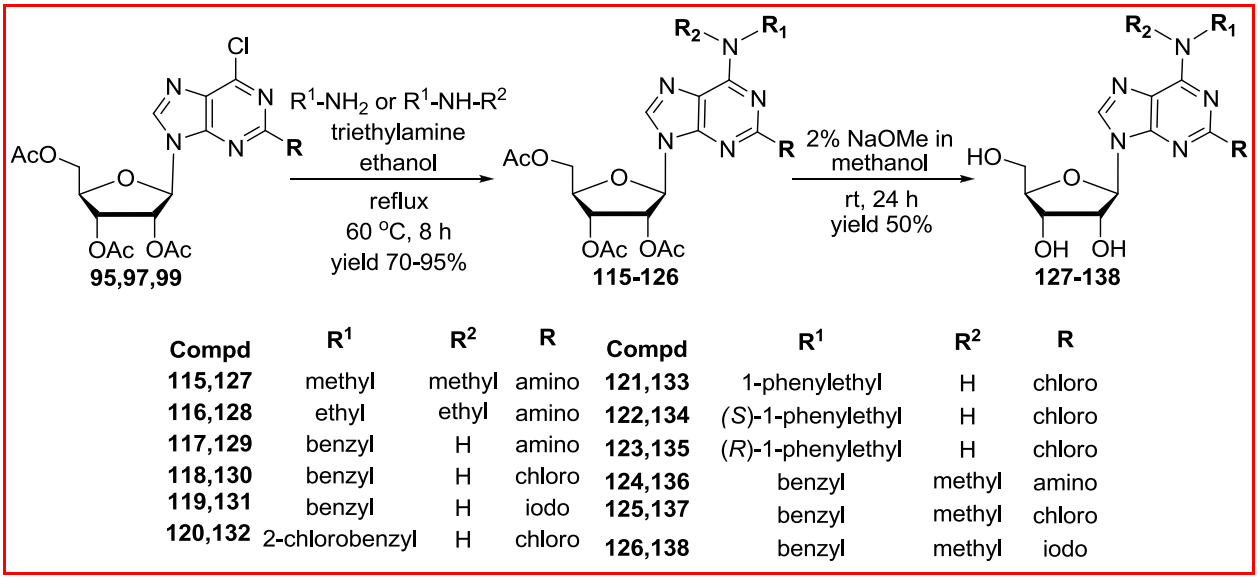

Compd	R^1	R^2	R
115,127	methyl	methyl	amino
116,128	ethyl	ethyl	amino
117,129	benzyl	H	amino
118,130	benzyl	H	chloro
119,131	benzyl	H	iodo
120,132	2-chlorobenzyl	H	chloro

Compd	R^1	R^2	R
121,133	1-phenylethyl	H	chloro
122,134	*(S)*-1-phenylethyl	H	chloro
123,135	(*R*)-1-phenylethyl	H	chloro
124,136	benzyl	methyl	amino
125,137	benzyl	methyl	chloro
126,138	benzyl	methyl	iodo

Scheme 27. Synthesis of 2-amino, 2-choro or 2-iodo-N^6-mono/dialkyl or aryl-purine ribosides (**127-138**)

6.5.2. Phosphorylation of 2,6-disubstituted purine ribosides (127-138)

All nucleoside derivatives **127-138** were phosphorylated using the earlier optimized method to give the target nucleotides **139-150** (Scheme 28).

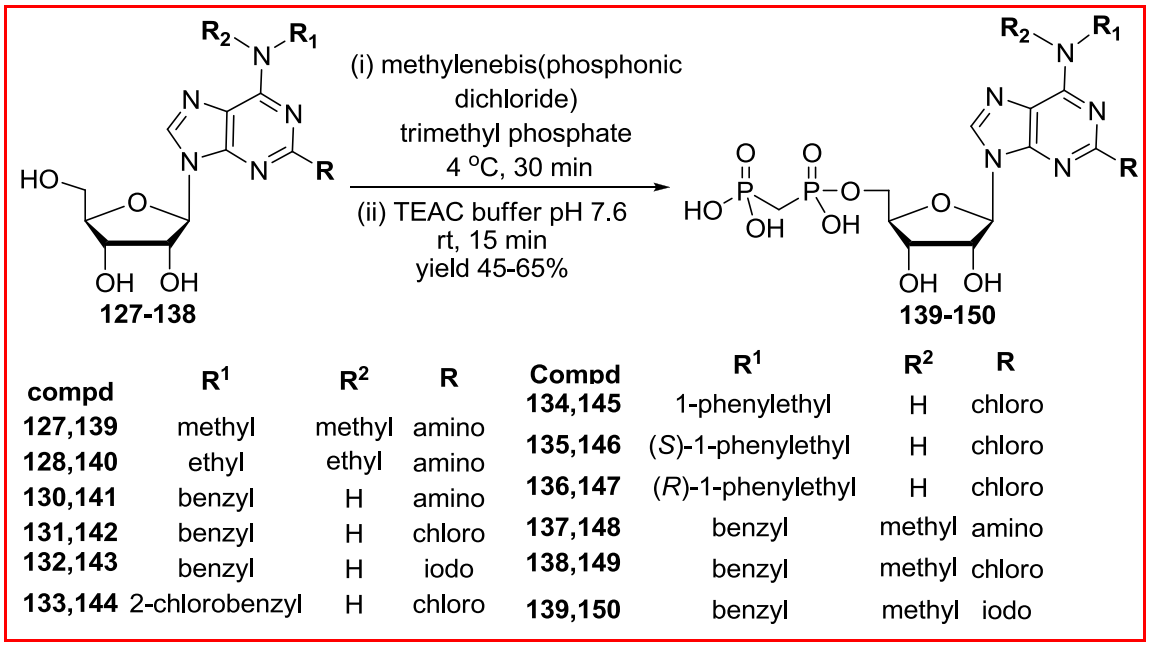

compd	R^1	R^2	R
127,139	methyl	methyl	amino
128,140	ethyl	ethyl	amino
130,141	benzyl	H	amino
131,142	benzyl	H	chloro
132,143	benzyl	H	iodo
133,144	2-chlorobenzyl	H	chloro

Compd	R^1	R^2	R
134,145	1-phenylethyl	H	chloro
135,146	(*S*)-1-phenylethyl	H	chloro
136,147	(*R*)-1-phenylethyl	H	chloro
137,148	benzyl	methyl	amino
138,149	benzyl	methyl	chloro
139,150	benzyl	methyl	iodo

Scheme 28. Synthesis of target nucleotides **139-150**

6.6. Phosphorylation of further nucleosides

Other nucleosides like inosine (**25**), guanosine (**93**), 6-chloropurine riboside (**28**), 2-amino-6-chloropurine riboside (**96**), 2,6-diaminopurine riboside (**155**) and isoguanosine (**157**) was phosphorylated to yield the corresponding nucleotides.

6.6.1. Phosphorylation of inosine (25)

Inosine (**25**) was phosphorylated using the earlier optimized method to give the target nucleotide **151**. It was purified by ion exchange chromatography followed by HPLC.

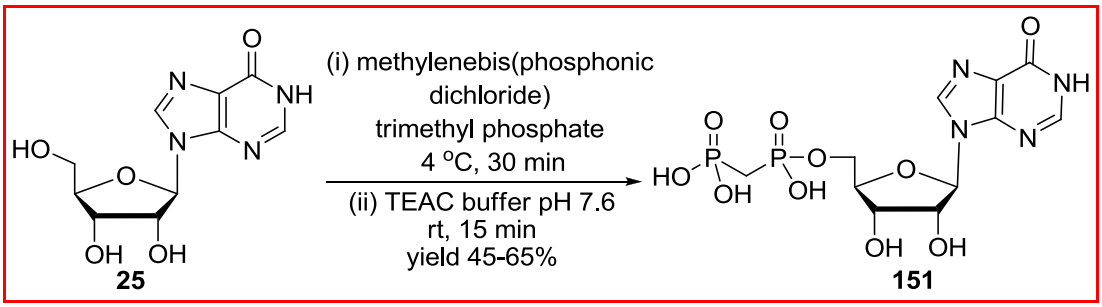

Scheme 29. Synthesis of inosine-5′-*O*-[(phosphonomethyl)phosphonic acid] (**151**)

6.6.2. Phosphorylation of 2-chloropurine riboside (28)

6-Chloro-purine riboside (**28**) was phosphorylated using the earlier optimized method to give the corresponding target nucleotide **152**.

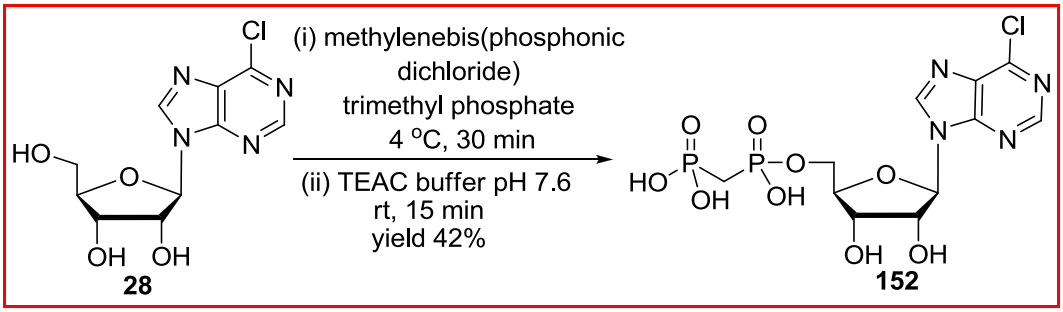

Scheme 30. 6-chloropurine riboside-5′-*O*-[(phosphonomethyl)phosphonic acid] (**152**)

6.6.3. Phosphorylation of guanosine (93)

Guanosine (**93**) was phosphorylated using the earlier optimized method to yield nucleotide **153**.

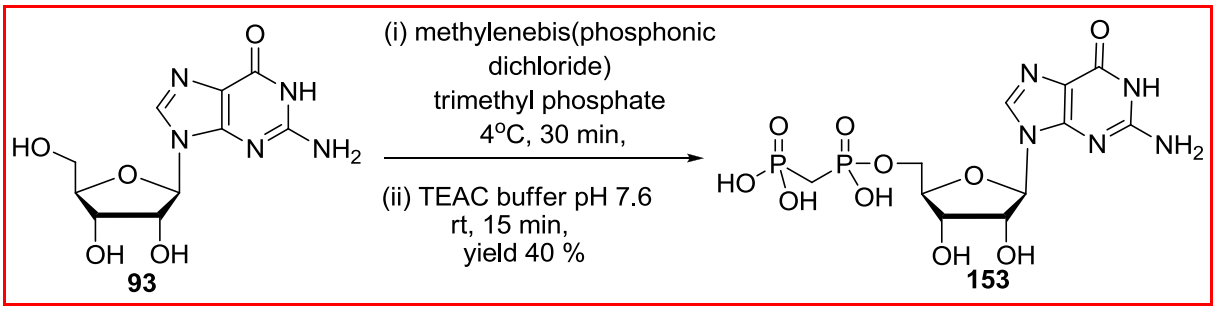

Scheme 31. Synthesis of guanosine-5′-*O*-[(phosphonomethyl)phosphonic acid] (**153**)

6.6.4. Phosphorylation of 2-amino-6-chloropurine riboside (96)

2-Amino-6-chloropurine riboside (**96**) was phosphorylated using the previously optimized method to give nucleotide **154**.

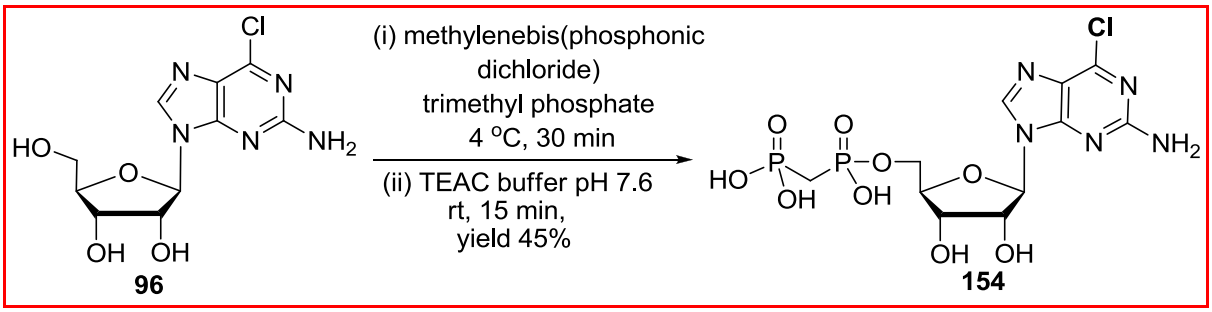

Scheme 32. Synthesis of 2-amino-6-chloropurine riboside-5′-*O*-[(phosphonomethyl)phosphonic acid] (**154**)

6.6.5. Synthesis and phosphorylation of 2,6-diaminopurine riboside (155)

2,6-Diaminopurine riboside (**155**) was synthesized from 2-amino-6-chloropurine riboside (**96**) by the same method as previously used for the synthesis of 2-chloro- and 2-iodo-adeonsine by treatment of **96** with ammonia in ethanolic solution. Compound **155** was phosphorylated using the previously optimized method to give nucleotide **156**.

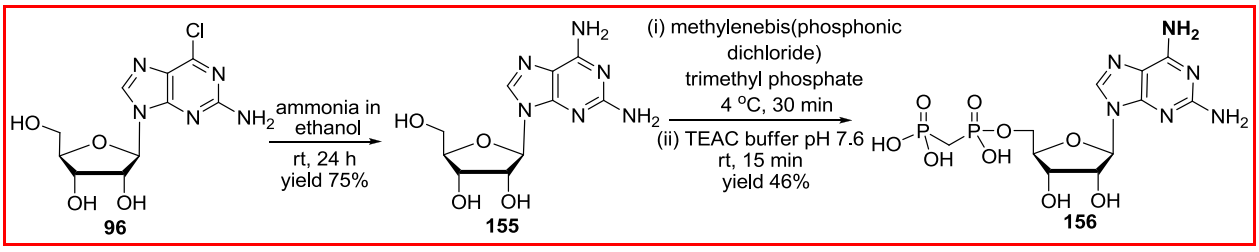

Scheme 32. Synthesis of 2,6-diaminopurine riboside-5′-*O*-[(phosphonomethyl)phosphonic acid] (**156**)

6.6.6. Synthesis and phosphorylation of isoguanosine (157)

Isoguanosine (**157**) was synthesized from 2,6-diaminopurine riboside (**155**) by selective deamination at the 2-position by nitrous acid.[162] Nitrous acid was generated *in situ* by using sodium nitrite and acetic acid. For this reaction sodium nitrite was used in excess. Isoguanosine was phosphorylated using the previously optimized method to give the nucleootide **158**.

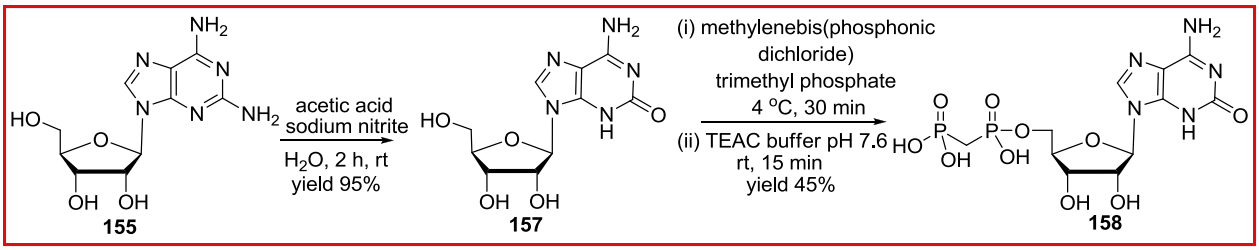

Scheme 33. Synthesis of isoguanosine-5′-*O*-[(phosphonomethyl)phosphonic acid] (**158**)

6.7. Synthesis of methylene diphosphonate-side chain-modified analogues of AOPCP (161, 162)

Various substituted bisphosphonates,e.g. etidronate, clodronate, alendronate etc are used as drugs for the treatment of osteoporosis.[163] We selected two non-nitrogen containing first-generation bisphosphonates, and commercially procured the compounds as free acids. The two compounds were clodronic acid [(dichloro-phosphono-methyl)phosphonic acid] and etidronic acid [(1-hydroxyethan-1,1-diyl)bis(phosphonic acid)]. They were employed for the preparation of the side-chain modified AOPCP analogues adenosine-5′-dichloromethylenediphosphonic acid (**161**) and adenosine-5′-(1-hydroxy)ethane-1,1-diphosphonic acid (**162**).

6.7.1. Synthesis of adenosine-5′-dichloromethylenediphosphonic acid (161)

There are several methods for the phosphorylation of adenosine by nucleophilic displacement of 5′-halogen or sulfonate ester derivative using activated bisphosphonate derivatives. For the synthesis of targeted compound we utilized the procedure by Davisson *et al*., where nucleophilic displacement of 5′-*O*-tosyl-nucleosides by the tris-(tetra-*n*-butylammonium) salt of substituted-bis(phosphonic acid)s affords the desired products.[137-139] But this is the multi-step method which involves protection of adenosine at the 2′,3′-position, tosylation at the 5′-position, followed by displacement of the tosyl moiety with tris-(tetra-*n*-butylammonium) bisphonates, and final deprotection at the 2′-,3′-position to gave the desired products.

The reaction was started from the commercially available adenosine. Adenosine was protected at the 2′-hydroxyl and 3′-hydroxyl group to give 2′,3′-*O*-isopropylidene-adenosine (**159**) by the earlier reported process using acetone, 2,2-dimethoxypropane and sulfuric acid. Protection of the 2′- hydroxyl and 3′-hydroxyl groups of ribose is essential for 5′-tosylation as all hydroxyl groups are reactive towards the tosylating reagent. 2′,3′-*O*-Isopropylidene-5′-tosyladenosine was prepared by reacting 2′,3′-*O*-isopropylidene-adenosine (**159**) with *p*-toluenesulphonyl chloride in the presence of DMAP as a catalyst and pyridine as a solvent.[138] After completion of the reaction 5′-tosylated adenosine was obtained as a white solid after evaporation of solvent pyridine *in vacuo* followed by extraction and crystallization. The substituted bisphosphonic acids were converted to their tris-(tetra-*n*-butylammonium) salts by trituration with tetra-butylammonium hydroxide in methanol, followed by evaporation of the methanol in vacuo and finally lyophilization of the obtained slurry after adding water to get white fine powders.[138]

The next step was the phosphoryation where tris-(tetra-*n*-butylammonium) dichloromethyl-enebis(phosphonic dichloride) dissolved in DMF in an air-tight flask was added slowly to the 5′-tosylated adenosine **160**.[138] After stirring of the mixture for 36 h, water was added and the mixture was lyophilized. It was purified by ion-exchange chromatography to give 2′,3′-*O*-isopropylidene- adenosine 5′-dichloromethylenediphosphonic acid, which was then deprotected by 6-8% trifluoroacetic acid in water : $CHCl_3$ (9 : 1), followed by a purification with HPLC to obtain the desired nucleotide adenosine-5′-dichloromethylenediphosphonic acid (**161**).

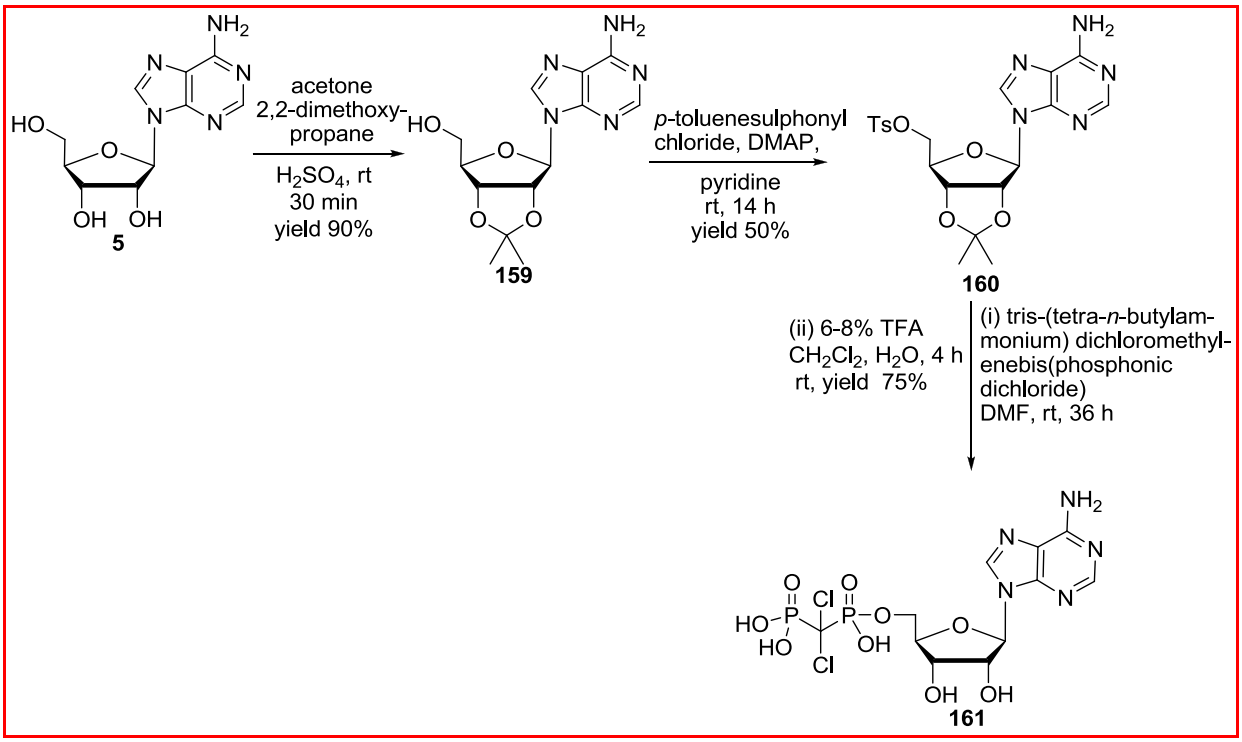

Scheme 34. Synthesis of adenosine-5′-dichloromethylenediphosphonic acid (**161**)

6.7.2. Synthesis of adenosine-5′-(1-hydroxy)ethane-1,1-diphosphonic acid (162)

The desired compound was obtained by same process as described for **161** where 5′-tosyldenosine derivative **160**, was reacted with tris(tetra-*n*-butylammonium) 1-hydroxyethane-1,1-diphosphonic acid.

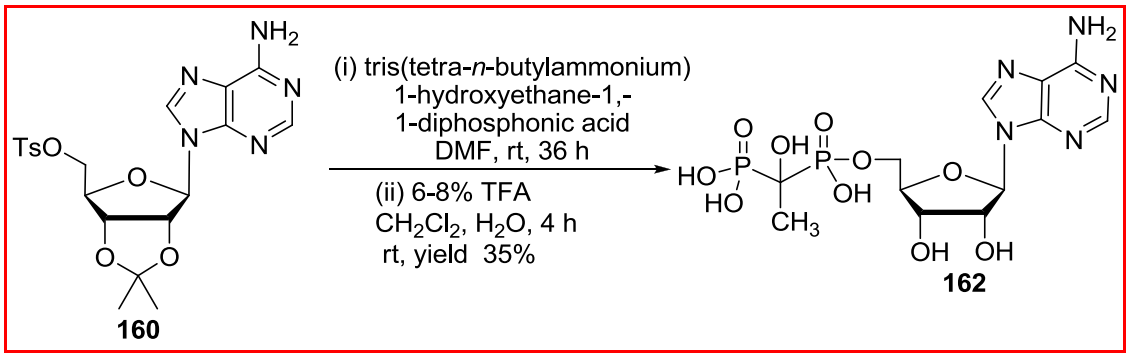

Scheme 35. Synthesis of adenosine-5′-(1-hydroxy)ethane-1,1-diphosphonic acid **(162)**

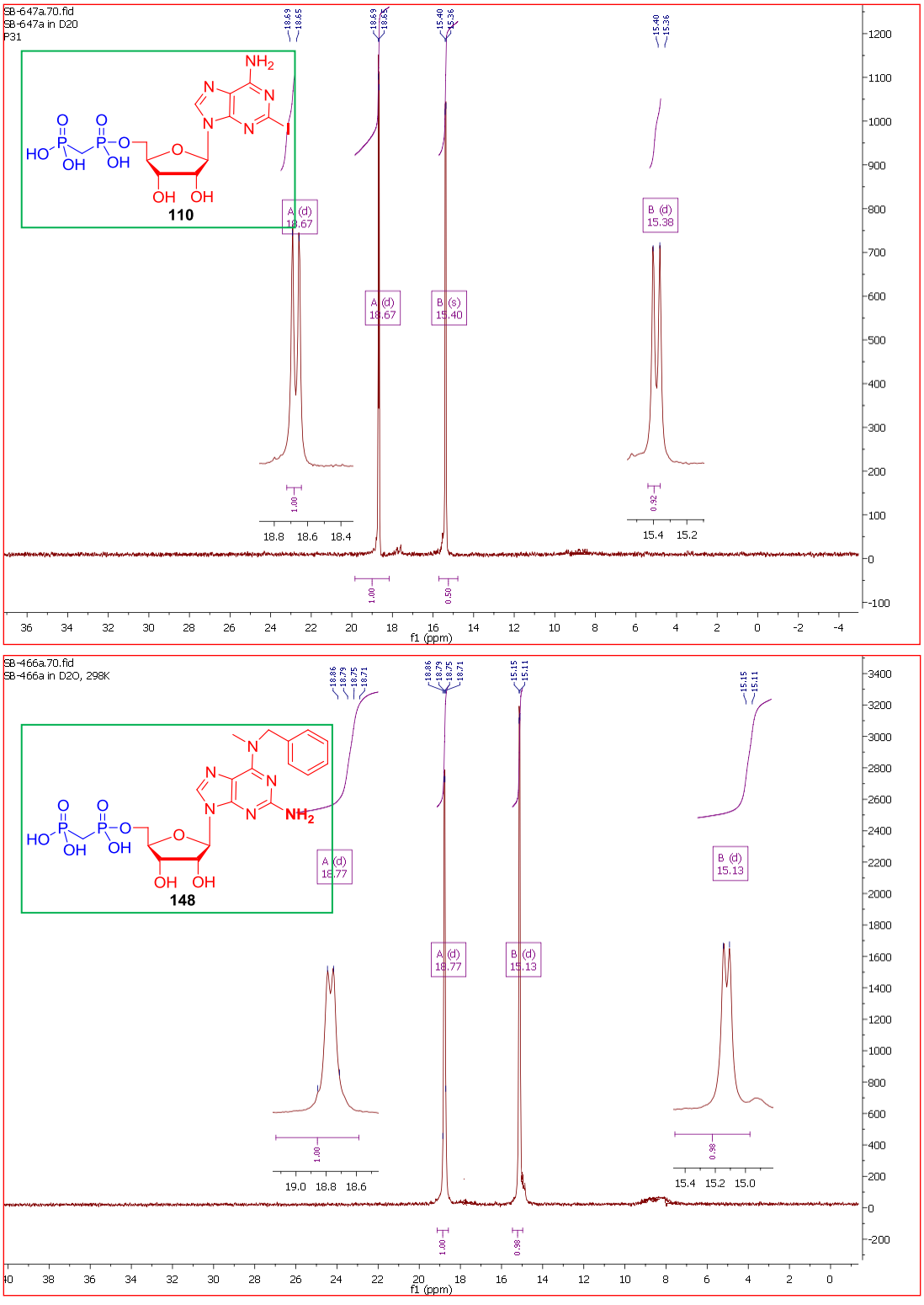

Figure 14. ^{31}P NMR spectra (202 MHz, D_2O) δ ppm: purity control of compound **110** and **148** respectively

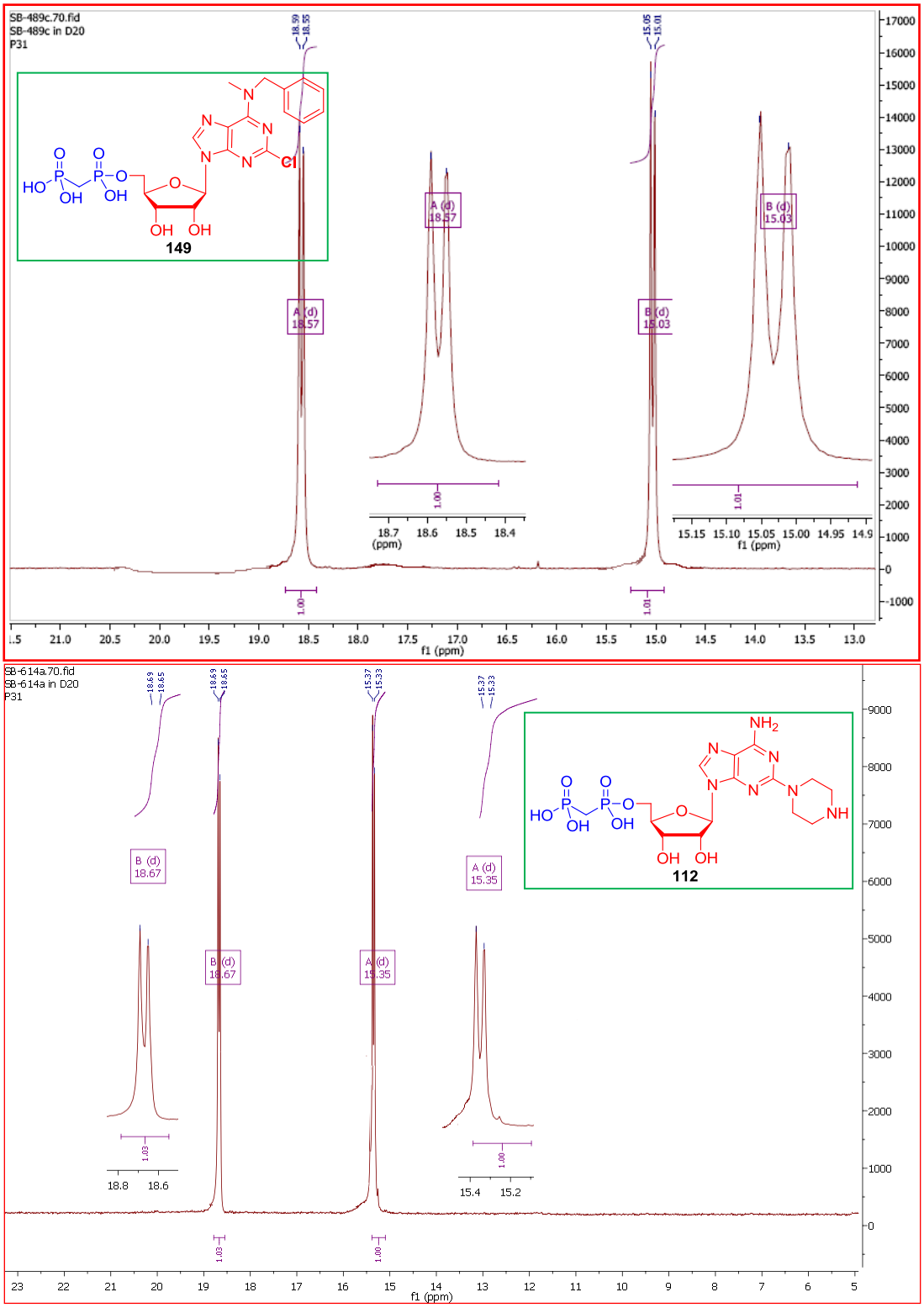

Figure 15. ^{31}P NMR spectra (202 MHz, D_2O) δ ppm: purity control of compound **149** and **112** respectively

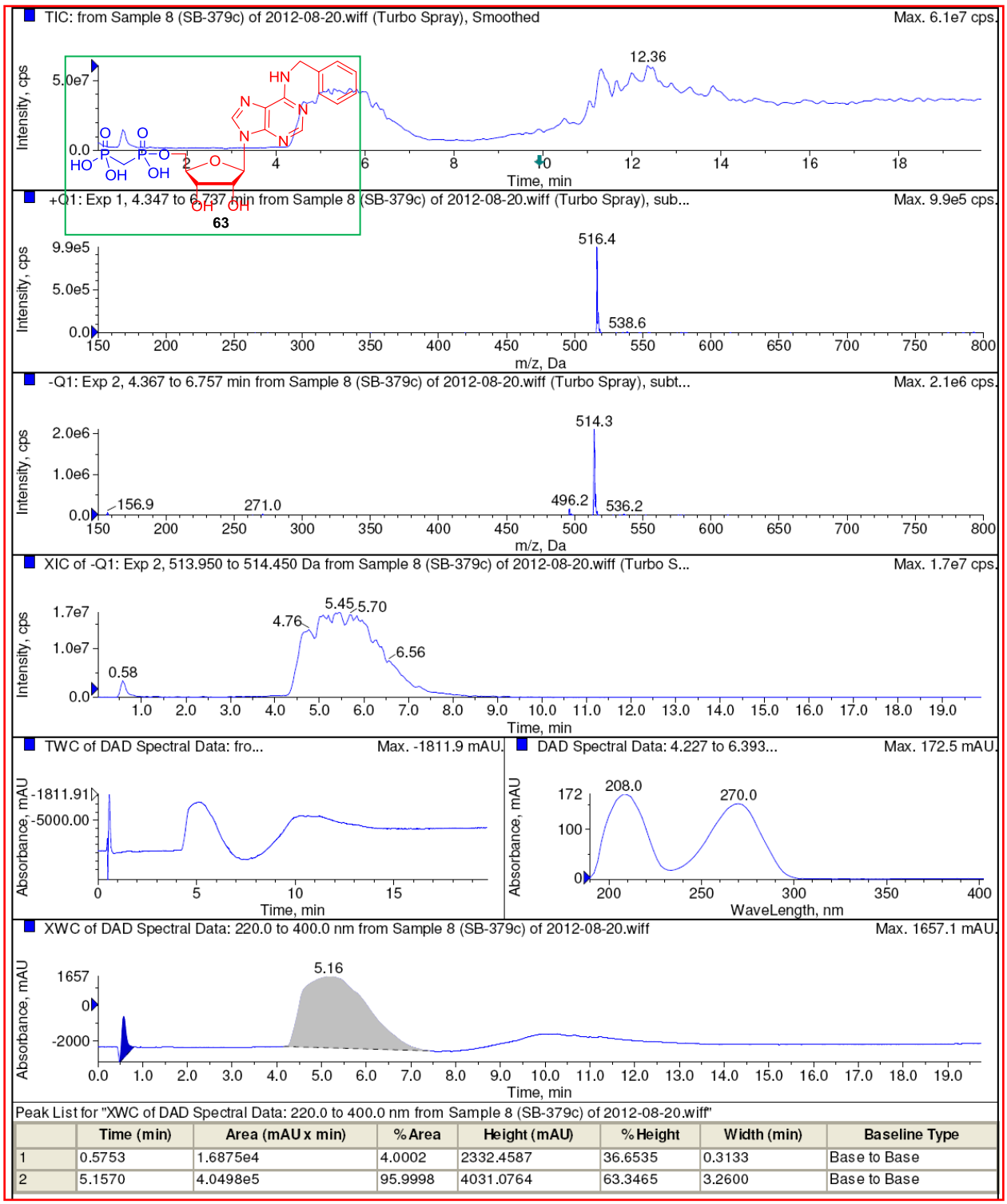

Peak List for "XWC of DAD Spectral Data: 220.0 to 400.0 nm from Sample 8 (SB-379c) of 2012-08-20.wiff"

	Time (min)	Area (mAU x min)	% Area	Height (mAU)	% Height	Width (min)	Baseline Type
1	0.5753	1.6875e4	4.0002	2332.4587	36.6535	0.3133	Base to Base
2	5.1570	4.0498e5	95.9998	4031.0764	63.3465	3.2600	Base to Base

Figure 16. LC/ESI-MS spectra of the synthesized nucleotide **63** (mass spectra in the positive and negative mode)**,** HPLC chromatogram of **63** and its purity determined by HPLC-DAD from 220-300 nm (100 %).

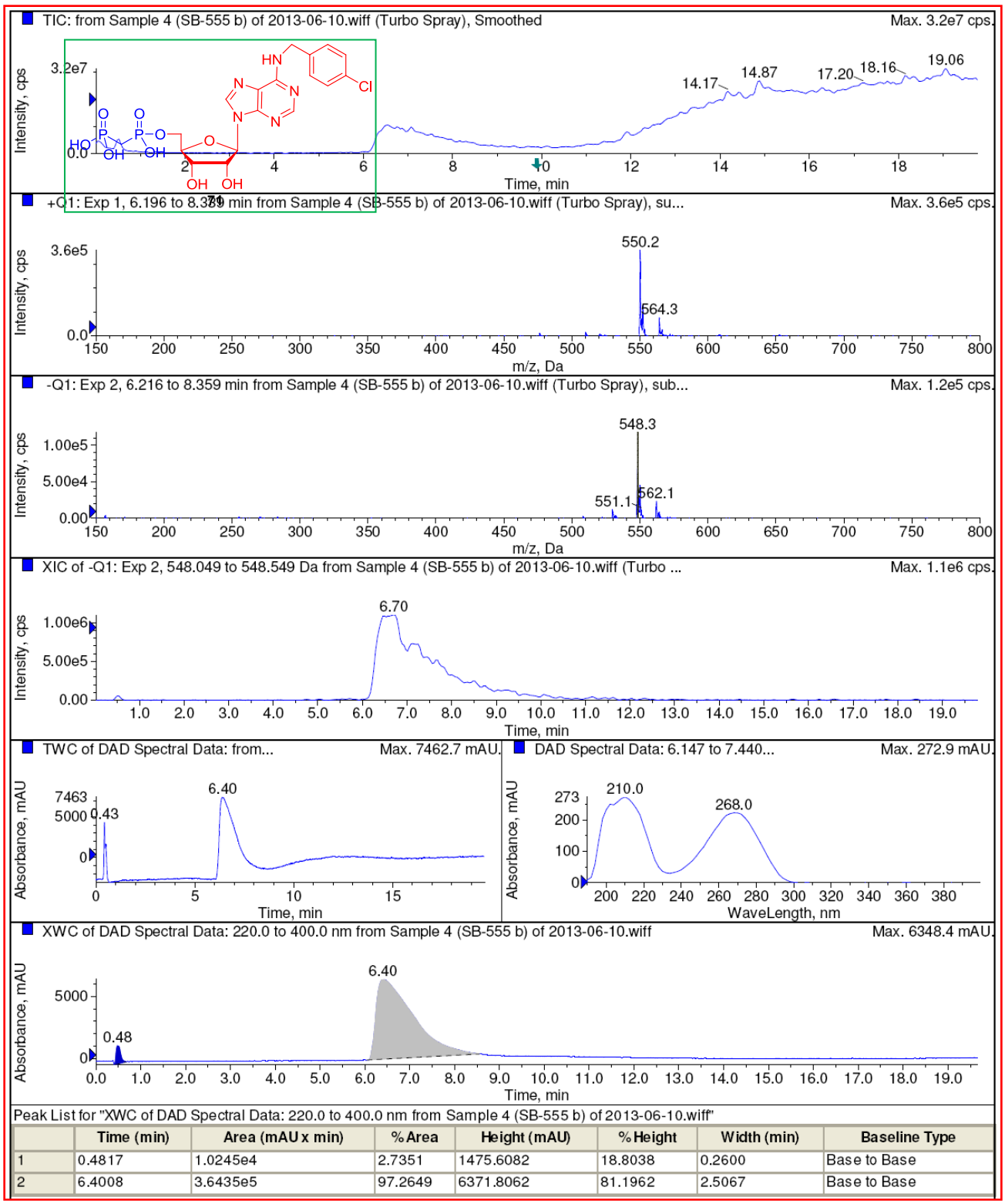

Peak List for "XWC of DAD Spectral Data: 220.0 to 400.0 nm from Sample 4 (SB-555 b) of 2013-06-10.wiff"

	Time (min)	Area (mAU x min)	% Area	Height (mAU)	% Height	Width (min)	Baseline Type
1	0.4817	1.0245e4	2.7351	1475.6082	18.8038	0.2600	Base to Base
2	6.4008	3.6435e5	97.2649	6371.8062	81.1962	2.5067	Base to Base

Figure 17. LC/ESI-MS spectra of the synthesized nucleotide **71** (mass spectra in the positive and negative mode)**,** HPLC chromatogram of **71** and its purity determined by HPLC-DAD from 220-300 nm (100 %).

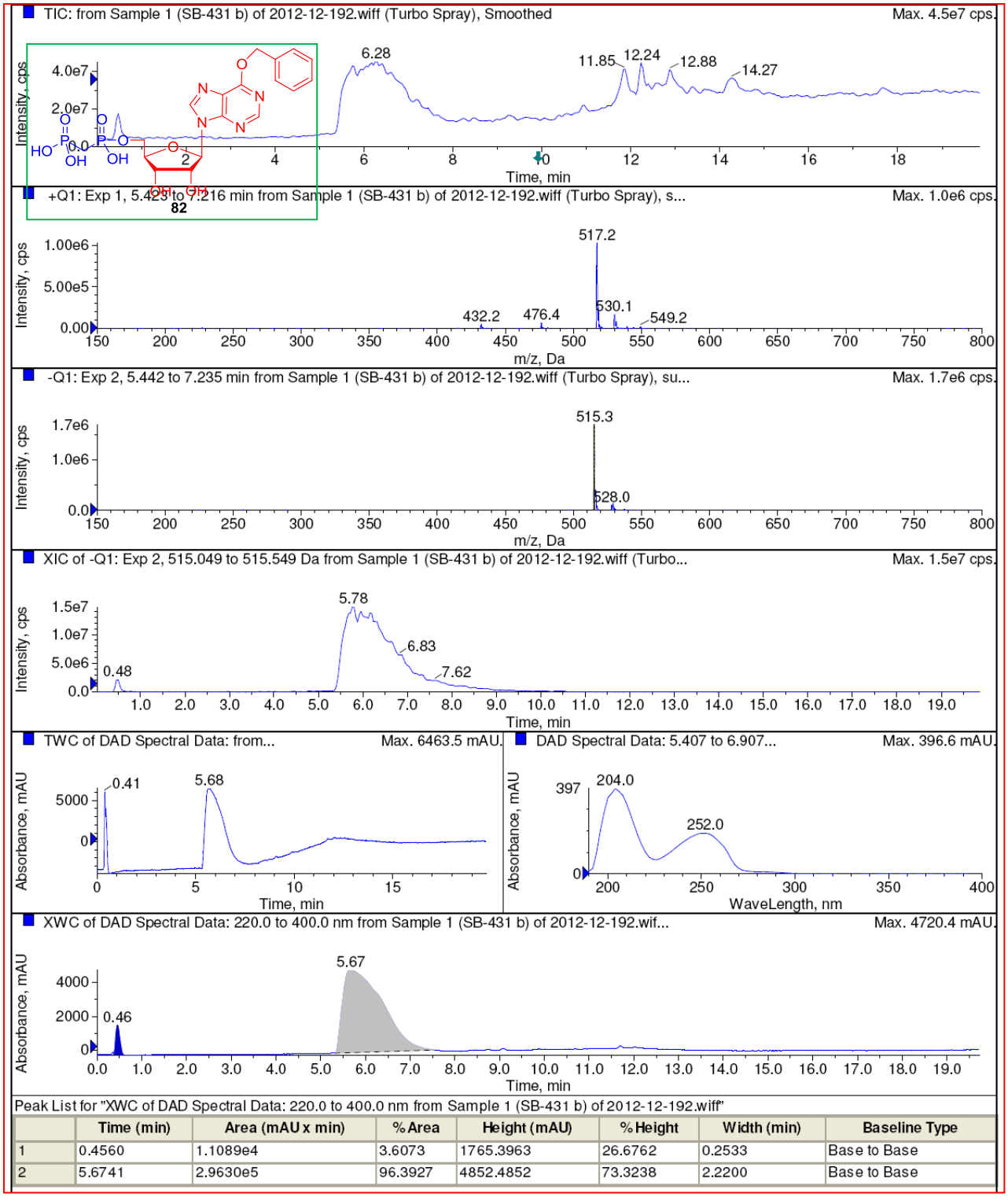

Peak List for "XWC of DAD Spectral Data: 220.0 to 400.0 nm from Sample 1 (SB-431 b) of 2012-12-192.wiff"

	Time (min)	Area (mAU x min)	% Area	Height (mAU)	% Height	Width (min)	Baseline Type
1	0.4560	1.1089e4	3.6073	1765.3963	26.6762	0.2533	Base to Base
2	5.6741	2.9630e5	96.3927	4852.4852	73.3238	2.2200	Base to Base

Figure 18. LC/ESI-MS spectra of the synthesized nucleotide **82** (mass spectra in the positive and negative mode)**,** HPLC chromatogram of **82** and its purity determined by HPLC-DAD from 220-300

7. Results and discussion - part II: Pharmacological Evaluation

Enzyme inhibition was determined in radiometric *e*N assay using [^{3}H]AMP as a substrate. The compounds were investigated in *e*N by Marianne Freundlieb.[118] Selectivity studies at *e*NPP 1-3 were done by Sang-Yong Lee, *e*NTPDase 1-3 by Amelie Zech and $P2Y_1$ and $P2Y_{12}$ receptor studies by Dr. Aliaa Abdelrahman.

Compounds were investigated in radiometric enzyme inhibition assay at recombinant rat *e*N at 10 different concentrations in triplicate. For all compounds full concentration-response curves were determined and K_i values were calculated from the obtained IC_{50} values using the Cheng-Prusoff equation.[164] Results are summarized in Table 12-17 and curves are shown in Figure 19.

7.1. Pharmacological Evaluation at rat *e*N

A series of 60 derivatives (see Table 12-17) were evaluated at rat *e*N. ADP and its methylene analog AOPCP tested under the same condition showed K_i values of 3880 and 197 nM, respectively. All tested inhibitors were competitive inhibitors of rat *e*N.

7.1.1. Structure-activity relationships of 6-substituted AOPCP derivatives at rat *ecto*-5′-nucleotidase

6-(Ar)alkylamino-substitution of AOPCP improved potency. But, 6-(ar)alkylamino-substituted 2′,3′-*O*-isopropylidene-protected-derivatives showed reduced potency as compared to the standard inhibitor AOPCP. There was a correlation between the substitution pattern and the compounds' potency. Studies were started with simpler alkyl groups like methyl and ethyl at the N^6-position. Substitution at the N^6-position appears to be beneficial as their inhibitory potency was improved. 2′,3′-*O*-Isopropylidene-protected compounds were also tested. All 2′,3′-*O*-isopropylidene-protected compounds were less potent than the corresponding unsubstituted ribosides. The lower potency of 2′,3′-*O*-isopropylidene-protected compounds indicates that free 2′,3′-hydroxyl group are important to form hydrogen bonds with aspartic acid and asparagine residues (as suggested by the crystal structure, PDB code 4H2I).[71, 72] Among the 2′,3′-*O*-isopropylidiene-protected compounds, the N^6-monoethyl-substituted derivative **54** was the best one with a K_i value of 365 nM. Among the N^6-alkyl-substituted derivatives, the rank order of potency was N^6-ethyl derivative **58** (K_i 43.8 nM, 4.5-fold improvement in potency as compared with AOPCP) > N^6-diethyl-substituted derivate **60** (K_i 68.0 nM, 3-fold improvement in potency as compared with AOPCP) > N^6-dimethyl-substituted derivate **59** (K_i 86.0 nM). Compound **54** is the 2′,3′-*O*-isopropylidene-protected derivative of **58**. Since the di-substituted derivatives will not yield adenosine receptor-activating metabolites we also synthesized derivatives with unsymmetrical alkyl-substitution at the N^6-position, i.e. N^6-ethyl-N^6-methyl-substituted derivative **61**, which showed a K_i value of 23.6 nM (8.5-fold improvement in potency as compared with AOPCP). This was the best compound among the N^6-alkyl-substituted derivatives.

Table 11. Inhibitory potency of N^6-substituted-purine riboside-5′-*O*-[(phosphonomethyl)phosphonic acid] derivatives at rat *ecto*-5′-nucleotidase

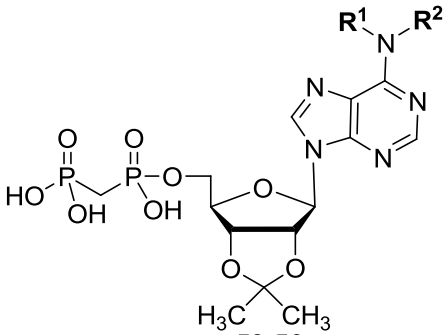

53-56

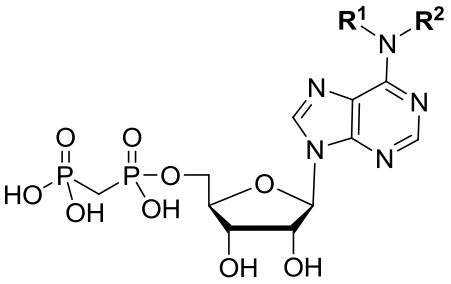

AOPCP, 57-76

Compd.	R^1	R^2	rat *e*N $K_i \pm SEM^a$ (nM)
AOPCP	H	H	**197** ± 5.00
53	methyl	H	**3870** ± 918
54	ethyl	H	**365** ± 31
55	methyl	methyl	**415** ± 60.0
56	ethyl	ethyl	**679** ± 49.0
57	methyl	H	**104** ± 13.0
58	ethyl	H	**43.8** ± 0.30
59	methyl	methyl	**86.0** ± 19.1
60	ethyl	ethyl	**68.0** ± 5.10
61	ethyl	methyl	**23.6** ± 4.90
62	phenyl	H	**36.8** ± 4.70
63	benzyl	H	**9.03** ± 1.24
64	2-phenylethyl	H	**8.04** ± 2.24
65	benzyl	methyl	**4.64** ± 0.20
66	benzyl	ethyl	**76.4** ± 5.00
67	benzyl	benzyl	**92.5** ± 8.50
68	4-aminobenzyl	H	**29.0** ± 1.70

69	4-chlorobenzyl	H	**7.23** ± 0.78
70	3-chlorobenzyl	H	**8.18** ± 3.85
71	2-chlorobenzyl	H	**3.56** ± 0.83
72	4-hydroxybenzyl	H	**9.06** ± 1.45
73	4-methoxybenzyl	H	**4.84** ± 0.30
74	1-phenylethyl	H	**3.39** ± 0.59
75	4-nitrobenzyl	H	**17.6** ± 1.50
76	4-sulphamoylbenzyl	H	**14.4** ± 1.70

[a][^{3}H]AMP (5 µM) was used a substrate (K_m value 59 µM).

From these results we concluded that hydrophobic groups are tolerated at the 6-position. Thus, we designed and synthesized aryl-substituted derivatives. Initially N^6-phenyl-substituted derivative **62** was synthesized, which showed K_i value of 36.8 nM (5-fold improvement in potency as compared with AOPCP). Since the aryl-substitution was also improving potency, we designed derivatives with increased length of the carbon chain between the amino group and the terminal aryl group. To serve this purpose N^6-benzyl-substituted derivative **63** and N^6-phenylethyl-substituted derivative **64** were synthesized. Both of these substituents produced a tremendous improvement in potency yielding low nano-molar range inhibitors. This indicated that longer and bulkier alkyl-substituents at the N^6-position are beneficial. N^6-benzyl-substituted derivative **63** and N^6-phenylethyl-substituted derivative **64** showed K_i values of 9.03 nM (22-fold improvement in potency as compared with AOPCP) and 8.04 nM (25-fold improvement in potency as compared with AOPCP) respectively. Elongation of the linker between the 6-amino group and the distal aromatic group led to an increase in potency, but the products were all monosubstituted derivatives. Their potential metabolites might activate adenosine receptors after the cleavage of the methylene diphosphate residue. Since N^6-phenylethyl-substitution is more

bulky than N^6-benzyl-substitution, we modified the N^6-benzyl-derivative yielding N^6-disubstituted derivatives. Symmetrical di-substitution as well as unsymmetrical derivatives with smaller alkyl groups like methyl and ethyl were obtained. N^6-benzyl-N^6-methyl-substituted derivative **65** showed a K_i value of 4.64 nM (43-fold improvement in potency as compared with AOPCP). Similarly, N^6-benzyl-N^6-ethyl-substituted derivative **66**, was synthesized as N^6-diethyl-substituted derivative **60** was more potent than N^6-dimethyl-substituted derivate **59**. Derivative **66** showed a slight improvement in potency with 76.4 nM. N^6-Dibenzyl-substituted derivative **66** was less potent with a K_i value of 76.4 nM. Surprisingly, we observed that introduction of unsymmetrical substitution at the N^6-position was better than a symmetrical substitution pattern (observable for N^6-ethyl-N^6-methyl derivative **61**, K_i 23.6 nM versus N^6-diethyl **60**, K_i 68.0 nM, and N^6-benzyl-N^6-methyl derivative **65**, K_i 4.64 nM versus N^6-dibenzyl, **67**, K_i 92 nM). These results also indicate that disubstitution at N^6 may increase the compounds' potency, but while one of the N^6-substituents may be large, the size of the second one is more limited and should preferably be a methyl group.

Table 12. Potency of inosine-5′-*O*-[(phosphonomethyl)phosphonic acid], 6-chloro-purine riboside-5′-*O*-[(phosphonomethyl)phosphonic acid], and O^6- and S^6-substituted-purine riboside-5′-*O*-[(phosphonomethyl)phosphonic acid] at rat *ecto*-5′-nucleotidase

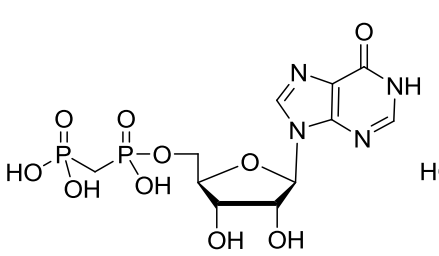

151

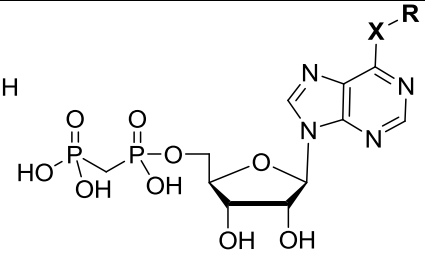

81-83

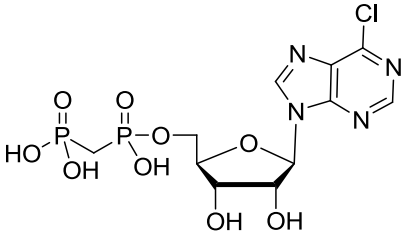

152

Compd.	**X**	**R**	**rat *e*N** $K_i \pm SEM^a$(nM)
151	see structure above		**2830** ± 421
81	O	ethyl	**32.0** ± 4.10

82	O	benzyl	**9.20** ± 0.52
83	S	benzyl	**9.50** ± 1.79
152	see structure above		**161** ± 0.14

[a][^{3}H]AMP (5 µM) was used a substrate (K_m value 59 µM).

The benzyl-substituted derivative **63** was selected for further modification due to its high potency, and because a large number of substituted benzylamine derivatives were easily accessible. So, we designed benzyl-substituted derivatives by making various substitutions on the benzyl ring like 4-amino, 4-chloro, 3-chloro, 2-chloro, 4-hydroxy, 4-methoxy, 4-nitro, 4-sulphamoyl and 1-phenylethyl. The order of potency was 1-phenylethyl derivative **74** (K_i 3.39 nM, 59-fold improvement in potency as compared with AOPCP) > 2-chlorobenzyl derivatives **71** (K_i 3.56 nM) > 4-methoxybenzyl derivatives **73** (K_i 4.84 nM) > 4-chlorobenzyl derivatives **69** (K_i 7.23 nM) > 3-chlorobenzyl derivatives **69** (K_i 8.18 nM) > 4-sulfamoylbenzyl-substituted derivative **76** (K_i 14.4 nM) > 4-nitrobenzyl-substituted derivative **75** (K_i 17.6 nM) > 4-aminobenzyl derivatives **68** (K_i 29.0 nM). Electron-withdrawing groups (e.g. Cl) appeared to be better tolerated in the *p*-position of the phenyl ring than electron-donating functions (NH_2). 1-Phenylethyl derivative **74** was the most potent compound among the 6-substitued derivatives. The nitrogen atom at 6-position of the adenine ring was exchanged for oxygen or sulfur yielding of O^6- and S^6-substituted derivatives. The synthesis of O^6- and S^6- substituted derivatives is also justified as their metabolites will also not yield adenosine receptor activating compounds. This offers the possibility to move away from adenine nucleotide derivatives, which might be metabolized to (N^6-substituted) adenosine derivatives after hydrolysis of the ester bond between the ribose and the diphosphonate moiety. Certain N^6-substituted adenosine derivatives are known to potently activate adenosine A_1 receptors and may thereby induce negative inotropic and

chronotropic effects, which might even lead to cardiac arrest.[166-167] All O^6- and S^6- substituted derivatives showed retainment of activity which confirmed the notion that hydrogen bond-donating groups are not required at position 6. When N^6-benzyl derivative **63** (K_i 9.03 nM), was compared with O^6-benzyl derivative **82** (K_i 9.20 nM), both gave comparable potency (21-fold improvement in potency as compared with AOPCP). Similarly, N^6-ethyl was replaced by O^6-ethyl also resulting in nearly comparable potency; derivative **81** with (K_i 32.0 nM) and derivative **58** with (K_i 43.8 nM). S^6-Benzyl derivative **83** (K_i 9.52 nM) also showed comparable activity (21-fold improvement in potency as compared with AOPCP). The bisphosphonic acid derivative of inosine **151**, showed a complete loss of activity. In the case of compound **152** (K_i 157 nM), when the amino group at the 6-position of AOPCP (K_i 197 nM) was substituted by a 6-chloro function, there was a slight improvement in activity. This could be due to different, non-aromatic tautomeric structure of **151** as compared to AOPCP and **152**.

7.1.2. Structure-activity relationships of 8-substituted AOPCP derivative at rat *ecto*-5′-nucleotidase

8-Substituted derivatives were also evaluated under the same assay conditions. Among 8-halo-substituted derivatives 8-chloro-substituted derivative **90** was more potent as compared to 8-bromo-substituted derivative **89**. Compound **90** showed a K_i value of 93.5 nM which is a 2-fold improvement in potency as compared with AOPCP. Other 8-substituted derivatives, 8-thioethyl- and 8-amoinomethyl-substituted derivative **91** and **92**, showed reduced potency. These results showed that only small substituents were tolerated at the purine 8-position. A reason for this may be that larger 8-substituents can induce a conformational change from the *anti*- to the *syn*-conformation around the nucleosidic bond, which is unfavourable for binding to the enzyme. [168]

Table 13. Potency of 8-substituted-adenosine-5′-*O*-[(phosphonomethyl)phosphonic acid] derivatives at rat *ecto*-5′-nucleotidase

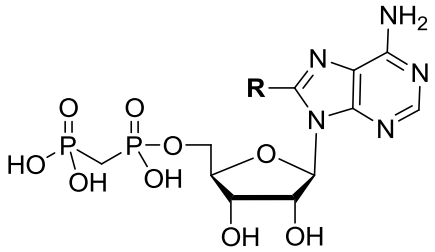

89-92

Compd.	R	rat *e*N K_i ± SEM[a](nM)
89	bromo	**491** ± 50
90	chloro	**93.5** ± 4.5
91	aminomethyl	**1720** ± 384
92	thioethyl	**3610** ± 576

[a][^{3}H]AMP (5 µM) was used a substrate (K_m value 59 µM).

7.1.3. Structure-activity relationships of 2-substituted AOPCP derivative at rat *ecto*-5′-nucleotidase

Several substituents at the 2-position produced improved potency. SARs were also studied for the 2-substituted AOPCP derivatives. Studies were started with nucleotide derivatives of guanosine and isoguanosine (isoguanosine > guanosine). Isoguanosine derivative **158** was 3-fold more potent than guanosine derivative **153**. But guanosine derivative **153** was more potent than inosine derivative **151**. Both of these nucleotides, guanosine derivative **153** and isoguanosine derivative **158** gave no improvement in potency as compared to AOPCP. The lower potency of guanosine and isoguanosine can be correlated to the low potency of inosine derivative **151**. 6-Chloro-2-amino-substituted derivative **154** was more potent as compared to guanosine derivative **153** and isoguanosine derivative **158**. 2,6-Diaminoadenosine nucleotide **156** was 2-fold more

potent as compared to AOPCP with a K_i value of 90.6 nM. Comparing the potency of derivatives **154** and **156** showed that the amino group at 2-position improves potency. Similarly, 2-halo-substitution produces a tremendous improvement in potency, e.g. 2-iodo substitution in **110** and 2-chloro-substitution in **109** gave K_i values of 15.1 nM and 18.6 nM, respectively. 2-Iodo substitution showed a 13-fold improvement in potency as compared to an 11-fold improvement in potency for the 2-chloro-substitution. 2-Iodo-substituted derivative **110** is the best derivative among the 2-substituted derivatives. Other 2-substituted derivatives like 2-hydrazinyl **111** did not significantly improve the activity but were more potent than AOPCP, however less potent than the 2,6-diamino-adenosine nucleotide **156**. 2-Piperazinyl-derivative **112** showed a complete loss of potency. The order of potency for 2-substituted compounds were: 2-iodo > 2-chloro > 2-amino > 2-hydrazinyl > 2-oxo >> piperazinyl. Among the 2-thio-substituted derivatives 2-cyclohexylethylthio derivative **114** was slightly more potent than 2-thioallyl-substituted derivative **113**. Compounds **113** and **114** were 3- and 3.5-fold more potent. From this various synthesized 2-substituted derivatives amino-, chloro- and iodo-substitution produced improvement in potency. So we combined these best 2-substituents with the best alkyl and aryl-substitution patterns to make derivatives with 6- and 2-disubstitution.

Table 14. Potency of 2-substituted-adenosine-5′-*O*-[(phosphonomethyl)phosphonic acid] derivatives at rat *ecto*-5′-nucleotidase

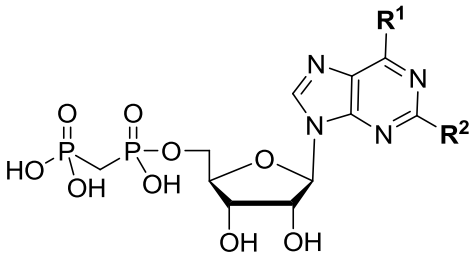

109-115, 153,154, 156,158

Compd.	R^1	R^2	rat eN $K_i \pm SEM^a$(nM)
153, guanosine dvts	oxo	amino	**1110** ± 350
158, isoguanosine dvts	amino	oxo	**326** ± 42
154	chloro	amino	**268** ± 21
156	amino	amino	**90.6** ±7.30
110	amino	iodo	**15.1** ± 1.20
109	amino	chloro	**18.6** ± 3.80
111	amino	hydrazinyl	**116** ± 18
112	amino	piperazinyl	**2290** ± 240
113	amino	thioallyl	**65.7** ± 5.60
114	amino	cyclohexylethylthio	**47.1** ± 8.30

[a][^{3}H]AMP (5 μM) was used a substrate (K_m value 59 μM).

7.1.4. Structure-activity relationships of 2,6-disubstituted AOPCP derivative at rat *ecto*-5′-nucleotidase

Various N^6-alkyl-substitutions was combined with a 2-amino residue. N^6-diethyl-, 2-amino-substituted derivative **140** was slightly more potent than the N^6-dimethyl-, 2-amino derivative **139**. Derivative **140** showed a K_i value of 29.8 nM. Compounds **140** and **139** were 6.6-fold and 5.7-fold more potent as compared to the lead compound AOPCP. These results were in accordance with results from 2-unsubstituted-N^6-disubstitiuted derivative, where the diethyl derivative was found to be more potent than the dimethyl derivative. These N^6-disubstituted compounds will not yield adenosine receptor-activating metabolites. Similarly N^6-benzyl was combined with the three best 2-substituents, namely chloro, iodo and amino. N^6-benzyl-2-amino-substituted derivative **141**, N^6-benzyl-2-chloro-derivative **142**, and N^6-benzyl-2-iodo-derivative **143** showed K_i values of 5.25, 1.23 and 1.53 nM, respectively. Compounds **142** was 160-fold more potent than the lead structure AOPCP. N^6-(2-Benzyl)-2-chloro derivative **144** (K_i = 0.34 nM) was 4-fold more potent than the N^6-benzyl-2-chloro derivative **142**, and 580-fold more potent as compared to AOPCP. Compound **144** is the most potent compound in the whole series. The potency of N^6-(1-phenylethyl)-2-chloro derivative **145** (K_i = 1.20 nM) was lower than that of N^6-(2-benzyl)-2-chloro derivative **144**. Since N^6-(1-phenylethyl)-2-chloro derivative **145** is racemic we also synthesized derivatives with different enantiomeric substituents which represent diastereomers. But there was no drastic difference in potency. N^6-((*S*)-1-Phenylethyl)-2-chloro derivative **146** (K_i = 0.92 nM) was slightly more potent as compared to N^6-((*R*)-1-phenylethyl)-2-chloro derivative **147** (K_i = 1.12 nM). Compound **146** showed 215-fold improvement in potency as compared to lead structure AOPCP. Since N^6-disubstituted derivatives are expected not to yield adenosine receptor-activating metabolites after hydrolysis, we synthesized derivatives combing N^6-benzyl-N^6-methyl and amino or iodo or chloro-substituents at the 2-

position. N^6-benzyl-N^6-methyl-2-amino derivative **148** showed a K_i value of 7.3 nM as compared to a K_i value of 2.20 nM for N^6-benzyl-N^6-methyl-2-iodo derivative **150** and a K_i value of 0.88 nM for N^6-benzyl-N^6-methyl-2-chloro derivative **149**. Compounds **149** and **150** showed 224- and 89-fold improvement in potency as compared to AOPCP.

Table 15. Potency of 2-amino, 2-chloro or 2-iodo-N^6-mono-/dialkyl- or aryl-adenosine-5′-*O*-[(phosphonomethyl)phosphonic acid] derivatives at rat *ecto*-5′-nucleotidase

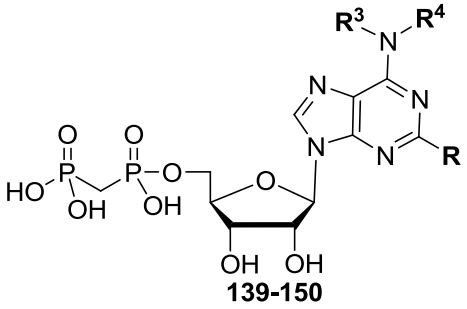

139-150

Compd.	R^3	R^4	R	rat *e*N $K_i \pm SEM^a$(nM)
139	methyl	methyl	amino	**34.1** ± 2.90
140	ethyl	ethyl	amino	**29.8** ± 1.70
141	benzyl	H	amino	**5.25** ± 1.10
142	benzyl	H	chloro	**1.23** ± 0.04
143	benzyl	H	iodo	**1.53** ± 0.24
144	2-chlorobenzyl	H	chloro	**0.34** ± 0.06
145	1-phenylethyl	H	chloro	**1.20** ± 0.04
146	(*S*)-1-phenylethyl	H	chloro	**0.92** ± 0.13
147	(*R*)-1-phenylethyl	H	chloro	**1.12** ± 0.28
148	benzyl	methyl	amino	**7.37** ± 1.36
149	benzyl	methyl	chloro	**0.88** ± 0.53
150	benzyl	methyl	iodo	**2.22** ± 0.11

[a][^{3}H]AMP (5 µM) was used a substrate (K_m value 59 µM).

7.1.5. Structure-activity relationships of AOPCP derivatives with modification of the methylene bis-phosphonate partial structure at rat *ecto*-5′-nucleotidase

Further derivatives with substitution in the methylene bisphosphonate side-chain of AOPCP were also synthesized. Adenosine-5′-dichloromethylenediphosphonic acid **161** and adenosine-5′-(1-hydroxy)ethane-1,1-diphosphonic acid **162** were tested the under same assay conditions. Both substitutions resulted in reduced potency.

Table 16. Potency of adenosine-5′-dichloromethylenediphosphonic acid and adenosine-5′-(1-hydroxy)ethane-1,1-diphosphonic acid

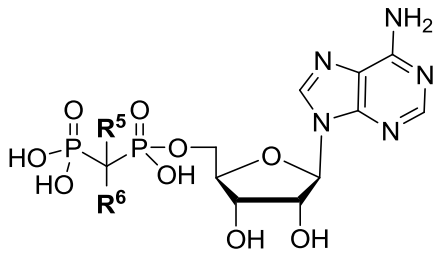

Compd.	R^5	R^6	rat *e*N K_i ± SEM[a](nM)
161	chloro	chloro	**292** ± 23
162	hydroxy	methyl	**4050** ± 240

[a][^{3}H]AMP (5 µM) was used a substrate (K_m value 59 µM).

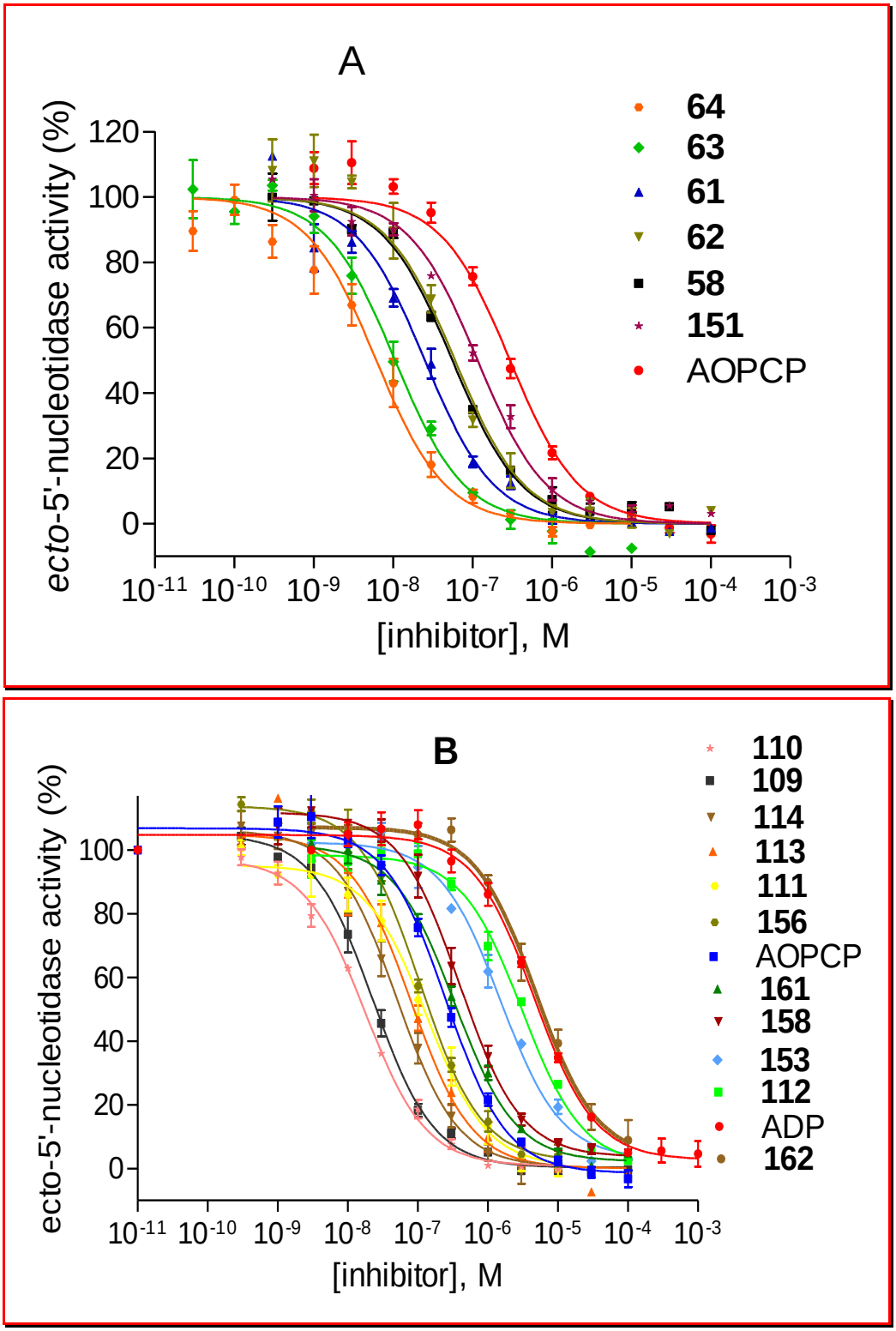

Figure 19. Radiometric assays at rat *e*N. Concentration-response curves of selected potent derivatives **58**, **61**, **62**, **63**, **64**, **109**, **110**, **111**, **113**, **114**, **151**, **153**, **156**, **158**, **161**, **162**, ADP and AOPCP (I). Rat enzyme K_m, 59 μM; AMP concentration, 5 μM. Data points are from three separate experiments performed in duplicate.

7.2. Selectivity studies

Selected potent compounds were further investigated at various purinergic targets including other *ecto*-nucleotidases like *e*NTPDase 1-3 and *e*NPP 1-3 as well as ADP-activated P2Y receptors ($P2Y_1$ and $P2Y_{12}$).

7.2.1. Activity at nucleoside triphosphate diphosphohydrolases and nucleotide phosphodiesterases

The lead compound AOPCP showed some inhibitory potency at *e*NPP 1 (K_i = 16500 nM). This mean that it has a 85-fold selectivity for *e*N versus *e*NPP 1. AOPCP has competitive mechanism of inhibition at *e*NPP 1.[106, 116] Most of the new compounds were inactive at the tested enzymes, which showed that we were able to achieve selectivity. The highest percentage of inhibition at human NTPDases 1 tested in the malachite green assay[117, 169] was observed for the compounds **61** (21 %) and **64** (16 %) at 10 μM concentration. At human NPP 1 all of the tested compounds were less active than AOPCP (percentage of inhibition at 10 μM of 21%) tested under same conditions, except for **140** which showed 31 % inhibition at 10 μM. The results are summarized in Table 18.

Table 17. Potency of selected derivatives at human NTPDase 1-3 and NPP 1-3

Compd.	human NTPDase % inhibition (at 20 µM), n=3 (% Effect ± SEM)[a,b] or K_i ± SEM (nM)			human NPP % inhibition (at 10 µM), n=3 (% Effect ± SEM)[a,b] or K_i ± SEM (nM)		
	NTPDase 1	**NTPDase 2**	**NTPDase 3**	**NPP 1**	**NPP 2**	**NPP 3**
AOPCP	>>10000 (1± 3)	>>10000 (-7 ± 8)	>>10000 (-4 ± 11)	**16500** ± 3.2 (21 ± 1)	>>10000 (4 ± 0)	>>10000 (1 ± 1)
ADP	n.d.	n.d.	n.d.	>10000 (28 ± 4)	>>10000 (4 ± 0)	>>10000 (2 ± 2)
61	>>10000 (-2± 4)	>10000 (27 ± 3)	>>10000 (-6 ± 9)	>>10000 (12 ± 0)	>>10000 (3 ± 1)	>>10000 (-1 ± 0)
63	>>10000 (9± 4)	>>10000 (-15 ± 11)	>>10000 (-17 ± 7)	>>10000 (9 ± 1)	>>10000 (2 ± 1)	>>10000 (-1 ± 1)
64	>>10000 (12± 5)	>>10000 (16 ± 12)	>>10000 (-5 ± 12)	>>10000 (13 ± 1)	>>10000 (-1 ± 3)	>>10000 (0 ± 4)
69	>>10000 (17± 3)	>>10000 (8 ± 5)	>>10000 (-12 ± 8)	>>10000 (10 ± 0)	>>10000 (2 ± 1)	>>10000 (1 ± 1)
82	>>10000 (3± 3)	>>10000 (14 ± 26)	>>10000 (-2 ± 17)	>>10000 (11 ± 3)	>>10000 (0 ± 2)	>>10000 (0 ± 1)
109	n.d.	n.d.	n.d.	>>10000 (16 ± 2)	>>10000 (4 ± 1)	>>10000 (0 ± 1)
114	n.d.	n.d.	n.d.	>>10000 (19 ± 1)	>>10000 (5 ± 2)	>>10000 (0 ± 2)
140	n.d.	n.d.	n.d.	>10000 (31 ± 2)	>>10000 (6 ± 2)	>>10000 (0 ± 2)
142	n.d.	n.d.	n.d.	>>10000 (8 ± 1)	>>10000 (8 ± 1)	>>10000 (1 ± 1)
144	n.d.	n.d.	n.d.	>10000 (27 ± 0)	>>10000 (-3 ± 4)	>>10000 (0 ± 4)
149	n.d.	n.d.	n.d.	>>10000 (14 ± 1)	>>10000 (4 ± 2)	>>10000 (4 ± 1)
150	n.d.	n.d.	n.d.	>>10000 (20 ± 3)	>>10000 (3 ± 1)	>>10000 (3 ± 2)
154	n.d.	n.d.	n.d.	>>10000 (22 ± 4)	>>10000 (2 ± 1)	>>10000 (0 ± 2)

[a]Screening was performed at a concentration of 10 µM for NPPs and 20 µM for NTPDases. [b]Effects were normalized to the effect induced by 400 µM of *p*-nitrophenylthymidine monophosphate for NPP 1 and 70 µM of ATP for NTPDase 1. [c]K_i value. (n.d., not determined)

7.2.2. Selectivity versus ADP-activated P2Y receptors

Selected compounds were further investigated at the P2Y receptor subtypes $P2Y_1$ and $P2Y_{12}$.[170] P2Y receptors are G protein-coupled receptors. The activators of P2Y receptors are nucleotides. ADP and its more potent analogue 2-MeSADP are agonists of both, $P2Y_1$ and $P2Y_{12}$ receptors. Our synthesized nucleotides are isosteres of ADP where an oxygen atom between two phosphoric acids has been replaced by methylene residue binding phosphonic acid derivatives. All tested nucleotide derivatives showed negligible potency at the investigated P2Y receptor subtypes which proved their selectivity versus both, $P2Y_1$ and $P2Y_{12}$ receptors. The results are summarized in Table 19.

Table 18. Potency of selected derivatives at ADP-activated P2Y receptor subtypes

Compd.	**human $P2Y_1$** EC_{50} ± SEM (nM) (% Effect[a] ± SEM)	**human $P2Y_{12}$** EC_{50} ± SEM (nM) (% Effect[a] ± SEM)
ADP	**289 ±** 6.7	**133** ± 2.6
AOPCP	>10000 (26 ± 7)	>>10000 (5 ± 4)
58	>>10000 (17 ± 7)	>>10000 (4 ± 5)
61	>>10000 (16 ± 12)	>>10000 (-2 ± 4)
63	>> 10000 (15 ± 1)	>>10000 (0 ± 2)
82	>> 10000 (20 ± 2)	>>10000 (1 ± 1)
109	>10000 (38 ± 6)	>>10000 (6 ± 5)
114	>>10000 (7 ± 9)	>10000 (34 ± 13)
145	>>10000 (20 ± 4)	>10000 (36 ± 5)
149	>>10000 (12 ± 3)	>>10000 (-1 ± 2)
154	>> 10000 (7 ± 4)	>>10000 (3 ± 4)

[a]Screening was performed at a concentration of 10 µM.

8. Results and discussion - part II: Metabolic stability studies

Metabolic stability is an important property of drug molecules, because this property determines both efficacy and safety (toxicity). Metabolic studies also determine parameters such as clearance, half-life, and bioavailability. Therefore, few selected, potent inhibitors were further investigated for their metabolic stability, (i) in rat liver microsomes in order to investigate potential metabolic degradation by liver enzymes, in order to identify stable inhibitors for extended pharmacological experiments, and (ii) in human blood, in order to determine plasma stability of the inhibitors. Inhibitors were incubated with microsomes, or plasma, respectively, at 37 °C and subsequently analyzed by LC-MS.[133]

8.1. Stability of inhibitors in liver microsomes

Metabolism increases clearance of clinical candidates. The main site of metabolism of drugs is the liver. Apart from the liver, the metabolism of drugs takes place in the gastrointestinal- (GI) tract, primarily the small intestine, and also in lungs, skin, nasal mucosa and kidneys. Metabolic studies are important as structural modification of the compounds with groups blocking or sterically interfering with metabolic sites increases metabolic stability.[171, 172] In drug discovery several pharmacologically important molecules are discarded at later stages of development because they are not sufficiently stable. So, the metabolic stability studies are a must for the successful development of stable compounds even at the lead optimization stage. An orally applied drug undergoes various enzymatic and chemical reactions in different parts of the body. In the GI-tract the molecule undergoes intestinal decomposition, in the liver it encounters hepatic metabolism and in plasma it undergoes plasma decomposition by hydrolytic and other enzymes

in the blood. Optimization of metabolic stability is one of the biggest challenges in drug discovery.[172]

8.1.1. Metabolism/ biotransformation

The metabolism reactions have been divided into two phases. Phase I reactions include structural modifications of drug molecules by addition or unmasking of polar and functional moiety, such as oxidation or dealkylation. Different enzymes which catalyze phase I reactions include monooxygenases, the cytochrome P450 (CYP) family and the flavine monooxygenase (FMO) family. Typical phase I reactions by CYP and FMO are oxidation, dealkylation etc. Other enzymes like esterases produce hydrolysis.[172]

Phase II reactions are additions or conjugations of polar groups to the molecular structure or the products of phase I reactions. However a compound may undergo phase II reaction before phase I reactions, if it has polar groups to allow conjugations. The common phase II reactions are glucuronidation, sulfation, acetylation, glycination, glutathione conjugation etc. The combining effects of phase I and II metabolism produce polar products with increased aqueous solubility which allows excretion from the body via bile and urine. Metabolism increases clearance and produces low bioavailability which results in a lower concentration of a drug at the therapeutic target.[172]

Metabolism has a direct relationship with clearance (CL). An increase in metabolism leads to an increase in clearance. CL and volume of distribution (V_d) directly affect the half-life of the drugs. Half-life determines how often the dose must be administered to achieve the desirable bioavailability, accounting absorption and clearance. So, the early metabolic study of chemical compounds determines the amount of drug to be administered during the animal experiments.

The phase 1 metabolism reactions depend on the binding of the compound to the metabolic enzyme as well as reactivity of specific site on the compounds to the reactive site of metabolic enzyme.[172] Structural changes reduce compound binding or reactivity and will increase metabolic stability. The strategies for increasing metabolic stability from phase I metabolism are blocking of metabolic site by adding blocking groups like halogens, removing labile functional groups or easily metabolizing groups, cyclization of molecular structure, change in ring size, change in chirality, reducing lipophilicity and removing unstable groups. Phase II metabolism can be reduced by introducing electron-withdrawing groups or steric hindrance and changing polar group to non-polar (e.g changing phenolic hydroxyl to cyclic urea or thiourea).[172] Phenolic hydroxyl groups can be converted to prodrugs thereby increasing phase II stability. There are both *in vitro* as well as *in vivo* metabolic stability models. The *in vivo* models are expensive and time-consuming, so in vitro models are more popular. In vitro metabolic stability data often guide structure modifications to improve stability. They can also provide information to select the optimal compound(s) for *in vivo* activity testing by predicting *in vivo* pharmacokinetic performance. [172]

8.1.2. Invitro-metabolic study models

Different in-vitro models are used for metabolic studies as detailed below.

I. Hepatocytes: They are prepared from fresh livers and are used for both phase I and phase II metabolic studies. They contain all the co-factors, enzymes and transporters for drug metabolism. They can be used for screening of the metabolic stability of drugs, for metabolite profiling, liver toxicity studies, and enzyme induction studies (P450 induction). They cannot be used for the study of drug-drug interaction and reaction phenotyping.[172, 173]

II. Liver Slices: They are similar to hepatocytes and they contain all the enzymes/transporters and co-factors for drug metabolism. They are harder to prepare but are the most physiologically relevant samples used for qualitative and quantitative measurement of hepatic metabolism. Like hepatocytes they are rarely used for absorption, distribution, metabolism, and excretion, (ADME) studies.[173]

III. Liver Microsomes: They contain all cytochrome P450s, flavin-containing monooxygenases (FMOs), and uridine 5'-diphospho-glucuronosyltransferases (UGTs). They are easy to prepare and can be stored for long periods (-80ºC), withstand several freeze and thaw cycles and can be re-used without significant loss of enzyme activity. The samples can also be pooled e.g. 20 to 150 liver samples of same or different animal species. They are used for drug half-life determination, metabolite profiling, enzyme mapping, reaction phenotyping study, study of drug-drug interaction, and mechanistic studies.[173]

IV. Liver S9 fraction: They are post-mitochondrial supernatant fraction which is the mixture of microsomes and cytosol. They are same as microsome fractions and contain many enzymes like CYPs, FMOs, carboxylesterases, epoxide hydrolase, UGTs, sulfotransferases, methyltransferases, acetyltransferases, glutathione S-transferases and other drug metabolism enzymes. They have the same advantages as microsomes but P450 activity is four to five-fold lower. It contains all enzymes for both phase I and phase II metabolic studies.[173]

8.1.3. Metabolic stability results

The aim of this metabolic study was primarily to check whether the compounds are stable enough for further *in vivo* studies. Studies were only limited to the time-dependent degradation of compounds and possible identification and structural elucidation of resulting metabolites. Four

inhibitors **150**, **149, 74** and **71** along with the standard inhibitors **AOPCP** and **ADP** were incubated at 37 °C and subsequently analyzed by high performance liquid chromatography coupled to electrospray ionization mass spectroscopy (LC-MS). To check the enzymatic activity of liver microsomes, a well studied drug, **diazepam**, was used for comparison as its in-vitro and in vivo metabolites are well documented.[171] Results are presented as percentage of remaining compound measured by LC-MS at different time intervals.

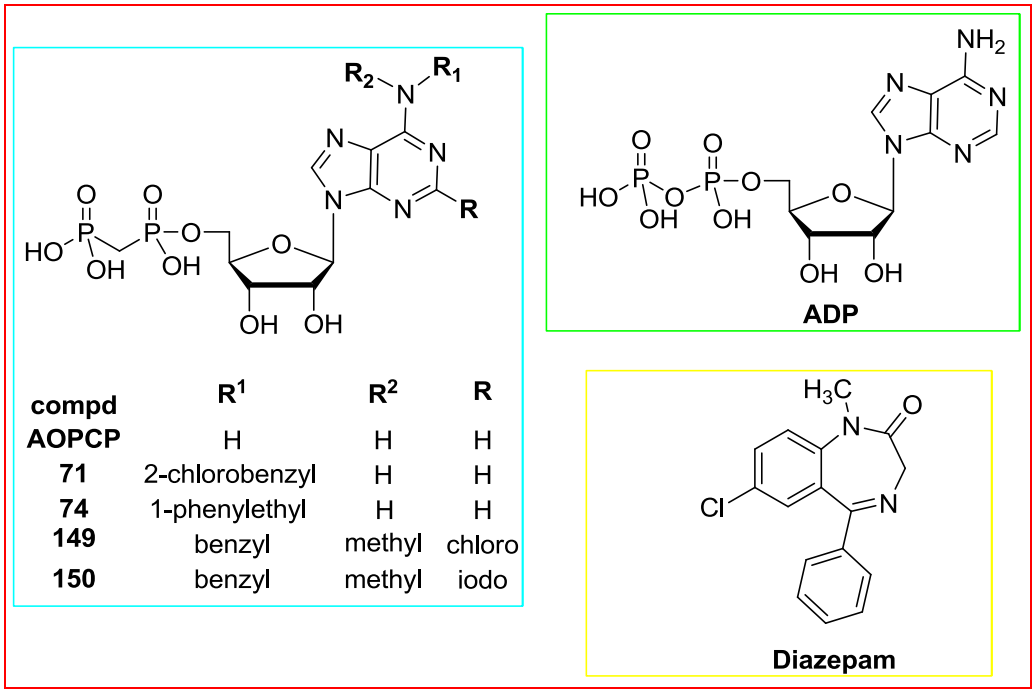

compd	R^1	R^2	R
AOPCP	H	H	H
71	2-chlorobenzyl	H	H
74	1-phenylethyl	H	H
149	benzyl	methyl	chloro
150	benzyl	methyl	iodo

Figure 20. Compounds used in the liver microsomal metabolic study

Incubation with rat liver microsomes showed that the inhibitors were relatively stable towards liver enzymes. Only a very small percentage (<10%) of inhibitors was metabolized under the applied conditions, while >90% of the compounds were recovered unchanged after incubation for 8 hours.

Table 20. Percentage remaining of AOPCP and ADP at different time intervals (min)

Time (min)	**% AOPCP**			**% ADP**		
0.0	100.00	100.00	100.00	100.00	100.00	100.00
2.5	100.00	96.11	96.22	31.60	35.78	23.34
5.0	54.51	44.84	74.10	27.24	23.41	6.67
7.5	33.21	23.69	34.63	24.00	11.17	1.11
10.0	22.57	13.89	17.29	1.70	1.67	0.00
15.0	16.58	9.47	9.83	0.00	1.91	0.00
30.0	0.00	0.00	0.00	0.00	0.00	0.00

The studies were validated by using diazepam. Diazepam on incubation with liver microsomes initially showed relatively high stability but on incubation for longer times showed many metabolities. We were able to elucidate at least three different metabolites. Diazepam (284.1 g/mol) got metabolized to oxazepam (286.1 g/mol) and also to nordiazepam (270.1 g/mol) and temazepam (270.1 g/mol) to a lesser extent. This shows that various cytochrome P450 enzymes like **CYP2C19** and **CYP3A4** (responsible for phase I metabolism of diazepam to oxazepam) are present in the liver microsome preparation. But, unfortunately, we could not elucidate any of the phase II products for diazepam metabolism.

Table 191. Percentage remaining of diazepam, **71**, **74**, **149** and **150** at different time intervals (hour)

Time (h)	% Diazepam			% **149**			% **150**		
0.0	100.00	100.00	100.00	100.00	100.00	100.00	100.00	100.00	100.00
2.0	94.70	94.77	96.22	100.00	100.00	100.00	100.00	100.00	100.00
8.0	91.10	91.10	90.00	100.00	100.00	94.80	86.79	90.70	94.01
30.0	75.00	75.53	78.80	65.83	61.34	67.76	58.92	64.58	62.37

Time (h)	**% 74**			**% 71**		
0.0	100.00	100.00	100.00	100.00	100.00	100.00
2.0	100.00	100.00	100.00	100.00	100.00	100.00
8.0	73.27	66.27	73.85	81.60	77.50	78.30
30.0	37.42	31.11	38.34	45.32	49.30	46.30

For both, ADP and AOPCP, low stability was observed. ADP was stable for 5 min as compared to 15 minutes for AOPCP. The low stability of ADP and its more stable analog AOPCP has been also documented in various *in vivo* experiments.[174, 175]

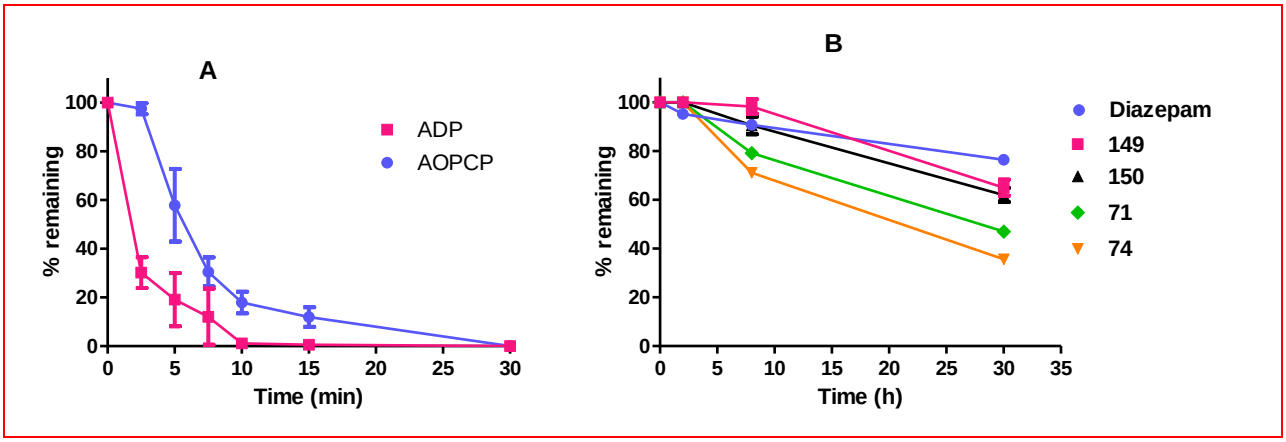

Figure 21. Metabolic stability studies of ADP, AOPCP, diazepam and AOPCP derivatives **71**, **74**, **149** and **150** in rat liver microsomes. Results are presented as percentage remaining of compounds measured by LC-MS at different time intervals. Data points are from three separate experiments performed in duplicate.

For ADP the metabolic products obtained were adenosine and adenine. For the bisphosphonic acids, the corresponding side-product of phosphonic acid ester cleavage at 5′-position was not observed. Probably it got further degraded to phosphonic acid. Adenine was only detected in the sample which was incubated for a long time, e.g. 2 h incubation. This may be because adenosine gets further degraded to adenine. Hydrolysis during the late phase I reactions are catalyzed by amidases and esterases. The mode of metabolism was hydrolytic cleavage of the glycosidic bond between ribose and adenine. For AOPCP, the metabolites obtained were adenosine, adenine and methylenebis(phosphonic acid). Hydrolysis is typical for a phase I reaction for nucleoside-derived drugs.

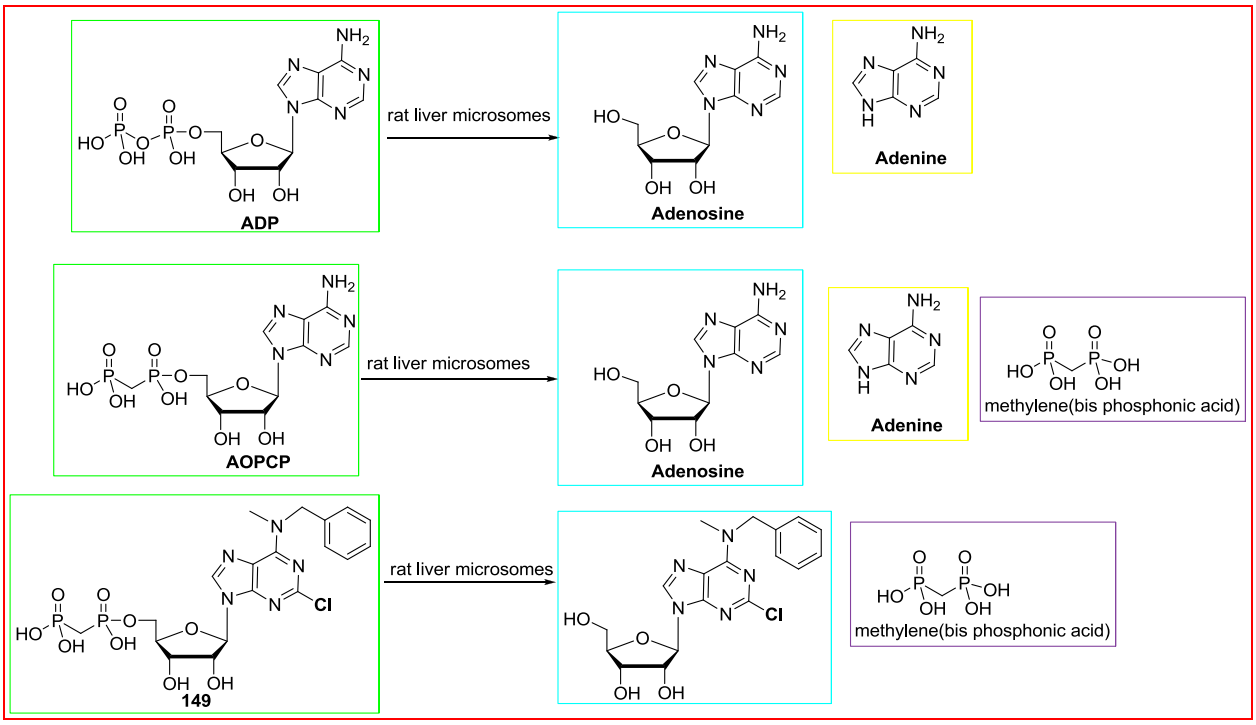

Figure 22. Phase 1 metabolic products of ADP, AOPCP and inhibitor **149** after incubation with rat liver microsomes

For our inhibitors, the studies were carried under the same conditions. Upon incubation for 5 hours, only few percentages of compounds were decomposed. So we incubated for longer time up to 30 hours. Among the inhibitors, **149** was most stable after incubation for 30 h. Only 34% of **149** was metabolized. Under the same conditions about 38% of **150**, 53% of **71** and 64% of **74** was metabolized. Diazepam was metabolized only by 23% after 30 h incubation. The metabolites identified from the inhibitors were analyzed as nucleoside, nucleobases and methylenebis(phosphonic acid). Since phase II metabolism products were not detected we performed more studies by adding an NADPH-regenerating system consisting of nicotinamide adenine dinucleotide phosphate (0.57 mM), nicotinamide adenine dinucleotide (0.57 mM), isocitrate (6.4 mM), isocitrate dehydrogenase (0.57 mM), and $MgCl_2$ (23.4 mM) maintained at pH 7.2, which will facilitate the conjugation with phase I metabolites.[133] The half-life of **149** and

74 in the studies with NADPH-regenerating system were found to be approximately 125 min (**149**), and 55 min (**74**), respectively. As expected NADPH-regenerating system addition favors phase II reaction by forward conjugation of sugars (products from the enzymatic activity of NADPH regenerating system) to the hydroxyl groups of compounds as well as metabolites. There were many metabolites with increased molecular weight by 180 and 192, probably due to the addition of glucose and isocitrate to the ribose moiety of metabolites and compounds.

Table 22. Percentage remaining of **74** and **149** at different time intervals (hour) under incubation with liver microsomes after adding NADPH regenerating system

Time (h)	% **74**			% **149**		
0.0	100.00	100.00	100.00	100.00	100.00	100.00
0.5	71.83	65.54	73.37	100.00	100.00	100.00
1.0	52.37	53.56	57.86	86.79	90.70	94.01
2.0	20.34	25.18	20.17	58.92	64.58	62.37
3.0	10.01	8.06	2.03	40.83	41.24	46.54
5.0	0.05	0.00	0.00	20.20	23.18	15.13
8.0	0.00	0.00	0.00	10.03	12.10	10.50

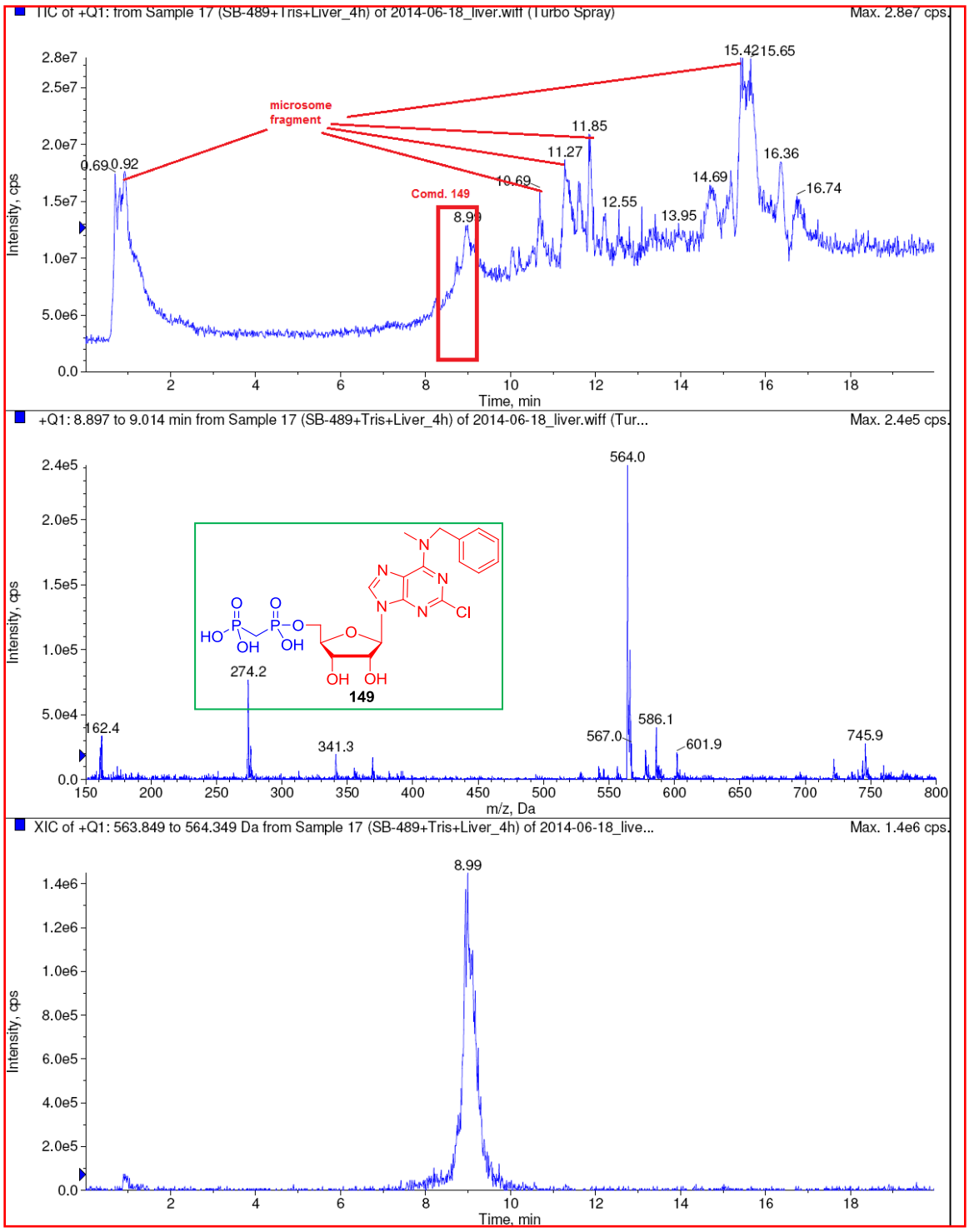

Figure 23. Representative HPLC chromatogram and corresponding MS spectra of compound **149** after 4 h incubation with rat liver microsomes at 37° C.The peak at the retention time of 8.99 min belongs to compound **149** (M= 563.82 g/mol).

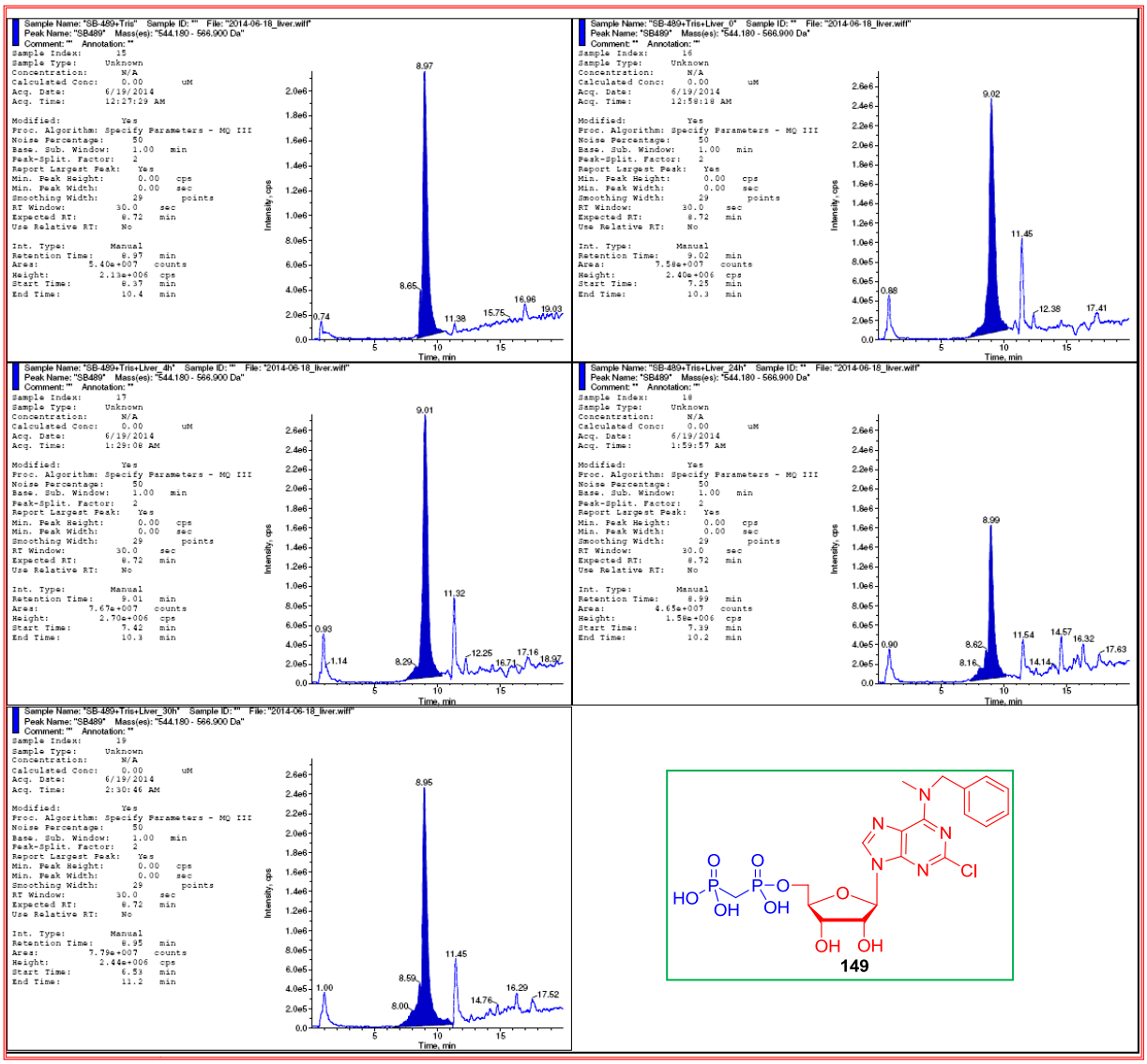

Figure 24. Representative HPLC chromatogram and corresponding MS spectra of compound **149** after incubation with rat liver microsomes at 37° C at different time intervals.The peak at the retention time of 8.97, 9.02, 9.01, 8.99, and 8.96 min belongs to compound **7** (M= 563.82 g/mol).

	Sample Name	File Name	Analyte Peak Area (counts)	Analyte Peak Height (cps)
1	ADP+Tris	Sanjay\2014-06-18_liver.wiff	2.53e+007	1.22e+006
2	ADP+Tris+Liver_0min	Sanjay\2014-06-18_liver.wiff	6.79e+006	1.56e+005
3	ADP+Tris+Liver_2.5min	Sanjay\2014-06-18_liver.wiff	2.43e+006	4.93e+004
4	ADP+Tris+Liver_5min	Sanjay\2014-06-18_liver.wiff	1.59e+006	3.20e+004
5	ADP+Tris+Liver_7.5min	Sanjay\2014-06-18_liver.wiff	7.97e+005	4.25e+004
6	ADP+Tris+Liver_10min	Sanjay\2014-06-18_liver.wiff	1.14e+006	3.82e+004
7	ADP+Tris+Liver_15min	Sanjay\2014-06-18_liver.wiff	1.13e+006	3.90e+004

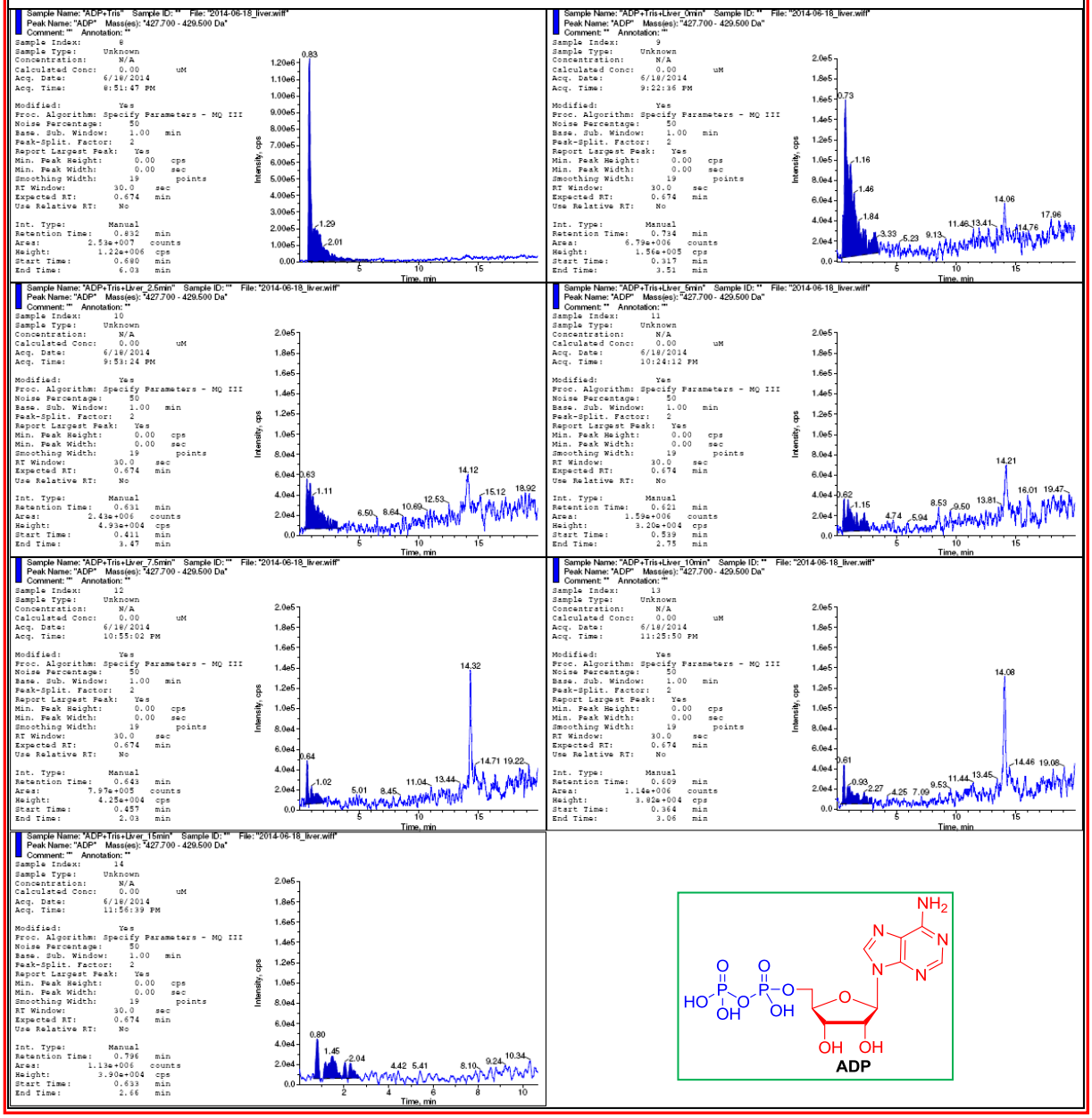

Figure 25. Representative HPLC chromatogram and corresponding MS spectra of **ADP** after incubation with rat liver microsomes at 37° C at different time intervals. The peak at the retention time of 0.83, 0.73, 0.63, 0.62, 0.61 and 0.80 min belongs to compound **ADP** (M= 427.20 g/mol).

	Sample Name	File Name	Analyte Peak Area (counts)	Analyte Peak Height (cps)
1	AOPCP+Tris	Sanjay\2014-06-18_liver.wiff	6.03e+007	2.86e+006
2	AOPCP+Tris+Liver_0min	Sanjay\2014-06-18_liver.wiff	2.99e+007	9.79e+005
3	AOPCP+Tris+Liver_2.5min	Sanjay\2014-06-18_liver.wiff	3.34e+007	9.41e+005
4	AOPCP+Tris+Liver_5min	Sanjay\2014-06-18_liver.wiff	1.63e+007	4.39e+005
5	AOPCP+Tris+Liver_7.5min	Sanjay\2014-06-18_liver.wiff	9.93e+006	2.32e+005
6	AOPCP+Tris+Liver_10min	Sanjay\2014-06-18_liver.wiff	6.75e+006	1.36e+005
7	AOPCP+Tris+Liver_15min	Sanjay\2014-06-18_liver.wiff	4.96e+006	9.28e+004

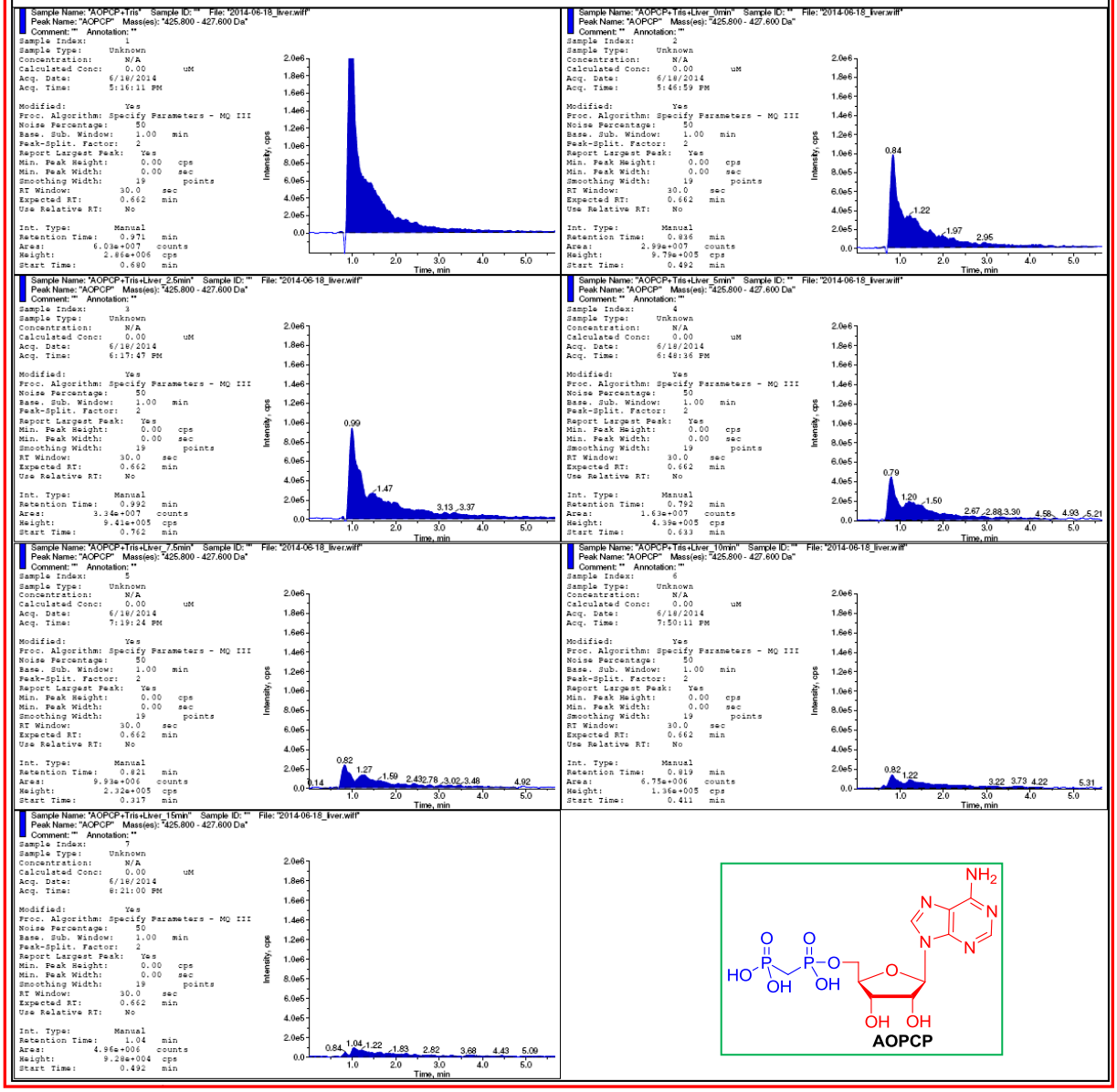

Figure 26. Representative HPLC chromatogram and corresponding MS spectra of **AOPCP** after incubation with rat liver microsomes at 37° C at different time intervals. The peak at the retention time of 0.84, 0.99, 0.79, 0.82and 0.84 min belongs to compound **AOPCP** (M= 425.23 g/mol).

8.2. Plasma stability

Compounds with certain functional groups can decompose in the bloodstream resulting in high clearance and short half-lives. These compounds have poor *in vivo* pharmacokinetics (PK) and disappointing pharmacological performance. Microsomal enzymes are different than plasma enzymes so, liver metabolic stability studies will yield different results than those in plasma. Instability in plasma should be accounted to eliminate erroneous PK. Pharmaceutical companies do not develop drugs that are unstable in plasma except they are prodrugs or antedrugs (soft drugs).[176] Therefore, it is important for researchers to anticipate and assess the plasma stability at an early stage. Blood contains a large number of hydrolytic enzymes, such as cholinesterase, dehydropeptidase, lipase, aldolase, alkaline and acid phosphatase. The compound with affinity for one of these enzymes can be decomposed in the plasma if it has a hydrolyzable group in the right position. The compound's pharmacological activity at the target protein can be modulated by replacing and removing the hydrolyzable group.[176] Hydrolysis in plasma is the major cause of compound clearance thereby restricting *in vivo* pharmacological efficacy. Thus it is important to either modify or deprioritize the series with unstable moieties at early discovery stage before spending a large amount of effort on activity optimization. The common functional group liable to plasma degradation includes ester, carbamate, amide, lactone, lactam, and sulfonamide functions. Plasma stability data are important for the succeeding *in vivo* studies. Typically, plasma stability is less in rodents than in humans.[176]

Substituting a less hydrolyzable group, e.g an amide, for a hydrolyzable group like an ester, increasing steric hindrance and removing electron-withdrawing groups are some basic tactics for improving plasma stability. Plasma stability data can be used to prioritize compounds for *in vivo*

animal studies by identification of easily liable structural motifs, and subsequently help structural modifications.[176]

8.2.1. Plasma stability results

The same sets of compounds was taken for the plasma stability studies (**ADP**, **AOPCP**, **150**, **149**, and **71**). Owing to the low stability of **74** in rat liver, it was left out for the plasma stability studies. Incubation with human blood showed that **ADP** was unstable, but the rest of the compounds was stable. **ADP** was degraded in less than 30 min as compared to liver microsomes where it got degraded in 5 min. The type of enzymes and their concentrations are different in liver and plasma. Plasma contains alkaline and acid phosphatases which are known to hydrolyze **ADP**. AOPCP was more stable than **ADP**. More than 50 % of AOPCP could be recovered after incubation under the same conditions. Inhibitors **150**, **149**, and **71** were also stable. Among them the most stable was **149** of which less than 5% was metabolized under the applied conditions, while >95% of the compounds were recovered unchanged after incubation for 5 hours. After 5 hour incubation the order of stability was **150** > **71** > **150** > **AOPCP**.

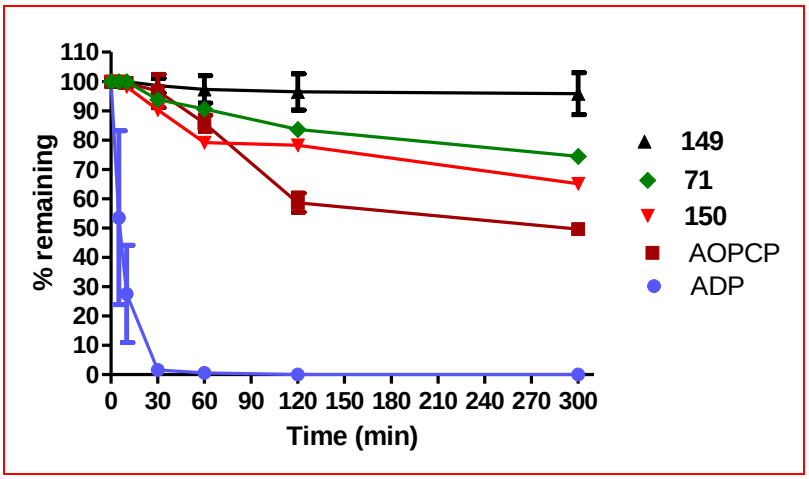

Figure 27. Stability studies of ADP, AOPCP and AOPCP derivatives **149**, **150 and 71** in human blood. Results are presented as percentage remaining of compounds measured by LC-MS at different time interval. Data points are from three separate experiments performed in duplicate.

Table 23. Percentage remaining of ADP, AOPCP, diazepam, **71**, **149** and **150** at different time intervals (min)

Time (min)	% **ADP**			% **AOPCP**			% **71**		
0.0	100.00	100.00	100.00	100.00	100.00	100.00	100.00	100.00	100.00
5.0	23.86	83.16	53.51	100.00	100.00	100.00	100.00	100.00	100.00
10.0	10.98	44.17	27.57	98.58	100.00	100.00	100.00	100.00	100.00
30.0	2.58	0.60	1.59	90.17	100.00	100.00	89.16	98.88	93.50
60.0	1.70	0.00	0.00	83.05	88.58	85.58	86.02	95.50	90.34
120.0	0.00	0.00	0.00	54.90	60.05	61.02	82.70	84.53	83.16
300.0	0.00	0.00	0.00	50.20	50.00	48.62	74.50	74.54	74.32

Time (min)	% **149**			% **150**		
0.0	100.00	100.00	100.00	100.00	100.00	100.00
5.0	100.00	100.00	100.00	100.00	100.00	100.00
10.0	100.00	100.00	100.00	100.00	96.14	98.52
30.0	100.00	100.00	95.74	87.22	98.47	85.22
60.0	100.00	100.00	91.86	76.52	79.58	81.32
120.0	100.00	100.00	89.32	75.51	81.98	77.35
300.0	100.00	100.00	87.59	70.12	49.51	75.82

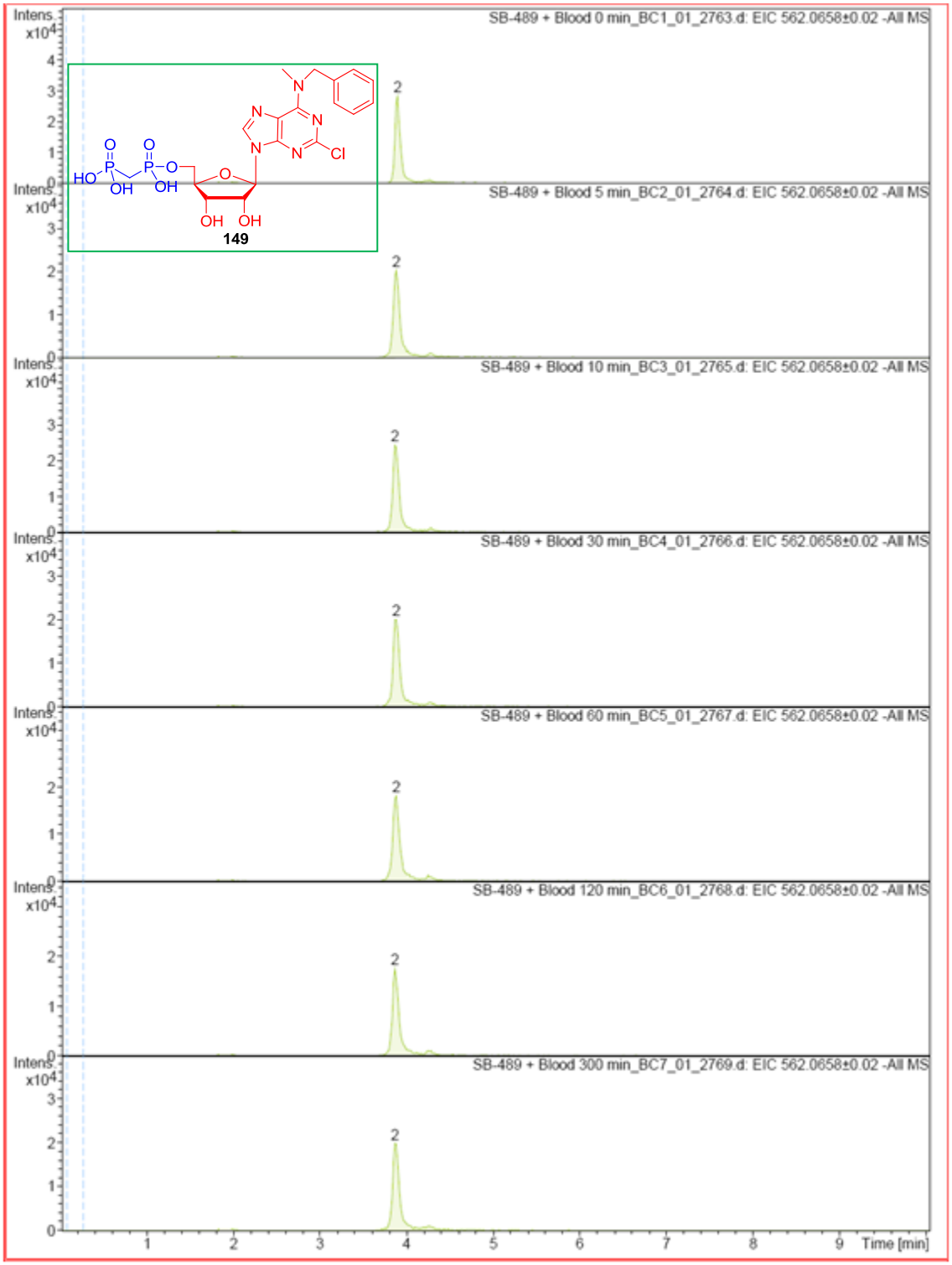

Figure 28. Representative HPLC chromatogram and corresponding MS spectra of **149** after incubation with human blood at 37° C at different time intervals. The peak 2 belongs to compound **149** (M= 563.82 g/mol).

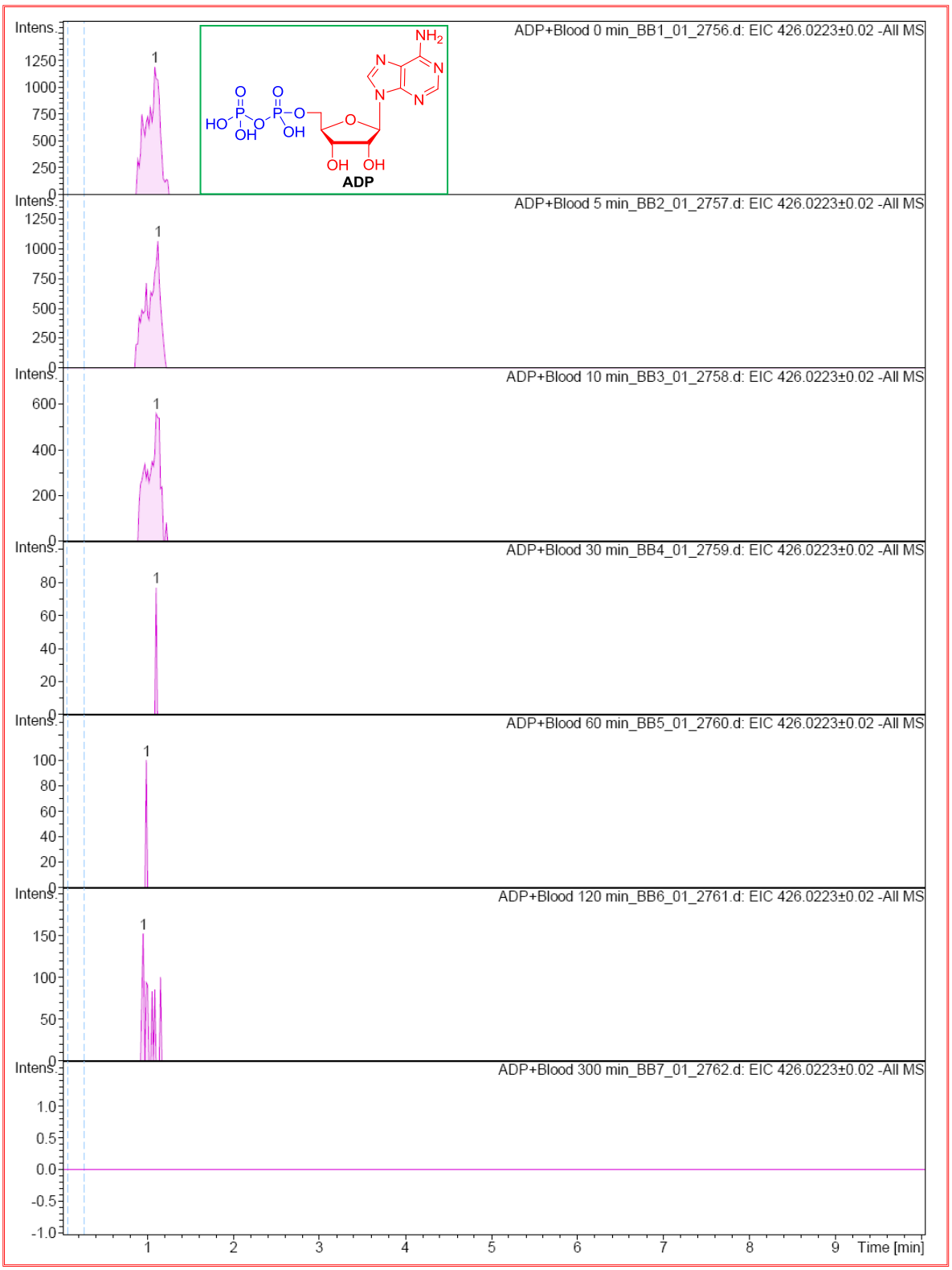

Figure 29. Representative HPLC chromatogram and corresponding MS spectra of **ADP** after incubation with human blood at 37° C at different time intervals. The peak belongs to compound **ADP** (M= 427.20 g/mol).

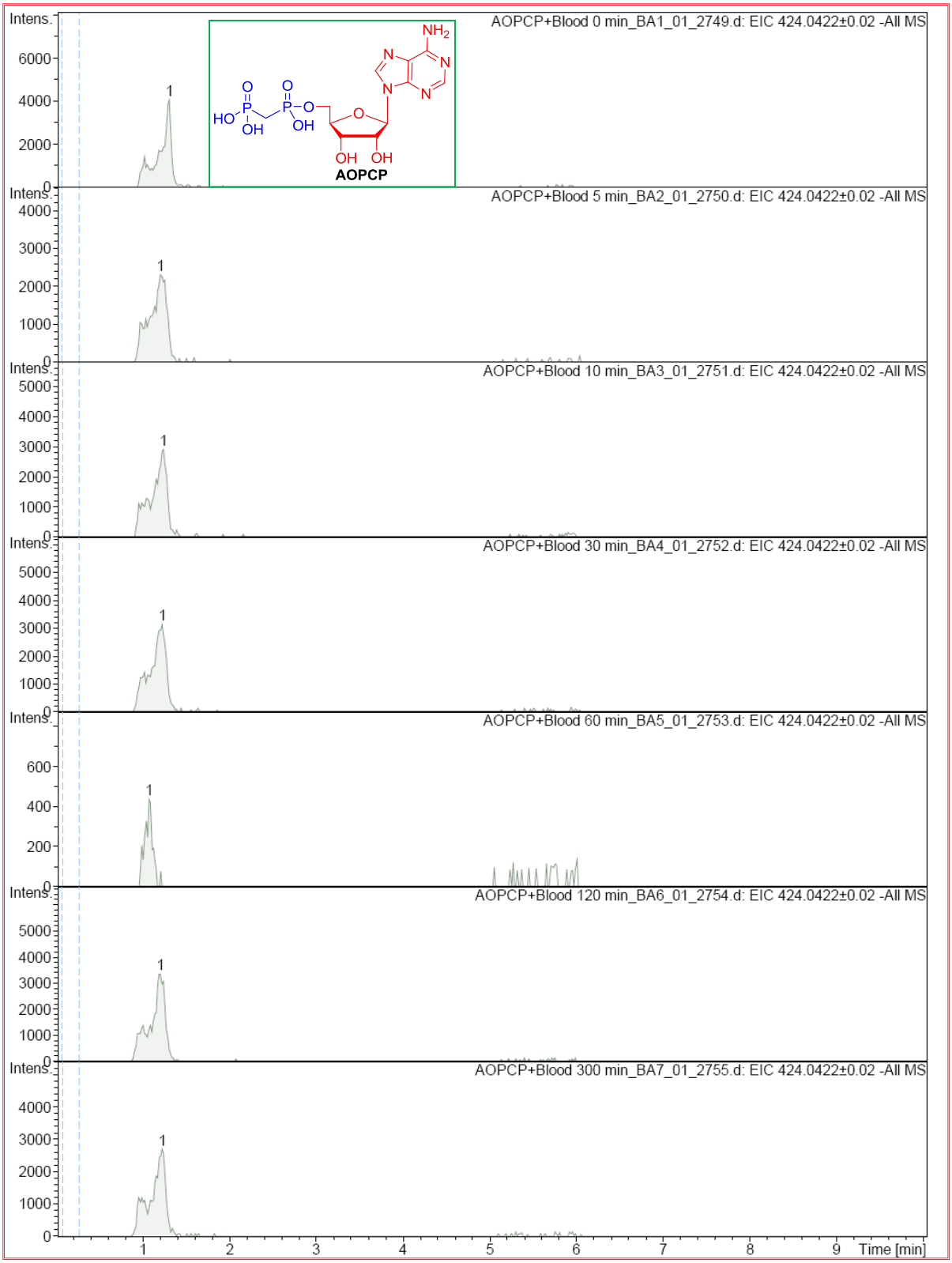

Figure 30. Representative HPLC chromatogram and corresponding MS spectra of **AOPCP** after incubation with human blood at 37° C at different time intervals. The peak belongs to compound **AOPCP** (M= 425.23 g/mol).

V. Experimental

9. Chemical synthesis

9.1. General remarks

All reagents were commercially obtained from various producers (Acros, Aldrich, Fluka, Merck, and Sigma) and used without further purification. The purity of all compounds including starting material was more than 95%. Commercial solvents of specific reagent grades were used, without additional purification or drying. The reactions were monitored by thin layer chromatography (TLC) using aluminum sheets with silica gel 60 F_{254} (Merck) using dichloromethane : methanol (9:1, 5:1, or 3:1) and *n*-butanol: acetic acid: water (2:1:1) as the mobile phase. Column chromatography was carried out with silica gel 0.060-0.200 mm, pore diameter ca. 6 nm. Mass spectra were recorded on an API 2000 (Applied Biosystems, Darmstadt, Germany) mass spectrometer (turbo ion spray ion source) coupled with a Waters HPLC system (Agilent 1100) using a Phenomenex Luna 3µ C18 column. The LC/MS samples were prepared by dissolving 1 mg/mL of compound in H_2O : MeOH (1:1) containing 2 mM ammonium acetate. A sample of 10 µL was injected into an HPLC instrument and elution was performed with a gradient of water: methanol (containing 2 mM ammonium acetate) from 90:10 to 0:100 for 20 min at a flow rate of 250 µL/ min. UV absorption was detected from 190 to 400 nm using a diode array detector. ^{1}H, ^{31}P, and ^{13}C NMR spectra were performed on a Bruker Avance 500 MHz spectrometer and Bruker Avance 600 MHz spectrometer. DMSO-d_6, MeOD-d_4, or D_2O were used as solvents. ^{31}P-NMR spectra were recorded at room temperature; orthophosphoric acid (85%) was used as an external standard. Shifts are given in ppm relative to the external standard (in ^{31}P-NMR) or relative to the remaining protons of the deuterated solvents used as internal standard (^{1}H-, ^{13}C-

NMR). Melting points were determined on a Buchi 530 melting point apparatus and are uncorrected. For the microwave reactions, a CEM focused microwave synthesis, Discover apparatus was used. For lyophilization, a freeze dryer (CHRIST ALPHA 1-4 LSC) was used. For HPLC purification (Knauer Smartline 1050 HPLC system) was used. For ion exchange chromatography FPLC instrument from Amersham Biosciences was used.

9.2. Preparation of triethylammonium hydrogen carbonate buffer (TEAC)

A 1 M solution of TEAC was prepared by adding dry ice slowly to 1 M triethylamine solution in water for several hours till the pH of approximately 7.4-7.6 was indicated in pH-meter.

9.3. Ion Exchange Chromatography

The crude nucleoside-5′-*O*-[(phosphonomethyl)phosphonic acid] derivatives were purified by ion exchange chromatography on an FPLC instrument (AKTA FPLC, from Amersham Biosciences) with an XK 26 mm X 20 cm length column (Pharmacia). The column was packed with Sephadex DEAE A-25 gel, HCO_3^- form, swelled in a 1 M solution of TEAC at 4 °C for 48 h. Before running purification the column was washed and equilibrated with deionized water. The sample was prepared by dissolving crude product in 5 mL of aqueous triethylammonium hydrogen carbonate buffer. Separation was achieved by running a solvent gradient of 0-900 mM TEAC buffer using approximately 3000 mL of solvent to elute the bis-phosphonic acids derivatives. The UV absorption was detected at 254 nm. Fractions were collected and appropriate fractions pooled, diluted in water, and lyophilized.

9.4. Preparative HPLC

Lyophilized nucleoside-5′-*O*-[(phosphonomethyl)phosphonic acid]s were dissolved in 5 mL of deionized water and injected into an RP-HPLC column (Knauer 20 mm i.d., Eurospher-100 C18). The column was eluted with a solvent gradient of 0- 65% of acetonitrile in 50 mM aqueous NH_4HCO_3 buffer for 40 min at a flow rate of 10 mL/min. The UV absorption was detected at 254 nm. Fractions were collected and appropriate fractions pooled, diluted with water, and lyophilized several times to remove the NH_4HCO_3 buffer, yielding the nucleotides as white powders.

10.1. 2',3',5'-Tri-O-acetylinosine (26)

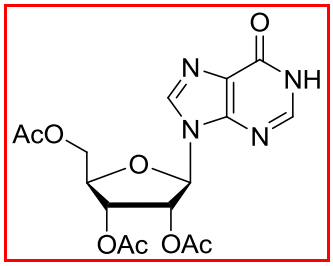

A solution of inosine (**25**, 10.0 g) and acetic anhydride (12.97 g) was suspended in 50 mL pyridine and was refluxed at 60 ^{o}C for 3 h until the solution become clear. After that 25 mL of methanol was added and stirred for 1 h to quench the unreacted acetic anhydride. Then the solution was evaporated *in vacuo* to get white oil which was dissolved in 100 mL of water. The aqueous layer was extracted with DCM (2 x 100 mL). The combined organic layers were washed with 2M HCl (2 x 50 mL) and brine (2 x 50 mL), dried, and evaporated. The resulting residue was triturated with ethanol to get a white precipitation which was filtered off to yield the crude product as a white solid.

Yield: 13.70 g (93%).

Melting Point (°C): 219-221 [**literature**, 238-243].[128, 153]

^{1}H NMR (500 MHz, DMSO-*d*$_6$): δ 8.29 (s, 1H, C8-H), 8.08 (s, 1H, C2-H), 6.14 – 6.17 (m, 1H, C1′-H), 5.87 – 5.89 (m, 1H, C3′-H), 5.51 – 5.53 (m, 1H, C2′-H), 4.38 (t, 1H, C4′-H), 4.21 – 4.25 (m, 2H, C5′-$\underline{H}_2$), 2.10 (s, 3H, OCOC$\underline{H}_3$), 2.03 (s, 3H, OCOC$\underline{H}_3$), 2.01 (s, 3H, OCOC$\underline{H}_3$).

^{13}C NMR (125 MHz, DMSO-*d*$_6$): δ 169.35, 169.65, 170.17, (3s, 3C, O$\underline{C}$OCH$_3$), 153.45 (1C, C6), 160.00 (1C, C2), 143.93 (1C, C4), 142.22 (1C, C8), 130.90 (1C, C5), 86.57 (1C, C1′), 80.81 (1C, C4′), 73.28 (1C, C3′), 70.52 (1C, C2′), 62.66 (1C, C5′), 20.35, 20.59, 20.70 (3C, $\underline{C}$H$_3$-CO).

LC/ESI-MS: negative mode 393 ([M - H]$^-$), positive mode 395 ([M + H]$^+$).

10.2. 6-Chloro-2',3',5'-tri-O-acetylinosine (27)

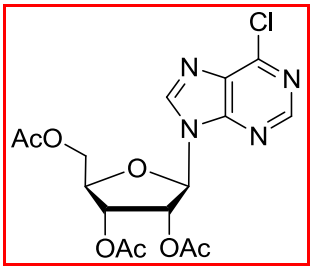

A suspension of **26** (2.45 g), *N*,*N*-dimethylaniline (0.83 mL), and phosphorus oxychloride (12.2 mL) was stirred at room temperature for 7 min under an atmosphere of argon. The flask was heated in a preheated oil bath at 100 °C for 13 min. After completion of reaction, the solution was evaporated, and the resulting oil was stirred in DCM (20 mL) and ice (20 mL). The aqueous layer was extracted with DCM (2 x 25 mL). The combined organic layers were washed with 2M HCl (4 x 20 mL) and brine (2 x 20 mL), dried with Na_2SO_4, and evaporated to yield 2.0 g of green oil. Purification using silica chromatography (1:10 MeOH/DCM) yielded the title compound **27** as a pale green solid.

Yield: 2.0 g (77%).

Melting Point (°C): 145-146 [**literature**, 122-123].[128]

^{1}H NMR (500 MHz, DMSO-*d*$_6$): δ 8.88 (s, 1H, C8-H), 8.83 (s, 1H, C2-H), 6.35 – 6.36 (m, 1H, C1′-H), 5.98 – 6.01 (m, 1H, C3′-H), 5.62 – 5.65 (m, 1H, C2′-H), 4.38 (t, 1H, C4′-H), 4.22 – 4.25 (m, 2H, C5′-$\underline{H}_2$), 2.11(s, 3H, OCOC$\underline{H}_3$), 2.03 (s, 3H, OCOC$\underline{H}_3$), 1.99 (s, 3H, OCOC$\underline{H}_3$).

^{13}C NMR (125 MHz, DMSO-*d*$_6$): δ 169.35, 169.6, 170.17 (3C, O$\underline{C}$OCH$_3$), 152.00 (1C, C2), 151.45 (1C, C6), 149.96 (1C, C4), 146.42 (1C, C8), 131.70 (1C, C5), 86.55 (1C, C1′), 79.88 (1C, C4′), 72.23 (1C, C3′), 70.54 (1C, C2′), 62.61 (1C, C5′), 20.39 – 20.51 (3C, $\underline{C}$H$_3$CO).

LC/ESI-MS: negative mode 411 ([M - H]$^-$), positive mode 413 ([M + H]$^+$).

10.3. 6-Chloropurine riboside (28)

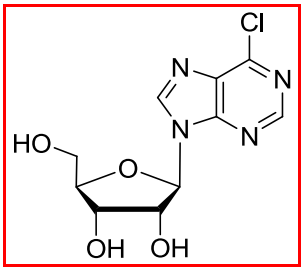

Compound **27** (2.0 g) was dissolve in 5 mL of methanol. To that, 20 mL of 7 N NH_3 in methanol was added while stirring at 0 °C. It was further stirred 3 h at 0 °C followed by stirring at rt for 16 h. Resulting precipitate was collected. The precipitate was washed with 2 M HCl (4 x 20 mL), brine (2 x 20 mL), and water (2 x 20 mL) and dried. Purification using silica chromatography (1:10 MeOH/DCM) yielded the title compound **28**.

Yield: 1.2 g (87%).

Melting Point (°C): 158-160 [**literature**, 161-163].[144, 177]

^{1}H NMR (500 MHz, DMSO-*d*$_6$): δ 8.96 (s, 1H, C8-H), 8.83 (s, 1H, C2-H), 6.03 (d, 1H, *J* = 5.1 Hz, C1′-H), 5.51 (d, 1H, *J* = 5.5 Hz, C2′-H), 5.30 (d, 1H, *J* = 5.4 Hz, C3′-H), 5.13 (t, 1H, *J* = 5.3

Hz, C4′-H), 4.57 (m, 1H, C5′-H), 4.22 (m, 1H, C5′-H), 4.12 (m, 1H, C5′-OH), 3.4 – 3.7 (m, 2H, C2′-OH and C3′-OH).

^{13}C NMR (125 MHz, DMSO-d_6): δ 152.93 (1C, C2), 151.41 (1C, C4), 143.26 (1C, C6), 142.84 (1C, C8), 133.52 (1C, C5), 87.31 (1C, C1′), 86.87 (1C, C4′), 73.52 (1C, C2′), 71.26 (1C, C3′), 62.08 (1C, C5′).

LC/ESI-MS: negative mode 285 ($[M - H]^-$), positive mode 287 ($[M + H]^+$).

11.1 General procedure for the synthesis of N^6-substituted-purine ribosides (29, 30, 33-48)

A mixture of 6-chloro-9-(*β*-D-ribofuranosyl)purine (**28**, 500 mg, 1.74 mmol), and (1.76 mmol) of amine, (1.6 mmol) of Et_3N and 25 mL of ethanol was refluxed at 60 ^oC for 18 h. After completion of reaction it was evaporated under high vacuo. Purification using silica chromatography and precipitation using acetone (1:8 MeOH/DCM) yielded the title compound.

11.2. Procedure for the synthesis of N^6-substituted-purine ribosides (31-32)

A mixture of 6-chloro-9-(*β*-D-ribofuranosyl)purine (**28**, 500 mg, 1.74 mmol), and diethylamine hydrochloride (191 mg, 1.76 mmol), or dimethylamine hydrochloride (144 mg, 1.76 mmol) was stirred vigorously in dimethylformamide (DMF) at 0 ^oC for 30 min. Triethylamine (1.6 mmol, 162 mg), was added and it was stirred at 0 ^oC for 2 h followed by stirring at rt for 16 h. Triethylamine hydrochloride formed was filtered off, and was washed with cold DMF. DMF was evaporated *in vacuo*. Purification using silica chromatography (1:8 MeOH/DCM) yielded the title compound **31-32** in the form of brown oil. Precipation using acetone and recrystallization in methanol yield **31-32** as solid.

11.3. N^6-Methylpurine riboside (29)

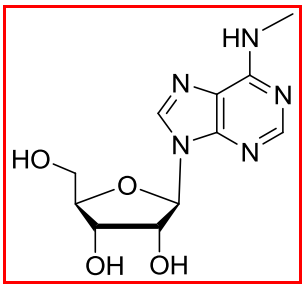

The compound was synthesized using 6-chloro-9-(*β*-D-ribofuranosyl)purine (**28**, 500 mg) and 120 mg of methylamine, and was isolated as a white solid.

Yield: 420 mg (95%).

Melting Point (°C): 169-171 [**literature**, 172].[178]

^{1}H NMR (500 MHz, D_2O-*d_6*): δ 8.65 (s, 1H, C8-H), 8.43 (s, 1H, C2-H), 6.45 (bs, 1H, NH), 6.17 – 6.18 (m, 1H, C1′-H), 4.70 – 4.72 (m, 1H, C2′-H), 4.54 – 4.56 (m, 1H, C3′-H), 4.40 – 4.41 (m, 1H, C4′-H), 4.30 (bs, H, C5′-OH), 4.18 – 4.20 (m, 2H, C5′-$\underline{H_2}$), 3.85 – 3.87 (m, 2H, C2′-OH and C3′-OH), 1.29 (s, 3H, $C\underline{H_3}$).

^{13}C NMR (125 MHz, D_2O-*d_6*): δ 158.53 (1C, C1), 153.41 (1C, C2), 149.82 (1C, C4), 142.24 (1C, C8), 120.26 (1C, C5), 93.32 (1C, C1′), 86.31 (1C, C4′), 72.87 (1C, C2′), 71.34 (1C, C3′), 62.82 (1C, C5′), 41.65 (1C, $\underline{C}H_3$).

LC/ESI-MS: negative mode 280 ($[M - H]^-$), positive mode 282 ($[M + H]^+$).

HPLC-UV (254 nm)-ESI-MS: 100%.

11.4. N^6-Ethylpurine riboside (30)

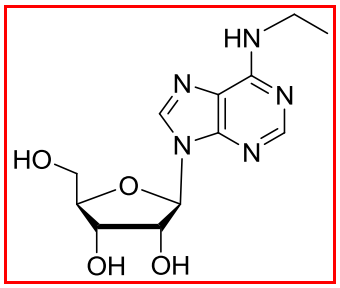

The compound was synthesized using 6-chloro-9-(*β*-D-ribofuranosyl)purine (**28**, 500 mg) and 159 mg of ethylamine, and was isolated as a white solid.

Yield: 390 mg (93%).

Melting Point (^{o}C): 189-191 [**literature**, 191-192][178]

^{1}H NMR (500 MHz, DMSO-d_6): δ 8.64 (s, 1H, C8-H), 8.42 (s, 1H, C2-H), 6.45 (m, 1H, NH), 6.17 – 6.18 (m, 1H, C1′-H), 4.68 – 4.70 (m, 1H, C2′-H), 4.53 – 4.56 (m, 1H, C3′-H), 4.14 (s, 1H, C4′-H), 4.21 – 4.22 (m, 2H, C5′-H_2), 4.05 (bs, H, C5′-OH), 3.83 – 3.85 (m, 2H, C2′-OH and C3′-OH), 3.61 – 3.63 (m, 2H, CH_2), 1.36 – 1.38 (m, 3H, CH_3).

^{13}C NMR (125 MHz, DMSO-d_6): δ 159.38 (1C, C6), 153.21 (1C, C2), 150.36 (1C, C4), 141.23 (1C, C8), 115.69 (1C, C5), 98.19 (1C, C1′), 88.21 (1C, C4′), 73.96 (1C, C2′), 71.53 (1C, C3′), 62.47 (1C, C5′), 37.85 (1C, CH_2), 17.89 (1C, CH_3).

LC/ESI-MS: negative mode 294 ($[M - H]^-$), positive mode 296 ($[M + H]^+$) .

HPLC-UV (254 nm)-ESI-MS: 98.7%.

11.5. N^6-Dimethylpurine riboside (31)

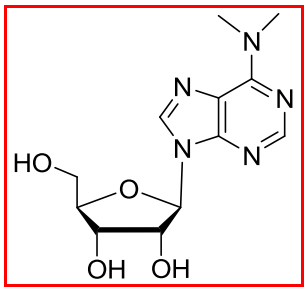

Yield: 390 mg (97%).

Melting Point (^{o}C): 182-183 [**literature**, 183-184][179]

^{1}H NMR (500 MHz, D_2O-d_6): δ 8.40 (s, 1H, C8-H), 8.20 (s, 1H, C2-H), 5.94 – 5.93 (m, 1H, C1′-H), 4.25 – 4.22 (m, 1H, C2′-H), 4.01 – 4.03 (m, 1H, C3′-H), 4.05 (bs, H, C5′-OH), 3.92 (s, 1H, C4′-H), 3.85 – 3.83 (m, 2H, C2′-OH and C3′-OH), 3.45 – 3.44 (m, 2H, C5′-$\underline{H_2}$), 2.90 – 3.18 (m, 2H, C$\underline{H_2}$), 1.88 – 1.91 (m, 6H, 2xC$\underline{H_3}$).

^{13}C NMR (125 MHz, D_2O-d_6): δ 154.38 (1C, C5), 152.05 (1C, C2), 150.54 (1C, C4), 138.13 (1C, C8), 119.42 (1C, C6), 97.39 (1C, C1′), 86.91 (1C, C4′), 83.84 (1C, C2′), 74.27 (1C, C3′), 67.31 (1C, C4′), 45.59 (2C, $\underline{C}H_3$).

LC/ESI-MS: negative mode 294 ($[M - H]^-$), positive mode 296 ($[M + H]^+$).

HPLC-UV (254 nm)-ESI-MS: 99.0%.

11.6. N^6-Diethylpurine riboside (32)

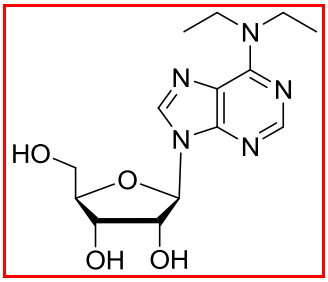

Yield: 320 mg (70%).

Melting Point (^{o}C): 178-180

^{1}H NMR (600 MHz, DMSO-d_6): δ 8.34 (s, 1H, C8-H), 8.19 (s, 1H, C2-H), 5.89 (d, *J* = 6.0 Hz, 1H, C1′-H), 5.40 (d, *J* = 6.2 Hz, 1H, C2′-H), 5.34 (dd, *J* = 7.0, 4.5 Hz, 1H, C3′-H), 5.13 (d, *J* = 4.7 Hz, 1H, C4′-H), 4.58 (td, *J* = 6.1, 4.9 Hz, 1H, C5′-H), 4.14 (td, *J* = 4.9, 3.2 Hz, 1H, C5′-H), 3.95 (q, *J* = 3.5 Hz, 1H, C5′-OH), 3.66 (q, *J* = 12.0, 4.5, 3.6 Hz, 1H, C3′-OH), 3.54 (q, *J* = 12.1, 7.0, 3.6 Hz, 1H, C2′-OH), 3.29 (s, 4H, 2xC$\underline{H}_2$), 1.19 (t, *J* = 7.0 Hz, 6H, 2xC$\underline{H}_3$).

^{13}C NMR (126 MHz, DMSO-d_6): δ 153.28 (1C, C5), 151.95 (1C, C6), 150.06 (1C, C2), 138.96 (1C, C4), 119.48 (1C, C8), 87.96 (1C, C1′), 85.92 (1C, C4′), 73.58 (1C, C2′), 70.71 (1C, C3′), 61.74 (1C, C5′), 42.55 (2C, $\underline{C}H_2$), 13.59 (2C, $\underline{C}H_3$).

LC-MS (*m*/*z*): negative mode 322 $[M-H]^-$, positive mode 324 $[M+H]^+$.

HPLC-UV (254 nm)-ESI-MS: 100%.

11.7. N^6-Ethyl-N^6-methyl-purine riboside (33)

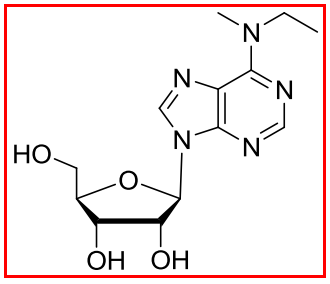

The compound was synthesized using 6-chloro-9-(*β*-D-ribofuranosyl)purine (**28**, 500 mg) and (123 mg, 2.08 mmol) of *N*-ethylmethylamine, and was isolated as a white solid.

Yield: 533 mg (98%).

Melting Point (^{o}C): 159-160

^{1}H NMR (500 MHz, DMSO-d_6): δ 8.34 (s, 1H, C8-H), 8.22 (s, 1H, C2-H), 6.13 (d, J = 3.0 Hz, 1H, C1′-H), 5.32 (dd, J = 6.2, 3.1 Hz, 1H, C2′-H), 5.18 (dd, J = 5.9, 5.1 Hz, 1H, C3′-H), 4.95 (dd, J = 6.2, 2.5 Hz, 1H, C4′-H), 4.21 (dt, J = 4.9, 2.4 Hz, 2H, C5′-$\underline{H_2}$), 4.07 – 4.05 (m, 3H, $C\underline{H_3}$), 3.51 – 3.60 (m, 2H, $C\underline{H_2}CH_3$), 1.54 (m, 3H, $CH_2C\underline{H_3}$).

^{13}C NMR (126 MHz, DMSO-d_6): δ 153.80 (1C, C5), 152.13 (1C, C6), 149.75 (1C, C2), 138.66 (1C, C4), 119.49 (1C, C8), 89.78 (1C, C1′), 86.57 (1C, C4′), 83.45 (1C, C2′), 81.50 (1C, C3′), 61.73 (1C, C5′), 27.22 (1C, $\underline{C}H_2$), 25.35 (2C, $\underline{C}H_3$).

LC-MS (m/z): negative mode 308 $[M-H]^-$, positive mode 310 $[M+H]^+$.

HPLC-UV (254 nm)-ESI-MS: 100%.

11.8. N^6-Phenylpurine riboside (34)

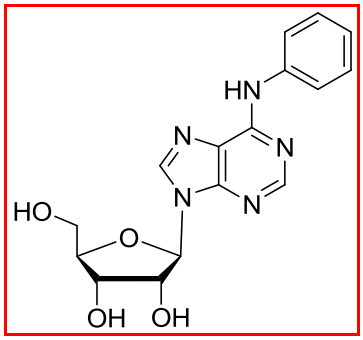

The compound was synthesized using 6-chloro-9-(β-D-ribofuranosyl)purine (**28**, 500 mg) and 328 mg of aniline, and was isolated as a white solid.

Yield: 533 mg (95%).

Melting Point (^{o}C): 186-187 [**literature**, 186-187].[180]

^{1}H NMR (500 MHz, DMSO-d_6): δ 8.55 (s, 1H, C8-H), 8.24 (s, 1H, C2-H), 7.44 – 7.48 (m, 2H, Ph), 7.39 – 7.42 (m, 2H, Ph), 7.23 – 7.26 (m, 1H, Ph), 6.12 – 6.15 (m, H, NH), 6.11 – 6.12 (m,

1H, C1′-H), 4.56 (s, 1H, C2′-H), 4.53 – 4.54 (m, 1H, C3′-H), 4.48 (bs, H, C5′-OH), 4.38 – 4.39 (m, 1H, C4′-H), 4.16 – 4.18 (m, 2H, C5′-$\underline{H_2}$), 3.78 – 3.82 (m, 2H, C2′-OH and C3′-OH).

^{13}C NMR (125 MHz, DMSO-*d_6*): δ 152.46 (1C, C2), 150.34 (1C, C4), 145.71 (1C, C6), 141.69 (1C, C8), 130.82 (2C, Ph), 128.91 (1C, Ph), 124.67 (1C, Ph), 120.43 (1C, C5), 118.65 (2C, Ph), 99.56 (1C, C1′), 88.32 (1C, C4′), 72.63 (1C, C2′), 70.72 (1C, C3′), 61.81 (1C, C5′).

LC/ESI-MS: negative mode 342 ($[M - H]^-$), positive mode 344 ($[M + H]^+$).

HPLC-UV (254 nm)-ESI-MS: 100%.

11.9. N^6-Benzylpurine riboside (35)

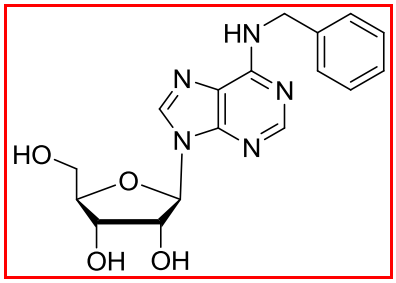

The compound was synthesized using 6-chloro-9-(*β*-D-ribofuranosyl)purine (**28**, 500 mg) and 378 mg of benzylamine, and was isolated as a white solid.

Yield: 533 mg (95%).

Melting Point (^{o}C): 177-178 [**literature**, 177-179].[178-180]

^{1}H NMR (500 MHz, D_2O-*d_6*): δ 8.48 (s, 1H, C8-H), 8.18 (s, 1H, C2-H), 7.28 – 7.38 (m, 5H, Ar-H), 6.66 (bs, 1H, NH), 6.09 – 6.10 (m, 1H, C1′-H), 4.81 (s, 1H, C2′-H), 4.70 – 4.72 (m, 2H, C$\underline{H_2}$-Ar), 4.64 (bs, H, C5′-OH), 4.52 – 4.53 (m, 1H, C3′-H), 4.36 – 4.37 (m, 1H, C4′-H), 4.15 – 4.16 (m, 2H, CH5′-$\underline{H_2}$), 4.03 – 4.05 (m, 2H, 2′-OH and 3′-OH).

^{13}C NMR (125 MHz, D_2O-*d_6*): δ 159.44 (1C, C6), 153.45 (1C, C2), 149.38 (1C, C4), 145.21 (1C, C8), 145.26 (1C, Ar), 128.53 (2C, Ar), 127.67 (2C, Ar), 126.32 (1C, Ar), 120.45 (1C, C5),

98.41 (1C, C1′), 88.42 (1C, C4′), 75.04 (1C, C2′), 71.31 (1C, C3′), 65.66 (1C, C5′), 42.81 (1C, $\underline{C}H_2$-Ar).

LC/ESI-MS: negative mode 356 ($[M - H]^-$), positive mode 358 ($[M + H]^+$).

HPLC-UV (254 nm)-ESI-MS: 100%.

11.10. N^6-(2-Phenylethyl)purine riboside (36)

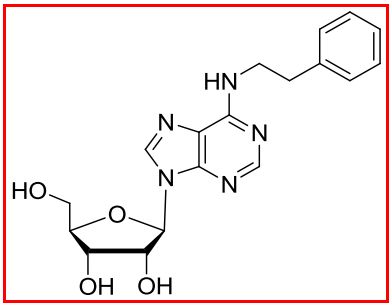

The compound was synthesized using 6-chloro-9-(*β*-D-ribofuranosyl)purine (**28**, 500 mg) and 251 mg of 2-phenylethylamine, and was isolated as a white solid.

Yield: 597 mg (91%).

Melting Point (^{o}C):170-171 [**literature**, 167-168].[181]

^{1}H NMR (500 MHz, DMSO-d_6): δ 8.33 (s, 1H, C8-H), 8.22 (s, 1H, C2-H), 7.33 – 7.23 (m, 5H, Ar-H), 7.21 – 7.13 (m, 1H, NH), 5.88 (d, *J* = 6.1 Hz, 1H, C1′-H), 5.43 – 5.34 (m, 2H, CH_2-$C\underline{H_2}$-Ar), 5.13 (d, *J* = 4.6 Hz, 1H, C2′-H), 4.60 (td, *J* = 6.2, 4.9 Hz, 1H, C3′-H), 4.14 (td, *J* = 4.8, 3.0 Hz, 1H, C4′-H), 3.96 (q, *J* = 3.5 Hz, 1H, C5′-H), 3.77 – 3.68 (m, 1H, 5′-OH), 3.66 (dd, *J* = 4.5, 3.6 Hz, 1H, C5′-H), 3.55 (q, *J* = 12.1, 7.3, 3.7 Hz, 1H, C3′-OH), 3.16 (d, *J* = 5.2 Hz, 1H, C2′-OH), 2.94 – 2.89 (m, 2H, $C\underline{H_2}$-CH_2-Ar).

^{13}C NMR (126 MHz, DMSO-d_6): δ 154.70 (1C, C6), 152.51 (1C, C2), 148.43 (1C, C4), 139.74 (1C, C8), 138.50 (1C, Ar), 128.61 (2C, Ar), 127.70 (2C, Ar), 126.16 (1C, Ar), 119.90 (1C, C5), 88.06 (1C, C1′), 86.02 (1C, C4′), 73.62 (1C, C2′), 70.78 (1C, C3′), 61.80 (1C, C5′), 41.40 (1C, $\underline{C}H_2$-CH_2), 35.12 (1C, $\underline{C}H_2$-Ar).

LC-MS (*m*/*z*): negative mode 370 $[M-H]^-$, positive mode 372 $[M+H]^+$.

HPLC-UV (254 nm)-ESI-MS: 100%.

11.11. N^6-Benzyl-N^6-methyl-purine riboside (37)

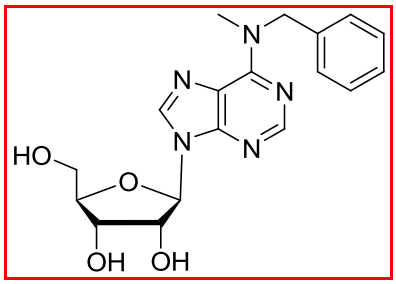

The compound was synthesized using 6-chloro-9-(*β*-D-ribofuranosyl)purine (**28**, 500 mg) and 426 mg of *N*-benzylmethylamine, and was isolated as a white solid.

Yield: 597 mg (90%).

Melting Point (^{o}C): 207-208

^{1}H NMR (500 MHz, DMSO-d_6): δ 8.45 (s, 1H, C8-H), 8.24 (s, 1H, C2-H), 7.36 – 7.37 (m, 5H, Ar-H), 6.14 – 6.15 (m, 1H, C1′-H), 5.26 – 5.28 (m, 2H, C$\underline{H}_2$), 4.87 (bs, H, C5′-OH), 4.74 – 4.76 (m, 1H, C2′-H), 4.56 – 5.58 (m, 1H, C3′-H), 4.53 – 4.56 (m, 1H, C4′-H), 4.12 – 4.14 (m, 2H, C5′-$\underline{H}_2$), 3.45 – 3.47 (m, 2H, C2′-OH and C3′-OH), 3.36 – 3.38 (m, 3H, C$\underline{H}_3$).

^{13}C NMR (125 MHz, DMSO-d_6): δ 159.62 (1C, C5), 154.84 (1C, C6), 152.71 (1C, C2), 150.16 (1C, C4), 140.36 (1C, C8), 138.72 (1C, Ar), 129.43 (2C, Ar), 125.47 (2C, Ar), 120.61 (1C, Ar), 98.12 (1C, C1′), 88.33 (1C, C4′), 74.61 (1C, C2′), 71.34 (1C, C3′), 62.52 (1C, C5′), 43.47 (1C, $\underline{C}H_3$).

LC/ESI-MS: negative mode 356 ($[M - H]^-$), positive mode 358 ($[M + H]^+$).

HPLC-UV (254 nm)-ESI-MS: 98.5%.

11.12. N^6-Benzyl-N^6-ethyl-purine riboside (38)

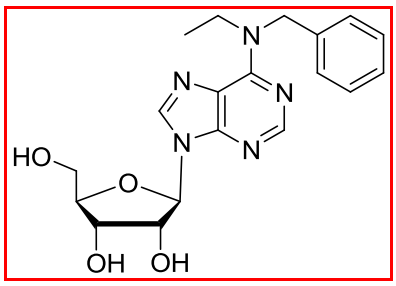

The compound was synthesized using 6-chloro-9-(*β*-D-ribofuranosyl)purine (**28**, 500 mg) and 281 mg of *N*-ethylbenzylamine, and was isolated as a white solid.

Yield: 559 mg (82%).

Melting Point (^{o}C): 224-225

^{1}H NMR (500 MHz, DMSO-d_6): δ 8.38 (s, 1H, C8-H), 8.24 (s, 1H, C2-H), 7.35 – 7.20 (m, 5H, Ar), 5.92 (d, *J* = 6.0 Hz, 1H, C1′-H), 5.41 (d, *J* = 6.2 Hz, 1H, C2′-H), 5.29 (t, *J* = 6.9, 4.6 Hz, 1H, C3′-H), 5.14 (d, *J* = 4.8 Hz, 1H, C4′-H), 4.60 (td, *J* = 6.1, 5.0 Hz, 1H, C5′-H), 4.15 (td, *J* = 4.9, 3.2 Hz, 1H, C5′-H), 3.96 (q, *J* = 3.6 Hz, 1H, C5′-OH), 3.67 (q, *J* = 12.0, 4.7, 3.7 Hz, 1H, C3′-OH), 3.55 (q, *J* = 12.0, 6.9, 3.7 Hz, 1H, C2′-OH), 3.12 – 3.10 (m, 2H, $C\underline{H}_2$-CH_3) 1.15 (s, 3H, CH_2-$C\underline{H}_3$).

^{13}C NMR (126 MHz, DMSO-d_6): δ 153.83 (1C, C5), 152.01 (1C, C6), 150.34 (1C, C2), 139.14 (1C, C4), 138.65 (1C, C8), 138.55 (1C, Ar), 127.43 (2C, Ar), 127.10 (2C, Ar), 119.47 (1C, Ar), 87.91 (1C, C1′), 85.92 (1C, C4′), 73.60 (1C, C2′), 70.69 (1C, C3′), 61.70 (1C, C5′), 50.63 (1C, $\underline{C}H_2$-Ar), 41.58 (1C, CH_3-$\underline{C}H_2$), 13.07 (1C, $\underline{C}H_3$-CH_2).

LC-MS (*m*/*z*): negative mode 384 [M-H], positive mode 386 $[M+H]^+$.

Purity by HPLC-UV (254 nm)-ESI-MS: 100%.

11.13. N^6-Dibenzylpurine riboside (39)

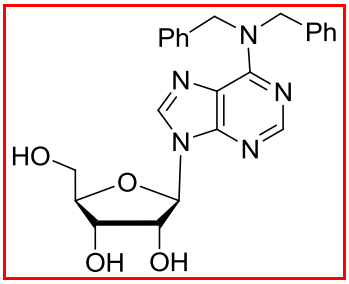

The compound was synthesized using 6-chloro-9-(*β*-D-ribofuranosyl)purine (**28**, 500 mg) and 410 mg of dibenzylamine, and was isolated as a white solid.

Yield: 603 mg (77%).

Melting Point (^{o}C): 260 (slow decomp.)

^{1}H NMR (500 MHz, DMSO-d_6): δ 8.41 (s, 1H, C8-H), 8.30 (s, 1H, C2-H), 7.36 – 7.18 (m, 10H, Ar-H), 5.95 (d, *J* = 6.0 Hz, 1H, C1′-H), 5.43 (d, *J* = 6.2 Hz, 1H, C2′-H), 5.24 (dd, *J* = 6.7, 4.7 Hz, 1H, C3′-H), 5.16 (d, *J* = 4.8 Hz, 1H, C4′-H), 4.91 (s, 4H, 2xCH_2), 4.62 (td, *J* = 6.1, 4.9 Hz, 1H, C5′-H), 4.16 (td, *J* = 4.9, 3.2 Hz, 1H, C5′-H), 3.97 (q, *J* = 3.6 Hz, 1H, C5′-OH), 3.71 – 3.62 (m, 1H, C3′-OH), 3.55 (q, *J* = 12.1, 6.8, 3.8 Hz, 1H, C2′-OH).

^{13}C NMR (126 MHz, DMSO-d_6): δ 154.37 (1C, C5), 152.07 (1C, C6), 150.64 (1C, C2), 148.26 (1C, C4), 139.34 (1C, C8), 137.92 (2C, Ar), 128.67 (4C, Ar), 128.34 (4C, Ar), 127.36 (1C, Ar), 119.49 (1C, Ar), 87.90 (1C, C1′), 85.96 (1C, C4′), 73.63 (1C, C2′), 70.69 (1C, C3′), 61.69 (1C, C5′), 52.25 (2C, $\underline{C}H_2$-Ar).

LC-MS (*m*/*z*): negative mode 446 $[M-H]^-$, positive mode 448 $[M+H]^+$.

Purity by HPLC-UV (254 nm)-ESI-MS: 99.2%.

11.14. N^6-(4-Aminobenzyl)purine riboside (40)

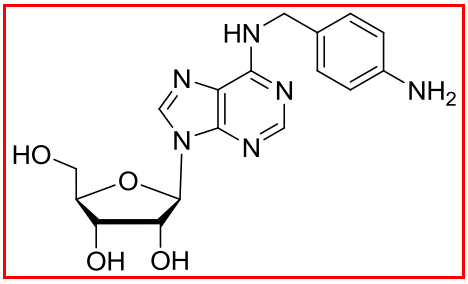

The compound was synthesized using 6-chloro-9-(*β*-D-ribofuranosyl)purine (**28**, 500 mg) and 294 mg of 4-aminobenzylamine, and was isolated as a yellow solid powder.

Yield: 509 mg (78%).

Melting Point (^{o}C):188-189

^{1}H NMR (500 MHz, DMSO-d_6): δ 8.33 (s, 1H, C8-H), 8.19 (s, 1H, C2-H), 8.13 (s, 1H, NH), 7.09 – 6.95 (m, 2H, Ar-H), 6.52 – 6.42 (m, 2H, Ar-H), 5.87 (d, *J* = 6.1 Hz, 1H, C1′-H), 5.42 – 5.33 (m, 2H, CH_2-Ar), 5.13 (d, *J* = 4.2 Hz, 1H, C2′-H), 4.87 (s, 2H, Ar-NH_2), 4.60 (q, *J* = 5.6 Hz, 1H, C3′-H), 4.52 (m, 2H, C5′-H_2), 4.17 – 4.11 (m, 1H, C4′-H), 3.96 (q, *J* = 3.4 Hz, 1H, C5′-OH), 3.67 (dt, *J* = 12.1, 4.0 Hz, 1H, C3′-OH), 3.54 (q, *J* = 12.2, 7.2, 3.6 Hz, 1H, C2′-OH).

^{13}C NMR (126 MHz, DMSO-d_6): δ 154.87 (1C, C6), 152.46 (1C, C2), 147.53 (1C, C4), 146.40 (1C, Ar), 139.83 (1C, C8), 128.36 (1C, Ar), 127.05 (2C, Ar), 120.87 (1C, C5), 113.80 (2C, Ar), 88.12 (1C, C1′), 86.03 (1C, C4′), 73.61 (1C, C2′), 70.79 (1C, C3′), 61.82 (1C, C5′), 40.92 (1C, CH_2-Ar).

LC-MS (*m*/*z*): negative mode 371 $[M-H]^-$, positive mode 373 $[M+H]^+$.

HPLC-UV (254 nm)-ESI-MS: 100%.

11.15. N^6-(4-Chlorobenzyl)-purine riboside (41)

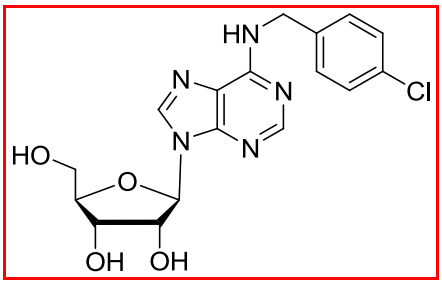

The compound was synthesized using 6-chloro-9-(*β*-D-ribofuranosyl)purine (**28**, 500 mg) and 490 mg of 4-chlorobenzylamine, and was isolated as a white solid.

Yield: 509 mg (95%).

Melting Point (^{o}C): 185-186 [**literature**, 181-182].[130, 178-180]

^{1}H NMR (500 MHz, DMSO-*d_6*): δ 8.51 (s, 1H, C8-H), 8.21 (s, 1H, C2-H), 7.29 – 7.32 (m, 4H, Ar-H), 6.42 (bs, 1H, NH), 6.10 – 6.11 (m, 1H, C1′-H), 4.82 – 4.84 (m, 2H, CH_2-Ar), 4.75 (m, 1H, C2′-H), 4.58 (bs, 1H, C5′-OH), 4.53 – 4.54 (m, 1H, C3′-H), 4.37 – 4.38 (m, 1H, C4′-H), 4.17 – 4.18 (m, 2H, C5′-H_2), 3.24 – 3.26 (m, 2H, C2′-OH and C3′-OH).

^{13}C NMR (125 MHz, DMSO-*d_6*): δ 160.12 (1C, C6), 152.63 (1C, C2), 149.71 (1C, C4), 141.57 (1C, C8), 138.44 (1C, Ar), 131.28 (2C, Ar), 126.89 (2C, Ar), 124.21 (1C, Ar), 117.31 (1C, C5), 93.72 (1C, C1′), 81.71 (1C, C4′), 74.26 (1C, C2′), 72.87 (1C, C3′), 62.82 (1C, C5′), 42.91 (1C, CH_2-Ar).

LC/ESI-MS: negative mode 390 ($[M - H]^-$), positive mode 392 ($[M + H]^+$).

HPLC-UV (254 nm)-ESI-MS: 98.5%.

11.16. N^6-(3-Chlorobenzyl)-purine riboside (42)

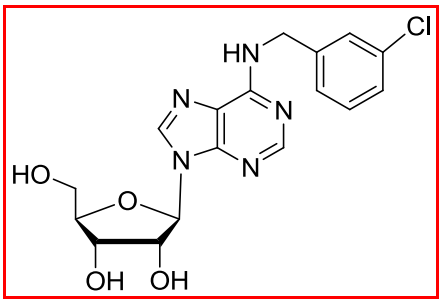

The compound was synthesized using 6-chloro-9-(*β*-D-ribofuranosyl)purine (**28**, 500 mg) and 490 mg of 3-chlorobenzylamine, and was isolated as a white solid.

Yield: 510 mg (95%).

Melting Point (^{o}C): 164-166 [**literature**, 164-165].[130]

^{1}H NMR (500 MHz, DMSO-d_6): δ 8.38 (s, 1H, C8-H), 8.20 (s, 1H, C2-H), 7.35 – 7.25 (m, 5H, Ar), 5.89 (d, *J* = 6.1 Hz, 1H, C1′-H), 5.40 – 5.38 (m, 1H, C2′-H), 5.31 – 5.27 (m, 1H, C3′-H), 5.14 – 5.10 (m, 1H, C4′-H), 4.75 – 4.67 (m, 2H, -CH_2-Ar), 4.64 – 4.52 (m, 1H, C5′-H), 4.15 (t, *J* = 5.0, 3.1 Hz, 1H, C5′-H), 3.96 (q, *J* = 3.5 Hz, 1H, C5′-OH), 3.67 (t, *J* = 12.0, 3.8 Hz, 1H, C3′-OH), 3.55 (t, *J* = 11.9, 3.6 Hz, 1H, C2′-OH).

^{13}C NMR (125 MHz, DMSO-d_6): δ 161.33 (1C, C6), 154.50 (1C, C2), 152.45 (1C, C4), 146.72 (1C, C8), 142.81 (1C, Ar), 140.17 (2C, Ar), 133.00 (2C, Ar), 130.25 (1C, Ar), 126.22 (1C, C5), 88.08 (1C, C1′), 86.00 (1C, C4′), 73.64 (1C, C2′), 70.74 (1C, C3′), 61.76 (1C, C5′), 45.04 (1C, -CH_2-Ar).

LC/ESI-MS: negative mode 390 ($[M - H]^-$), positive mode 392 ($[M + H]^+$).

HPLC-UV (254 nm)-ESI-MS: 100%.

11.17. N^6-(2-Chlorobenzyl)-purine riboside (43)

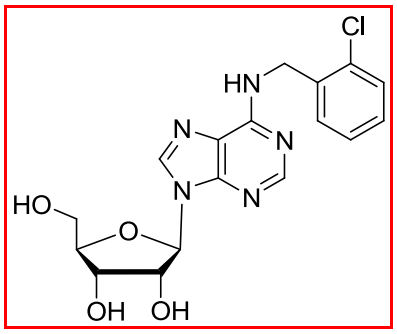

The compound was synthesized using 6-chloro-9-(*β*-D-ribofuranosyl)purine (**28**, 500 mg) and 490 mg of 2-chlorobenzylamine, and was isolated as a white solid.

Yield: 509 mg (95%).

Melting Point (^{o}C): 182-183 [**literature**, 183-184].[130]

^{1}H NMR (500 MHz, DMSO-*d_6*): δ 8.42 (s, 1H, C8-H), 8.18 (s, 1H, C2-H), 7.59 – 7.50 (bs, 1H, NH), 7.46 – 7.36 (m, 2H, Ar), 7.29 – 7.18 (m, 3H, Ar), 5.90 (d, *J* = 6.0 Hz, 1H, C1′-H), 5.42 (s, 1H, C2′-H), 5.32 (s, 2H, -C$\underline{H_2}$-Ar), 5.16 (s, 1H, C3′-H), 4.81 – 4.73 (m, 2H, C5′-$\underline{H_2}$), 4.61 (d, *J* = 6.3 Hz, 1H, C4′-H), 3.96 (q, *J* = 3.5 Hz, 1H, C5′-OH), 3.66 (dd, *J* = 12.1, 3.8 Hz, 1H, C3′-OH), 3.56 – 3.42 (m, 1H, C2′-OH).

^{13}C NMR (125 MHz, DMSO-*d_6*): δ 154.66 (1C, C6), 152.50 (1C, C2), 148.76 (1C, C4), 140.29 (1C, Ar), 136.77 (1C, C8), 131.86 (1C, Ar), 130.76 (1C, Ar), 129.21 (1C, Ar), 128.45 (1C, Ar), 127.25 (1C, Ar), 120.03 (1C, C5), 88.07 (1C, C1′), 86.05 (1C, C4′), 73.64 (1C, C2′), 70.78 (1C, C3′), 61.79 (1C, C5′), 41.17 (1C, -$\underline{C}H_2$-Ar).

LC/ESI-MS: negative mode 390 ($[M - H]^-$), positive mode 392 ($[M + H]^+$).

HPLC-UV (254 nm)-ESI-MS: 97.2%.

11.18. N^6-(4-Hydroxybenzyl)-purine riboside (44)

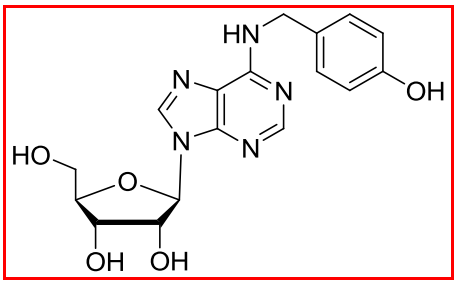

The compound was synthesized using 6-chloro-9-(*β*-D-ribofuranosyl)purine (**28**, 500 mg) and 432 mg of 4-hydroxybenzylamine, and was isolated as a white solid.

Yield: 509 mg (95%).

Melting Point (^{o}C): 201-202 [**literature**, 201-204].[182]

^{1}H NMR (500 MHz, DMSO-*d*$_6$): δ 8.33 (s, 1H, C8-H), 8.16 (s, 1H, C2-H), 7.11 – 6.93 (m, 2H, Ar-H), 6.53 – 6.37 (m, 2H, Ar-H), 5.87 (d, *J* = 6.1 Hz, 1H, C1′-H), 5.13 (d, *J* = 4.2 Hz, 1H, C2′-H), 4.87 (s, 2H, -C$\underline{H_2}$-Ar), 4.60 (q, *J* = 5.6 Hz, 1H, C3′-H), 4.52 (m, 2H, C5′-$\underline{H_2}$), 4.21 – 4.12 (m, 1H, C4′-H), 3.96 (q, *J* = 3.4 Hz, 1H, C5′-OH), 3.67 (dt, *J* = 12.1, 4.0 Hz, 1H, C3′-OH), 3.54 (q, *J* = 12.1, 7.2, 3.7 Hz, 1H, C2′-OH).

^{13}C NMR (125 MHz, DMSO-*d*$_6$): δ 154.60 (1C, C6), 152.46 (1C, C2), 148.49 (1C, C4), 147.53 (1C, Ar), 139.83 (1C, C8), 128.36 (1C, Ar), 127.05 (2C, Ar), 119.86 (1C, C5), 113.80 (2C, Ar), 88.12 (1C, C1′), 86.03 (1C, C4′), 73.61 (1C, C2′), 70.79 (1C, C3′), 61.82 (1C, C5′), 52.73 (1C, $\underline{C}H_2$-Ar).

LC/ESI-MS: negative mode 372 ($[M - H]^-$), positive mode 373 ($[M + H]^+$).

HPLC-UV (254 nm)-ESI-MS: 98.2%.

11.19. N^6-(4-Methoxybenzyl)-purine riboside (45)

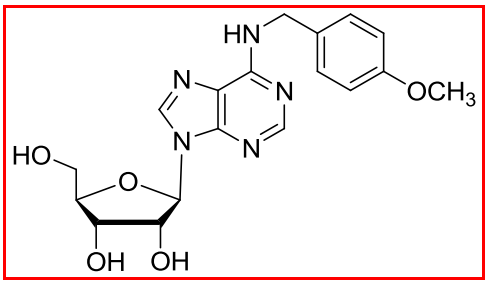

The compound was synthesized using 6-chloro-9-(*β*-D-ribofuranosyl)purine (**28**, 500 mg, 1.74 mmol), and 442 mg of 4-methoxybenzylamine, and was isolated as a white solid.

Yield: 509 mg (95%).

Melting Point (^{o}C): 161-163 [**literature**, 154-156].[130]

^{1}H NMR (500 MHz, DMSO-d_6): δ 8.35 (s, 1H, C8-H), 8.18 (s, 1H, C2-H), 8.12 (bs, 1H, NH), 7.43 (d, *J* = 7.6 Hz, 2H, Ar-H), 7.25 – 7.21 (m, 2H, Ar-H), 7.10 – 7.05 (m, 2H, Ar-H), 6.16 – 6.10 (m, *J* = 6.1 Hz, 1H, C1′-H), 5.75 – 5.73 (m, 1H, C2′-H), 5.50 (d, *J* = 6.2, Hz, 1H, C3′-H), 5.45 – 5.40 (m, 1H, C$\underline{H}_2$-Ar), 4.70 – 4.68 (m, 1H, C4′-H), 4.10 – 4.00 (m, 1H, C5′-H), 3.95 – 3.90 (m, 1H, C5′-H), 3.83 (d, *J* = 7.0 Hz, 3H, -OC$\underline{H}_3$) 3.79 (dt, 1H, C5′-OH), 3.58 (dq, *J* = 11.7, 1H, C3′-OH), 3.54 – 3.51 (m, 1H, C2′-OH).

^{13}C NMR (125 MHz, DMSO-d_6): δ 158.69 (1C, C6), 154.78 (1C, C2), 152.37 (1C, C4), 140.38 (1C, Ar), 132.20 (1C, C8), 130.57 (2C, Ar), 126.40 (2C, Ar), 121.20 (1C, Ar), 119.40 (1C, C5), 97.03 (1C, C1′), 87.49 (1C, C4′), 73.76 (1C, C2′), 70.50 (1C, C3′), 61.67 (1C, C5′), 55.86 (1C, -O$\underline{C}$H$_3$), 48.92 (1C, $\underline{C}$H-Ar).

LC/ESI-MS: negative mode 386 ($[M - H]^-$), positive mode 388 ($[M + H]^+$).

HPLC-UV (254 nm)-ESI-MS: 98.0%.

11.20. N^6-(1-Phenylethyl)-purine riboside (46)

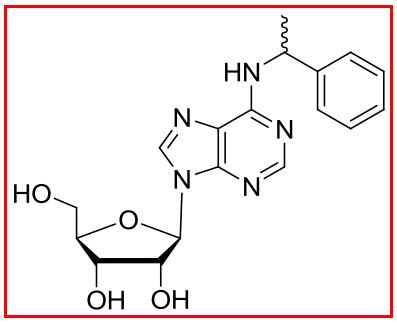

The compound was synthesized using 6-chloro-9-(*β*-D-ribofuranosyl)purine (**28**, 500 mg, 1.74 mmol), and 426 mg of 1-phenylethylamine, and was isolated as a white solid.

Yield: 509 mg (95%).

Melting Point (^{o}C): 201-202.

^{1}H NMR (500 MHz, DMSO-*d_6*): δ 8.36 (s, 1H, C8-H), 8.29 (s, 1H, C2-H), 8.15 (bs, 1H, NH), 7.43 (d, *J* = 7.6 Hz, 2H, Ar-H), 7.27 (td, *J* = 7.6, 1.3 Hz, 2H, Ar-H), 7.24 – 7.13 (m, 1H, Ar-H), 5.87 (dd, *J* = 6.1, 3.6 Hz, 1H, C1′-H), 5.51 – 5.43 (m, 1H, C2′-H), 5.40 (dd, *J* = 6.2, 3.1 Hz, 1H, H3′), 5.36 – 5.27 (m, 1H, C<u>H</u>-Ar), 5.14 (d, *J* = 4.6 Hz, 1H, C4′-H), 4.59 (dd, *J* = 8.6, 5.4 Hz, 1H, C5′-H), 4.13 (td, *J* = 4.8, 3.0 Hz, 1H, C5′-H), 3.95 (dt, *J* = 6.2, 3.4 Hz, 1H, C5′-OH), 3.65 (dq, *J* = 11.7, 3.8 Hz, 1H, C3′-OH), 3.54 – 3.46 (m, 1H, C2′-OH), 1.53 (d, *J* = 7.0 Hz, 3H, α-C<u>H$_3$</u>).

^{13}C NMR (125 MHz, DMSO-*d_6*): δ 161.59 (1C, C6), 153.98 (1C, C2), 152.37 (1C, C4), 148.68 (1C, Ar), 145.30 (1C, C8), 139.87 (2C, Ar), 126.65 (2C, Ar), 126.28 (1C, Ar), 119.89 (1C, C5), 88.02 (1C, C1′), 85.99 (1C, C4′), 73.56 (1C, C2′), 70.75 (1C, C3′), 61.77 (1C, C5′), 48.92 (1C, <u>C</u>H-Ar), 22.66 (1C, α-<u>C</u>H$_3$).

LC/ESI-MS: negative mode 370 ($[M - H]^-$), positive mode 372 ($[M + H]^+$).

HPLC-UV (254 nm)-ESI-MS: 99.0%.

11.21. N^6-(4-Nitrobenzyl)purine riboside (47)

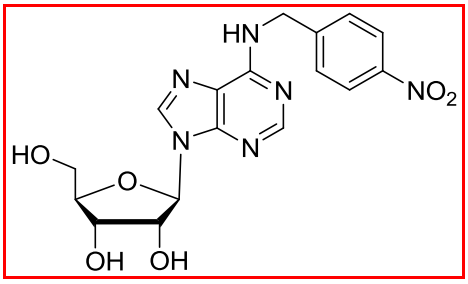

The compound was synthesized using 6-chloro-9-(*β*-D-ribofuranosyl)purine (**28**, 500 mg, 1.74 mmol), and 392 mg of 4-nitrobenzylamine, and was isolated as a yellow powder.

Yield: 531 mg (75%).

Melting Point (^{o}C): 169-171 [**literature**, 167-168].[183]

^{1}H NMR (500 MHz, DMSO-d_6): δ 8.57 (s, 1H, C8-H), 8.39 (s, 1H, C2-H), 8.19 (s, 1H, NH), 8.17 (d, *J* = 2.0 Hz, 2H, Ar-H), 8.15 (d, *J* = 1.9 Hz, 1H, Ar-H), 7.58 (d, *J* = 2.0 Hz, 1H, Ar-H), 5.93 – 5.83 (m, 1H, C1′-H), 5.35 (d, *J* = 58.6 Hz, 2H, C$\underline{H_2}$-Ar), 5.15 – 5.10 (m, 1H, C2′-H), 4.82 – 4.75 (m, 1H, C3′-H), 4.60 (tt, *J* = 9.8, 4.9 Hz, 1H, C4′-H), 4.20 – 4.06 (m, 1H, C5′-H), 3.58 – 3.52 (m, 1H, C5′-H), 3.71 – 3.70 (m, 1H, C5′-OH), 3.96 (q, *J* = 3.8 Hz, 1H, C3′-OH), 3.70 – 3.63 (m, 1H, C2′-OH).

^{13}C NMR (126 MHz, DMSO-d_6): δ 152.45 (1C, C6), 151.81(1C, C2), 146.52 (1C, C4), 142.54 (1C, Ar), 140.28 (1C, C8), 130.53 (1C, Ar), 128.17 (2C, Ar), 123.59 (2C, Ar), 119.25 (1C, C5), 88.00 (1C, C1′), 85.95 (1C, C4′), 75.42 – 72.64 (1C, C2′), 72.06 – 68.46 (1C, C3′), 64.28 – 60.68 (1C, C5′), 54.12 (1C, $\underline{C}H_2$-Ar).

LC-MS (*m*/*z*): negative mode 401 $[M-H]^-$, positive mode 403 $[M+H]^+$.

Purity by HPLC-UV (254 nm)-ESI-MS: 98.0%.

11.22. N^6-(4-Sulfamoylbenzyl)adenosine (48)

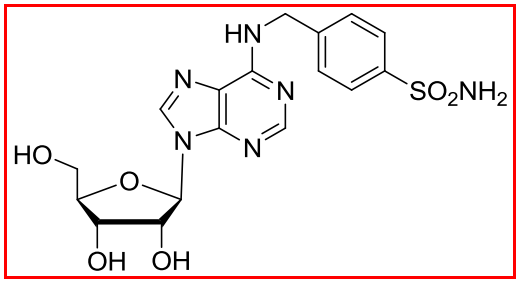

The compound was synthesized using 6-chloro-9-(*β*-D-ribofuranosyl)purine (**28**, 500 mg) and 463 mg of 4-sulfamoylbenzylamine, and was isolated as a white powder.

Yield: 517 mg (67%).

Melting Point (^{o}C): 215-216

^{1}H NMR (500 MHz, DMSO-d_6): δ 8.50 (s, 1H, C8-H), 8.38 (s, 1H, C2-H), 8.19 (s, 1H, NH), 7.79 – 7.69 (m, 2H, Ar-H), 7.48 (d, *J* = 8.0 Hz, 2H, Ar-H), 7.23 (s, 2H, CH_2-Ar), 5.89 (d, *J* = 6.1 Hz, 1H, C1′-H), 5.39 – 5.37 (m, 1H, C2′-H), 5.30 – 5.25 (m, 1H, C3′-H), 5.14 – 5.10 (m, 1H, C4′-H), 4.76 (s, NH_2), 4.60 (t, *J* = 5.6 Hz, 1H, C5′-H), 4.14 (dd, *J* = 5.0, 3.0 Hz, 1H, C5′-H), 3.96 (q, *J* = 3.5 Hz, 1H, C5′-OH), 3.66 (dd, *J* = 12.0, 3.7 Hz, 1H, C3′-OH), 3.58 – 3.48 (m, 1H, C2′-OH).

^{13}C NMR (126 MHz, DMSO-d_6): δ 154.56 (1C, C6), 152.45 (1C, C2), 148.70 (1C, C4), 144.25 (1C, Ar), 142.59 (1C, Ar), 140.17 (1C, C8), 127.44 (2C, Ar), 125.79 (2C, Ar), 121.30 (1C, C5), 88.06 (1H, C4′), 86.01 (1H, C4′), 73.64 (1H, C2′), 70.75 (1H, C3′), 61.77 (1H, C5′), 42.83 (1H, CH_2-Ar).

LC-MS (*m*/*z*): negative mode 435 $[M-H]^-$, positive mode 437 $[M+H]^+$.

HPLC-UV (254 nm)-ESI-MS: 94.8%.

12.1. Procedure for the synthesis of N^6-substituted 2′,3′-*O*-isopropylidene-purine ribosides 49-52

About 1 g of **29-32** was suspended in a mixture of 45 mL of dry acetone and 5 mL of 2′,3′-dimethoxypropane. To this was added 0.5 mL of conc. H_2SO_4. It was then vigorously stirred for 1 h. Then 3 mL of Et_3N was added and the resulting solution was evaporated under high vacuo. Purification using silica chromatography (1:12 MeOH/DCM) yielded the title compound in the form of colourless oil. Precipation using hexane and recrystallization in methanol yielded **49-52** as white solids.

12.2. 2′,3′-O-Isopropylidene-N^6-methyl-purine riboside (49)

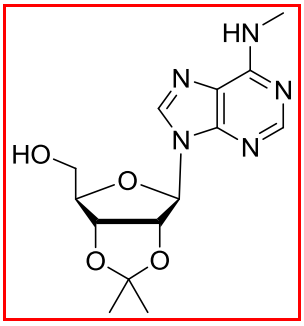

Yield: 315 mg (91%).

Melting Point (^{o}C): 170-171

^{1}H NMR (500 MHz, DMSO-d_6): δ 8.31 (s, 1H, C8-H), 8.23 (s, 1H, C2-H), 7.76 (s, 1H, NH), 6.12 (d, *J* = 3.1 Hz, 1H, C1′-H), 5.33 (dd, *J* = 6.2, 3.1 Hz, 1H, C2′-H), 5.19 (dd, *J* = 6.0, 5.1 Hz, 1H, C3′-H), 4.96 (dd, *J* = 6.2, 2.5 Hz, 1H, C4′-H), 4.21 (td, *J* = 4.9, 2.5 Hz, 1H, C5′-OH), 3.65 – 3.49 (m, 2H, C5′-H_2), 2.95 (s, 3H, NH-CH_3), 1.54 (d, *J* = 0.8 Hz, 3H, C-CH_3), 1.32 (d, *J* = 0.8 Hz, 3H, C-CH_3).

^{13}C NMR (126 MHz, DMSO-d_6): δ 155.21 (1C, C6), 152.78 (1C, C2), 147.96 (1C, C4), 139.53 (1C, C8), 119.75 (1C, CH_3-$\underline{C}$-CH_3), 113.18 (1C, C5), 89.77 (1C, C1′), 86.52 (1C, C4′), 83.40 (1C, C2′), 81.50 (1C, C3′), 61.73 (1C, C5′), 27.22 (1C, $\underline{C}H_3$), 25.34 (2C, C-$\underline{C}H_3$).

LC-MS (*m*/*z*): negative mode 320 $[M-H]^-$, positive mode 322 $[M+H]^+$.

HPLC-UV (254 nm)-ESI-MS: 97.8%.

12.3. 2',3'-Isopropylidiene-N^6-ethyl-purine riboside (50).

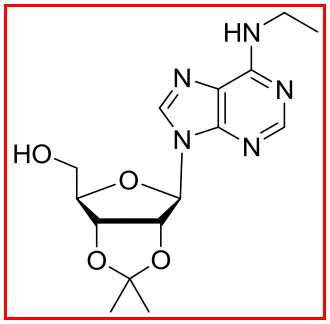

Yield: 261 mg (78%).

Melting Point (°C): 185-187 [**literature**, 109-111].[184]

^{1}H NMR (500 MHz, DMSO-d_6): δ 8.31 (s, 1H, C8-H), 8.21 (s, 1H, C2-H), 7.81 (s, 1H, NH), 6.11 (d, *J* = 3.0 Hz, 1H, C1′-H), 5.63 – 5.20 (m, 2H, C2′-H), 4.96 (dd, *J* = 6.2, 2.5 Hz, 1H, C3′-H), 4.20 (td, *J* = 4.9, 2.5 Hz, 1H, C4′-H), 3.55 (td, *J* = 10.7, 9.8, 3.6 Hz, 2H, C5′-$\underline{H_2}$), 3.47 – 3.40 (m, 2H, -$C\underline{H_2}$-Ar), 1.54 (s, 3H, $C\underline{H_3}$), 1.32 (s, 3H, $C\underline{H_3}$), 1.17 (t, *J* = 7.1 Hz, 3H, CH_2-$C\underline{H_3}$).

^{13}C NMR (126 MHz, DMSO-d_6): δ 154.63 (1C, C6), 152.73 (1C, C2), 148.17 (1C, C4), 139.52 (1C, C8), 119.60 (1C, CH_3-$\underline{C}$-CH_3), 113.15 (1C, C5), 89.77 (1C, C1′), 86.53 (1C, C4′), 83.39 (1C, C2′), 81.50 (1C, C3′), 61.72 (1C, C5′), 34.69 (1C, $\underline{C}H_2$-CH_3), 27.21 (1C, C-$\underline{C}H_3$), 25.33 (1C, C-$\underline{C}H_3$), 14.92 (1C, CH_2-$\underline{C}H_3$).

LC-MS (*m*/*z*): negative mode 334 $[M-H]^-$, positive mode 336 $[M+H]^+$.

Purity by HPLC-UV (254 nm)-ESI-MS: 100%.

12.4. 2',3'-Isopropylidiene-N^6-dimethyl-purine riboside (51)

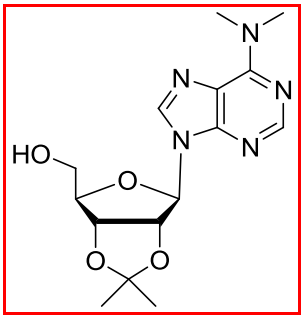

Yield: 436 mg (88%).

Melting Point (^{o}C): 177-179 [**literature**, 176-177].[184]

^{1}H NMR (600 MHz, DMSO-d_6): δ 8.34 (s, 1H, C8-H), 8.22 (s, 1H, C2-H), 6.13 (d, *J* = 3.0 Hz, 1H, C1′-H), 5.32 (dd, *J* = 6.1, 3.0 Hz, 1H, C2′-H), 5.18 (t, *J* = 5.5 Hz, 1H, C3′-H), 4.95 (dd, *J* = 6.2, 2.5 Hz, 1H, C4′-H), 3.38 – 3.33 (m, 1H, C5′-OH), 4.21 (td, *J* = 4.8, 2.5 Hz, 1H, C5′-H), 3.56 (dt, *J* = 11.7, 5.0 Hz, 1H, C5′-H), 3.44 (s, 6H, 2xCH_3), 1.54 (s, 3H, C-C$\underline{H_3}$), 1.32 (s, 3H, C-C$\underline{H_3}$).

^{13}C NMR (151 MHz, DMSO-d_6): δ 154.40 (1C, C5), 152.03 (1C, C2), 149.76 (1C, C4), 138.53 (1C, C8), 119.70 (2C, CH_3-$\underline{C}$-CH_3), 113.14 (1C, C6), 89.77 (1C, C1′), 86.56 (1C, C4′), 83.44 (1C, C2′), 81.50 (1C, C3′), 61.71 (1C, C5′), 27.20 (2C, 2x**C**H_3), 25.33 (2C, $\underline{C}H_3$-C-$\underline{C}H_3$).

LC-MS (*m*/*z*): negative mode 334 $[M-H]^-$, positive mode 336 $[M+H]^+$.

HPLC-UV (254 nm)-ESI-MS: 99.7%.

12.5. 2',3'-Isopropylidene-N^6-diethylpurine riboside (52)

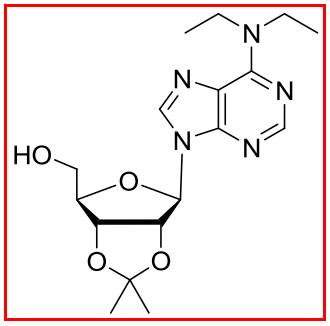

Yield: 254 mg (66%).

Melting Point (^{o}C): 195-197

^{1}H NMR (500 MHz, DMSO-d_6): δ 8.34 (s, 1H, C8-H), 8.21 (s, 1H, C2-H), 6.13 (d, *J* = 3.1 Hz, 1H, C1′-H), 5.80 – 5.75 (m, 1H, C2′-H), 5.32 (dd, *J* = 6.2, 3.1 Hz, 1H, C3′-H), 4.97 (q, *J* = 10.9, 6.2, 2.7 Hz, 1H, C4′-H), 4.21 (td, *J* = 4.9, 2.6 Hz, 2H, C5′-H_2), 3.93 (s, 4H, 2xCH_2-CH_3), 3.55 (tt, *J* = 12.1, 6.1 Hz, 1H, C5′-OH), 1.53 (d, *J* = 3.8 Hz, 3H, -C-CH_3), 1.32 (d, *J* = 5.7 Hz, 3H, -C-CH_3), 1.23 – 1.18 (m, 6H, 2xCH_3).

^{13}C NMR (126 MHz, DMSO-d_6): δ 153.25 (1C, C5), 149.78 (1C, C6), 138.78 (1C, C2), 126.83 (1C, C4), 119.24 (1C, CH_3-C-CH_3), 113.13 (1C, C8), 89.78 (1C, C1′), 86.59 (1C, C4′), 83.46 (1C, C2′), 81.51(1C, C3′), 61.73 (1C, C5′), 27.22 (2C, 2xCH_2-CH_3), 25.34 (2C, 2xC-CH_3), 13.56 (2C, 2xCH_2-CH_3).

LC-MS (*m*/*z*): negative mode 362 $[M-H]^-$, positive mode 364 $[M+H]^+$.

HPLC-UV (254 nm)-ESI-MS: 98.6%.

13.1. General procedure for the synthesis of nucleotides (53-56)

A solution of methylenebis(phosphonic dichloride) (2 mmol) in trimethyl phosphate (2 mL), cooled to 0 ^{o}C was added to a suspension of corresponding N^6-substitued-nucleosides, **49-52** (1 mmol) in trimethyl phosphate at 0 ^{o}C. The reaction mixture was stirred at 0 ^{o}C and samples were

withdrawn at 10 min interval for TLC to check the disappearance of nucleosides. After 1 h, on disappearance of nucleoside, 7 mL of cold 0.5 M aqueous TEAC solution (pH 7.4-7.6) was added. It was stirred at 0 ^{o}C for 15 min followed by stirring at room temperature for 1h. Trimethyl phosphate was extracted using (2 x 100 mL) of *tert*.butylmethyl ether and the aqueous layer was lyophilized. The mixture of nucleotide and dinucleotide was separated by ion-exchange chromatography on DEAE Sephadex (A-25, HCO^{-}_{3} form), using linear gradient of aqueous TEAC. Fractions containing the product were pooled and evaporated to dryness, with ethanol added repeatedly to remove TEAC buffer. The compound was then purified by RP-HPLC using a gradient of 50 Mm ammoniumbicarbonate/ACN from 100:0 to 40:60 and suitable fraction were pooled and lyophilized to obtain the final product as a glassy solid.

13.2. 2',3'-O-Isopropylidene-N^{6}-methylpurine riboside-5'-O-[(phosphonomethyl)phosphonic acid] (53)

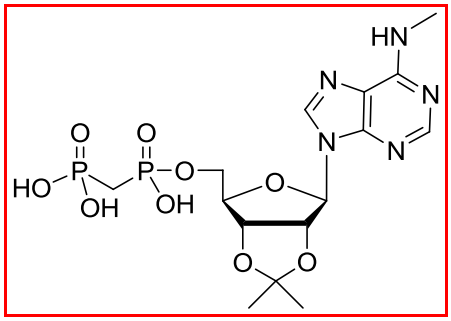

^{1}H NMR (600 MHz, methanol-*d*$_4$): δ 8.64 (s, 1H, C8-H), 8.38 (s, 1H, C2-H), 6.25 (d, *J* = 3.2 Hz, 1H, C1′-H), 5.53 – 5.30 (m, 1H, C2′-H), 5.22 (dd, *J* = 6.0, 2.2 Hz, 1H, C3′-H), 4.59 (d, *J* = 3.7 Hz, 1H, C4′-H), 4.26 (m, 2H, C5′-$\underline{H_2}$), 2.42 – 2.24 (m, 2H, P-C$\underline{H_2}$-P), 1.64 (s, 3H, C-C$\underline{H_3}$), 1.43 (s, 3H, C-C$\underline{H_3}$), 1.35 (t, *J* = 7.3 Hz, 3H, C$\underline{H_3}$).

^{13}C NMR (151 MHz, methanol-*d*$_4$): δ 153.39 (1C, C6), 149.61 (1C, C2), 148.49 (1C, C4), 142.69 (1C, C8), 120.19 (1C, CH_3-$\underline{C}$-CH_3), 115.49 (1C, C5), 92.94 (1C, C1′), 87.53 (1C, C4′),

87.31 – 86.18 (1C, C2′), 83.40 (1C, C3′), 66.31 (1C, C5′), 46.13 (1C, P-$\underline{C}H_2$-P), 27.80 (1C, $\underline{C}H_3$), 25.82 (1C, 2xC-$\underline{C}H_3$).

^{31}P NMR (243 MHz, methanol-*d*$_4$): δ 18.86 (**P$_\alpha$**), 14.60 (**P$_\beta$**).

LC-MS (*m*/*z*): negative mode 478 $[M-H]^-$, positive mode 480 $[M+H]^+$.

Purity by HPLC-UV (254 nm)-ESI-MS: 100%.

13.3. 2',3'-O-Isopropylidene-N^6-ethylpurine riboside-5'-O-[(phosphonomethyl)phosphonic acid] (54)

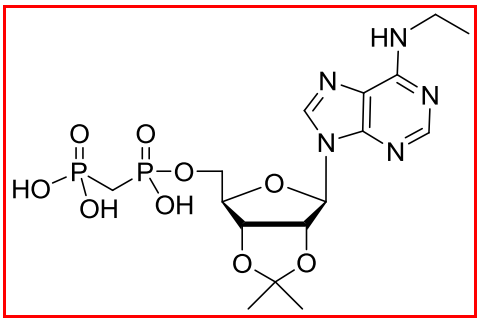

^{1}H NMR (500 MHz, methanol-*d*$_4$): δ 8.59 (s, 1H, C8-H), 8.33 (s, 1H, C2-H), 6.25 (d, *J* = 3.2 Hz, 1H, C1′-H), 5.38 (s, 1H, C2′-H), 5.21 (dd, *J* = 6.0, 2.2 Hz, 1H, C3′-H), 4.56 – 4.50 (m, 1H, C4′-H), 4.20-4.15 (m, 2H, C5′-$\underline{H}_2$), 3.77 – 3.55 (m, 2H, -$\underline{C}H_2$-CH_3), 3.26 – 3.22 (m, 3H, -CH_2-$\underline{C}H_3$), 2.30 (td, *J* = 19.9, 4.5 Hz, 2H, P-$\underline{C}H_2$-P), 1.64 (s, 3H, C-$\underline{C}H_3$), 1.43 (s, 3H, C-$\underline{C}H_3$).

^{13}C NMR (126 MHz, methanol-*d*$_4$): δ 155.10 (1C, C6), 152.47 (1C, C2), 149.28 (1C, C4), 134.62 (1C, C8), 130.07 (1C, CH_3-$\underline{C}$-CH_3), 115.01 (1C, C5), 92.02 (1C, C1′), 86.85 (1C, C4′), 85.77 (1C, C2′), 82.9 (1C, C3′), 65.81 (1C, C5′), 47.66 (1C, P-$\underline{C}H_2$-P), 27.35 (1C, -$\underline{C}H_2$-CH_3), 25.37 (2C, 2xC-$\underline{C}H_3$), 9.02 (1C, -CH_2-$\underline{C}H_3$).

^{31}P NMR (202 MHz, methanol-*d*$_4$): δ 18.82 (**P$_\alpha$**), 14.41(**P$_\beta$**).

LC-MS (*m*/*z*): negative mode 492 $[M-H]^-$, positive mode 494 $[M+H]^+$.

Purity by HPLC-UV (254 nm)-ESI-MS: 98.5%.

13.4. 2',3'-O-Isopropylidene-N^6-dimethylpurine riboside-5'-O-[(phosphonomethyl)phosphonic acid] (55)

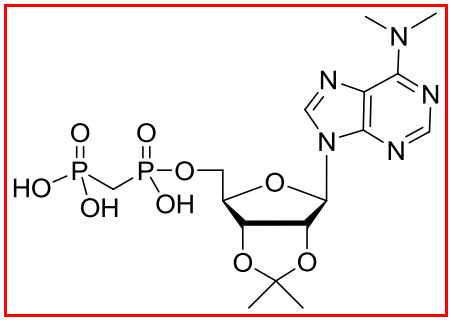

^{1}H NMR (500 MHz, methanol-d_4): δ 8.57 (s, 1H, C8-H), 8.39 (s, 1H, C2-H), 6.27 (d, *J* = 3.0 Hz, 1H, C1′-H), 5.41 (dd, *J* = 6.1, 3.0 Hz, 1H, C2′-H), 5.22 (dd, *J* = 6.2, 2.1 Hz, 1H, C3′-H), 4.58 (d, *J* = 3.4 Hz, 1H, C4′-H), 4.28 – 4.17 (m, 2H, C5′-$\underline{H}_2$), 3.35 (q, *J* = 3.3, 1.7, 0.5 Hz, 6H, signal overlap with water of MeOD, 2xCH_3), 2.35 – 2.23 (m, 2H, P-C$\underline{H}_2$-P), 1.64 (s, 3H, C-C$\underline{H}_3$), 1.43 (s, 3H, C-C$\underline{H}_3$).

^{13}C NMR (126 MHz, methanol-d_4): δ 152.53 (1C, C5), 149.41 (1C, C2), 148.36 (1C, C4), 141.66 (1C, C8), 121.30 (1C, CH_3-$\underline{C}$-CH_3), 115.54 (1C, C6), 94.25 – 92.42 (1C, C1′), 87.41 (1C, C4′), 87.09 – 85.48 (1C, C2′), 85.48 – 82.70 (1C, C3′), 66.34 (1C, C5′), 48.21 (1C, P-$\underline{C}H_2$-P), 27.76 (1C, $\underline{C}H_3$), 25.80 (1C, $\underline{C}H_3$), 9.50 (2C, -CH_2-$\underline{C}H_3$).

^{31}P NMR (202 MHz, methanol-d_4): δ 20.65 ($\mathbf{P_\alpha}$), 16.94 ($\mathbf{P_\beta}$).

LC-MS (*m*/*z*): negative mode 492 $[M-H]^-$, positive mode 494 $[M+H]^+$.

Purity by HPLC-UV (254 nm)-ESI-MS: 100%.

13.5. 2',3'-O-Isopropylidene-N^6-diethylpurine riboside-5'-O-[(phosphonomethyl)phosphonic acid] (56)

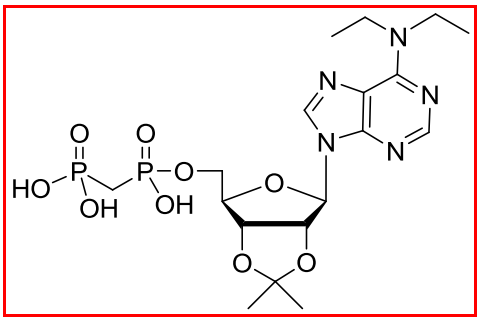

^{1}H NMR (600 MHz, methanol-*d*$_4$): δ 8.47 (s, 1H, C8-H), 8.30 (s, 1H, C2-H), 6.25 (d, *J* = 3.3 Hz, 1H, C1′-H), 5.39 (dd, *J* = 6.1, 3.4 Hz, 1H, C2′-H), 5.22 (dd, *J* = 6.2, 2.2 Hz, 1H, C3′-H), 4.52 (dd, *J* = 4.1, 2.4 Hz, 1H, C4′-H), 4.18 (dd, *J* = 5.9, 3.9 Hz, 2H, C5′-$\underline{H_2}$), 4.05 (s, 5H, $C\underline{H_2}$-$C\underline{H_3}$), 3.22 (q, *J* = 7.0 Hz, 5H, $C\underline{H_2}$-$C\underline{H_3}$), 2.36 – 2.24 (m, 2H, P-$C\underline{H_2}$-P), 1.65 (s, 3H, C-$C\underline{H_3}$), 1.43 (s, 3H, C-$C\underline{H_3}$).

^{13}C NMR (151 MHz, methanol-*d*$_4$): δ 154.02 (1C, C5), 152.03 (1C, C6), 150.70 (1C, C2), 140.18 (1C, C4), 120.71 (1C, $\underline{C}$-CH_3), 115.32 (1C, C8), 91.91 (1C, C1′), 86.70 (1C, C4′), 85.79 (1C, C2′), 83.34 (1C, C3′), 66.12 (1C, C5′), 47.80 (1C, P-$\underline{C}H_2$-P), 28.40 – 26.99 (2C, 2x$\underline{C}H_2$-CH_3), 25.72 (2C, 2xC-$\underline{C}H_3$), 9.30 (2C, 2xCH_2-$\underline{C}H_3$).

^{31}P NMR (243 MHz, methanol-*d*$_4$): δ 18.83 (d, *J* = 7.0 Hz, $\mathbf{P_\alpha}$), 14.33 (d, *J* = 6.8 Hz, $\mathbf{P_\beta}$).

LC-MS (*m*/*z*): negative mode 520 $[M-H]^-$, positive mode 522 $[M+H]^+$.

Purity by HPLC-UV (254 nm)-ESI-MS: 100%.

13.6. General procedure for the synthesis of nucleotides (57-60)

2′,3′-*O*-Isopropylidene-nucleoside-5′-*O*-[(phosphonomethyl)phosphonic acid]s **53-56** (100 mg) was dissolved in 4.5 mL dichloromethane then, 0.5 mL of water and 0.65 mL of triflouroacetic acid was added to it. It was stirred at room temperature for 3 hours. After completion of the reaction, the mixture was evaporated and the solid was precipitated adding diethyl ether. Then the crude solid product was dissolved in 6 mL water and 0.6 mL methanol. It was then purified by RP-HPLC using a gradient of H_2O/MeOH from 100:0 to 0:100, and finally appropriate fraction were pooled and lyophilized to get final product.

13.7. N^6-Methylpurine riboside-5'-O-[(phosphonomethyl)phosphonic acid] (57)

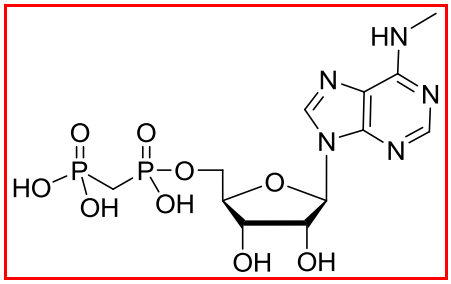

^{1}H NMR (500 MHz, D_2O): δ 8.66 (s, 1H, C8-H), 8.43 (s, 1H, C2-H), 6.18 (d, *J* = 5.1 Hz, 1H, C1′-H), 4.82 (m, 1H, C2′-H), 4.56 (t, *J* = 4.4 Hz, 1H, C3′-H), 4.46 – 4.32 (m, 1H, C4′-H), 4.21 – 4.18 (m, 2H, C5′-$\underline{H_2}$), 2.27 (t, *J* = 19.3 Hz, 2H, P-C$\underline{H_2}$-P), 1.29 (t, *J* = 7.3 Hz, 3H, C$\underline{H_3}$).

^{13}C NMR (126 MHz, D_2O): δ 153.49 (1C, C6), 150.46 (1C, C2), 148.83 (1C, C4), 145.89 (1C, C8), 122.82 (1C, C5), 91.85 (1C, C1′), 88.13 (1C, C4′), 78.33 (1C, C2′), 74.06 (1C, C3′), 67.45 (1C, C5′), 50.59 (1C, P-$\underline{C}H_2$-P), 12.10 (1C, $\underline{C}H_3$).

^{31}P NMR (202 MHz, D_2O): δ 19.78 (P_α), 17.20 (P_β).

LC-MS (*m*/*z*): negative mode 438 $[M-H]^-$, positive mode 440 $[M+H]^+$.

Purity by HPLC-UV (254 nm)-ESI-MS: 100%.

13.8. N^6-Ethylpurine riboside-5'-O-[(phosphonomethyl)phosphonic acid] (58)

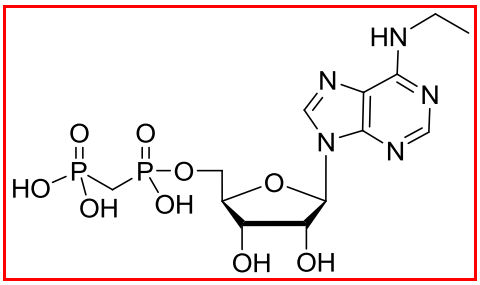

^{1}H NMR (500 MHz, D_2O): δ 8.64 (s, 1H, C8-H), 8.42 (s, 1H, C2-H), 6.18 (d, *J* = 5.1 Hz, 1H, C1′-H), 4.83 (d, *J* = 2.1 Hz, 1H, C2′-H), 4.56 (t, *J* = 4.5 Hz, 1H, C3′-H), 4.46 – 4.38 (m, 1H, C4′-

H), 4.23 – 4.21 (m, 2H, C5′-$\underline{H_2}$), 3.63 (d, *J* = 13.2 Hz, 2H, $C\underline{H_2}$-CH_3), 2.32 (t, *J* = 19.4 Hz, 2H, P-$C\underline{H_2}$-P), 1.43 – 1.35 (m, 3H, CH_2-$C\underline{H_3}$).

^{13}C NMR (126 MHz, D_2O): δ 154.56 (1C, C6), 152.48 (1C, C2), 148.73 (1C, C4), 145.85 (1C, C8), 121.38 (1C, C5), 91.84 (1C, C1′), 88.15 (1C, C4′), 78.32 (1C, C2′), 74.07 (1C, C3′), 67.50 (1C, C5′), 50.59 (1C, P-$\underline{C}H_2$-P), 30.63 (1C, $\underline{C}H_2$-CH_3), 12.10 (1C, CH_2-$\underline{C}H_3$).

^{31}P NMR (202 MHz, D_2O): δ 19.05 ($\mathbf{P_\alpha}$), 17.11 ($\mathbf{P_\beta}$).

LC-MS (*m*/*z*): negative mode 452 $[M-H]^-$, positive mode 454 $[M+H]^+$.

Purity by HPLC-UV (254 nm)-ESI-MS: 100%.

13.9. N^6-Dimethylpurine riboside-5'-O-[(phosphonomethyl)phosphonic acid] (59)

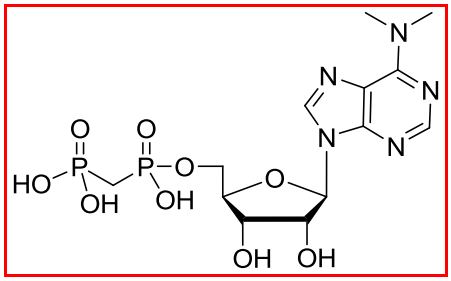

^{1}H NMR (600 MHz, D_2O): δ 8.54 (s, 1H, C8-H), 8.25 (s, 1H, C2-H), 6.13 (d, *J* = 5.4 Hz, 1H, C1′-H), 4.78-4.75 (m, 1H, C2′-H), 4.55 (t, *J* = 4.4 Hz, 1H, C3′-H), 4.39 (q, *J* = 3.2 Hz, 1H, C4′-H), 4.27 – 4.13 (m, 2H, C5′-$\underline{H_2}$), 3.54 – 3.43 (m, 6H, 2x$C\underline{H_3}$), 2.19 (t, *J* = 19.3 Hz, 2H, P-$C\underline{H_2}$-P).

^{13}C NMR (151 MHz, D_2O): δ 154.95 (1C, C5), 152.21 (1C, C2), 151.55 (1C, C4), 141.90 (1C, C8), 121.95 (1C, C6), 90.01 (1C, C1′), 86.95 (1C, C4′), 77.10 (1C, C2′), 73.10 (1C, C3′), 66.36 (1C, C5′), 49.52 (1C, P-$\underline{C}H_2$-P), 11.07 (2C, $\underline{C}H_3$).

^{31}P NMR (243 MHz, D_2O): δ 18.67 ($\mathbf{P_\alpha}$), 15.18 ($\mathbf{P_\beta}$).

LC-MS (*m*/*z*): negative mode 452 $[M-H]^-$, positive mode 454 $[M+H]^+$.

Purity by HPLC-UV (254 nm)-ESI-MS: 100%.

13.10. N^6-Diethylpurine riboside-5'-O-[(phosphonomethyl)phosphonic acid] (60)

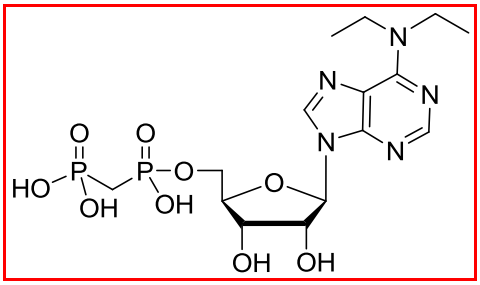

^{1}H NMR (500 MHz, D_2O): δ 8.62 (s, 1H, C8-H), 8.38 (s, 1H, C2-H), 6.19 (d, *J* = 5.2 Hz, 1H, C1′-H), 4.84 – 4.82 (m, 1H, C2′-H), 4.56 (dd, *J* = 5.1, 4.1 Hz, 1H, C3′-H), 4.41 (q, *J* = 4.4, 3.0, 1.5 Hz, 1H, C4′-H), 4.36 – 4.18 (m, 4H, 2x$C\underline{H_2}$-CH_3), 3.78 (s, 2H, C5′-$\underline{H_2}$), 2.39 – 2.25 (m, 2H, P-$C\underline{H_2}$-P), 1.37 (t, *J* = 7.2 Hz, 6H, 2xCH_2-$C\underline{H_3}$).

^{13}C NMR (126 MHz, D_2O): δ 150.80 (1C, C5), 149.98 (1C, C6), 147.86 (1C, C2), 143.63 (1C, C4), 121.79 (1C, C8), 90.77 (1C, C1′), 87.03 (1C, C4′), 77.25 (1C, C2′), 73.01 (1C, C3′), 66.53 (1C, C5′), 49.94 (2C, 2x$\underline{C}H_2$-CH_3), 48.11 (1C, P-$\underline{C}H_2$-P), 13.77 (1C, 2xCH_2-$\underline{C}H_3$).

^{31}P NMR (202 MHz, D_2O): δ 19.41 (d, $\mathbf{P_\alpha}$), 16.94 ($\mathbf{P_\beta}$).

LC-MS (*m*/*z*): negative mode 480 $[M-H]^-$, positive mode 482 $[M+H]^+$.

Purity by HPLC-UV (254 nm)-ESI-MS: 100%.

13.11. General procedure for the synthesis of nucleotides (61-76)

A solution of methylenebis(phosphonic dichloride) (5 mmol) in trimethyl phosphate (2 mL), cooled to 0 °C was added to a suspension of corresponding N^6-substitued-nucleosides **33-48** (1 mmol) in trimethyl phosphate at 0 °C. The reaction mixture was stirred at 0 °C and samples were withdrawn at 10 min interval for TLC to check the disappearance of nucleosides. After 30 min, on disappearance of nucleoside, 7 mL of cold 0.5 M aqueous TEAC solution (pH 7.4-7.6) was added. It was stirred at 0 °C for 15 min followed by stirring at room temperature for 1 h. Trimethyl phosphate was extracted using (2 x 100 mL) of *tert*.butylmethyl ether and the aqueous

layer was lyophilized. The crude product was then purified by RP-HPLC using a gradient of 50 Mm ammoniumbicarbonate/ACN from 100:0 to 60:40 to get final product. Since there was no formation of dinucleotide, ion exchange chromatography was not used.

13.12. N^6-Ethyl-N^6-methylpurine riboside-5'-O-[(phosphonomethyl)phosphonic acid] (61)

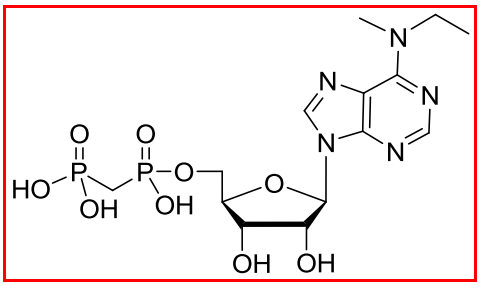

^{1}H NMR (500 MHz, D_2O): δ 8.37 (s, 1H, C8-H), 8.04 (s, 1H, C2-H), 6.04 (t, *J* = 3.8 Hz, 1H, C1′-H), 4.75 – 4.73 (m, 1H, C2′-H), 4.52 (t, *J* = 4.6 Hz, 1H, C3′-H), 4.35 (t, *J* = 3.6 Hz, 1H, C4′-H), 4.16 (dd, *J* = 5.3, 2.7 Hz, 2H, C5′-H_2), 3.80 (s, 2H, $C\underline{H_2}$-CH_3), 3.23 (s, 3H, CH_2-$C\underline{H_3}$), 2.12 (t, *J* = 19.6 Hz, 2H, P-$C\underline{H_2}$-P), 1.15 (td, *J* = 7.3, 2.6 Hz, 3H, $C\underline{H_3}$).

^{13}C NMR (126 MHz, D_2O): δ 156.38 (1C, C5), 154.90 (1C, C6), 151.90 (1C, C2), 140.52 (1C, C4), 121.45 (1C, C8), 89.74 (1C, C1′), 86.44 (1C, C4′), 76.96 (1C, C2′), 72.91 (1C, C3′), 66.21 (1C, C5′), 50.21 (1C, $\underline{C}H_2$-CH_3) 48.73 (1C, P-$\underline{C}H_2$-P), 39.19 (1C, $\underline{C}H_3$), 14.72 (1C, CH_2-$\underline{C}H_3$).

^{31}P NMR (202 MHz, D_2O): δ 20.17 (**P_α**), 13.67 (**P_β**).

LC-MS (*m*/*z*): negative mode 466 $[M-H]^-$, positive mode 468 $[M+H]^+$.

Purity by HPLC-UV (254 nm)-ESI-MS: 100%.

13.13. N^6-Phenylpurine riboside-5'-O-[(phosphonomethyl)phosphonic acid] (62)

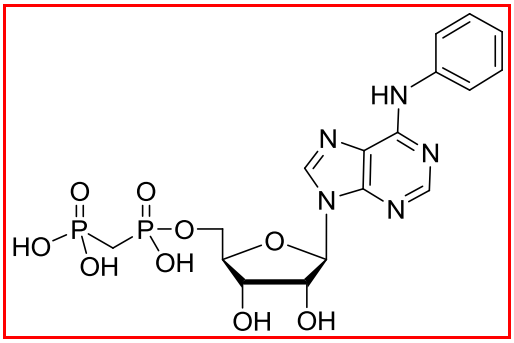

^{1}H NMR (500 MHz, D_2O): δ 8.55 (s, 1H, C8-H), 8.24 (s, 1H, C2-H), 7.44 (q, *J* = 8.5, 4.9, 2.4 Hz, 4H, Ar-H), 7.33 – 7.12 (m, 1H, Ar-H), 6.12 (t, *J* = 5.2 Hz, 1H, C1′-H), 4.76 – 4.71 (m, 1H, C2′-H), 4.55 (dd, *J* = 5.2, 4.0 Hz, 1H, C3′-H), 4.39 (tq, *J* = 3.7, 1.6 Hz, 1H, C4′-H), 4.19 (dd, *J* = 5.4, 3.3 Hz, 2H, C5′-$\underline{H_2}$), 2.21 (tt, *J* = 19.9, 2.5 Hz, 2H, P-C$\underline{H_2}$-P).

^{3}C NMR (126 MHz, D_2O): δ 154.73 (1C, C2), 154.34 (1C, C4), 151.65 (1C, C6), 143.20 (1C, C8), 139.64 (2C, Ar-H), 132.10 (1C, Ar-H), 128.44 (1C, Ar-H), 125.85 (1C, C5), 122.21 (2C, Ar-H), 89.99 (1C, C1′), 86.79 (1C, C4′), 77.12 (1C, C2′), 73.09 (1C, C3′), 66.39 (1C, C5′), 53.10 (1C, P-$\underline{C}H_2$-P).

^{31}P NMR (202 MHz, D_2O): δ 24.86 – 18.08 (d, $\mathbf{P_\alpha}$), 15.29 (d, *J* = 9.6 Hz, $\mathbf{P_\beta}$).

LC-MS (*m*/*z*): negative mode 500 $[M-H]^-$, positive mode 502 $[M+H]^+$.

Purity by HPLC-UV (254 nm)-ESI-MS: 100%.

13.14. N^6-Benzylpurine riboside-5'-O-[(phosphonomethyl)phosphonic acid] (63)

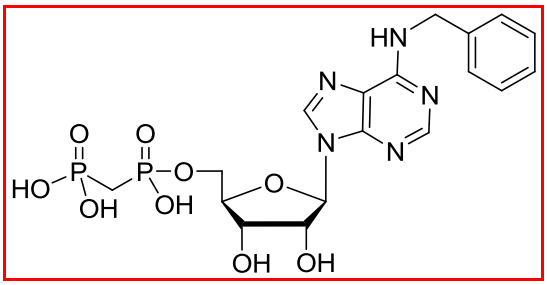

^{1}H NMR (500 MHz, D_2O): δ 8.48 (s, 1H, C8-H), 8.18 (s, 1H, C2-H), 7.63 – 7.14 (m, 5H, Ar-H), 6.10 (dd, *J* = 6.5, 2.3 Hz, 1H, C1′-H), 5.03 – 5.01 (m, 2H, C$\underline{H_2}$-Ar), 4.53 (dd, *J* = 5.2, 3.7 Hz, 1H, C2′-H) (dd, *J* = 5.2, 3.7 Hz, 1H, C3′-H), 4.37 (td, *J* = 4.1, 2.7 Hz, 1H, C4′-H), 4.16 (dt, *J* = 6.5, 3.3 Hz, 2H, C5′-$\underline{H_2}$), 2.19 (ddt, *J* = 22.3, 18.5, 3.3 Hz, 2H, P-C$\underline{H_2}$-P).

^{13}C NMR (126 MHz, D_2O): δ 157.35 (1C, C2), 155.69 (1C, C4), 151.11 (1C, C6), 142.28 (1C, C8), 131.55 (2C, Ar-H), 130.16 (1C, Ar-H), 129.76 (2C, Ar-H), 121.82 (1C, C5), 89.69 (1C, C1′), 86.78 (1C, C4′), 77.02 (1C, C2′), 73.13 (1C, C3′), 66.41 (1C, C5′), 53.50 (1C, $\underline{C}H_2$-Ar), 46.82 (1C, P-$\underline{C}H_2$-P).

^{31}P NMR (202 MHz, D_2O): δ 18.67 (d, 9.6 Hz, $\mathbf{P_\alpha}$), 15.03 (td, 9.6 Hz, $\mathbf{P_\beta}$).

LC-MS (*m*/*z*): negative mode 514 $[M-H]^-$, positive mode 516 $[M+H]^+$.

Purity by HPLC-UV (254 nm)-ESI-MS: 100%.

13.15. N^6-(2-Phenylethyl)purine riboside-5'-O-[(phosphonomethyl)phosphonic acid] (64)

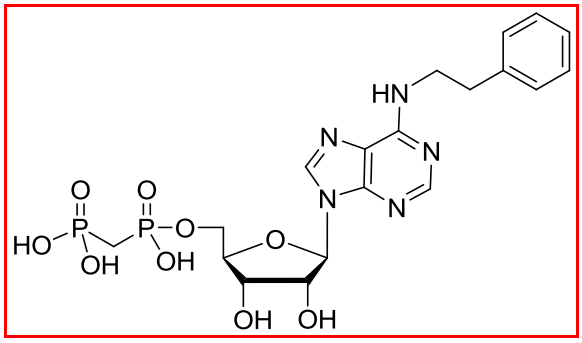

^{1}H NMR (500 MHz, D_2O): δ 8.41 (s, 1H, C8-H), 8.13 (s, 1H, C2-H), 7.30 – 7.15 (m, 5H, Ar-H), 6.06 (d, *J* = 5.5 Hz, 1H, C1′-H), 4.74 – 4.68 (m, 1H, C2′-H), 4.52 (dd, *J* = 5.2, 3.8 Hz, 1H, C3′-H), 4.36 (d, *J* = 3.5 Hz, 1H, C4′-H), 4.20 – 4.08 (m, 2H, C5′-$\underline{H_2}$), 3.80 (s, 2H, CH_2-C$\underline{H_2}$-Ar), 3.01 – 2.88 (m, 2H, C$\underline{H_2}$-CH_2-Ar), 2.26 – 2.12 (m, 2H, P-C$\underline{H_2}$-P).

^{13}C NMR (126 MHz, D_2O): δ 157.39 (1C, C6), 155.49 (1C, C2), 150.79 (1C, C4), 142.00 (1C, C8), 139.50 (1C, Ar-H), 131.86 (2C, Ar-H), 131.31 (2C, Ar-H), 129.24 (1C, Ar-H), 121.63 (1C,

C5), 89.63 (1C, C1′), 86.73 (1C, C4′), 76.99 (1C, C2′), 73.11 (1C, C3′), 66.40 (1C, C5′), 54.28 (1C, $\underline{C}H_2$-CH_2-Ar), 44.81 (1C, P-$\underline{C}H_2$-P), 37.73 (1C, CH_2-$\underline{C}H_2$-Ar).

^{31}P NMR (202 MHz, D_2O): δ 18.81 (P_α), 15.01 (P_β).

LC-MS (*m*/*z*): negative mode 528 [M-H], positive mode 530 $[M+H]^+$.

Purity by HPLC-UV (254 nm)-ESI-MS: 100%.

13.16. N^6-Benzyl-N^6-methylpurine riboside-5'-O-[(phosphonomethyl)phosphonic acid] (65)

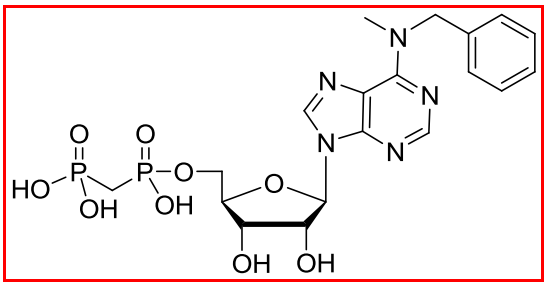

^{1}H NMR (500 MHz, D_2O): δ 8.46 (s, 1H, C8-H), 8.24 (s, 1H, C2-H), 7.48 – 7.21 (m, 5H, Ar-H), 6.15 (dd, *J* = 5.8, 1.7 Hz, 1H, C1′-H), 5.25 (s, 2H, $C\underline{H_2}$-Ar), 4.74 (d, *J* = 2.3 Hz, 1H, C2′-H), 4.54 (dd, *J* = 5.2, 3.5 Hz, 1H, C3′-H), 4.45 – 4.33 (m, 1H, C4′-H), 4.17 (t, *J* = 4.2 Hz, 2H, C5′-$\underline{H_2}$), 3.36 (s, 3H, CH_3), 2.18 (t, *J* = 19.7 Hz, 2H, P-$C\underline{H_2}$-P).

^{13}C NMR (126 MHz, D_2O): δ 157.23 (1C, C5), 154.80 (1C, C6), 152.52 (1C, C2), 141.19 (1C, C4), 139.89 (1C, C8), 131.68 (1C, Ar-H), 130.14 (2C, Ar-H), 128.35 (2C, Ar-H), 121.94 (1C, Ar-H), 89.61 (1C, H1′), 86.80 (1C, H4′), 76.95 (1C, H2′), 73.13 (1C, H3′), 66.42 (1C, H5′), 56.81 (1C, $\underline{C}H_2$-Ar), 45.32 (1C, P-$\underline{C}H_2$-P), 30.27 (1C, $\underline{C}H_3$).

^{31}P NMR (202 MHz, D_2O): δ 18.73 (P_α), 15.18 (P_β).

LC-MS (*m*/*z*): negative mode 528 $[M-H]^-$, positive mode 530 $[M+H]^+$.

Purity by HPLC-UV (254 nm)-ESI-MS: 100%.

13.17. N^6-Benzyl-N^6-ethylpurine riboside-5'-O-[(phosphonomethyl)phosphonic acid] (66)

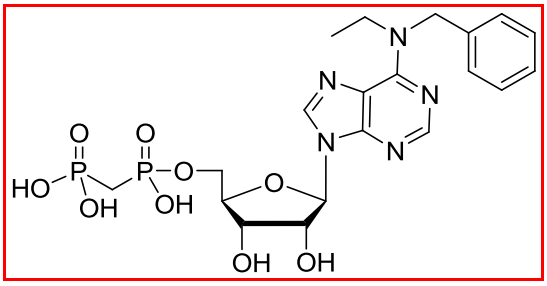

^{1}H NMR (500 MHz, D_2O): δ 8.61 (s, 1H, C8-H), 8.44 (s, 1H, C2-H), 7.51 – 7.32 (m, 5H, Ar-H), 6.21 (d, *J* = 5.3 Hz, 1H, C1′-H), 5.62 (s, 2H, -C$\underline{H_2}$-Ar), 4.74 (t, *J* = 0.7 Hz, 1H, C2′-H), 4.56 (t, *J* = 4.5 Hz, 1H, C3′-H), 4.42 (d, *J* = 3.7 Hz, 1H, C4′-H), 4.21 (dt, *J* = 11.7, 7.2 Hz, 2H, C5′-$\underline{H_2}$), 3.95 – 3.65 (m, 2H, -C$\underline{H_2}$-CH_3), 2.29 (td, *J* = 19.9, 15.6 Hz, 2H, P-C$\underline{H_2}$-P), 1.51 – 1.23 (m, 3H, -CH_2-C$\underline{H_3}$).

^{13}C NMR (126 MHz, D_2O): δ 156.18 (1C, C5), 151.08 (1C, C6), 148.15 (1C, C2), 143.73 (1C, C4), 138.78 (1C, C8), 131.89 (1C, Ar-H), 131.11 (2C, Ar-H), 129.89 (2C, Ar-H), 122.03 (1C, Ar-H), 90.88 (1C, C1′), 87.15 (1C, C4′), 77.27 (1C, C2′), 73.05 (1C, C3′), 66.56 (1C, C5′), 56.36 – 53.01 (1C, -C$\underline{H_2}$-Ar′) , 47.87 (1C, P-C$\underline{H_2}$-P), 41.58 (1C, -C$\underline{H_2}$-CH_3), 13.57 (1C, -CH_2-C$\underline{H_3}$).

^{31}P NMR (202 MHz, D_2O): δ 18.80 ($\mathbf{P_\alpha}$), 16.88 ($\mathbf{P_\beta}$).

LC-MS (*m*/*z*): negative mode 542 $[M-H]^-$, positive mode 544 $[M+H]^+$.

Purity by HPLC-UV (254 nm)-ESI-MS: 100%.

13.18. N^6-Dibenzylpurine riboside-5'-O-[(phosphonomethyl)phosphonic acid] (67)

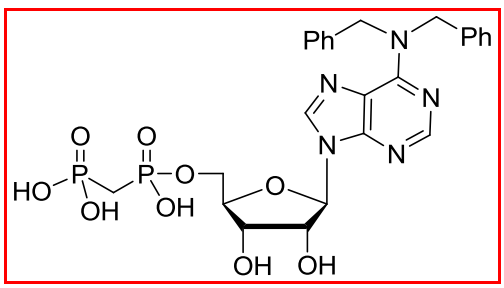

^{1}H NMR (500 MHz, D_2O): δ 8.50 (s, 1H, C8-H), 8.34 (s, 1H, C2-H), 7.45 – 7.19 (m, 10H, Ar-H), 6.17 (d, *J* = 5.6 Hz, 1H, C1′-H), 5.19 (s, 4H, 2xC$\underline{H_2}$-Ar), 4.82 (d, *J* = 0.8 Hz, 1H, C2′-H), 4.54 – 4.51 (m, 1H, C3′-H), 4.39 – 4.34 (m, 1H, C4′-H), 4.19 – 4.16 (m, 2H, C5′-$\underline{H_2}$), 2.22 (t, *J* = 19.4 Hz, 2H, P-C$\underline{H_2}$-P).

^{13}C NMR (126 MHz, D_2O): δ 155.99 (1C, C5), 152.56 (1C, C6), 151.82 (1C, C2), 142.26 (1C, C4), 138.63 (1C, C8), 131.71 (2C, Ar-H), 130.64 (4C, Ar-H), 130.14 (4C, Ar-H), 121.96 (2C, Ar-H), 90.22 (1C, C1′), 87.03 (1C, C4′), 77.08 (1C, C2′), 73.11 (1C, C3′), 66.53 (1C, C5′), 54.64 (1C, P-$\underline{C}H_2$-P), 30.01 (2C, 2x$\underline{C}H_2$-Ar).

^{31}P NMR (202 MHz, D_2O): δ 18.16 (**P_α**), 16.10 (**P_β**).

LC-MS (*m*/*z*): negative mode 604 $[M-H]^-$, positive mode 606 $[M+H]^+$.

Purity by HPLC-UV (254 nm)-ESI-MS: 100%.

13.19. N^6-(4-Aminobenzyl)purine riboside-5'-O-[(phosphonomethyl)phosphonic acid] (68)

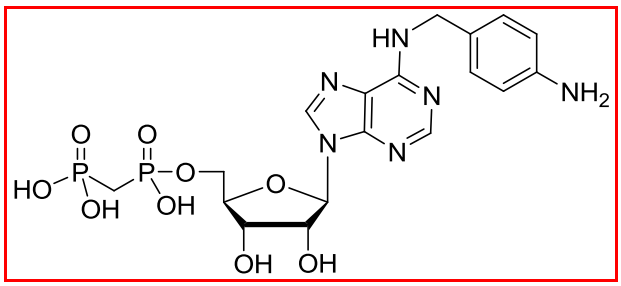

^{1}H NMR (500 MHz, D_2O): δ 8.50 (s, 1H, C8-H), 8.21 (s, 1H, C2-H), 7.38 (d, *J* = 8.0 Hz, 2H, Ar-H), 7.14 (d, *J* = 8.0 Hz, 2H, Ar-H), 6.11 (d, *J* = 5.7 Hz, 1H, C1′-H), 5.13 (d, 1H, C2′-H), 4.87 (s, 2H, C$\underline{H_2}$-Ar), 4.61 – 4.48 (m, 1H, C3′-H), 4.38 (dq, *J* = 4.4, 2.9 Hz, 1H, C4′-H), 4.17 (dd, *J* = 5.4, 3.2 Hz, 2H, C5′-$\underline{H_2}$), 2.19 (td, *J* = 19.8, 2.3 Hz, 2H, P-C$\underline{H_2}$-P).

^{13}C NMR (126 MHz, D_2O): δ 156.95 (1C, C6), 152.52 (1C, C2), 149.80 (1C, C4), 146.46 (1C, Ar-H), 138.55 (1C, C8), 137.62 (1C, Ar-H), 131.23 (2C, Ar-H), 128.77 (1C, C5), 119.42 (1C,

2C, Ar-H), 89.75 (1C, C1′), 86.90 – 86.85 (1C, C4′), 77.04 (1C, C2′), 73.11 (1C, C3′), 66.41 (1C, C5′), 55.65 (1C, $\underline{C}H_2$-Ar), 49.25 (1C, P-$\underline{C}H_2$-P) .

^{31}P NMR (202 MHz, D_2O): δ 18.71 (d, *J* = 9.7 Hz, **P_α**), 15.14 (d, *J* = 9.7 Hz, **P_β**).

LC-MS (*m*/*z*): negative mode 529 $[M-H]^-$, positive mode 531 $[M+H]^+$.

Purity by HPLC-UV (254 nm)-ESI-MS: 100%.

13.20. N^6-(4-Chlorobenzyl)purine riboside-5′-O-[(phosphonomethyl)phosphonic acid] (69)

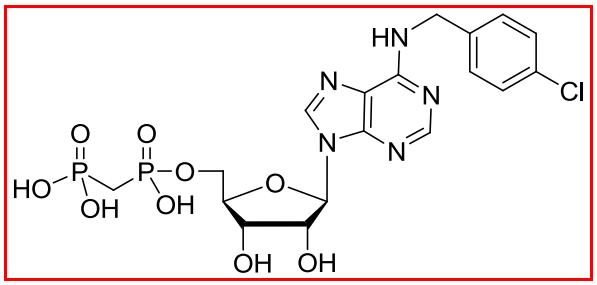

^{1}H NMR (500 MHz, D_2O): δ 8.51 (s, 1H, C8-H), 8.22 (s, 1H, C2-H), 7.29 – 7.21 (m, 4H, Ar-H), 6.11 (d, *J* = 5.6 Hz, 1H, C1′-H), 4.82 (d, *J* = 1.0 Hz, 1H, C2′-H), 4.76 (s, 2H, $C\underline{H_2}$-Ar), 4.74 (d, *J* = 1.3 Hz, 1H, C3′-H), 4.54 (dd, *J* = 5.2, 3.9 Hz, 1H, C4′-H), 4.18 (dd, *J* = 5.5, 3.3 Hz, 2H, C5′-$\underline{H_2}$), 2.20 (td, *J* = 19.8, 1.4 Hz, 2H, P-$C\underline{H_2}$-P).

^{13}C NMR (126 MHz, D_2O): δ 157.08 (1C, C6), 155.40 (1C, C2), 149.28 (1C, C4), 142.46 (1C, C8), 139.72 (1C, Ar-H), 135.14 (1C, Ar-H), 131.31 (2C, Ar-H), 129.45 (2C, Ar-H), 121.83 (1C, C5), 89.73 (1C, C1′), 86.81 (1C, C4′), 77.05 (1C, C2′), 73.13 (1C, C3′), 66.40 (1C, C5′), 46.21 (1C, P-$\underline{C}H_2$-P), 37.61 (1C, $\underline{C}H_2$-Ar).

^{31}P NMR (202 MHz, D_2O): δ 21.30 – 17.66 (**P_α**), 15.26 (**P_β**).

LC-MS (*m*/*z*): negative mode 548 $[M-H]^-$, positive mode 550 $[M+H]^+$.

Purity by HPLC-UV (254 nm)-ESI-MS: 99.0%.

13.21. N^6-(3-Chlorobenzyl)purine riboside-5'-O-[(phosphonomethyl)phosphonic acid] (70)

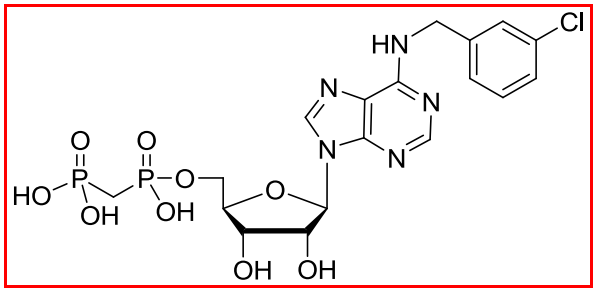

^{1}H NMR (500 MHz, D_2O): δ 8.52 (s, 1H, C8-H), 8.21 (s, 1H, C2-H), 7.35 (s, 1H, Ar-H), 7.31 – 7.19 (m, 3H, Ar-H), 6.11 (d, *J* = 5.6 Hz, 1H, C1′-H), 4.76 (t, *J* = 5.4 Hz, 1H, C2′-H), 4.54 (dd, *J* = 5.2, 3.9 Hz, 1H, C3′-H), 4.43 – 4.33 (m, 1H, C4′-H), 4.18 (dd, *J* = 5.5, 3.2 Hz, 2H, C5′-H_2), 2.20 (td, *J* = 19.8, 1.9 Hz, 2H, P-CH_2-P).

^{13}C NMR (126 MHz, D_2O): δ 153.88 (1C, C6), 152.21 (1C, C2), 139.94 (1C, C4), 133.72 (1C, C8), 130.03 (1C, Ar-H), 132.50 (1C, Ar-H), 126.53 (2C, Ar-H), 125.20 (2C, Ar-H), 118.90 (1C, C4), 86.91 (1C, C1′), 83.91 (1C, C4′), 74.19 (1C, C2′), 70.21 (1C, C3′), 63.50 (1C, C5′), 46.59 (1C, P-CH_2-P), 40.10 (1C, CH_2-Ar).

^{31}P NMR (202 MHz, D_2O): δ 18.69 (d, *J* = 9.9 Hz, $\mathbf{P_\alpha}$), 15.22 (d, *J* = 9.7 Hz, $\mathbf{P_\beta}$).

LC-MS (*m*/*z*): negative mode 548 $[M-H]^-$, positive mode 550 $[M+H]^+$.

Purity by HPLC-UV (254 nm)-ESI-MS: 100%.

13.22. N^6-(2-Chlorobenzyl)purine riboside-5'-O-[(phosphonomethyl)phosphonic acid] (71)

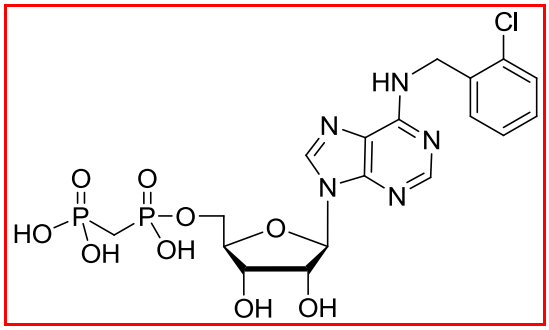

^{1}H NMR (500 MHz, D_2O): δ 8.48 (s, 1H, C8-H), 8.20 (s, 1H, C2-H), 7.38 – 7.32 (m, 1H, Ar-H), 7.29 (d, *J* = 7.3 Hz, 1H, Ar-H), 7.18 (dt, *J* = 18.9, 7.5 Hz, 2H, Ar-H), 6.03 (d, *J* = 5.4 Hz, 1H, C1′-H), 4.74 (d, *J* = 2.8 Hz, 1H, C2′-H), 4.68 – 4.57 (m, 2H, CH_2-Ar), 4.55 – 4.40 (m, 1H, C3′-H), 4.30 (t, *J* = 3.5 Hz, 1H, C4′-H), 4.15 – 3.99 (m, 2H, C5′-H_2), 2.13 (t, *J* = 19.8 Hz, 2H, P-CH_2-P).

^{13}C NMR (126 MHz, D_2O): δ 154.34 (1C, C6), 152.10 (1C, C2), 143.40 (1C, C4), 136.71 (1C, Ar), 135.64 (2C, Ar), 132.98 – 131.26 (2C, Ar), 130.04 (1C, Ar), 121.61 (1C, C5), 90.21 (1C, C1′), 86.92 (1C, C4′), 77.22 (1C, C2′), 73.04 (1C, C3′), 66.38 (1C, C5′), 49.50 (1C, CH_2-Ar), 45.69 (1C, P-CH_2-P).

^{31}P NMR (202 MHz, D_2O): δ 18.54 (**P_α**), 5.69 (d, *J* = 24.4 Hz, **P_β**).

LC-MS (*m*/*z*): negative mode 548 $[M-H]^-$, positive mode 550 $[M+H]^+$.

Purity by HPLC-UV (254 nm)-ESI-MS: 99.0%.

13.23. N^6-(4-Hydroxybenzyl)purine riboside-5'-O-[(phosphonomethyl)phosphonic acid] (72)

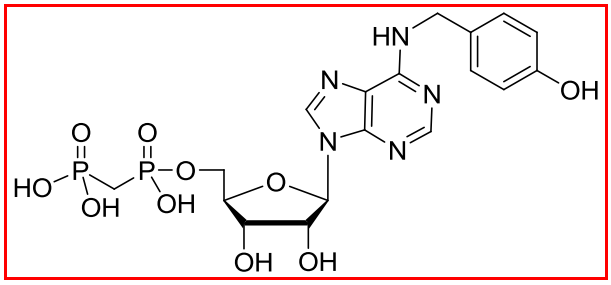

^{1}H NMR (500 MHz, D_2O): δ 8.50 (s, 1H, C8-H), 8.21 (s, 1H, C2-H), 7.38 (d, *J* = 7.9 Hz, 2H, Ar-H), 7.14 (d, *J* = 8.0 Hz, 2H, Ar-H), 6.11 (d, *J* = 5.7 Hz, 1H, C1′-H), 4.65 – 4.50 (m, 1H, C2′-H), 4.41 – 4.29 (m, 1H, C3′-H), 4.17 (dd, *J* = 5.4, 3.2 Hz, 2H, C5′-H_2), 3.59 (d, *J* = 10.7 Hz, 1H, C4′-H), 2.19 (td, *J* = 19.8, 2.3 Hz, 2H, P-CH_2-P).

^{13}C NMR (126 MHz, D_2O): δ 156.54 (1C, Ar), 154.08 (1C, C6), 152.35 (1C, C2), 149.89 (1C, C4), 139.60 (1C, C8), 133.41 (1C, Ar), 128.33 (2C, Ar), 120.75 (1C, C5), 114.99 (2C, Ar), 86.83 (1C, C1′), 84.00 (1C, C4′), 74.13 (1C, C2′), 70.22 (1C, C3′), 63.50 (1C, C5′), 52.70 (1C, CH_2-Ar), 46.61 (1C, P-CH_2-P).

^{31}P NMR (202 MHz, D_2O): δ 18.71 (d, J = 9.7 Hz, $\mathbf{P_\alpha}$), 15.14 (d, J = 9.7 Hz, $\mathbf{P_\beta}$).

LC-MS (*m*/*z*): negative mode 530 $[M-H]^-$, positive mode 532 $[M+H]^+$.

Purity by HPLC-UV (254 nm)-ESI-MS: 100%.

13.24. N^6-(4-Methoxybenzyl)purine riboside-5'-O-[(phosphonomethyl)phosphonic acid] (73)

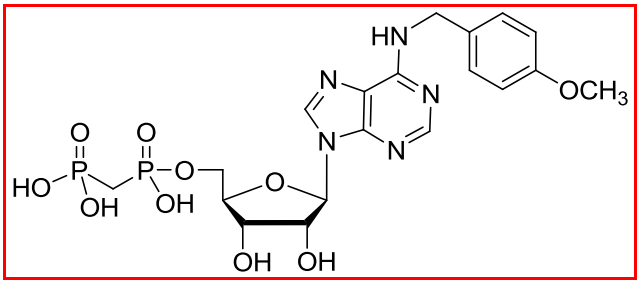

^{1}H NMR (500 MHz, D_2O): δ 8.58 (s, 1H, C8-H), 8.30 (s, 1H, C2-H), 7.33 (d, J = 8.2 Hz, 2H, Ar-H), 6.98 – 6.83 (m, 2H, Ar-H), 6.12 (d, J = 5.4 Hz, 1H, C1′-H), 4.75 – 4.71 (m, 1H, C2′-H), 4.55 (t, J = 4.5 Hz, 1H, C3′-H), 4.39 (q, J = 3.4 Hz, 1H, C4′-H), 4.26 – 4.07 (m, 2H, C5′-H_2), 3.82 (m, OCH_3), 2.30 – 2.10 (m, 2H, P-CH_2-P).

^{13}C NMR (126 MHz, D_2O): δ 158.24 (1C, Ar), 155.26 (1C, C6), 152.27 (1C, C2), 144.17 (1C, C4), 140.60 (1C, C8), 132.45 (1C, Ar), 129.30 (2C, Ar), 128.75 (1C, C5), 121.11 (2C, Ar), 87.31 (1C, C1′), 84.04 (1C, C4′), 74.36 (1C, C2′), 70.17 (1C, C3′), 63.47 (1C, C5′), 55.28 (1C, OCH_3), 55.21 (1C, CH_2-Ar), 46.62 (1C, P-CH_2-P).

^{31}P NMR (202 MHz, D_2O): δ 18.62 (d, J = 9.7 Hz, $\mathbf{P_\alpha}$), 15.47 ($\mathbf{P_\beta}$).

LC-MS (*m*/*z*): negative mode 544 $[M-H]^-$, positive mode 546 $[M+H]^+$.

Purity by HPLC-UV (254 nm)-ESI-MS: 100%.

13.25. N^6-(1-Phenylethyl)purine riboside-5'-O-[(phosphonomethyl)phosphonic acid] (74)

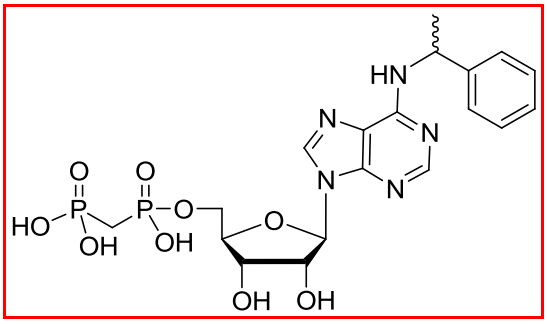

^{1}H NMR (500 MHz, D_2O): δ 8.48 (s, 1H, C8-H), 8.12 (s, 1H, C2-H), 7.44 (d, *J* = 7.4 Hz, 2H, Ar-H), 7.36 (td, *J* = 7.6, 1.6 Hz, 2H, Ar-H), 7.27 (td, *J* = 7.2, 1.4 Hz, 1H, Ar-H), 6.09 (d, *J* = 5.7 Hz, 1H, C1′-H), 5.32 (s, 2H, C$\underline{H_2}$-Ar), 4.75 – 4.71 (m, 1H, C2′-H), 4.56 – 4.49 (m, 1H, C3′-H), 4.36 (tq, *J* = 3.6, 1.6 Hz, 1H, C4′-H), 4.16 (dd, *J* = 5.3, 3.3 Hz, 2H, C5′-$\underline{H_2}$), 2.18 (td, *J* = 19.9, 2.0 Hz, 2H, P-C$\underline{H_2}$-P), 1.61 (d, *J* = 6.9 Hz, 3H, α-C$\underline{H_3}$).

^{13}C NMR (126 MHz, D_2O): δ 156.64 (1C, C6), 155.67 (1C, C2), 146.81 (1C, C4), 142.21 (1C, Ar), 131.64 (1C, C8), 130.13 (2C, Ar), 128.58 (1C, Ar), 121.84 (1C, C5), 89.64 (1C, C1′), 86.78 (1C, C4′), 77.02 (1C, C2′), 73.12 (1C, C3′), 66.40 (1C, C5′), 53.21 (1C, $\underline{C}H_2$-Ar), 45.42 (1C, P-$\underline{C}H_2$-P) 25.15 (1C, α-$\underline{C}H_3$).

^{31}P NMR (202 MHz, D_2O): δ 18.90 (**P_α**), 15.05 (**P_β**).

LC-MS (*m*/*z*): negative mode 528 $[M-H]^-$, positive mode 530 $[M+H]^+$.

Purity by HPLC-UV (254 nm)-ESI-MS: 99.0%.

13.26. N^6-(4-Nitrobenzyl)purine riboside-5'-O-[(phosphonomethyl)phosphonic acid] (75)

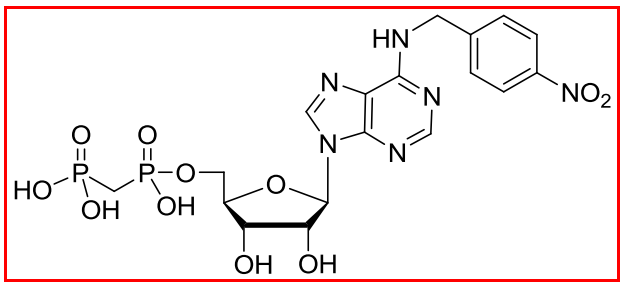

^{1}H NMR (500 MHz, D_2O): δ 8.53 (s, 1H, C8-H), 8.20 (s, 1H, C2-H), 8.10 (d, *J* = 8.5 Hz, 2H, Ar-H), 7.51 (d, *J* = 8.5 Hz, 2H, Ar-H), 6.10 (d, *J* = 5.5 Hz, 1H, C1′-H), 4.87 (d, *J* = 9.4 Hz, 2H, CH_2-Ar), 4.74 (d, *J* = 1.2 Hz, 1H, C2′-H), 4.54 (t, *J* = 4.6 Hz, 1H, C3′-H), 4.40 – 4.30 (m, 1H, C4′-H), 4.18 (dd, *J* = 5.5, 3.2 Hz, 2H, C5′-H_2), 2.21 (t, *J* = 19.8 Hz, 2H, P-CH_2-P).

^{13}C NMR (126 MHz, D_2O): δ 156.65 (1C, C6), 155.02 (1C, C2), 149.48 (1C, C4), 149.01 (1C, Ar), 142.79 (1C, C8), 130.46 (2C, Ar), 127.67 – 125.05 (2C, Ar), 121.75 (1C, Ar), 119.63 (1C, C5), 89.89 (1C, C1′), 86.83 (1C, C4′), 77.13 (1C, C2′), 73.11 (1C, C3′), 66.4 (1C, C5′), 47.00 (1C, C6, CH_2-Ar), 46.46 (1C, C6, P-CH_2-P).

^{31}P NMR (202 MHz, D_2O): δ 18.68 (**P_α**), 15.39 (**P_β**).

LC-MS (*m*/*z*): negative mode 559 $[M-H]^-$, positive mode 561 $[M+H]^+$.

Purity by HPLC-UV (254 nm)-ESI-MS: 99.0%.

13.27. N^6-(4-Sulfamoylbenzyl)purine riboside-5'-O-[(phosphonomethyl)phosphonic acid] (76)

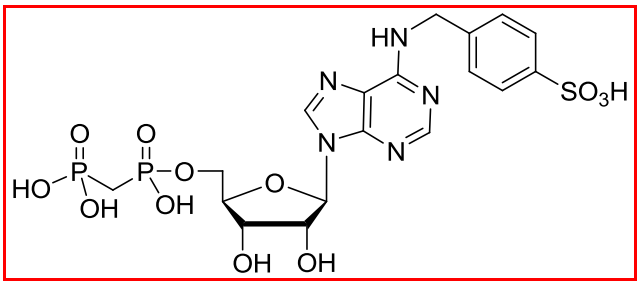

^{1}H NMR (500 MHz, D_2O): δ 8.55 (s, 1H, C8-H), 8.25 (s, 1H, C2-H), 7.83 (d, *J* = 8.3 Hz, 2H, Ar-H), 7.55 (d, *J* = 8.2 Hz, 2H, Ar-H), 6.12 (d, *J* = 5.5 Hz, 1H, C1′-H), 5.01 – 4.84 (m, 2H, CH_2-Ar), 4.74 – 4.70 (m, 1H, C2′-H), 4.54 (dd, *J* = 5.1, 4.0 Hz, 1H, C3′-H), 4.38 (dd, *J* = 4.0, 1.6 Hz, 1H, C4′-H), 4.19 (dt, *J* = 5.8, 2.7 Hz, 2H, C5′-H_2), 2.21 (td, *J* = 19.9, 1.2 Hz, 2H, P-CH_2-P).

^{13}C NMR (126 MHz, D_2O): δ 155.11 (1C, C6), 154.40 (1C, C2), 150.62 (1C, C4), 146.13 (1C, Ar), 142.94 (1C, C8), 139.34 (1C, Ar), 132.07 (2C, Ar), 130.54 (2C, Ar), 128.98 (1C, C5), 90.03 (1C, C1′), 86.86 (1C, C4′), 77.15 (1C, C2′), 73.05 (1C, C3′), 66.37 (1C, C5′), 57.84 (1C, CH_2-Ar), 49.49 (1C, P-CH_2-P).

^{31}P NMR (202 MHz, D_2O): δ 18.59 (d, *J* = 10.2 Hz, $\mathbf{P_\alpha}$), 15.46 (d, *J* = 9.9 Hz, $\mathbf{P_\beta}$).

LC-MS (*m*/*z*): negative mode 593 $[M-H]^-$, positive mode 595 $[M+H]^+$.

Purity by HPLC-UV (254 nm)-ESI-MS: 98.0%.

14.1. General procedure for the synthesis 6-O-alkylpurine riboside (77, 78)

A mixture of 6-chloro-9-(*β*-D-ribofuranosyl)purine 500 mg and 3 mL of 1.0 M sodium (ar)alkoxide in 8 mL of subsequent (ar)alkyl alcohol was stirred at rt for 3 h. After completion of reaction, as indicated in TLC it was evaporated under high vacuo. Purification using silica chromatography (1:8 MeOH/DCM) yielded the title compound **77** or **78** as white solid.

14.2. 6-Ethoxypurine riboside (77)

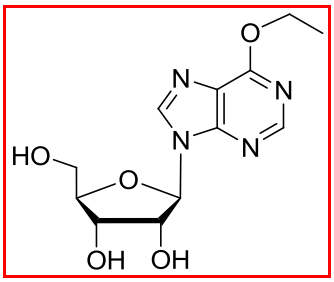

The compound was synthesized using 6-chloro-9-(*β*-D-ribofuranosyl)purine (**28**, 500 mg) and 3 mL of 1.0 M sodium ethoxide in 8 mL of ethanol, and was isolated as a white solid.

Yield: 303 mg (71%).

Melting Point (^{o}C): 195-197

^{1}H NMR (500 MHz, DMSO-d_6): δ 8.60 (s, 1H, C8-H), 8.52 (s, 1H, C2-H), 5.98 (d, *J* = 5.7 Hz, 1H, C1′-H), 5.47 (d, *J* = 5.8 Hz, 1H, C2′-H), 5.19 (d, *J* = 4.8 Hz, 1H, C3′-H), 5.11 (t, *J* = 5.8 Hz, 1H, C4′-H), 4.59 (d, *J* = 7.0 Hz, 2H, C5′-$\underline{H_2}$), 4.16 (dd, *J* = 5.1, 2.8 Hz, 1H, C5′-OH), 3.96 (q, *J* = 3.8 Hz, 1H, C3′-OH), 3.68 (dt, *J* = 12.0, 4.4 Hz, 1H, C2′-OH), 3.56 (q, *J* = 12.0, 5.9, 3.9 Hz, 2H, -$C\underline{H_2}$-CH_3), 1.40 (t, *J* = 7.1 Hz, 3H, CH_2-$C\underline{H_3}$).

^{13}C NMR (126 MHz, DMSO-d_6): δ 160.21 (1C, C6), 151.87 (1C, C2), 142.43 (1C, C4), 126.62 (1C, C8), 121.27 (1C, C5), 87.93 (1C, C1′), 85.85 (1C, C4′), 73.90 (1C, C2′), 70.48 (1C, C3′), 62.71 (1C, C5′), 61.48 (1C, $\underline{C}H_2$-CH_3), 14.52 (1C, CH_2-$\underline{C}H_3$).

LC-MS (*m*/*z*): negative mode 295 $[M-H]^-$, positive mode 297 $[M+H]^+$.

Purity by HPLC-UV (254 nm)-ESI-MS: 98.0%.

14.3. 6-Benzyloxypurine riboside (78)

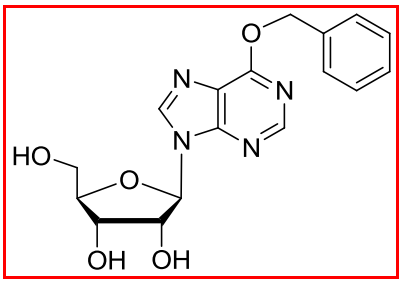

The compound was synthesized using 6-chloro-9-(*β*-D-ribofuranosyl)purine (**28**, 500 mg) and 3 mL of 1.0 M sodium benzyloxide in 8 mL of benzyl alcohol, and was isolated as a white solid.

Yield: 383 mg (75%).

Melting Point (^{o}C): 207-208

^{1}H NMR (600 MHz, DMSO-d_6): δ 8.62 (s, 1H, C8-H), 8.56 (s, 1H, C2-H), 7.54 – 7.47 (m, 2H, Ar), 7.43 – 7.31 (m, 3H, Ar), 5.99 (d, *J* = 5.7 Hz, 1H, C1′-H), 5.64 (d, *J* = 2.1 Hz, 2H, CH_2-Ar), 5.47 (d, *J* = 6.0 Hz, 1H, C2′-H), 5.19 (d, *J* = 4.9 Hz, 1H, C3′-H), 5.10 (dd, *J* = 6.1, 5.1 Hz, 1H, C4′-H), 4.59 (q, *J* = 5.6 Hz, 1H, C5′-H), 4.16 (td, *J* = 4.9, 3.5 Hz, 1H, C5′-H), 3.96 (q, *J* = 3.8 Hz, 1H, C5′-OH), 3.68 (q, *J* = 11.9, 5.0, 3.9 Hz, 1H, C3′-OH), 3.56 (q, *J* = 12.0, 6.2, 4.0 Hz, 1H, C2′-OH).

^{13}C NMR (151 MHz, DMSO-d_6): δ 159.97 (1C, C6), 152.15 (1C, C2), 151.72 (1C, C4), 142.69 (1C, C8), 136.41 (1C, Ar-H), 129.40 (2C, Ar-H), 127.75 (3C, Ar-H), 121.30 (1C, C5), 87.96 (1C, C1′), 85.87 (1C, C4′), 73.93 (1C, C2′), 70.48 (1C, C3′), 67.98 (1C, C5′), 61.47 (1C, $\underline{C}H_2$-Ar).

LC-MS (*m*/*z*): negative mode 357 $[M-H]^-$, positive mode 359 $[M+H]^+$.

Purity by HPLC-UV (254 nm)-ESI-MS: 97.6%.

14.4. 6-Benzylthiopurine riboside (80)

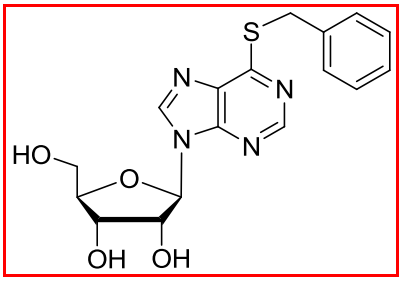

6-Chloropurine riboside (**28**, 500 mg) was put in a 10 mL glass vial with a small magnetic stirrer. To this was added 2 mL ethanol, thiourea (200 mg, 2.61 mmol), and the solution was refluxed for 1 h. Precipitate of *S*-(purin-6-yl)isothiourea hydrochloride was formed followed by addition of benzyl chloride (330 mg, 2.61 mmol) and K_2CO_3 (480 mg, 3.48 mmol). Then the mixture was

put in the microwave synthesis apparatus and irradiated at 200 W at 100 ^{o}C for 10 min. After evaporation of the solvent, the crude product was purified by column chromatography over silica (1:8 MeOH/DCM) yielded the title compound as yellowish white solid.

Yield: 222 mg (76%).

Melting Point (^{o}C): 216-217

^{1}H NMR (600 MHz, DMSO-d_6): δ 8.78 (s, 1H, C8-H), 8.70 (s, 1H, C2-H), 7.48 – 7.42 (m, 2H, Ar-H), 7.34 – 7.27 (m, 2H, Ar-H), 7.27 – 7.21 (m, 1H, Ar-H), 5.99 (d, *J* = 5.5 Hz, 1H, C1′-H), 5.49 (d, *J* = 5.9 Hz, 1H, C2′-H), 5.20 (d, *J* = 5.0 Hz, 1H, C3′-H), 5.08 (t, *J* = 5.6 Hz, 1H, C4′-H), 4.70 – 4.62 (m, 2H, C$\underline{H_2}$-Ar), 4.59 (q, *J* = 5.5 Hz, 1H, C5′-H), 4.17 (td, *J* = 4.9, 3.6 Hz, 1H, C5′-H), 3.97 (q, *J* = 3.9 Hz, 1H, C5′-OH), 3.68 (q, *J* = 12.0, 5.1, 4.0 Hz, 1H, C3′-OH), 3.56 (q, *J* = 12.0, 6.1, 4.0 Hz, 1H, C2′-OH).

^{13}C NMR (151 MHz, DMSO-d_6): δ 159.34 (1C, C6), 151.63 (1C, C2), 148.45 (1C, C4), 143.50 (1C, C8), 137.91 (1C, Ar-H), 131.11 (1C, C5), 129.11 (2C, Ar-H), 128.65 (1C, Ar-H), 127.35 (1C, Ar-H), 87.99 (1C, H1′), 85.87 (1C, H4′), 73.94 (1C, H2′), 70.41 (1C, H3′), 61.38 (1C, H5′), 31.79 (1C, $\underline{C}H_2$-Ar).

LC-MS (*m*/*z*): negative mode 373 $[M-H]^-$, positive mode 375 $[M+H]^+$.

Purity by HPLC-UV (254 nm)-ESI-MS: 100%.

15.1. General procedure for the synthesis of nucleotides (81-83)

A solution of methylenebis(phosphonic dichloride) (5 mmol) in trimethyl phosphate (2 mL), cooled to 0 ^{o}C was added to a suspension of corresponding O^6– and S^6–substituted nucleosides, **77**, **78** and **80** (1 mmol) in trimethyl phosphate at 0 ^{o}C. The reaction mixture was stirred at 0 ^{o}C and samples were withdrawn at 10 min interval for TLC to check the disappearance of

nucleosides. After 30 min, on disappearance of nucleoside, 7 mL of cold 0.5 M aqueous TEAC solution (pH 7.4-7.6) was added. It was stirred at 0 °C for 25 min followed by stirring at room temperature for 1 h. Trimethyl phosphate was extracted using (2 x 100 mL) of *tert*.butylmethyl ether and the aqueous layer was lyophilized. The crude product was then purified by RP-HPLC using a gradient of 50 mM ammoniumbicarbonate/ACN from 100:0 to 60:40 to get final product. Since there was no formation of dinucleotide, ion exchange chromatography was not used.

15.2. 6-Ethoxypurine riboside-5'-O-[(phosphonomethyl)phosphonic acid] (81)

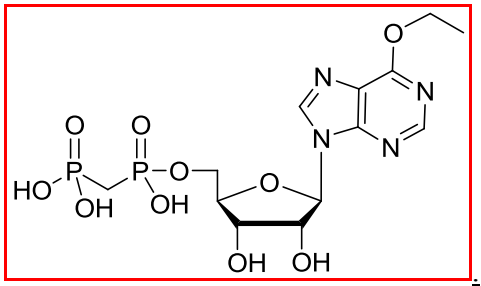

^{1}H NMR (500 MHz, D_2O): δ 8.69 (s, 1H, C8-H), 8.48 (s, 1H, C2-H), 6.20 (d, *J* = 5.4 Hz, 1H, C1′-H), 4.74 (d, *J* = 0.8 Hz, 1H, C2′-H), 4.63 (q, *J* = 7.1 Hz, 2H, $C\underline{H_2}$-CH_3), 4.56 (dd, *J* = 5.2, 4.0 Hz, 1H, C3′-H), 4.40 (q, *J* = 3.4 Hz, 1H, C4′-H), 4.20 (dt, *J* = 6.1, 3.0 Hz, 2H, C5′-$\underline{H_2}$), 2.24 (td, *J* = 19.9, 1.6 Hz, 2H, P-$C\underline{H_2}$-P), 1.40 – 138 (m, 3H, CH_2-$C\underline{H_3}$).

^{13}C NMR (126 MHz, D_2O): δ 163.31 (1C, C6), 155.10 (1C, C2), 153.96 (1C, C4), 144.59 (1C, C8), 123.25 (1C, C5), 90.33 (1C, C1′), 86.81 (1C, C4′), 77.06 (1C, C2′), 73.02 (1C, C3′), 67.39 (1C, C5′), 66.37 (1C, $\underline{C}H_2$-CH_3′), 49.49 (1C, P-$\underline{C}H_2$-P), 16.46 (1C, CH_2-$\underline{C}H_3$).

^{31}P NMR (202 MHz, D_2O): δ 18.09 ($\mathbf{P_\alpha}$), 16.59 ($\mathbf{P_\beta}$).

LC-MS (*m*/*z*): negative mode 453 $[M-H]^-$, positive mode 455 $[M+H]^+$.

Purity by HPLC-UV (254 nm)-ESI-MS: 100%.

15. 3. 6-Benzyloxypurine riboside-5'-O-[(phosphonomethyl)phosphonic acid] (82)

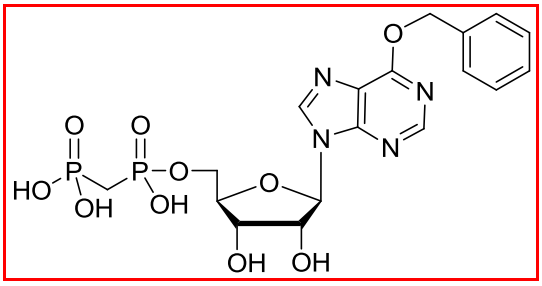

^{1}H NMR (500 MHz, D_2O): δ 8.70 (s, 1H, C8-H), 8.52 (s, 1H, C2-H), 7.57 (dd, *J* = 8.1, 1.6 Hz, 2H, Ar-H), 7.47 – 7.34 (m, 3H, Ar-H), 6.21 (dd, *J* = 5.7, 1.1 Hz, 1H, C1′-H), 5.67 (s, 2H, CH_2-Ar), 4.74 (d, *J* = 1.2 Hz, 1H, C2′-H), 4.59 – 4.50 (m, 1H, C3′-H), 4.40 (td, *J* = 3.9, 2.5 Hz, 1H, C4′-H), 4.19 (td, *J* = 3.9, 1.3 Hz, 2H, C5′-H_2), 2.32 – 2.15 (m, 2H, P-CH_2-P).

^{13}C NMR (126 MHz, D_2O): δ 163.10 (1C, C6), 155.09 (1C, C2), 154.33 (1C, C4), 144.90 (1C, C8), 138.52 (1C, Ar-H), 131.65 (2C, Ar-H), 131.40 (2C, Ar-H), 130.73 (1C, Ar-H), 123.58 (1C, C5), 90.26 (1C, C1′), 86.90 (1C, C4′), 77.07 (1C, C2′), 72.56 (1C, C3′), 68.55 – 65.68 (1C, C5′), 61.47 (1C, CH_2-Ar), 49.51 (1C, P-CH_2-P).

^{31}P NMR (202 MHz, D_2O): δ 18.40 (d, *J* = 23.6 Hz, $\mathbf{P_\alpha}$), 16.03 (d, *J* = 21.0 Hz, $\mathbf{P_\beta}$).

LC-MS (*m*/*z*): negative mode 515 $[M-H]^-$, positive mode 517 $[M+H]^+$.

Purity by HPLC-UV (254 nm)-ESI-MS: 100%.

15.4. 6-Benzylthiopurine riboside-5'-O-[(phosphonomethyl)phosphonic acid] (83)

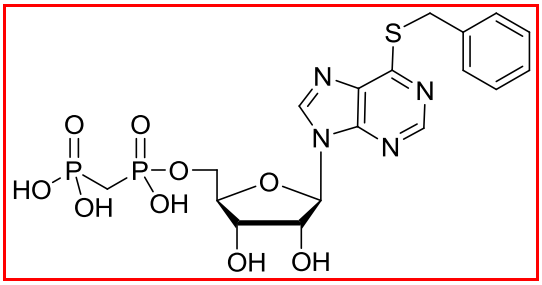

^{1}H NMR (500 MHz, D_2O): δ 8.72 (s, 1H, C8-H), 8.67 (s, 1H, C2-H), 7.36 – 7.21 (m, 5H, Ar-H), 6.18 (d, *J* = 5.4 Hz, 1H, C1′-H), 4.74 (d, *J* = 2.0 Hz, 1H, C2′-H), 4.61 (s, 2H, CH_2-Ar), 4.55 (dd,

J = 5.2, 4.1 Hz, 1H, C3′-H), 4.44 – 4.35 (m, 1H, C4′-H), 4.19 (q, *J* = 5.6, 3.3, 1.8 Hz, 2H, C5′-H_2), 2.20 (td, *J* = 20.0, 1.1 Hz, 2H, P-CH_2-P).

^{13}C NMR (126 MHz, D_2O): δ 163.32 (1C, C6), 154.77 (1C, C2), 150.62 (1C, C4), 145.62 (1C, C8), 139.86 (1C, Ar-H), 133.51 (1C, C5), 131.64 (1C, Ar-H), 130.43 (1C, Ar-H), 129.35 (1C, Ar-H), 90.23 (1C, C1′), 86.84 (1C, C4′), 77.09 (1C, C2′), 73.06 (1C, C3′), 66.34 (1C, C5′), 50.53 (1C, P-CH_2-P), 35.56 (1C, CH_2-Ar).

^{31}P NMR (202 MHz, D_2O): δ 18.71 (d, *J* = 10.3 Hz, $\mathbf{P_\alpha}$), 15.31 (td, *J* = 9.7 Hz, $\mathbf{P_\beta}$).

LC-MS (*m*/*z*): negative mode 531 $[M-H]^-$, positive mode 533 $[M+H]^+$.

Purity by HPLC-UV (254 nm)-ESI-MS: 97.0%.

16.1. 8-Bromoadenosine (84)

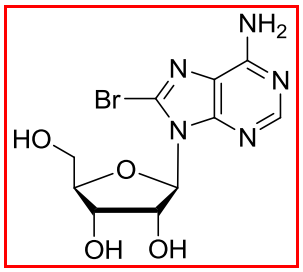

Bromine-water is a mixture of 2.8% conc. bromine dissolved in water (%w/w). Adenosine (500 mg) and 8 mL of bromine-water was stirred at pH 4.0 maintained by acetate buffer (0.1 M) for 4 h. The solution was decolorized with $NaHSO_3$ and the resulting precipitate was washed with water followed by 1N sodium bicarbonate solution, then dried to yield orange red solid as the title compound **84**.

Yield: 254 mg (75%).

Melting Point (^{o}C): 185-186

^{1}H NMR (500 MHz, DMSO-*d*$_6$): δ 8.40 (s, 1H, C2-H), 6.56 (bs, 2H, NH_2), 4.59 – 4.50 (m, 1H, C1′-H), 4.53 – 4.45 (m, 1H, C2′-H), 4.33 – 4.28 (m, 1H, C3′-H), 4.20 (bs, H, C5′-OH), 4.15 – 4.13 (m, 2H, C5′-H_2), 3.56 – 3.58 (m, 2H, C2′-OH and C3′-OH), 3.17 – 3.10 (m, 1H, C4′-H).

^{13}C NMR (125 MHz, DMSO-*d*$_6$): δ 155.8 (1C, C2), 152.5 (1C, C6), 150.1 (1C, C4), 128.1 (1C, C8), 120.3 (1C, C5), 95.7 (1C, C1′), 88.3 (1C, C4′), 74.5 (1C, C2′), 71.3 (1C, C3′), 62.8 (1C, C5′).

LC/ESI-MS: negative mode 345 ($[M - H]^-$), positive mode 347 ($[M + H]^+$).

16.2. 8-Chloroadenosine (86)

8-Bromoadenosine (**84,** 500 mg) was put in a 10 mL glass vial with a small magnetic stirrer. To this was added 2 mL ethanol, thiourea (200 mg), and the solution was refluxed for 1 h. Precipitate was filterd off. The filtrate was evapotated and purified by HPLC to get 8-thioadenosine (**85**). Compound **86** was synthesized by stirring 8-thioadenosine (200 mg), 3mL of *N*-chlorosuccinimide and 5 mL of methanol at rt for 3 h. Then it was evaporated in vacuo and purified by RP-HPLC to get desired compound as white solid. (110 mg, 52% yield).

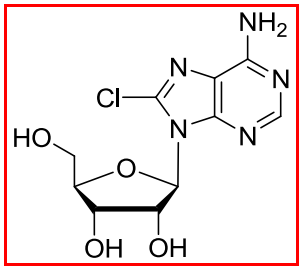

Melting Point (^{o}C): 190-191 [**literature**, 189-191][185]

^{1}H NMR (600 MHz, DMSO-*d*$_6$): δ 8.12 (s, 1H, C2-H), 7.55 (s, 2H, NH_2), 5.83 (d, *J* = 6.7 Hz, 1H, C1′-H), 5.08 (dd, *J* = 6.8, 5.2 Hz, 1H, C2′-H), 4.19 (dd, *J* = 5.2, 2.4 Hz, 1H, C3′-H), 3.97 (td,

J = 4.0, 2.4 Hz, 1H, C4′-H), 3.67 (dd, *J* = 12.1, 4.0 Hz, 1H, C5′-H), 3.52 (dd, *J* = 12.2, 4.2 Hz, 1H, C5′-H).

^{13}C NMR (151 MHz, DMSO-*d*$_6$): δ 155.16 (1C, C6), 152.40 (1C, C2), 149.99 (1C, C4), 127.31 (1C, C8), 119.81 (1C, C5), 90.54 (1C, C1′), 86.82 (1C, C4′), 74.32 (1C, C2′), 71.11 (1C, C3′), 62.22 (1C, C5′).

LC-MS (*m*/*z*): negative mode 302 $[M-H]^-$, positive mode 300 $[M+H]^+$.

Purity by HPLC-UV (254 nm)-ESI-MS: 97.6%.

16.3. 8-Ethylthioadenosine (87)

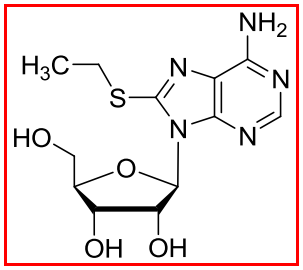

8-Bromoadenosine (**84**, 500 mg) was put in a 10 mL glass vial with a small magnetic stirrer. To this was added 2 mL ethanol, thiourea (200 mg), and the solution was refluxed for 1 h. Precipitate of *S*-(purin-6-yl)isothiourea hydroiodide was formed followed by addition of ethyl iodide (330 mg) and K_2CO_3 (480 mg). Then the mixture was put in the microwave synthesis apparatus and irradiated at 200 W at 100 ^oC for 10 min. After evaporation of the solvent, the crude product was purified by column chromatography over silica (1:8 MeOH/DCM) yielded the title compound as white solid. (383 mg, 56% yield).

Melting Point (^{o}C): 169-170 [**literature**, 176][186]

^{1}H NMR (600 MHz, DMSO-d_6): δ 8.05 (s, 1H, C2-H), 7.24 (s, 2H, NH_2), 5.76 (d, *J* = 6.8 Hz, 1H, C1′-H), 5.59 (dd, *J* = 8.8, 3.7 Hz, 1H, C2′-H), 5.38 – 5.33 (m, 1H, C3′-H), 5.17 – 5.12 (m, 1H, C4′-H), 5.03 – 4.95 (m, 1H, C5′-H), 4.15 (dt, *J* = 4.8, 2.4 Hz, 1H, C5′-H), 3.96 (td, *J* = 3.9, 2.3 Hz, 1H, C5′-OH), 3.66 (dt, *J* = 12.1, 3.6 Hz, 1H, C3′-OH), 3.56 – 3.47 (m, 1H, C2′-OH), 3.39 – 3.19 (m, 2H, $C\underline{H_2}$-CH_3), 1.35 (t, *J* = 7.3 Hz, 3H, CH_2-$C\underline{H_3}$).

^{13}C NMR (151 MHz, DMSO-d_6): δ 154.71 (1C, C8), 151.41 (1C, C6), 150.55 (1C, C2), 148.65 (1C, C4), 119.79 (1C, C5), 89.02 (1C, C1′), 86.72 (1C, C4′), 71.42 (1C, C2′), 71.11 (1C, C3′), 62.36 (1C, C5′), 26.92 (1C, $\underline{C}H_2$-CH_3), 14.95 (1C, CH_2-$\underline{C}H_3$).

LC-MS (*m*/*z*): negative mode 295 $[M-H]^-$, positive mode 297 $[M+H]^+$.

Purity by HPLC-UV (254 nm)-ESI-MS: 97.6%.

16.4. 8-Aminomethyl-adenosine (88)

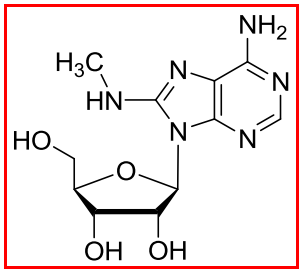

The compound **88** was synthesized from 8-chloroadenosine (500 mg), by stirring with methyl amine (120 mg) and triethyl amine (150 mg) for 20 h at room temperature. Then the resulting solution was evaporated in vacuo and separated by column chromatography and was isolated as a purplish solid (456 mg, 93% yield).

Melting Point (^{o}C): 217–218

^{1}H NMR (600 MHz, DMSO-d_6): δ 7.88 (s, 1H, C2-H), 6.88 (q, *J* = 4.6 Hz, 1H, N<u>H</u>-CH_3), 6.48 (s, 2H, NH_2), 5.87 – 5.82 (m, 2H, C1′-H and C2′-H), 5.20 (d, *J* = 6.6 Hz, 1H, C3′-H), 5.09 (d, *J* = 4.1 Hz, 1H, C4′-H), 4.67 (td, *J* = 6.9, 5.3 Hz, 1H, C5′-H), 4.11 – 4.09 (m, 1H, C5′-H), 3.95 (q, *J* = 2.4 Hz, 1H, C5′-OH), 3.69 – 3.54 (m, 2H, C2′-OH and C3′-OH), 2.88 (d, *J* = 4.6 Hz, 3H, NHC<u>H</u>$_3$).

^{13}C NMR (151 MHz, DMSO-d_6): δ 152.58 (1C, C8), 152.21 (1C, C6), 149.97 (1C, C2), 148.62 (1C, C4), 117.33 (1C, C5), 86.68 (1C, C1′), 85.80 (1C, C4′), 71.09 (1C, C2′), 70.89 (1C, C3′), 61.83 (1C, C5′), 29.26 (1C, NH<u>C</u>H_3).

LC-MS (*m*/*z*): negative mode 295 $[M-H]^-$, positive mode 297 $[M+H]^+$.

Purity by HPLC-UV (254 nm)-ESI-MS: 97.4%.

<u>17.1. General procedure for the synthesis of nucleotides (89-92)</u>

A solution of methylenebis(phosphonic dichloride) (5-6 mmol) in trimethyl phosphate (2 mL), cooled to 0 ^{o}C was added to a suspension of corresponding 8-substitued nucleosides, **84**, **86**, **87** and **88** (1 mmol) in trimethyl phosphate at 0 ^{o}C. The reaction mixture was stirred at 0 ^{o}C and samples were withdrawn at 10 min interval for TLC to check the disappearance of nucleosides. After 60 min, on disappearance of nucleoside, 7 mL of cold 0.5 M aqueous TEAC solution (pH 7.4-7.6) was added. It was stirred at 0 ^{o}C for 15 min followed by stirring at room temperature for 1 h. Trimethyl phosphate was extracted using (2 x 100 mL) of *tert*.butylmethyl ether and the aqueous layer was lyophilized. The crude product was then purified by RP-HPLC using a gradient of 50 Mm ammoniumbicarbonate/ACN from 100:0 to 60:40 to get final product. Since there was no formation of dinucleotide, ion exchange chromatography was not used.

17.2. 8-Bromoadenosine-5'-O-[(phosphonomethyl)phosphonic acid] (89)

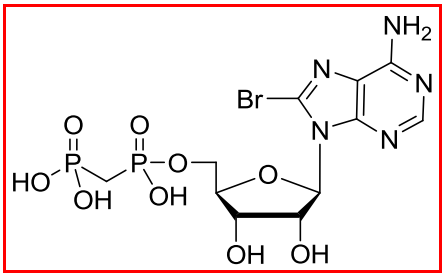

^{1}H NMR (500 MHz, D_2O): δ 8.40 (s, 1H, C2-H), 5.98 (d, *J* = 5.2 Hz, 1H, C1′-H), 4.54 (t, *J* = 4.7 Hz, 1H, C2′-H), 4.33 (q, *J* = 3.9 Hz, 1H, C3′-H), 4.16 (dt, *J* = 6.6, 3.5 Hz, 2H, C5′-H_2), 3.97 (td, *J* = 4.0, 2.4 Hz, 1H, C4′-H), 2.14 (t, *J* = 19.8 Hz, 2H, P-CH_2-P).

^{13}C NMR (126 MHz, D_2O): δ 162.36 (1C, C2), 156.06 (1C, C8), 153.31 (1C, C4), 145.04 (1C, C8), 126.81 (1C, C5), 90.26 (1C, C1′), 86.58 (1C, C4′), 76.55 (1C, C2′), 73.03 (1C, C3′), 66.28 (1C, C5′), 49.47 (1C, P-CH_2-P).

^{31}P NMR (202 MHz, D_2O): δ 23.04 – 18.65 (m, $\mathbf{P_\alpha}$), 14.47 (d, *J* = 9.6 Hz, $\mathbf{P_\beta}$).

LC-MS (*m*/*z*): negative mode 503 $[M-H]^-$, positive mode 505 $[M+H]^+$.

Purity by HPLC-UV (254 nm)-ESI-MS: 100%.

17.3. 8-Chloroadenosine-5'-O-[(phosphonomethyl)phosphonic acid] (90)

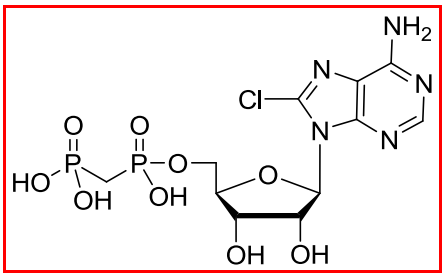

^{1}H NMR (500 MHz, D_2O): δ 8.46 (s, 1H, C2-H), 6.01 (d, *J* = 5.0 Hz, 1H, C1′-H), 4.98 (td, *J* = 4.0, 2.4 Hz, 1H, C2′-H), 4.52 (t, *J* = 4.8 Hz, 1H, C3′-H), 4.34 (q, *J* = 3.7 Hz, 1H, C4′-H), 4.14 (t, *J* = 4.4 Hz, 2H, C5′-H_2), 2.07 (t, *J* = 19.5 Hz, 2H, P-CH_2-P).

^{13}C NMR (126 MHz, D_2O): δ 163.14 (1C, C6), 156.60 (1C, C2), 152.91 (1C, C4), 142.91 (1C, C8), 120.49 (1C, C5), 90.04 (1C, C1′), 86.66 – 86.60 (1C, C4′), 77.09 (1C, C2′), 72.84 (1C, C3′), 66.05 (1C, C5′), 49.48 (1C, P-$\underline{C}H_2$-P).

^{31}P NMR (202 MHz, D_2O): δ 21.25 (**P_α**), 12.84 (**P_β**).

LC-MS (*m*/*z*): negative mode 458 $[M-H]^-$, positive mode 460 $[M+H]^+$.

Purity by HPLC-UV (254 nm)-ESI-MS: 100%.

<u>17.4. 8-Ethylthioadenosine-5'-O-[(phosphonomethyl)phosphonic acid] (91)</u>

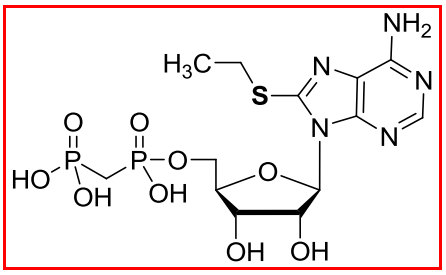

^{1}H NMR (500 MHz, D_2O): δ 8.05 (s, 1H, C2-H), 6.11 (dd, *J* = 15.8, 5.4 Hz, 1H, C1′-H), 5.33 – 5.23 (m, 1H, C2′-H), 4.62 – 4.51 (m, 1H, C3′-H), 4.42 – 4.28 (m, 1H, C4′-H), 4.17 (td, *J* = 8.7, 4.8 Hz, 2H, C5′-$\underline{H_2}$), 3.23 – 3.21 (m, 2H, $\underline{C}H_2$-CH_3), 2.19 (t, *J* = 19.8 Hz, 2H, P-$\underline{C}H_2$-P), 1.30 (t, *J* = 7.5, 3.7 Hz, 3H, CH_2-$\underline{C}H_3$).

^{13}C NMR (126 MHz, D_2O): δ 167.64 (1C, C8), 157.32 (1C, C6), 152.90 (1C, C2), 142.11 (1C, C4), 118.83 (1C, C5), 89.77 (1C, C1′), 86.48 (1C, C4′), 76.82 (1C, C2′), 73.05 (1C, C3′), 66.43 (1C, C5′), 49.46 (1C, P-$\underline{C}H_2$-P), 25.12 (1C, $\underline{C}H_2$-CH_3), 14.04 (1C, CH_2-$\underline{C}H_3$).

^{31}P NMR (202 MHz, D_2O): δ 18.68 (d, *J* = 9.7 Hz, **P_α**), 15.27 (d, *J* = 9.4 Hz, **P_β**).

LC-MS (*m*/*z*): negative mode 484 $[M-H]^-$, positive mode 486 $[M+H]^+$.

Purity by HPLC-UV (254 nm)-ESI-MS: 100%.

17.5. 8-Aminomethyladenosine-5'-O-[(phosphonomethyl)phosphonic acid] (92)

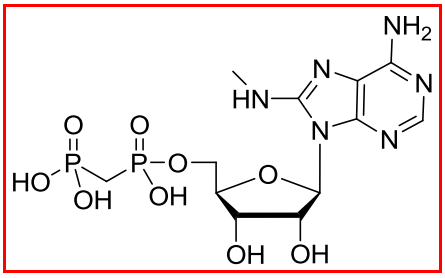

^{1}H NMR (500 MHz, D_2O): δ 8.01 (s, 1H, C2-H), 5.98 (s, 1H, C1′-H), 4.97 – 4.95 (m, 1H, C2′-H), 4.56 (d, *J* = 25.2 Hz, 1H, C3′-H), 4.35 (d, *J* = 10.1 Hz, 1H, C4′-H), 4.26 – 4.15 (m, 2H, C5′-H_2), 2.27 – 2.02 (m, 2H, P-CH_2-P), 2.86 (d, *J* = 4.6 Hz, 3H, -NH-CH_3).

^{13}C NMR (126 MHz, D_2O): δ 165.98 (1C, C6), 157.10 (1C, C4), 152.80 (1C, C2), 142.75 (1C, C8), 120.14 (1C, C5), 90.89 (1C, C1′), 86.69 (1C, C4′), 75.81 (1C, C2′), 73.11 (1C, C3′), 66.45 (1C, C5′), 49.51 (1C, P-CH_2-P), 33.07 (1C, -NH-CH_3).

^{31}P NMR (202 MHz, D_2O): δ 18.49 (**P_α**), 16.14 (**P_β**).

LC-MS (*m*/*z*): negative mode 453 $[M-H]^-$, positive mode 455 $[M+H]^+$.

Purity by HPLC-UV (254 nm)-ESI-MS: 100%.

18.1. 2-Amino-2',3',5'-tri-O-acetylinosine (94)

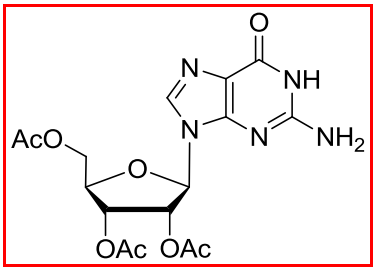

To 8.92 g of commercial guanosine was added 0.2 g DMAP, 8.8 g of EDMA and 10.2 g of acetic anhydride. The resulting suspension was suspended in 100 mL of acetonitrile. It was stirred for 15 min at rt until a clear solution was obtained. Excess acetic anhydride was destroyed by adding

20 mL methanol and stirred for additional 15 min. Finally the reagents are removed in vacuo and the residue is recrystallized from isopropanol, followed by acetone and methanol.

Yield: 8.03 g (95%).

Melting Point (°C): 225-227 [**literature**, 224-229].[187]

^{1}H NMR (500 MHz, DMSO-*d*$_6$): δ 8.34 (s, 1H, C2-H), 8.13 (s, 1H, C8-H), 6.49 (bs, 2H, N$\underline{H_2}$), 6.19 (d, *J* =5.7, 1H, C1′-H), 5.92 (t, *J* = 5.4, 1H, C2′-H), 5.58 (t, *J* = 5.6, 1H, C3′-H), 4.38 – 4.51 (m, 3H, H4′, C5′-$\underline{H_2}$), 2.19 (s, 3H, OAc), 2.17 (s, 3H, OAc), 2.13 (s, 3H, OAc).

^{13}C NMR (125 MHz, DMSO-*d*$_6$): δ 169.31, 169.84, 171.28 (3 xCO), 156.01 (1C, C6), 142.47 (1C, C2), 145.83 (1C, C4), 136.26 (1C, C8), 125.42 (1C, C5), 87.65 (1C, C1′), 82.44 (1C, C4′), 73.42 (1C, C2′), 70.81 (1C, C3′), 65.09 (1C, C5′), 22.61, 22.74, 22.85 (3C, 3xOAc).

LC/ESI-MS: negative mode 408 ([M - H]$^-$), positive mode 410 ([M + H]$^+$).

<u>18.2. 2-Amino-6-chloro-2',3',5'-tri-O-acetylinosine (95)</u>

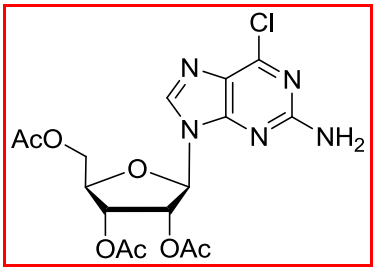

A suspension of **94** (2.45 g), *N*,*N*-dimethylaniline (0.83 mL), tetraethylammonium chloride (1.88 g) and phosphorus oxychloride (12.2 mL) was stirred at room temperature for 7 min under an atmosphere of argon. The flask was heated in a preheated oil bath at 90 °C for 13 min. The solution was evaporated, and the resulting oil was stirred in DCM (20 mL) and ice (20 mL). The aqueous layer was extracted with DCM (2 x 25 mL). The combined organic layers were washed with 2M HCl (4 x 20 mL) and brine (2 x 20 mL), dried, and evaporated to yield 2.0 g of green

oil. Purification using silica chromatography (1:10 MeOH/DCM) yielded the title compound **95** as a pale orange oil, which was subsequently crystallized in hexane to pale orange solid.

Yield: 254 mg (95%).

Melting Point (^{o}C): 174-175 [**literature**, 174].[188]

^{1}H NMR (500 MHz, DMSO-*d*$_6$): δ 8.28 (s, 1H, C8-H), 6.20 (d, 1H, C1′-H), 5.77 (d, 1H, C3′-H), 5.53 (d, 1H, C2′-H), 4.46 (t, 1H, C4′-H), 4.40 (d, 2H, C5′-$\underline{H}_2$), 2.14 (s, 3H, OCOC$\underline{H}_3$), 2.12 (s, 3H, OCOC$\underline{H}_3$), 2.06 (s, 3H, OCOC$\underline{H}_3$).

^{13}C NMR (125 MHz, DMSO-*d*$_6$): δ 170.17 (1C, O$\underline{C}$OCH$_3$), 169.65 (1C, O$\underline{C}$OCH$_3$), 169.35 (1C, O$\underline{C}$OCH$_3$), 160.03 (1C, C2), 153.45 (1C, C6), 143.91 (1C, C4), 142.28 (1C, C8), 130.90 (1C, C5), 86.52 (1C, C1′), 80.83 (1C, C4′), 73.21 (1C, C3′), 70.56 (1C, C2′), 62.61 (1C, C5′), 20.79 (1C, $\underline{C}$H$_3$-CO), 20.51 (1C, $\underline{C}$H$_3$-CO), 20.32 (1C, $\underline{C}$H$_3$-CO).

LC/ESI-MS: negative mode 413 ([M - H]$^-$), positive mode 415 ([M + H]$^+$).

18.3. 2-Amino-6-chloropurine riboside (96)

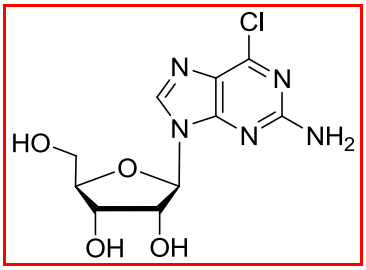

Compound **95** (2.0 g) was dissolve in methanol. To it was added, 2% of sodium methoxide in methanol. It was stirred 24 h at rt. Resulting precipitate was collected. The resulting solution was evaporated and purification using silica chromatography (1:10 MeOH/DCM) yielded the title compound **99.**

Yield: 995 mg (67%).

Melting Point (°C): 174-176 [**literature**, 171-172].[190]

^{1}H NMR (500 MHz, DMSO-d_6): δ 8.83 (s, 1 H, C8-H), 6.49 (bs, 2H, $N\underline{H_2}$), 6.03 (d, 1 H, *J* = 5.1 Hz, C1′-H), 5.51 (d, 1 H, *J* = 5.5 Hz, C2′-H), 5.30 (d, 1 H, *J* = 5.4 Hz, C3′-H), 5.13 (t, 1 H, *J* = 5.3 Hz, C4′-H), 4.57 – 4.45 (m, 1 H, C5′-H), 4.22 – 4.13 (m, 1 H, C5′-H), 4.12 – 4.08 (m, 1 H, C5′-OH), 3.4 – 3.7 (m, 2H, C2′-OH and C3′-OH).

^{13}C NMR (125 MHz, DMSO-d_6): δ 152.98 (1C, C2), 151.41 (1C, C6), 143.27 (1C, C4), 142.82 (1C, C8), 133.54 (1C, C5), 87.32 (1C, C1′), 86.81 (1C, C4′), 73.55 (1C, C2′), 71.21 (1C, C3′), 62.01 (1C, C5′).

LC/ESI-MS: negative mode 299 ($[M - H]^-$), positive mode 302 ($[M + H]^+$).

18.4. 2,6-dichloro-2',3', 5'-triacetyl-purine riboside (97)

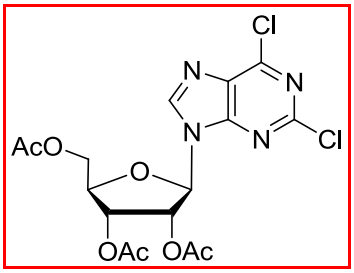

2-Amino-6-chloro-2',3',5'-triacetylribofuranoslypurine (0.6 g) and acetyl chloride (0.92 g) were added under argon atmosphere in 20 mL of anhydrous dichloromethane. Under ice cooling, 0.8 g BTEA-nitrite dissolved in 10 mL of anhydrous dichloromethane was added dropwise within an hour. It was stirred under ice-cooling and the progress of reaction was monitored in TLC. After completion of reaction after five hour, the solution was extracted three times with 100 mL of water. The organic phase is dried over magnesium sulfate, filtered and freed from solvent to yield the desired compound.

Yield: 254 mg (67%).

Melting Point (°C): 160-161 [**literature**, 159].[191]

^{1}H NMR (500 MHz, DMSO-d_6): δ 8.28 (s, 1H, C8-H), 6.20 – 6.10 (m, 1H, C1′-H), 5.77 – 5.67 (m, 1H, C2′-H), 5.53 – 5.45 (m, 1H, C3′-H), 4.46 (t, 1H, C4′-H), 4.40 – 4.23 (m, 2H, C5′-H_2), 2.15 (s, 3H, OCOCH_3), 2.12 (s, 3H, OCOCH_3), 2.07(s, 3H, OCOCH_3).

^{13}C NMR (125 MHz, DMSO-d_6): δ 170.17, 169.60, 169.35 (3C, 3xOCOCH$_3$), 153.00 (1C, C2), 152.45 (1C, C6), 152.19 (1C, C4), 143.21 (1C, C8), 131.35 (1C, C5), 86.5 (1C, C1′), 80.8 (1C, C4′), 73.21 (1C, C2′), 70.5 (1C, C3′), 62.6 (1C, C5′), 20.7 (1C, 3xOCOCH$_3$).

LC/ESI-MS: negative mode 446 ($[M - H]^-$), positive mode 448 ($[M + H]^+$).

18.5. 2-Chloroadenosine (98)

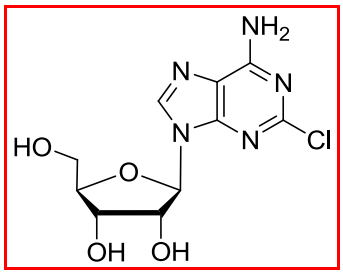

Ammoniacal ethanol solution is prepared by introducing ammonia gas in 100 mL of dry ethanol, under ice-cooling. The solution is used without further workup. 0.5 g of 2,6-dichoro-2',3',5'-triacetylribofuranosylpurine (**97**) was dissolved in 25 mL of ammoniacal ethanol solution and stirred for three days at room temperature. The solvent is removed under reduced pressure and the crude product was applied to a silica gel column with dichloromethane: methanol elution (9:1). The collected fractions were freed from solvent, and a reversed-phase chromatography (HPLC) with an increasing gradient methanol (10:90 to 90:10 over 70 min) in water was used to remove acetamide. The solvent was removed by lyophilization to yield the title compound **98**.

Yield: 254 mg (67%).

Melting Point (^{o}C): 174-176 [**literature**, 135].[192]

^{1}H NMR (500 MHz, DMSO-d_6): δ 8.36 (s, 1H, C8-H), 7.80 (d, 2H, N$\underline{H_2}$), 5.97 (d, *J* = 5.99 Hz, 1H, C1′-H), 5.42 (d, *J* = 5.99 Hz, 1H, C2′-H), 5.16 (d, *J* = 5.04 Hz, 1H, C3′-H), 5.01 (d, *J* = 5.67 Hz, 1H, C4′-H), 4.51 – 4.41 (m, 1H, C5′-H), 4.12 – 4.01 (m, 1H, C5′-H), 3.93 – 3.82 (m, 1H, C5′-OH) , 3.56 – 3.54 (m, 1H, C3′-OH), 3.51 – 3.41 (m, 1H, C2′-OH).

^{13}C NMR (125 MHz, DMSO-d_6): δ 156.95 (1C, C6), 153.14 (1C, C2), 150.49 (1C, C4), 140.17 (1C, C8), 118.33 (1C, C5), 87.53 (1C, C1′), 85.86 (1C, C4′), 73.57 (1C, C2′), 70.53 (1C, C3′), 61.53 (1C, C5′).

LC/ESI-MS: negative mode 300 ($[M - H]^-$), positive mode 302 ($[M + H]^+$).

18.6. 6-Chloro-2-iodo-2',3',5'-triacetyl-purine riboside (99)

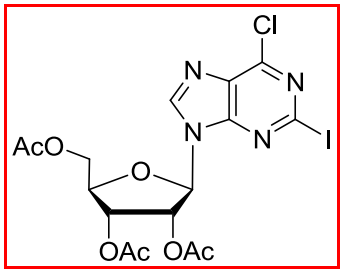

Isoamyl nitrate (4350 g) was added to the mixture of **95** (500 mg), I_2 (1000 mg), diiodomethane (30 mL) and CuI (2394 g) in THF (50 mL). The mixture was heated at 80 ^{o}C for 2 h. Insoluble material was removed by filteration and the filtrate was evaporated in vacuo. Then it was subjected to column chromatography. The desired compound was eluted with 2% methanol in DCM as brownish solid.

Yield: 254 mg (47%).

Melting Point (^{o}C): 174-176.

^{1}H NMR (500 MHz, DMSO-d_6): δ 8.26 (s, 1H, C8-H), 6.02 (d, 1H, C1′-H), 5.80 (d, J = 5.8 Hz, 1H, C2′-H), 5.42 (d, J = 6.2 Hz, 1H, C3′-H), 5.25 (q, J = 1.5 Hz, 1H, C4′-H), 5.13 (d, J = 1.5 Hz, 2H, C5′-$\underline{H}_2$), 2.16 (s, 3H, COC$\underline{H}_3$), 2.11 (s, 3H, COC$\underline{H}_3$), 2.06 (s, 3H, COC$\underline{H}_3$).

^{13}C NMR (125 MHz, DMSO-d_6): δ 170.12 – 168.36 (3C, $\underline{C}OCH_3$), 154.23 (1C, C6), 151.30 (1C, C2), 150.45 (1C, C4), 138.20 (1C, C8), 131.35 (1C, C5), 87.65 (1C, C1′), 85.80 (1C, C4′), 73.28 (1C, C2′), 70.58 (1C, C3′), 61.66 (1C, C5′), 20.68 (1C, CO$\underline{C}H_3$), 20.34 (1C, CO$\underline{C}H_3$), 20.12 (1C, CO$\underline{C}H_3$).

LC/ESI-MS: negative mode 537 ($[M - H]^-$), positive mode 539 ($[M + H]^+$).

18.7. 2-Iodoadenosine (100)

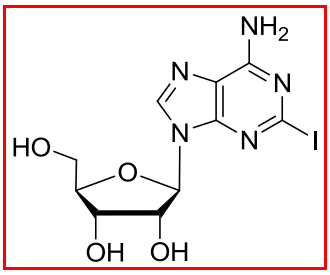

6-Chloro-2-iodo-2',3',5'-triacetylribofuranosylpurine (0.5 g) was dissolved in 25 mL of ammoniacal ethanol solution and was stirred for three days at room temperature. The solvent was removed under reduced pressure and the crude product was applied to a silica gel column with dichloromethane: methanol (9:1) elution. The collected fractions were freed from solvent, and a reversed-phase chromatography (HPLC) with an increasing gradient of methanol in water (10:90 to 90:10 over 70 min) was used to remove acetamide. The solvent was removed by lyophilization to yield desired compound.

Yield: 254 mg (67%).

Melting Point (^{o}C): 185-186 [**literature**, 185-187].[193]

^{1}H NMR (500 MHz, DMSO-d_6): δ 8.36 (s, 1H, C8-H), 7.80 (d, 2H, N$\underline{H_2}$), 5.97 (d, *J* = 5.99 Hz, 1H, C1′-H), 5.42 (d, *J* = 5.99 Hz, 1H, C2′-H), 5.16 (d, *J* = 5.04 Hz, 1H, C3′-H), 5.01 (d, *J* = 5.67 Hz, 1H, C4′-H), 4.51 (m, 1H, C5′-H), 4.12 – 4.05 (m, 1H, C5′-H), 3.93 – 3.85 (m, 1H, C5′-OH) , 3.56 – 5.51 (m, 1H, C3′-OH), 3.43 – 3.41 (m, 1H, C2′-OH).

^{13}C NMR (125 MHz, DMSO-d_6): δ 156.95 (1C, C6), 153.14 (1C, C2), 150.49 (1C, C4), 140.17 (1C, C8), 118.33 (1C, C5), 87.53 (1C, C1′), 85.86 (1C, C4′), 73.57 (1C, C2′), 70.53(1C, C3′), 61.53 (1C, C5′).

LC/ESI-MS: negative mode 392 ($[M - H]^-$), positive mode 394 ($[M + H]^+$).

18.8. 2-Hydrazinyladenosine (101)

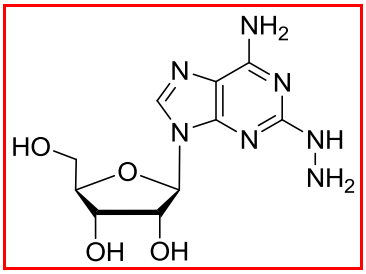

Solution of **100** (1.5 g, 5 mmol) in 5 mL of hydrazine hydrate was allowed to stir over night till disappearance of **100** determined by TLC (CH_2Cl_2: MeOH = 3:1). 2-Propanol (50 mL) was added to the reaction mixture and the formed gum was taken in water (100 mL) and stirred for additional 5 h. The precipitated product was filtered, washed with water, and dried to give the pure product.

Yield: 254 mg (67%).

Melting Point (^{o}C): 157-159.

^{1}H NMR (500 MHz, DMSO-d_6): δ 8.24 (s, 1H, C8-H), 7.45 (bs, 2H, N$\underline{H_2}$), 7.41 (s, 1H, N$\underline{H}$-NH_2), 5.90 – 5.85 (m, 1H, C1′-H), 5.48 – 5.40 (m, 1H, C2′-H), 5.06 – 5.01 (m, 1H, C3′-H), 4.98

– 4.85 (m, 1H, C4′-H), 4.45 – 4.40 (m, 1H, C5′-H), 4.35 – 4.37 (m, 1H, C5′-H), 3.91 – 3.88 (m, 1H, C5′-OH) , 3.85 – 3.81 (m, 1H, C3′-OH), 3.78 – 3.65 (m, 1H, C2′-OH).

^{13}C NMR (125 MHz, DMSO-*d*$_6$): δ 160.05 (1C, C1), 152.04 (1C, C2), 151.40 (1C, C4), 140.37 (1C, C8), 113.43 (1C, C5), 88.33 (1C, C1′), 87.46 (1C, C4′), 73.77 (1C, C2′), 70.50 (1C, C3′), 61.63 (1C, C5′).

LC/ESI-MS: negative mode 296 ($[M - H]^-$), positive mode 298 ($[M + H]^+$).

18.9. 2-Boc-piperazinyladenosine (102)

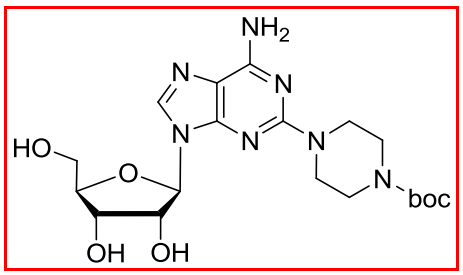

A mixture of 2-chloropurine riboside (500 mg), and 1-boc piperazine (5 mL), 5 mL of Et_3N in 1:1 mixture of 20 mL of ethanol and water was refluxed at 160 ^oC for 18 h. After completion of reaction it was evaporated under high vacuo. Purification using silica chromatography and precipitation using acetone (1:8 MeOH/DCM) yielded the title compound as white solid.

Yield: 254 mg (67%).

Melting Point (^{o}C): 178-179.

^{1}H NMR (500 MHz, DMSO-*d*$_6$): δ 8.36 (s, 1H, C8-H), 6.84 (s, 2H, $N\underline{H_2}$), 5.74 (d, *J* = 5.9 Hz, 1H, C1′-H), 5.31 – 5.20 (m, 1H, C2′-H), 5.10 – 4.95 (m, 1H, C3′-H), 4.87 – 4.78 (m, 1H, C4′-H), 4.60 (t, *J* = 5.5 Hz, C5′-H), 4.13 (dd, *J* = 5.2, 3.2 Hz, 1H, C5′-H), 3.87 (q, *J* = 4.2 Hz, 1H, C5′-OH), 3.68 – 3.64 (m, 2H, C3′-OH and C2′-OH), 3.40 – 3.34 (m, 4H, piperazinyl), 1.38 (s, 9H, 3xCH_3).

^{13}C NMR (125 MHz, DMSO-d_6): δ 158.59 (1C, C2), 155.89 (1C, C6), 154.15 (1C, NCOO), 151.60 (1C, C4), 137.24 (1C, C8), 113.69 (1C, C5), 87.00 (1C, C1′), 85.20 (1C, C4′), 79.07 (1C, C-3xCH_3), 73.09 (1C, C2′), 70.68 (1C, C3′), 61.80 (1C, C5′), 45.50 (2C, piperazinyl), 44.05 (2C, piperazinyl), 28.23 (3C, 3xCH_3).

LC/ESI-MS: negative mode 450 ($[M - H]^-$), positive mode 452 ($[M + H]^+$).

18.10. 2-piperazinyladenosine (103)

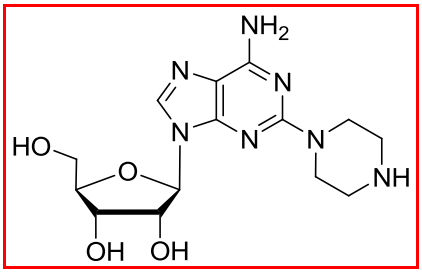

Compound **102** (500 mg) was dissolved in 4.5 mL dichloromethane then, 0.5 mL of water and 0.65 mL of triflouroacetic acid was added to it. It was stirred at room temperature for 3 h. After completion of the reaction, the mixture was evaporated and the solid was precipitated adding diethyl ether. Then the crude solid product was dissolved in 6 mL water and 0.6 mL methanol. It was then purified by RP-HPLC using a gradient of H_2O/MeOH from 100: 0 to 0: 100, and finally appropriate fraction were pooled and lyophilized to get final product.

Yield: 254 mg (67%).

Melting Point (^{o}C): 169-171.

^{1}H NMR (500 MHz, DMSO-d_6): δ 8.35 (s, 1H, C8-H), 5.72 (d, J = 5.9 Hz, 1H, C1′-H), 5.35 – 5.21 (m, 1H, C2′-H), 5.14 – 5.11 (m, 1H, C3′-H), 4.95 – 4.78 (m, 1H, C4′-H), 4.65 (t, J = 5.5 Hz, C5′-H), 4.25 (dd, J = 5.2 Hz, 1H, C5′-H), 3.97 (q, 1H, C5′-OH), 3.78 – 3.76 (m, 2H, C3′-OH and C2′-OH), 3.41 – 3.36 (m, 4H, piperazinyl).

^{13}C NMR (125 MHz, DMSO-d_6): δ 160.69 (1C, C2), 157.88 (1C, C6), 151.64 (1C, C4), 140.23 (1C, C8), 113.64 (1C, C5), 97.03 (1C, C1′), 84.24 (1C, C4′), 73.79 (1C, C2′), 70.56 (1C, C3′), 61.86 (1C, C5′), 48.00 (2C, piperazinyl), 45.85 (2C, piperazinyl).

LC/ESI-MS: negative mode 350 ($[M - H]^-$), positive mode 352 ($[M + H]^+$).

18.11. Synthesis of 2-allylthio- and 2-cyclohexylethylthio-adenosine (107, 108)

2-Thioadenosine (500 mg, 1 mmol) was dissolved in 20 mL of water: ethanol (1: 1) mixture, then 4 mL of sodium hydroxide (0.5 N) was added to the reaction mixture, followed by the addition of allyl bromide (243 mg, 1.2 mmol) or cyclohexylethyl bromide (385 mg, 1.2 mmol). The reaction mixture was stirred for 5 h at rt, and the completion of the reaction was determined by TLC (CH_2Cl_2: MeOH = 9:1). The crude product was extracted by ethyl acetate and evaporated to dryness under reduced pressure. The crude product was purified by silica gel column chromatography (CH_2Cl_2: MeOH = 9: 1) to afford the pure product.

18.12. 2-Allylthioadenosine (107)

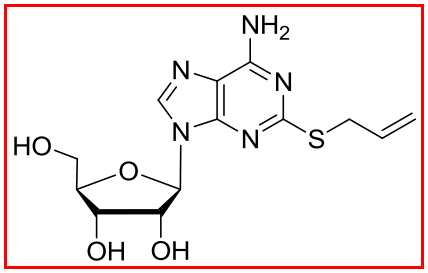

Yield: 254 mg (67%).

Melting Point (^{o}C): 171-172.

^{1}H NMR (500 MHz, DMSO-d_6): δ 8.22 (s, 1H, C8-H), 7.35 (s, 2H, NH_2), 6.02 – 5.88 (m, 1H, C1′-H), 5.82 (d, J = 5.8 Hz, 1H, S-CH_2-C<u>H</u>=CH_2), 5.38 (d, J = 6.2 Hz, 1H, C2′-H), 5.32 (q, J = 1.5 Hz, 1H, C3′-H), 5.13 (d, J = 4.9 Hz, 1H, S-CH_2-CH=C<u>H</u>$_2$), 5.10 – 5.05 (m, 1H, S-CH_2-

CH=C<u>H</u>$_2$), 4.99 (dd, *J* = 6.0, 5.2 Hz, 1H, C4′-H), 4.56 (td, *J* = 6.0, 5.1 Hz, 1H, C5′-H), 4.12 (td, *J* = 5.0, 3.5 Hz, 1H, C5′-H), 3.91 (q, *J* = 4.0 Hz, 1H, C5′-OH), 3.83 – 3.73 (m, 2H, S-C<u>H</u>$_2$-CH=CH$_2$), 3.63 (q, *J* = 11.9, 5.3, 4.2 Hz, 1H, C3′-OH), 3.53 (q, *J* = 12.0, 6.1, 4.3 Hz, 1H, C2′-OH).

^{13}C NMR (125 MHz, DMSO-*d*$_6$): δ 163.12 (1C, C2), 155.66 (1C, C6), 150.26 (1C, C4), 138.83 (1C, C8), 134.63 (1C, S-CH$_2$-C<u>H</u>=CH$_2$), 120.40 (1C,C5), 117.28 (1C, S-CH$_2$-CH=C<u>H</u>$_2$), 87.44 (1C, C1′), 85.57 (1C, C4′), 73.55 (1C, C2′), 70.58 (1C, C3′), 61.67 (1C, C5′), 33.22 (1C, S-C<u>H</u>$_2$-CH=CH$_2$).

LC/ESI-MS: negative mode 338 ([M - H]$^-$), positive mode 340 ([M + H]$^+$).

Purity by HPLC-UV (254 nm)-ESI-MS: 98.5%.

<u>18.13. 2-Cyclohexylethylthio-adenosine (108)</u>

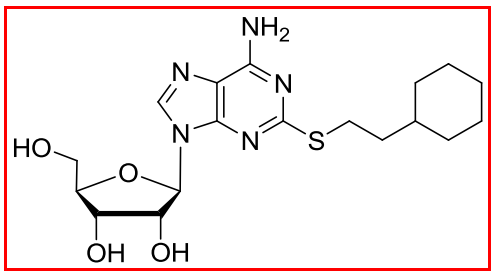

Yield: 254 mg (67%).

Melting Point (^{o}C): 181-183.

^{1}H NMR (500 MHz, DMSO-*d*$_6$): δ 8.19 (s, 1H, C8-H), 7.28 (bs, 2H, NH$_2$), 5.80 (d, *J* = 5.99 Hz, 1H, C1′-H), 5.36 – 5.25 (m, 1H, C2′-H), 5.10 – 5.05 (m, 1H, C3′-H), 4.98 (t, *J* = 5.51 Hz, 1H, C4′-H), 4.59 (t, *J* = 5.35 Hz, 1H, C5′-H), 4.11 (t, *J* = 5.35 Hz, 1H, C5′-H), 3.90 (q, *J* = 3.99 Hz, 1H, C5′-OH), 3.64 – 3.50 (q, *J* = 3.99 Hz, 2H, C3′-OH and C2′-OH), 3.14 – 3.00 (m, 2H, C<u>H</u>$_2$), 1.74 – 1.61 (m, 2H, C<u>H</u>$_2$), 1.60 – 0.87 (m, 11H, cyclohexane).

^{13}C NMR (125 MHz, DMSO-d_6): δ 163.94 (1C, C2), 155.63 (1C, C6), 150.31 (1C, C4), 138.86 (1C, C8), 117.05 (1C, C5), 87.42 (1C, C1′), 85.57 (1C, C4′), 73.31 (1C, C2′), 70.60 (1C, C3′), 61.75 (1C, C5′), 36.82 (1C, $\underline{C}H_2$-CH_2- cyclohexane), 36.61 (1C, cyclohexane), 32.46 (1C, CH_2-$\underline{C}H_2$-cyclohexane), 27.94 (2C, cyclohexane), 26.26 (2C, cyclohexane), 25.89 (1C, cyclohexane).

LC/ESI-MS: negative mode 408 ($[M - H]^-$), positive mode 410 ($[M + H]^+$).

Purity by HPLC-UV (254 nm)-ESI-MS: 100%.

19.1. General procedure for the synthesis of nucleotides (109-114)

A solution of methylenebis(phosphonic dichloride) (5 mmol) in trimethyl phosphate (2 mL), cooled to 0 °C was added to a suspension of corresponding nucleosides, **98**, **100**, **101**, **103**, **107** and **108** (1 mmol) in trimethyl phosphate at 0 °C. The reaction mixture was stirred at 0 °C and samples were withdrawn at 10 min interval for TLC to check the disappearance of nucleosides. After 30 min, on disappearance of nucleoside, 7 mL of cold 0.5 M aqueous TEAC solution (pH 7.4-7.6) was added. It was stirred at 0 °C for 15 min followed by stirring at room temperature for 1 h. Trimethyl phosphate was extracted using (2 x 100 mL) of *tert*.butylmethyl ether and the aqueous layer was lyophilized. The crude product was then purified by RP-HPLC using a gradient of 50 mM ammoniumbicarbonate/ACN from 100:0 to 60:40 to get final product. Since there was no formation of dinucleotide, ion exchange chromatography was not used.

19.2. 2-Chloroadenosine-5'-O-[(phosphonomethyl)phosphonic acid] (109)

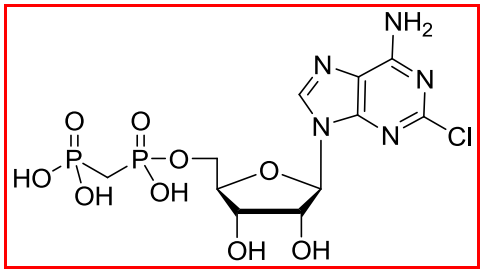

^{1}H NMR (500 MHz, D_2O): δ 8.46 (s, 1H, C8-H), 6.01 (d, *J* = 5.0 Hz, 1H, C1′-H), 4.71 (d, *J* = 4.8 Hz, 1H, C2′-H), 4.52 (t, *J* = 4.8 Hz, 1H, C3′-H), 4.34 (q, *J* = 3.7 Hz, 1H, C4′-H), 4.15 (d, *J* = 4.5 Hz, 2H, C5′-$\underline{H_2}$), 2.07 (t, *J* = 19.5 Hz, 2H, P-C$\underline{H_2}$-P).

^{13}C NMR (126 MHz, D_2O): δ 159.10 (1C, C6), 156.60 (1C, C2), 152.91 (1C, C4), 142.91 (1C, C8), 120.50 (1C, C5), 90.04 (1C, C1′), 86.63 (1C, C4′), 77.09 (1C, C2′), 72.84 (1C, C3′), 66.05 (1C, C5′), 49.48 (1C, P-$\underline{C}H_2$-P).

^{31}P NMR (202 MHz, D_2O): δ 21.25 (**P_α**), 12.84 (**P_β**).

LC-MS (*m*/*z*): negative mode 458 $[M-H]^-$, positive mode 460 $[M+H]^+$.

Purity by HPLC-UV (254 nm)-ESI-MS: 100%.

19.3. 2-Iodoadenosine-5′-O-[(phosphonomethyl)phosphonic acid] (110)

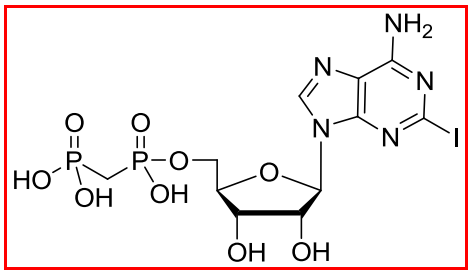

^{1}H NMR (600 MHz, D_2O): δ 8.43 (s, 1H, C8-H), 6.05 (d, *J* = 5.4 Hz, 1H, C1′-H), 4.74 (t, *J* = 5.3 Hz, 1H, C2′-H), 4.54 (dd, *J* = 5.1, 4.1 Hz, 1H, C3′-H), 4.38 (dt, *J* = 4.2, 2.3 Hz, 1H, C4′), 4.22 – 4.09 (m, 2H, C5′-$\underline{H_2}$), 2.20 (td, *J* = 19.9, 2.0 Hz, 2H, P-C$\underline{H_2}$-P).

^{13}C NMR (151 MHz, D_2O): δ 155.38 (1C, C6), 149.51 (1C, C2), 139.57 (1C, C4), 119.44 (1C, C8), 118.50 (1C, C5), 87.05 (1C, C1′), 83.90 (1C, C4′), 74.29 (1C, C2′), 70.13 (1C, C3′), 63.42 (1C, C5′), 46.62 (1C, P-$\underline{C}H_2$-P).

^{31}P NMR (243 MHz, D_2O): δ 18.67 (d, *J* = 9.7 Hz, **P_α**), 15.38 (d, *J* = 9.8 Hz, **P_β**).

LC-MS (*m*/*z*): negative mode 550 $[M-H]^-$, positive mode 552 $[M+H]^+$.

Purity by HPLC-UV (254 nm)-ESI-MS: 100%.

19.4. 2-Hydrazinyladenosine-5'-O-[(phosphonomethyl)phosphonic acid] (111)

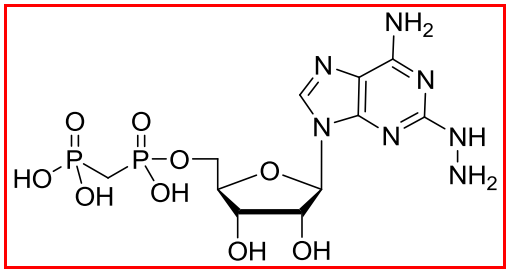

^{1}H NMR (600 MHz, D_2O): δ 8.30 (s, 1H, C8-H), 5.98 (s, 1H, C1′-H), 4.98 (m, 1H, C2′-H), 4.56 (d, *J* = 25.2 Hz, 1H, C3′-H), 4.35 (d, *J* = 10.1 Hz, 1H, C4′-H), 4.27 – 4.14 (m, 2H, C5′-H_2), 2.28 – 2.13 (m, 2H, P-CH_2-P).

^{13}C NMR (151 MHz, D_2O): δ 159.06 (1C, C6), 157.10 (1C, C2), 152.80 (1C, C4), 142.75 (1C, C8), 120.14 (1C, C5), 90.89 (1C, C1′), 86.69 (1C, C4′), 75.81 (1C, C2′), 73.11 (1C, C3′), 66.45 (1C, C5′), 49.51 (1C, P-CH_2-P).

^{31}P NMR (243 MHz, D_2O): δ 18.49 (P_α), 16.14 (P_β).

LC-MS (*m*/*z*): negative mode 454 $[M-H]^-$, positive mode 456 $[M+H]^+$.

Purity by HPLC-UV (254 nm)-ESI-MS: 100%.

19.5. 2-Piperazinyladenosine-5'-O-[(phosphonomethyl)phosphonic acid] (112)

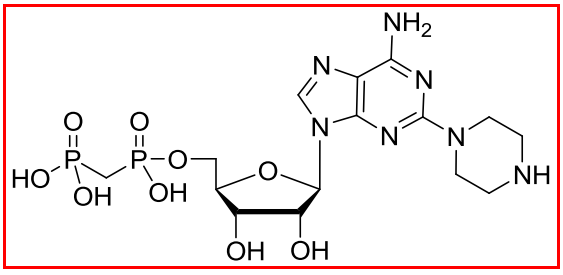

^{1}H NMR (600 MHz, D_2O): δ 8.15 (s, 1H, C8-H), 6.02 (d, *J* = 5.3 Hz, 1H, C1′-H), 4.87 (d, *J* = 5.3 Hz, 1H, C2′-H), 4.54 (t, *J* = 4.8 Hz, 1H, C3′-H), 4.37 – 4.24 (m, 1H, C4′-H), 4.14 (q, *J* =

21.8, 8.7, 4.7 Hz, 2H, C5′-$\underline{H_2}$), 3.99 (s, 2H, piperazinyl-H), 3.33 (s, 2H, piperazinyl-H), 2.90 (s, 1H, piperazinyl-H), 2.13 (t, *J* = 19.3 Hz, 2H, P-C$\underline{H_2}$-P).

^{13}C NMR (151 MHz, D_2O): δ 161.50 (1C, C2), 158.82 (1C, C6), 154.30 (1C, C4), 141.32 (1C, C8), 120.14 (1C, C6), 90.00 (1C, C1′), 86.07 (1C, C4′), 76.05 (1C, C2′), 73.06 (1C, C3′), 66.58 (1C, C5′), 47.53 (2C, piperazine), 45.89 (2C, piperazine), 44.46 (1C, P-$\underline{C}H_2$-P).

^{31}P NMR (243 MHz, D_2O): δ 19.73 (**P_α**), 14.49 (**P_β**).

LC-MS (*m*/*z*): negative mode 508 $[M-H]^-$, positive mode 510 $[M+H]^+$.

Purity by HPLC-UV (254 nm)-ESI-MS: 100%.

19.6. 2-Allylthioadenosine-5'-O-[(phosphonomethyl)phosphonic acid] (113)

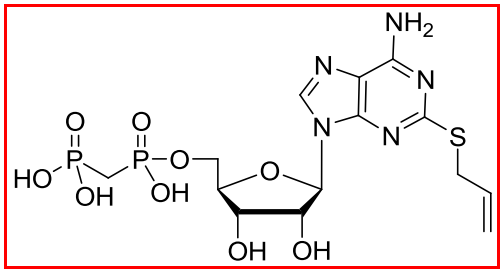

^{1}H NMR (500 MHz, D_2O): δ 8.34 (s, 1H, C8-H), 6.09 (dd, *J* = 5.2, 1.8 Hz, 1H, C1′-H), 6.06 – 5.99 (m, 1H, C2′-H), 5.36 (t, *J* = 17.1, 1.5 Hz, 1H, C3′-H), 5.16 (dt, *J* = 10.1, 1.4 Hz, 1H, C4′-H), 4.82 (d, *J* = 2.2 Hz, 1H, Allyl-H), 4.55 (dd, *J* = 5.8, 4.0 Hz, 1H, Allyl-H), 4.34 (dt, *J* = 3.4, 1.7 Hz, 1H, Allyl-H), 4.22 – 4.01 (m, 2H, C5′-H_2), 3.82 (dt, *J* = 6.8, 1.4 Hz, 2H, Allyl-H), 2.15 (td, *J* = 19.8, 1.9 Hz, 2H, P-C$\underline{H_2}$-P).

^{13}C NMR (126 MHz, D_2O): δ 167.39 (1C, C2), 158.06 (1C, C6), 152.94 (1C, C4), 142.12 (1C, C8), 136.87 (1C, Allyl), 120.55 (1C, C5), 119.27 (1C, Allyl), 90.08 (1C, C1′), 86.38 (1C, C4′), 76.71 (1C, C2′), 73.02 (1C, C3′), 66.38 (1C, C5′), 49.50 (1C, P-$\underline{C}H_2$-P), 36.51 (1C, Allyl).

^{31}P NMR (202 MHz, D_2O): δ 19.33 (**P_α**), 14.47 (**P_β**).

LC-MS (*m*/*z*): negative mode 496 $[M-H]^-$, positive mode 498 $[M+H]^+$.

Purity by HPLC-UV (254 nm)-ESI-MS: 100%.

19.7. 2-Cyclohexylethylthioadenosine-5'-O-[(phosphonomethyl)phosphonic acid] (114)

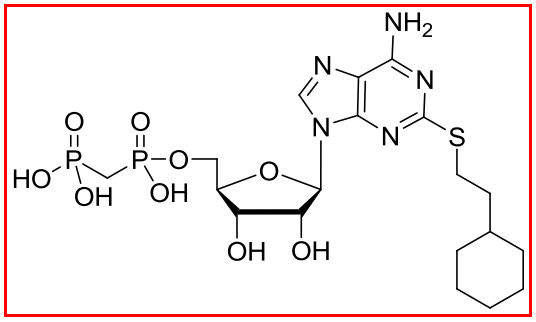

^{1}H NMR (500 MHz, D_2O): δ 8.37 (s, 1H, C8-H), 6.11 (dd, *J* = 15.8, 5.4 Hz, 1H, C1′-H), 4.56 (dt, *J* = 20.6, 4.7 Hz, 1H, C2′-H), 4.34 (dq, *J* = 7.4, 3.6 Hz, 1H, C3′-H), 4.28 – 4.21 (m, 1H, C4′-H), 4.17 (td, *J* = 8.7, 4.8 Hz, 2H, C5′-H_2), 3.16 – 3.01 (m, 2H, -CH_2-CH_2-), 2.19 (t, *J* = 19.8 Hz, 2H, P-CH_2-P), 1.61 – 0.74 (m, 13H, -CH_2-CH_2-Cyclohexane-H).

^{13}C NMR (126 MHz, D_2O): δ 167.64 (1C, C2), 157.32 (1C, C6), 152.90 (1C, C4), 142.11 (1C, C8), 118.83 (1C, C5), 89.77 (1C, C1′), 86.48 (1C, C4′), 76.82 (1C, C2′), 73.05 (1C, C3′), 66.43 (1C, C5′), 39.46 (1C, P-CH_2-P), 35.46 (1C, CH_2-CH_2-), 31.60 (1C, Cyclohexane), 30.34 (1C, -CH_2-CH_2-Cyclohexane), 29.06 (2C, Cyclohexane), 28.71 (3C, Cyclohexane).

^{31}P NMR (202 MHz, D_2O): δ 18.68 (d, *J* = 9.8 Hz, $\mathbf{P_\alpha}$), 15.27 (d, *J* = 9.4 Hz, $\mathbf{P_\beta}$).

LC-MS (*m*/*z*): negative mode 566 $[M-H]^-$, positive mode 568 $[M+H]^+$.

Purity by HPLC-UV (254 nm)-ESI-MS: 100%.

20.1. General Procedure for the synthesis of nucleoside derivatives (115-126 and 127-138)

A mixture 2-amino-6-chloro-2', 3',5'-triacetylribofuranoslypurine (500 mg) or 2,6-dichloro-2',3', 5'-triacetylribofuranoslypurine (500 mg) or 2-amino-6-iodo-2',3',5'-triacetylribofuranoslypurine (500 mg), (1.76 mmol) of respective amine, (1.6 mmol) of Et_3N and 25 mL of ethanol was refluxed at 60 ^{o}C for 18 h. After completion of reaction it was evaporated under high vacuo.

Purification using silica chromatography and precipitation using acetone (1:8 MeOH/DCM) yielded the title compounds **115-126** as white solid. White solid compound (100 mg) was dissolved in 5 mL of 2% sodium methoxide in methanol. It was stirred at room temperature for 10 hours. After completion of the reaction, the mixture was evaporated and the solid was precipitated adding diethyl ether. Then the crude solid product was dissolved in 6 mL water and 0.6 mL methanol. It was then purified by RP-HPLC using a gradient of H_2O/MeOH from 100:0 to 0:100, and finally appropriate fraction were pooled and lyophilized to get final products **127-138**.

20.2. N^6-Dimethyl-2-aminopurine riboside (127)

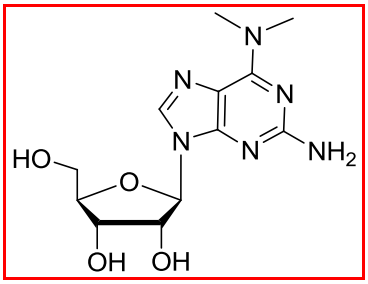

The compound synthesized using 2',3',5'-tri-*O*-acetyl-6-chloro-2-amino-9-(*β*-D-ribofuranosyl)purine (500 mg), and 123 mg of dimethylamine and was isolated as a white solid.

Yield: 533 mg (95%).

Melting Point (^{o}C): 201-202 [**literature**, 200-202].[152]

^{1}H NMR (500 MHz, DMSO-d_6): δ 8.45 (s, 1H, C8-H), 7.92 (bs, 2H, N$\underline{H_2}$), 5.97 (d, *J* = 2.9 Hz, 1H, C1′-H), 5.23 (dd, *J* = 6.3, 2.9 Hz, 1H, C2′-H), 5.13 (dd, *J* = 5.9, 5.2 Hz, 1H, C3′-H), 4.98 (dd, *J* = 6.2, 2.9 Hz, 1H, C4′-H), 4.12 (td, *J* = 5.0, 2.9 Hz, 1H, C5′-$\underline{H_2}$), 3.59 – 3.53 (m, 1H, C5′-OH), 3.50 (q, *J* = 11.4, 5.9, 5.0 Hz, 2H, C3′- and C2′-OH), 1.52 (d, *J* = 0.8 Hz, 3H, C$\underline{H_3}$), 1.31 (d, *J* = 0.8 Hz, 3H, C$\underline{H_3}$).

^{13}C NMR (126 MHz, DMSO-*d*$_6$): δ 159.50 (1C, C5), 157.49 (1C, C2), 151.62 (1C, C6), 135.18 (1C, C4), 113.49 (1C, C8), 98.78 (1C, C1′), 86.56 (1C, C4′), 73.37 (1C, C2′), 70.46 (1C, C3′), 61.85 (1C, C5′), 27.24 (2C, 2xCH$_3$).

LC-MS (*m*/*z*): negative mode 309 $[M-H]^-$, positive mode 311 $[M+H]^+$.

Purity by HPLC-UV (254 nm)-ESI-MS: 95.0%.

20.3. N^6-Diethyl-2-aminopurine riboside (128)

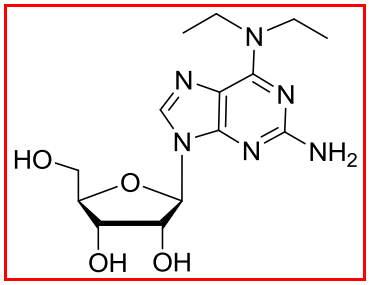

The compound was synthesized using 2',3',5'-tri-*O*-acetyl-6-chloro-2-amino-9-(*β*-D-ribofuranosyl)purine (500 mg), and 251 mg of diethylamine, and was isolated as a white solid.

Yield: 597 mg (92%).

Melting Point (^{o}C): 170-172

^{1}H NMR (500 MHz, DMSO-*d*$_6$): δ 8.36 (s, 1H, C8-H), 6.92 (s, 2H, N$\underline{H_2}$), 5.77 (dd, *J* = 30.2, 6.0 Hz, 1H, C1′-H), 5.32 – 5.19 (m, 1H, C2′-H), 5.09 (d, *J* = 31.4 Hz, 1H, C3′-H), 4.47 (t, *J* = 5.7 Hz, 1H, C4′-H), 4.10 (q, *J* = 13.2, 4.7, 3.0 Hz, 1H, C5′-$\underline{H_2}$), 3.97 – 3.80 (m, 1H, C5′-OH), 3.70 – 3.58 (m, 1H, C3′-OH), 3.53 (q, *J* = 12.1, 9.4, 3.9 Hz, 1H, C2′-OH), 3.42 – 3.35 (m, 4H, 2xC$\underline{H_2}$-CH$_3$), 1.15 – 1.10 (m, *J* = 6.9 Hz, 6H, 2xCH$_2$-C$\underline{H_3}$).

^{13}C NMR (126 MHz, DMSO-*d*$_6$): δ 159.94 (1C, C5), 154.19 (1C, C2), 149.64 (1C, C6), 141.31 (1C, C4), 123.67 (1C, C8), 86.97 (1C, C1′), 85.54 (1C, C4′), 73.54 (1C, C2′), 70.57 (1C, C3′), 61.58 (1C, C5′), 41.54 (2C, 2x$\underline{C}$H$_2$-CH$_3$), 22.63 (2C, 2xCH$_2$-$\underline{C}$H$_3$).

LC-MS (*m*/*z*): negative mode 337 $[M-H]^-$, positive mode 339 $[M+H]^+$.

Purity by HPLC-UV (254 nm)-ESI-MS: 96.0%.

20.4. N^6-Benzyl-2-aminopurine riboside (129)

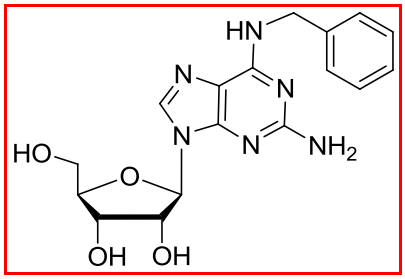

The compound was synthesized using 2',3',5'-tri-*O*-acetyl-6-chloro-2-amino-9-(*β*-D-ribofuranosyl)purine (500 mg), and 281 mg of benzylamine, and was isolated as a white solid.

Yield: 610 mg (99%).

Melting Point (^{o}C): 208-210 [**literature**, 120].[194]

^{1}H NMR (500 MHz, DMSO-d_6): δ 8.38 (s, 1H, C8-H), 8.24 (s, 1H, NH), 7.35 – 7.20 (m, 5H, Ar-H), 5.92 (d, *J* = 6.0 Hz, 1H, C1′-H), 5.41 (d, *J* = 6.2 Hz, 1H, C2′-H), 5.29 (dd, *J* = 6.9, 4.6 Hz, 1H, C3′-H), 5.14 (d, *J* = 4.8 Hz, 1H, C4′-H), 4.60 (td, *J* = 6.1, 5.0 Hz, 1H, C5′-H), 4.15 (td, *J* = 4.9, 3.2 Hz, 1H, C5′-H_2), 3.96 (q, *J* = 3.6 Hz, 1H, C5′-OH), 3.67 (q, *J* = 12.0, 4.7, 3.7 Hz, 1H, C3′-OH), 3.55 (q, *J* = 12.0, 6.9, 3.7 Hz, 1H, C2′-OH).

^{13}C NMR (126 MHz, DMSO-d_6): δ 160.09 (1C, C2), 154.76 (1C, C6), 151.11 (1C, C4), 146.05 (1C, Ar), 140.63 (1C, Ar), 136.21 (2C, Ar), 128.22 (1C, Ar), 127.34 (1C, Ar), 125.64 (1C, C5), 87.17 (1C, C1′), 85.64 (1C, C4′), 73.37 (1C, C2′), 70.83 (1C, C3′), 61.87 (1C, C5′), 42.70 (1C, CH_2-Ar).

LC-MS (*m*/*z*): negative mode 371 [M-H], positive mode 373 $[M+H]^+$.

Purity by HPLC-UV (254 nm)-ESI-MS: 100%.

20.5. N^6-Benzyl-2-chloropurine riboside (130)

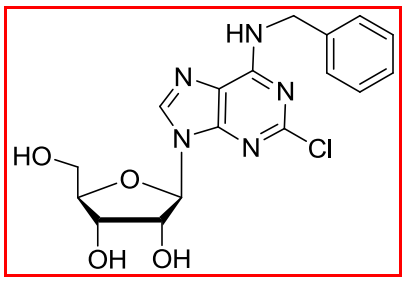

The compound was synthesized using 2',3',5'-tri-*O*-acetyl-2,6-dichloro-9-(*β*-D-ribofuranosyl)purine (500 mg) and 410 mg of benzylamine, and was isolated as a white solid.

Yield: 603 mg (98%).

Melting Point (^{o}C): 225-228 (slow decomp.)

^{1}H NMR (500 MHz, DMSO-d_6): δ 8.86 (s, 1H, C8-H), 8.43 (s, 1H, NH), 7.32 (dd, *J* = 11.8, 7.5 Hz, 4H, Ar-H), 7.25 – 7.20 (m, 1H, Ar-H), 5.84 (d, *J* = 6.1 Hz, 1H, C1′-H), 5.44 (d, *J* = 6.1 Hz, 1H, C2′-H), 5.25 (m, 1H, C3′-H), 4.65 (d, *J* = 6.8 Hz, 2H, C5′-H_2), 4.49 (q, *J* = 5.2 Hz, 1H, C4′-H), 4.15 – 4.03 (m, 1H, C5′-OH), 3.94 (dd, *J* = 11.3, 3.9 Hz, 1H, C3′-OH), 3.85 (dd, *J* = 11.2, 3.9 Hz, 1H, C2′-OH).

^{13}C NMR (126 MHz, DMSO-d_6): δ 155.08 (1C, C6), 153.38 (1C, C2), 150.20 (1C, C4), 139.73 (1C, C8), 139.35 (1C, Ar), 128.41 (2C, Ar), 127.35 (2C, Ar), 126.92 (1C, Ar), 118.33 (1C, C5), 98.34 (1C, C1′), 86.90 (1C, C4′), 83.73 (1C, C2′), 71.13 (1C, C3′), 66.06 (1C, C5′), 43.27 (1C, CH_2-Ar).

LC-MS (*m*/*z*): negative mode 446 $[M-H]^-$, positive mode 448 $[M+H]^+$.

Purity by HPLC-UV (254 nm)-ESI-MS: 100%.

20.6. N^6-Benzyl-2-iodopurine riboside (131)

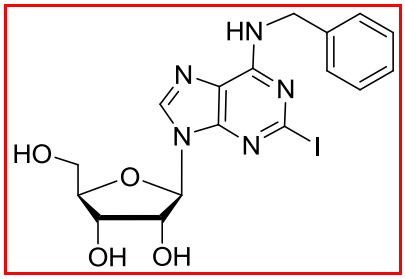

The compound was synthesized using 2',3',5'-tri-*O*-acetyl-6-chloro-2-iodo-9-(*β*-D-ribofuranosyl)purine (500 mg) and benzylamine (294 mg), and was isolated as a yellow solid powder.

Yield: 550 mg (94%).

Melting Point (^{0}C): 188-189

^{1}H NMR (500 MHz, DMSO-d_6): δ 8.30 (s, 1H, C8-H), 7.51 – 7.41 (m, 1H, Ar-H), 7.33 (m, 2H, Ar-H), 7.26 – 7.15 (m, 2H, Ar-H), 5.81 (d, *J* = 6.0 Hz, 1H, C1′-H), 5.42 – 5.31 (m, 1H, C2′-H), 4.77 (d, *J* = 1.4 Hz, 1H, C3′-H), 4.61 (s, 2H, CH_2-Ar), 4.51 (t, *J* = 5.5 Hz, 1H, C4′-H), 4.18 – 4.07 (m, 2H, C5′-H_2), 3.93 (q, *J* = 3.8 Hz, 1H, C5′-OH).

^{13}C NMR (126 MHz, DMSO-d_6): δ 161.88 (1C, C6), 154.05 (1C, C2), 149.28 (1C, C4), 139.58 (1C, C8), 130.86 (1C, Ar), 128.36 (1C, Ar), 127.69 (3C, Ar), 120.84 (1C, C5), 85.94 (1C, C1′), 73.74 (1C, C4′), 70.62 (1C, C2′), 64.07 (1C, C3′), 61.55 (1C, C5′), 44.72 (1C, CH_2-Ar).

LC-MS (*m*/*z*): negative mode 482 $[M-H]^-$, positive mode 484 $[M+H]^+$.

Purity by HPLC-UV (254 nm)-ESI-MS: 100%.

20.7. N^6-(2-Chlorobenzyl)-2-chloropurine riboside (132)

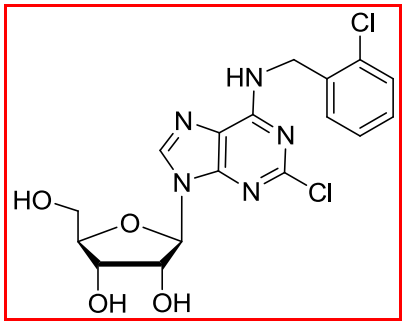

The compound was synthesized using 2',3',5'-tri-*O*-acetyl-2,6-dichloro-9-(*β*-D-ribofuranosyl)purine (500 mg), and 392 mg of 2-chlorobenzylamine, and was isolated as a yellow powder.

Yield: 631 mg (95%).

Melting Point (^{0}C): 202-203

^{1}H NMR (500 MHz, DMSO-d_6): δ 8.84 (s, 1H, C8-H), 8.44 (s, 1H, NH), 7.50 – 7.41 (m, 1H, Ar-H), 7.38 – 7.22 (m, 3H, Ar-H), 5.84 (d, *J* = 5.9 Hz, 1H, C1′-H), 5.20 (d, *J* = 25.0 Hz, 1H, C2′-H), 4.80 – 4.66 (m, 1H, C3′-H), 4.53 – 4.45 (m, 1H, C4′-H), 4.14 (d, *J* = 5.2 Hz, 2H, C5′-$\underline{H_2}$), 3.99 – 3.89 (m, 1H, C5′-OH), 3.74 – 3.60 (m, 1H, C3′-OH), 3.55 (d, *J* = 11.9 Hz, 1H, C2′-OH).

^{13}C NMR (126 MHz, DMSO-d_6): δ 155.19 (1C, C6), 153.22 (1C, C2), 149.94 (1C, C4), 140.40 (1C, Ar), 136.09 (1C, C8), 132.04 (1C, Ar), 129.29 (1C, Ar), 128.59 (2C, Ar), 127.33 (1C, Ar), 118.85 (1C, C5), 87.63 (1C, C1′), 85.90 (1C, C4′), 73.85 (1C, C2′), 70.52 (1C, C3′), 61.50 (1C, C5′), 41.35 (1C, $\underline{C}H_2$-Ar).

LC-MS (*m*/*z*): negative mode 425 $[M-H]^-$, positive mode 427 $[M+H]^+$.

Purity by HPLC-UV (254 nm)-ESI-MS: 95.0%.

20.8. N^6-(1-Phenylethylamine)-2-chloropurine riboside (133)

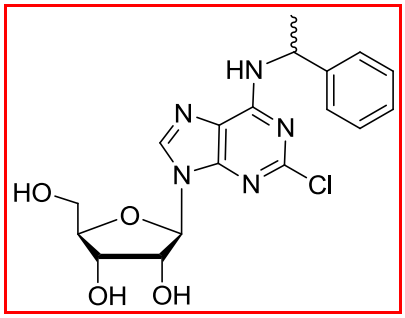

The compound was synthesized using 2',3',5'-tri-*O*-acetyl-2,6-dichloro-9-(*β*-D-ribofuranosyl)purine (500 mg) and 392 mg of α-methylbenzylamine, and was isolated as a yellow powder.

Yield: 567 mg (90%).

Melting Point (^{o}C): 202-203

^{1}H NMR (500 MHz, DMSO-d_6): δ 8.80 (s, 1H, C8-H), 7.43 (d, *J* = 7.5 Hz, 2H, Ar), 7.34 – 7.26 (m, 3H, Ar), 5.81 (dd, *J* = 5.9, 1.2 Hz, 1H, C1′-H), 5.41 (d, *J* = 14.1 Hz, 2H, C$\underline{H_2}$-Ar), 5.15 – 5.08 (m, 1H, C2′-H), 5.01 – 4.89 (m, 1H, C3′-H), 4.49 (t, *J* = 6.0 Hz, C4′-H), 4.11 – 4.08 (m, 1H, C5′-H), 4.00 (q, *J* = 6.6 Hz, 1H, C5′-H), 3.93 (q, *J* = 3.8 Hz, 1H, C5′-OH), 3.64 (d, *J* = 12.1 Hz, 1H, C3′-OH), 3.54 (d, *J* = 12.0 Hz, 1H, C2′-OH), 1.63 – 1.43 (m, 3H, α-C$\underline{H_3}$).

^{13}C NMR (126 MHz, DMSO-d_6): δ 153.14 (1C, C6), 149.87 (1C, C2), 147.93 (1C, C4), 144.46 (1C, Ar), 139.99 (1C, C8), 128.29 (2C, Ar), 126.99 – 124.13 (3C, Ar), 118.60 (1C, C5), 85.84 (1C, C1), 73.83 (1C, C4), 70.48 (1C, C2), 61.48 (1C, C3), 50.71 (1C, C5), 49.21 (1C, $\underline{C}H_2$-Ar), 25.80 (1C, α-$\underline{C}H_3$).

LC-MS (*m*/*z*): negative mode 404 $[M-H]^-$, positive mode 406 $[M+H]^+$.

Purity by HPLC-UV (254 nm)-ESI-MS: 97.0%.

Optical rotation: -53.8^o

20.9. N^6-((S)-1-Phenylethylamine)-2-chloropurine riboside (134)

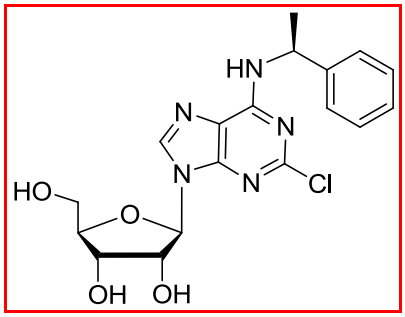

The compound was synthesized using 2',3',5'-tri-*O*-acetyl-2,6-dichloro-9-(*β*-D-ribofuranosyl)purine (500 mg) and 392 mg of (*S*)-α-methylbenzylamine, and was isolated as a yellow powder.

Yield: 599 mg (95%).

Melting Point (^{o}C): 202-203

^{1}H NMR (500 MHz, DMSO-d_6): δ 8.39 (s, 1H, C8-H), 7.42 (d, *J* = 7.5 Hz, 2H, Ar), 7.34 – 7.26 (m, 2H, Ar), 7.22 – 7.13 (m, 1H, Ar), 5.81 (d, *J* = 5.8 Hz, 1H, C1′-H), 5.40 (d, *J* = 14.3 Hz, 1H, C2′-H), 5.15 – 5.10 (m, 1H, C3′-H), 5.01 (t, *J* = 5.7 Hz, 1H, C4′-H), 4.48 (q, *J* = 4.8 Hz, 1H, C5′-H), 4.11 (q, *J* = 3.7 Hz, 1H, C5′-H), 4.00 (q, *J* = 6.6 Hz, 1H, C<u>H</u>-CH_3), 3.93 (q, *J* = 3.7 Hz, 1H, C5′-OH), 3.63 – 3.61 (m, 1H, C3′-OH), 3.52 – 3.45 (m, 1H, C2′-OH), 1.52 (s, 3H, α-C<u>H</u>$_3$).

^{13}C NMR (126 MHz, DMSO-d_6): δ 154.31 (1C, C6), 153.15 (1C, C2), 149.87 (1C, C4), 144.47 (1C, Ar), 139.99 (1C, C8), 128.29 (2C, Ar), 126.57 (3C, Ar), 118.59 (1C, C5), 87.54 (1C, C1′), 85.82 (1C, C4′), 73.88 (1C, C2′), 70.46 (1C, C3′), 61.45 (1C, C5′), 50.70 (1C, <u>C</u>H-CH_3), 25.78 (1C, α-<u>C</u>H_3).

LC-MS (*m*/*z*): negative mode 404 $[M-H]^-$, positive mode 406 $[M+H]^+$.

Purity by HPLC-UV (254 nm)-ESI-MS: 97.0%.

Optical rotation: -57.2^o

20.10. N^6-((R)-1-Phenylethylamine)-2-chloropurine riboside (135)

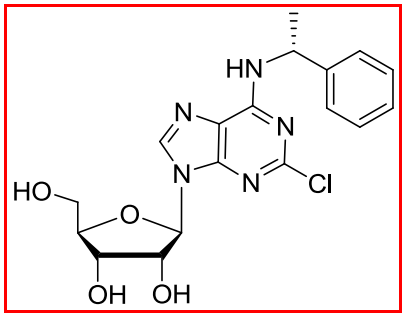

The compound was synthesized using 2',3',5'-tri-*O*-acetyl-2,6-dichloro-9-(*β*-D-ribofuranosyl)purine (500 mg) and 392 mg of (*R*)-α-methylbenzylamine, and was isolated as a yellow powder.

Yield: 580 mg (92%).

Melting Point (^{o}C): 198-199

^{1}H NMR (500 MHz, DMSO-*d_6*): δ 8.39 (s, 1H, C8-H), 7.43 (d, *J* = 7.6 Hz, 2H, Ar), 7.29 (td, *J* = 7.8, 6.1 Hz, 2H, Ar), 7.22 – 7.12 (m, 1H, Ar), 5.80 (d, *J* = 5.9 Hz, 1H, C1′-H), 5.42 – 5.25 (m, 1H, C2′-H), 5.15 – 5.08 (m, 1H, C3′-H), 5.01 (d, *J* = 6.5 Hz, 1H, C4′-H), 4.50 – 4.37 (m, 1H, C5′-H), 4.11 (q, 1H, C5′-H), 4.00 (q, *J* = 6.6 Hz, 1H, C<u>H</u>-CH_3), 3.93 (q, *J* = 3.8 Hz, 1H, C5′-OH), 3.64 – 3.61 (m, 1H, C3′-OH), 3.54 – 3.48 (m, 1H, C2′-OH), 1.53 (d, *J* = 7.0 Hz, 3H, α-C<u>H</u>$_3$).

^{13}C NMR (126 MHz, DMSO-*d_6*): δ 154.33 (1C, C6), 153.14 (1C, C2), 144.43 (1C, C4), 140.06 (1C, Ar), 133.28 (1C, C8), 128.29 (2C, Ar), 127.81 – 124.62 (3C, Ar), 118.64 (1C, C5), 87.60 (1C, C1′), 85.85 (1C, C4′), 73.76 (1C, C2′), 70.50 (1C, C3′), 61.49 (1C, C5′), 50.70 (1C, <u>C</u>H-CH_3), 25.80 (1C, α-<u>C</u>H$_3$).

LC-MS (*m*/*z*): negative mode 404 $[M-H]^-$, positive mode 406 $[M+H]^+$.

Purity by HPLC-UV (254 nm)-ESI-MS: 100%.

Optical rotation: -46.5°

20.11. 2-Iodo-N^6-methyl-N^6-benzyl-purine riboside (136)

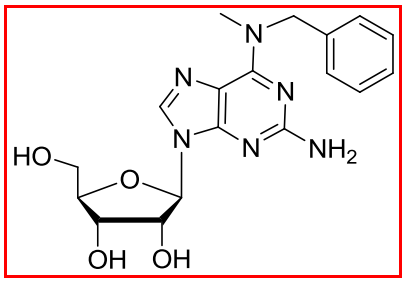

The compound was synthesized using 2',3',5'-tri-*O*-acetyl-2-amino-6-chloro-9-(*β*-D-ribofuranosyl)purine (500 mg) and 395 mg of *N*-benzylmethylamine, and was isolated as a white powder.

Yield: 626 mg (98%).

Melting Point (°C): 207-208

^{1}H NMR (500 MHz, DMSO-d_6): δ 8.23 (s, 1H, C8-H), 7.32 – 7.28 (m, 2H, Ar-H), 7.23 – 7.12 (m, 3H, Ar-H), 5.82 (d, 1H, C1′-H), 5.76 (d, J = 6.2 Hz, 1H, C2′-H), 5.33 (d, J = 6.1 Hz, C3′-H), 5.32 – 5.22 (m, 1H, CH_2-Ar), 5.07 (d, J = 4.6 Hz, 1H, C4′-H), 4.55 – 4.44 (m, 1H, C5′-H), 4.09 (td, J = 4.8, 3.2 Hz, 1H, C5′-H), 3.89 (q, J = 3.6 Hz, 1H, C5′-OH), 3.62 (dt, J = 12.0, 4.1 Hz, 1H, C3′-OH), 3.52 (q, J = 12.0, 6.4, 3.7 Hz, 1H, C2′-OH), 3.28 – 3.13 (m, 3H, CH_3).

^{13}C NMR (126 MHz, DMSO): δ 159.55 (1C, C5), 154.75 (1C, C2), 152.95 (1C, C6), 151.28 (1C, C4) 140.32 (1C, C8), 138.61 (1C, Ar), 128.60 (1C, Ar), 127.52 (2C, Ar), 127.09 (1C, Ar), 86.95 (1C, C1′), 85.55 (1C, C4′), 73.41 (1C, C2′), 70.76 (1C, C3′), 61.81 (1C, C5′), 51.78 (1C, CH_2-Ar), 27.01 (1C, CH_3).

LC-MS (*m*/*z*): negative mode 385 $[M-H]^-$, positive mode 387 $[M+H]^+$.

Purity by HPLC-UV (254 nm)-ESI-MS: 100%.

20.12. 2-Chloro-N^6-methyl-N^6-benzylpurine riboside (137)

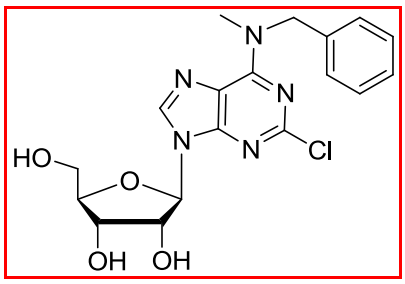

The compound was synthesized using 2',3',5'-tri-*O*-acetyl-2,6-dichloro-9-(*β*-D-ribofuranosyl)purine (500 mg) and 400 mg of *N*-benzylmethylamine, and was isolated as a white powder.

Yield: 599 mg (95%).

Melting Point (^{o}C): 180-182

^{1}H NMR (500 MHz, DMSO-d_6): δ 8.42 (s, 1H, C8-H), 7.43 – 7.30 (m, 2H, Ar-H), 7.31 – 7.22 (m, 3H, Ar-H), 5.86 (d, *J* = 5.8 Hz, 1H, C1′-H), 5.45 (d, *J* = 6.1 Hz, 1H, C2′-H), 5.17 (d, *J* = 5.0 Hz, C3′-H), 5.17 (d, *J* = 5.0 Hz, 1H, CH_2-Ar), 5.01 (t, *J* = 5.6 Hz, 1H, C4′-H), 4.51 (q, *J* = 5.7 Hz, 1H, C5′-H), 4.13 (td, *J* = 5.0, 3.5 Hz, 1H, C5′-H), 3.94 (q, *J* = 3.8 Hz, 1H, C5′-OH), 3.71 – 3.62 (m, 1H, C3′-OH), 3.54 (q, *J* = 12.0, 6.1, 4.0 Hz, 1H, C2′-OH), 3.07 – 3.01 (m, 3H, CH_3).

^{13}C NMR (126 MHz, DMSO): δ 154.63 (1C, C5), 152.74 (1C, C2), 151.51 (1C, C6), 151.28 (1C, C4) 140.30 (1C, C8), 137.59 (1C, Ar), 128.75 (1C, Ar), 127.43 (2C, Ar), 118.59 (1C, Ar), 87.45 (1C, C1′), 85.55 (1C, C4′), 73.83 (1C, C2′), 70.43 (1C, C3′), 61.41 (1C, C5′), 53.53 (1C, CH_2-Ar), 37.58 (1C, CH_3).

LC-MS (*m*/*z*): negative mode 404 $[M-H]^-$, positive mode 406 $[M+H]^+$.

Purity by HPLC-UV (254 nm)-ESI-MS: 100%.

20.13. 2-Iodo-N^6-Benzyl-N^6-methyl-purine riboside (138)

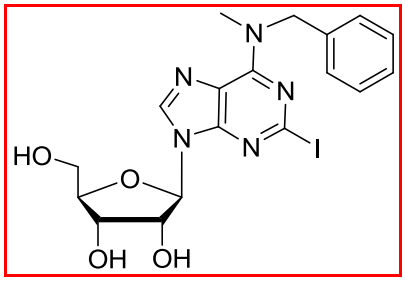

The compound was synthesized using 2',3',5'-tri-*O*-acetyl-6-chloro-2-iodo-9-(*β*-D-ribofuranosyl)purine (500 mg) and 392 mg of *N*-benzylmethylamine, and was isolated as a white powder.

Yield: 542 mg (90%).

Melting Point (^{o}C): 207-208

^{1}H NMR (500 MHz, DMSO-d_6): δ 8.27 (s, 1H, C8-H), 7.33 (t, *J* = 7.5 Hz, 2H, Ar-H), 7.27 (d, *J* = 7.2 Hz, 3H, Ar-H), 5.87 (d, *J* = 5.1 Hz, 1H, C1′-H), 5.56 (d, *J* = 5.7 Hz, 1H, C2′-H), 5.37 (d, *J* = 5.5 Hz, 1H, C3′-H), 4.56 (q, *J* = 5.3 Hz, 1H, C4′-H), 4.32 – 4.25 (m, 1H, C5′-H), 4.20 – 4.14 (m, 2H, C$\underline{H}_2$-Ar), 4.07 (dt, *J* = 6.1, 4.2 Hz, 1H, C5′-H), 3.04 (q, 1H, C5′-OH), 2.01 (s, 3H, C$\underline{H}_3$).

^{13}C NMR (126 MHz, DMSO): δ 170.25 (1C, C5), 153.66 (1C, C6), 148.19 (1C, C2), 139.86 (1C, C4), 138.53 (1C, C8), 128.72 (1C, Ar-H), 127.43 (3C, Ar-H), 119.40 (2C, Ar-H), 87.47 (1C, C1′), 81.96 (1C, C4′), 73.14 (1C, C2′), 70.44 (1C, C3′), 63.96 (1C, C5′), 46.86 (1C, $\underline{C}H_2$-Ar), 20.74 (1C, $\underline{C}H_3$).

LC-MS (*m*/*z*): negative mode 496 $[M-H]^-$, positive mode 498 $[M+H]^+$.

Purity by HPLC-UV (254 nm)-ESI-MS: 100%.

21.1. General procedure for the synthesis of nucleotides (139-150)

A solution of methylenebis(phosphonic dichloride) (5 mmol) in trimethyl phosphate (2 mL), cooled to 0 °C was added to a suspension of corresponding nucleosides **127-138** (1 mmol) in 2 mL of trimethyl phosphate at 0 °C. The reaction mixture was stirred at 0 °C and samples were withdrawn at 10 min interval for TLC to check the disappearance of nucleosides. After 30 min., on disappearance of nucleoside, 7 mL of cold 0.5 M aqueous TEAC solution (pH 7.4-7.6) was added. It was stirred at 0 °C for 15 min followed by stirring at room temperature for 1 h. Trimethyl phosphate was extracted using (2 x 100 mL) of *tert*.butylmethyl ether and the aqueous layer was lyophilized. The crude product was then purified by RP-HPLC using a gradient of 50 Mm ammoniumbicarbonate/ACN from 100:0 to 60:50 to get final product. Since there was no formation of dinucleotide, ion exchange chromatography was not used.

21.2. 2-Amino-N^6-dimethylpurine riboside-5'-O-[(phosphonomethyl)phosphonic acid] (139)

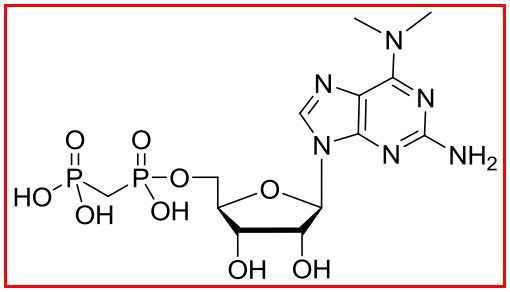

^{1}H NMR (500 MHz, D_2O): δ 8.49 (s, 1H, C8-H), 5.92 (m, 1H, C1′-H), 4.70 (m, 1H, C2′-H), 4.51 (m, 1H, C3′-H), 4.37 – 4.30 (m, 1H, C4′-H), 4.22 – 4.17 (m, 2H, C5′-H_2), 3.89 – 2.98 (m, 6H, 2xCH_3), 2.28 – 2.23 (m, 2H, P-CH_2-P).

^{13}C NMR (126 MHz, D_2O): δ 157.75 (1C, C5), 155.25 (1C, C2), 153.08 (1C, C6), 149.21 (1C, C4), 140.79 (1C, C8), 90.72 (1C, C1′), 87.11 (1C, C4′), 76.49 (1C, C2′), 72.96 (1C, C3′), 66.76 (1C, C5′), 49.53 (1C, P-CH_2-P), 11.07 (1C, 2xCH_3).

^{31}P NMR (202 MHz, D_2O): δ 20.52 (P_α), 18.02 (P_β).

LC-MS (*m*/*z*): negative mode 467 $[M-H]^-$, positive mode 469 $[M+H]^+$.

Purity by HPLC-UV (254 nm)-ESI-MS: 99.0%.

21.3. 2-Amino-N^6-diethylpurine riboside-5'-O-[(phosphonomethyl)phosphonic acid] (140)

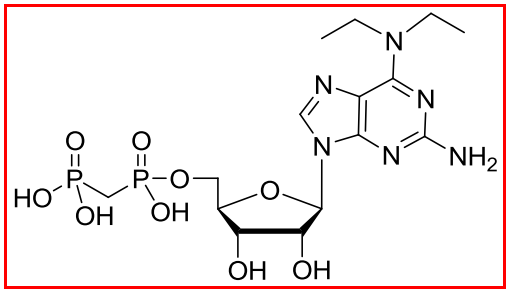

^{1}H NMR (500 MHz, D_2O): δ 8.41 (d, *J* = 1.3 Hz, 1H, C8-H), 5.94 (dd, *J* = 5.9, 1.4 Hz, 1H, C1′-H), 4.72 (d, *J* = 1.3 Hz, 1H, C2′-H), 4.58 – 4.45 (m, 1H, C3′-H), 4.32 (dd, *J* = 3.6, 1.9 Hz, 1H, C4′-H), 4.22 – 4.05 (m, 2H, C5′-$\underline{H_2}$), 3.90 – 3.68 (m, 4H, 2x-C$\underline{H_2}$-CH_3), 2.18 (td, *J* = 19.8, 1.5 Hz, 2H, P-C$\underline{H_2}$-P), 1.19 (td, *J* = 7.1, 1.4 Hz, 6H, 2x-CH_2-C$\underline{H_3}$).

^{13}C NMR (126 MHz, D_2O): δ 162.12 (1C, C5), 156.44 (1C, C2), 154.35 (1C, C6), 138.47 (1C, C4), 115.99 (1C, C8), 89.08 (1C, C1′), 86.51 (1C, C4′), 76.39 (1C, C2′), 73.15 (1C, C3′), 66.46 (1C, C5′), 64.13 (2C, 2x-$\underline{C}H_2$-CH_3), 45.99 (1C, P-$\underline{C}H_2$-P), 15.54 (2C, 2x-CH_2-$\underline{C}H_3$).

^{31}P NMR (202 MHz, D_2O): δ 21.04 – 17.40 (d, P_α), 15.07 (d, *J* = 9.8 Hz, P_β).

LC-MS (*m*/*z*): negative mode 495 $[M-H]^-$, positive mode 497 $[M+H]^+$.

Purity by HPLC-UV (254 nm)-ESI-MS: 99.0%.

21.4. 2-Amino-N^6-benzylpurine riboside-5′-O-[(phosphonomethyl)phosphonic acid] (141)

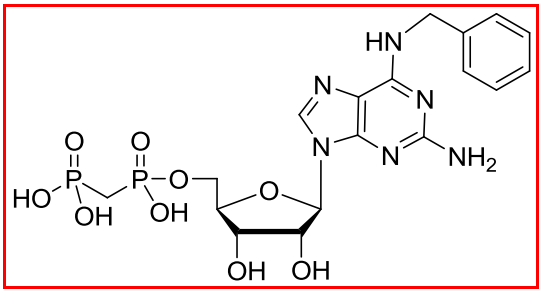

^{1}H NMR (500 MHz, D_2O): δ 8.43 (s, 1H, C8-H), 7.37 (d, *J* = 27.7 Hz, 5H, Ar-H), 5.90 (d, *J* = 6.2 Hz, 1H, C1′-H), 5.03 – 4.95 (m, 2H, CH_2-Ar), 4.74 (d, *J* = 1.3 Hz, 1H, C2′-H), 4.62 (t, *J* = 5.7 Hz, 1H, C3′-H), 4.50 (q, *J* = 4.5 Hz, 1H, C4′-H), 4.33 (d, *J* = 21.8 Hz, 2H, C5′-H_2), 2.23 (t, *J* = 19.8 Hz, 2H, P-CH_2-P).

^{13}C NMR (126 MHz, D_2O): δ 157.35 (1C, C2), 155.69 (1C, C6), 151.11 (1C, C4), 139.71 (1C, C8), 131.68 (1C, Ar), 130.15 (2C, Ar), 129.76 (3C, Ar), 121.82 (1C, C5), 89.69 (1C, C1′), 86.78 (1C, C4′), 76.56 (1C, C2′), 72.91 (1C, C3′), 66.76 (1C, C5′), 49.52 (1C, P-CH_2-P), 44.61 (1C, CH_2-Ar).

^{31}P NMR (202 MHz, D_2O): δ 19.12 (**P_α**), 15.08 (d, *J* = 10.9 Hz, **P_β**).

LC-MS (*m*/*z*): negative mode 529 $[M-H]^-$, positive mode 531 $[M+H]^+$.

Purity by HPLC-UV (254 nm)-ESI-MS: 99.0%.

21.5. N^6-Benzyl-2-chloropurine riboside-5′-O-[(phosphonomethyl)phosphonic acid] (142)

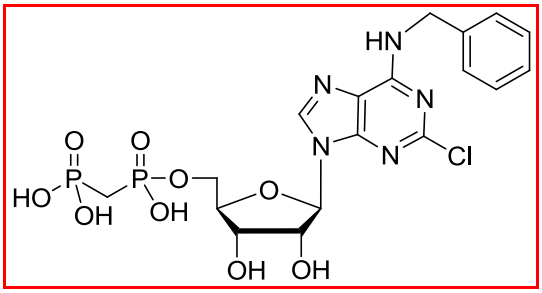

^{1}H NMR (600 MHz, D_2O): δ 8.53 (s, 1H, C8-H), 7.46 – 7.38 (m, 5H, Ar-H), 6.06 (dd, *J* = 12.1, 6.4 Hz, 1H, C1′-H), 5.20 – 4.92 (m, 1H, C2′-H), 4.76 – 4.70 (m, 2H, CH_2-Ar), 4.54 (t, *J* = 4.5 Hz, 1H, C3′-H), 4.36 (dd, *J* = 23.3, 3.6 Hz, 1H, C4′-H), 4.17 (dt, *J* = 6.1, 2.8 Hz, 2H, C5′-H_2), 2.26 – 2.14 (m, 2H, P-CH_2-P).

^{13}C NMR (126 MHz, D_2O): δ 163.10 (1C, C6), 155.09 (1C, C2), 154.33 (1C, C4), 142.42 (1C, C8), 139.57 (1C, Ar), 131.65 (2C, Ar), 130.73 (3C, Ar), 123.58 (1C, C5), 88.72 (1C, C1′), 85.83 (1C, C4′), 80.29 (1C, C2′), 75.80 (1C, C3′), 73.13 (1C, C5′), 66.36 (1C, CH_2-Ar), 49.51 (1C, P-CH_2-P).

^{31}P NMR (243 MHz, D_2O): δ 18.69 (d, *J* = 10.0 Hz, $\mathbf{P_\alpha}$), 15.32 (d, *J* = 9.9 Hz, $\mathbf{P_\beta}$).

LC-MS (*m*/*z*): negative mode 548 $[M-H]^-$, positive mode 5550 $[M+H]^+$.

Purity by HPLC-UV (254 nm)-ESI-MS: 99.0%.

21.6. N^6-Benzyl-2-iodopurine riboside-5′-O-[(phosphonomethyl)phosphonic acid] (143)

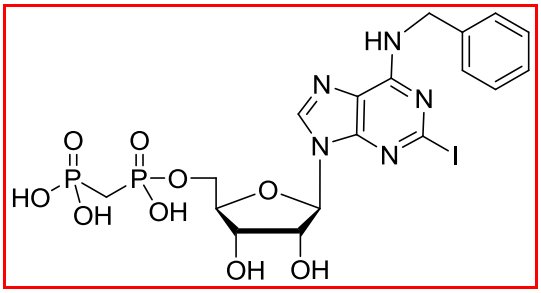

^{1}H NMR (500 MHz, D_2O): δ 8.48 (s, 1H, C8-H), 7.39 – 7.32 (m, 4H, Ar-H), 7.30 – 7.25 (m, 1H, Ar-H), 6.10 (dd, *J* = 6.5, 2.3 Hz, 1H. C1′-H), 4.82 (s, 2H, CH_2-Ar), 4.70 – 4.68 (m, 1H, C2′-H), 4.53 (dd, *J* = 5.1, 3.8 Hz, 1H, C3′-H), 4.37 (td, *J* = 4.1, 2.7 Hz, 1H, C4′-H), 4.16 (dt, *J* = 6.5, 3.3 Hz, 2H, C5′-H_2), 2.19 (q, *J* = 21.8, 18.2, 3.0 Hz, 2H, P-CH_2-P).

^{13}C NMR (126 MHz, D_2O): δ 162.83 (1C, C6), 157.35 (1C, C2), 155.69 (1C, C4), 142.28 (1C, C8), 141.18 (1C, Ar), 131.55 (2C, Ar), 129.96 (3C, Ar), 121.82 (1C, C5), 89.60 (1C, C1′), 86.78

(1C, C4′), 77.02(1C, C2′), 73.13 (1C, C3′), 66.41 (1C, C5′), 46.82 (1C, $\underline{C}H_2$-Ar), 42.94 (1C, P-$\underline{C}H_2$-P).

^{31}P NMR (202 MHz, D_2O): δ 18.67 ($\mathbf{P_\alpha}$), 15.03 (d, J = 9.8 Hz, $\mathbf{P_\beta}$).

LC-MS (*m*/*z*): negative mode 640 $[M-H]^-$, positive mode 642 $[M+H]^+$.

Purity by HPLC-UV (254 nm)-ESI-MS: 99.0%

21.7. N^6-(2-Chlorobenzyl)-2-chloropurine riboside-5'-O-[(phosphonomethyl)phosphonic acid] (144).

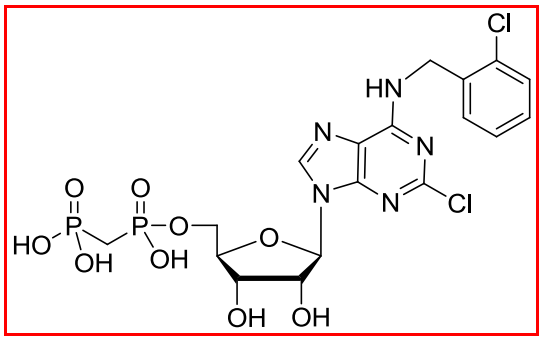

^{1}H NMR (500 MHz, D_2O): δ 8.46 (s, 1H, C8-H), 7.43 (q, J = 13.3, 7.4, 2.2 Hz, 2H, Ar-H), 7.28 (q, J = 7.0, 4.8, 1.9 Hz, 2H, Ar-H), 6.03 (d, J = 5.6 Hz, 1H, C1′-H), 4.82 (s, 2H, C$\underline{H_2}$-Ar), 4.74 (q, J = 1.1 Hz, 1H, C2′-H), 4.59 – 4.49 (m, 1H, C3′-H), 4.43 – 4.30 (m, 1H, C4′-H), 4.17 (dd, J = 5.5, 3.2 Hz, 2H, C5′-$\underline{H_2}$), 2.21 (td, J = 19.9, 1.6 Hz, 2H, P-C$\underline{H_2}$-P).

^{13}C NMR (126 MHz, D_2O): δ 158.04 (1C, C6), 157.99 (1C, C2), 152.20 (1C, C4), 142.49 (1C, Ar-H), 137.60 (1C, C8), 135.68 (1C, Ar-H), 131.87 (2C, Ar-H), 129.97 (2C, Ar-H), 121.06 (1C, C5), 89.77 (1C, C1′), 86.87 (1C, C4′), 77.18 (1C, C2′), 73.10 (1C, C3′), 66.41 (1C, C5′), 49.51 (1C, $\underline{C}H_2$-Ar), 45.03 (1C, P-$\underline{C}H_2$-P).

^{31}P NMR (202 MHz, D_2O): δ 18.60 (d, J = 10.1 Hz, $\mathbf{P_\alpha}$), 15.60 (d, J = 9.7 Hz, $\mathbf{P_\beta}$).

LC-MS (*m*/*z*): negative mode 583 $[M-H]^-$, positive mode 585 $[M+H]^+$.

Purity by HPLC-UV (254 nm)-ESI-MS: 99.0%.

21.8. 2-Chloro-N^6-(1-phenylethyl)- purine riboside-5′-O-[(phosphonomethyl)phosphonic acid] (145)

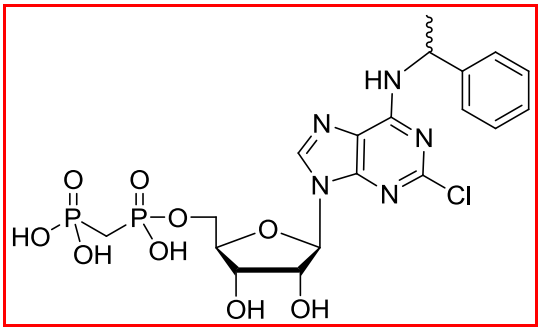

^{1}H NMR (600 MHz, D_2O): δ 8.56 (s, 1H, C8-H), 7.30 (t, *J* = 7.3 Hz, 2H, Ar-H), 7.24 – 7.17 (m, 2H, Ar-H), 7.13 (q, *J* = 7.6, 6.5 Hz, 1H, Ar-H), 5.83 (t, *J* = 4.8 Hz, 1H, C1′-H), 5.16 (s, 1H, C<u>H</u>-Ar), 4.38 (t, *J* = 4.3 Hz, 1H, C2′-H), 4.33 (t, *J* = 4.5 Hz, 1H, C3′-H), 4.18 – 4.08 (m, 1H, C4′-H), 4.04 – 3.94 (m, 2H, C5′-H), 2.18 (dt, *J* = 50.5, 19.9 Hz, 2H, P-C<u>H</u>$_2$-P), 1.44 (dd, *J* = 7.1, 3.4 Hz, 3H, α-C<u>H</u>$_3$).

^{13}C NMR (151 MHz, D_2O): δ 154.48 (1C, C6), 150.91 (1C, C2), 149.37 (1C, C4), 143.64 (1C, Ar-H), 139.47 (1C, C8), 128.79 (1C, Ar-H), 127.39 (1C, Ar-H), 125.90 (1C, Ar-H), 117.71 (1C, C5), 86.76 (1C, C1′), 83.97 (1C, C4′), 74.21 (1C, C2′), 70.23 (1C, C3′), 63.48 (1C, C5′), 60.32 (1C, <u>C</u>H-Ar), 50.02 (1C, P-<u>C</u>H$_2$-P), 21.78 (1C, α-<u>C</u>H$_3$).

^{31}P NMR (243 MHz, D_2O): δ 18.75 (d, *J* = 9.8 Hz, **P_α**), 15.10 (d, *J* = 9.6 Hz, **P_β**).

LC-MS (*m*/*z*): negative mode 562 $[M-H]^-$, positive mode 564 $[M+H]^+$.

Purity by HPLC-UV (254 nm)-ESI-MS: 100%.

21.9. 2-Chloro-N^6-((S)- 1-phenylethyl)-purine riboside-5'-O-[(phosphonomethyl)phosphonic acid] (146)

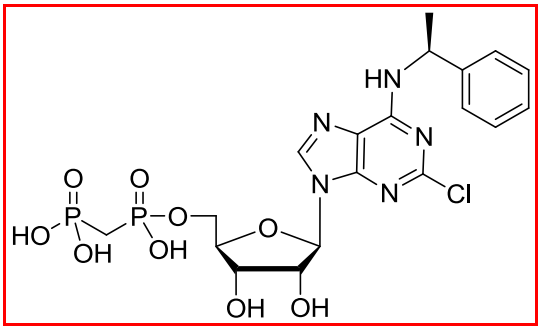

^{1}H NMR (600 MHz, D_2O): δ 8.50 (s, 1H, C8-H), 7.45 (d, *J* = 7.7 Hz, 2H, Ar-H), 7.37 (t, *J* = 7.6 Hz, 2H, Ar-H), 7.29 (t, *J* = 7.4 Hz, 1H, Ar-H), 6.00 (d, *J* = 5.2 Hz, 1H, C1′-H), 5.31 (s, 1H, C<u>H</u>-Ar), 4.70 (t, *J* = 5.2 Hz, 1H, C2′-H), 4.51 (t, *J* = 4.6 Hz, 1H, C3′-H), 4.37 (dt, *J* = 5.2, 2.8 Hz, 1H, C4′-H), 4.18 (d, *J* = 3.0 Hz, 2H, C5′-<u>H</u>$_2$), 2.38 – 2.12 (m, 2H, P-C<u>H</u>$_2$-P), 1.61 (d, *J* = 6.9 Hz, 3H, α-C<u>H</u>$_3$).

^{13}C NMR (151 MHz, D_2O): δ 157.22 (1C, C6), 151.98 (1C, C2), 146.21 (1C, C4), 142.11 (1C, Ar), 131.62 (1C, C8), 130.26 (2C, Ar), 128.78 (3C, Ar), 120.14 (1C, C6), 90.01 (1C, C1′), 86.68 (1C, C4′), 77.11 (1C, C2′), 72.93 (1C, C3′), 72.42 (1C, C5′), 66.43 (1C, <u>C</u>H-Ar), 53.19 (1C, P-<u>C</u>H$_2$-P), 24.52 (1C, α-<u>C</u>H$_3$).

^{31}P NMR (243 MHz, D_2O): δ 17.72 (d, *J* = 10.3 Hz, **P_α**), 17.51 (d, *J* = 10.0 Hz, **P_β**).

LC-MS (*m*/*z*): negative mode 562 $[M-H]^-$, positive mode 564 $[M+H]^+$.

Purity by HPLC-UV (254 nm)-ESI-MS: 100%.

21.10. 2-Chloro-N^6-((R) -1-phenylethyl)- purine riboside-5'-O-[(phosphonomethyl)phosphonic acid] (147)

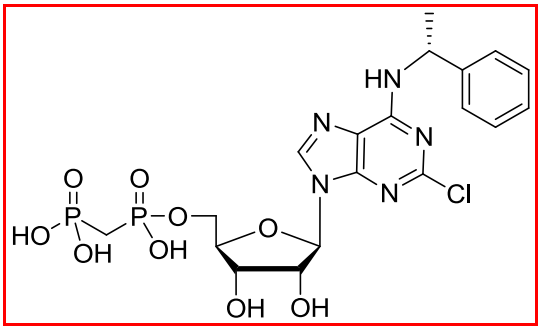

^{1}H NMR (600 MHz, D_2O + NaOD): δ 8.12 (s, 1H, C8-H), 7.20 (d, *J* = 7.7 Hz, 2H, Ar-H), 7.13 (t, *J* = 7.5 Hz, 2H, Ar-H), 7.06 (d, *J* = 7.3 Hz, 1H, Ar-H), 5.55 (d, *J* = 5.3 Hz, 1H, C1′-H), 4.29 (s, 1H, C<u>H</u>-Ar), 4.02 – 3.96 (m, 1H, C2′-H), 3.93 (d, *J* = 5.0 Hz, 1H, C3′-H), 3.86 (dd, *J* = 12.0, 5.5 Hz, 1H, C4′-H), 3.81 – 3.67 (m, 2H, C5′-<u>H_2</u>), 1.75 (t, *J* = 19.3 Hz, 2H, P-C<u>H_2</u>-P), 1.36 (d, *J* = 7.0 Hz, 3H, α-C<u>H_3</u>).

^{13}C NMR (151 MHz, D_2O): δ 157.22 (1C, C6), 151.98 (1C, C2), 146.21 (1C, C4), 142.11 (1C, Ar), 131.62 (1C, C8), 130.26 (1C, Ar), 128.78 (1C, Ar), 120.14 (1C, C5), 90.01 (1C, C1′), 86.68 (1C, C4′), 77.11 (1C, C2′), 72.93 (1C, C3′), 72.42 (1C, C5′), 66.43 (1C, <u>C</u>H-Ar), 53.19 (1C, P-<u>C</u>H_2-P), 24.52 (1C, α-<u>C</u>H_3).

^{31}P NMR (243 MHz, D_2O): δ 23.22 (d, *J* = 8.5 Hz, **P_α**), 12.83 (d, *J* = 8.5 Hz, **P_β**).

LC-MS (*m*/*z*): negative mode 562 $[M-H]^-$, positive mode 564 $[M+H]^+$.

Purity by HPLC-UV (254 nm)-ESI-MS: 100%.

21.11. 2-Amino-N^6-benzyl-N^6-methylpurine riboside-5'-O-[(phosphonomethyl)phosphonic acid] (148)

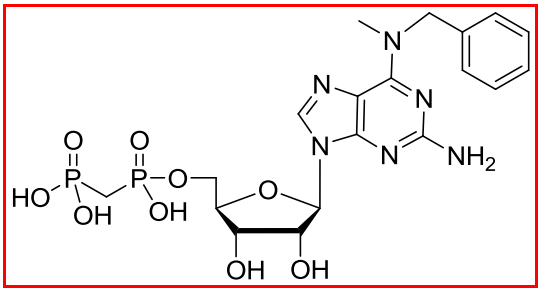

^{1}H NMR (600 MHz, D_2O): δ 8.14 (s, 1H, C8-H), 7.40 – 7.33 (m, 2H, Ar-H), 7.32 – 7.23 (m, 3H, Ar-H), 5.97 (d, *J* = 5.9 Hz, 1H, C1′-H), 5.16 (s, 2H, CH_2-Ar), 4.72 (t, *J* = 5.6 Hz, 1H, C2′-H), 4.51 (dd, *J* = 5.2, 3.6 Hz, 1H, C3′-H), 4.34 (q, *J* = 3.6 Hz, 1H, C4′-H), 4.15 (t, *J* = 4.2 Hz, 2H, C5′-H_2), 3.27 (s, 3H, CH_3), 2.18 (t, *J* = 19.8 Hz, 2H, P-CH_2-P).

^{13}C NMR (151 MHz, D_2O): δ 161.65 (1C, C5), 157.66 (1C, C2), 154.12 (1C, C6), 140.13 (1C, C4), 138.81 (1C, C8), 131.66 (1C, Ar), 130.20 (2C, Ar), 116.47 (3C, Ar), 89.30 (1C, C1′), 86.65 (1C, C4′), 76.53 (1C, C2′), 73.15 (1C, C3′), 66.53 (1C, C5′), 58.14 (1C, CH_2-Ar), 49.49 (1C, P-CH_2-P), 39.28 (1C, CH_3).

^{31}P NMR δ (243 MHz, D_2O): 18.77 (d, *J* = 10.0 Hz, $\mathbf{P_\alpha}$), 15.13 (d, *J* = 9.9 Hz, $\mathbf{P_\beta}$).

LC-MS (*m*/*z*): negative mode 543 $[M-H]^-$, positive mode 545 $[M+H]^+$.

Purity by HPLC-UV (254 nm)-ESI-MS: 100%.

21.12. N^6-Benzyl-N^6-methyl-2-chloropurine riboside-5'-O-[(phosphonomethyl)phosphonic acid] (149)

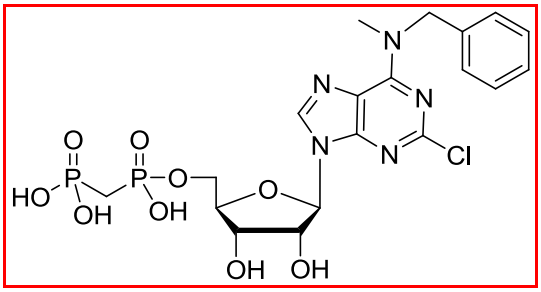

^{1}H NMR (600 MHz, D_2O): δ 8.40 (s, 1H, C8-H), 7.37 – 7.32 (m, 2H, Ar-H), 7.30 – 7.20 (m, 3H, Ar-H), 6.04 (t, *J* = 5.5 Hz, 1H, C1′-H), 5.19 (s, 2H, CH_2-Ar), 4.72 (t, *J* = 5.3 Hz, 1H, C2′-H), 4.52 (dd, *J* = 5.1, 4.1 Hz, 1H, C3′-H), 4.40 – 4.31 (m, 1H, C4′-H), 4.22 – 4.09 (m, 2H, C5′-H_2), 3.53 – 3.06 (m, 3H, CH_3), 2.25 (t, *J* = 19.7 Hz, 2H, P-CH_2-P).

^{13}C NMR (151 MHz, D_2O): δ 157.80 (1C, C5), 156.46 (1C, C2), 153.84 (1C, C6), 141.10 (1C, C4), 139.58 (1C, C8), 131.65 (1C, Ar), 130.12 (2C, Ar), 120.97 (3C, Ar), 89.56 (1C, C1′), 86.71

(1C, C4′), 77.10 (1C, C2′), 73.04 (1C, C3′), 66.56 (1C, C5′), 66.40 (1C, $\underline{C}H_2$-Ar), 56.56 (1C, P-$\underline{C}H_2$-P), 39.34 (1C, $\underline{C}H_3$).

^{31}P NMR (243 MHz, D_2O): δ 18.57 (d, *J* = 9.7 Hz, **P_α**), 15.03 (d, *J* = 9.8 Hz, **P_β**).

LC-MS (*m*/*z*): negative mode 562 $[M-H]^-$, positive mode 564 $[M+H]^+$.

Purity by HPLC-UV (254 nm)-ESI-MS: 100%.

21.14. N^6-Benzyl-N^6-methyl-2-iodopurine riboside-5′-O-[(phosphonomethyl)phosphonic acid] (150)

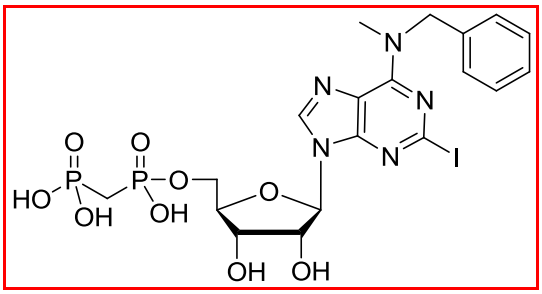

^{1}H NMR (600 MHz, D_2O): δ 8.33 (s, 1H, C8-H), 7.38 – 7.34 (m, 2H, Ar-H), 7.31 (d, *J* = 7.8 Hz, 3H, Ar-H), 6.06 (d, *J* = 5.3 Hz, 1H, C1′-H), 5.15 (s, 2H, $C\underline{H_2}$-Ar), 4.73 – 4.67 (m, 1H, C2′-H), 4.54 (t, *J* = 4.6 Hz, 1H, C3′-H), 4.38 (q, *J* = 3.6 Hz, 1H, C4′-H), 4.18 (dd, *J* = 5.4, 3.2 Hz, 2H, C5′-$\underline{H_2}$), 3.85 – 3.12 (m, 3H, $C\underline{H_3}$), 2.20 (td, *J* = 20.0, 2.1 Hz, 2H, P-$C\underline{H_2}$-P).

^{13}C NMR (151 MHz, D_2O): δ 154.15 (1C, C5), 150.45 (1C, C2), 137.89 (1C, C6), 137.85 (1C, C4), 137.01 (1C, C8), 128.86 (1C, Ar), 127.68 (1C, Ar), 127.51 (2C, Ar), 119.83 (1C, Ar), 119.18 (1C, Ar), 87.04 (1C, C1′), 83.84 (1C, C4′), 74.33 (1C, C2′), 70.21 (1C, C3′), 63.60 (1C, C5′), 53.78 (1C, $\underline{C}H_2$-Ar), 45.76 (1C, P-$\underline{C}H_2$-P), 38.70 (1C, $\underline{C}H_3$).

^{31}P NMR δ (243 MHz, D_2O): 18.58 (**P_α**), 15.49 (**P_β**).

LC-MS (*m*/*z*): negative mode 654 $[M-H]^-$, positive mode 656 $[M+H]^+$.

Purity by HPLC-UV (254 nm)-ESI-MS: 100%.

22.1. 2,6-Diaminoadenosine (156)

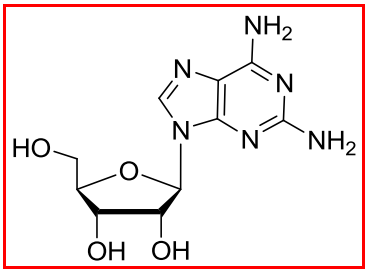

A suspension containing 0.5 g of 2-amino-6-chloro-ribofuranosylpurine (**96**) dissolved in 25 mL of ammoniacal ethanol solution was stirred at rt for three days. The solvent was removed under reduced pressure and the crude product was applied to a silica gel column with dichloromethane: methanol (9:1) elution. The collected fractions were freed from solvent, and a reversed-phase chromatography (HPLC) with an increasing gradient of methanol in water (10:90 to 90:10 over 70 min) was used. The solvent was removed by lyophilization to get the desired compound.

Yield: 531 mg (98%).

Melting Point (^{o}C): 235-237 [**literature**, 248][195]

^{1}H NMR (500 MHz, DMSO-*d*$_6$): δ 8.30 (s, 1H, C8-H), 6.75 (bs, 1H, N$\underline{H_2}$), 5.82 – 5.65 (m, 1H, H1′), 5.47 – 5.27 (m, 1H, C2′-H), 5.06 (d, *J* = 4.5 Hz, 1H, C3′-H), 4.51 (td, *J* = 6.2, 4.9 Hz, 1H, C4′-H), 4.09 (td, *J* = 4.7, 2.9 Hz, 2H, C5′-$\underline{H_2}$), 3.90 (q, *J* = 3.4 Hz, 1H, C5′-OH), 3.69 – 3.56 (m, 1H, C3′-OH), 3.53 (q, *J* = 12.1, 7.1, 3.6 Hz, 1H, C2′-OH).

^{13}C NMR (126 MHz, DMSO-*d*$_6$): δ 160.16 (1C, C6), 156.40 (1C, C2), 151.57 (1C, C4), 136.43 (1C, C8), 113.76 (1C, C5), 87.25 (1C, C1′), 85.68 (1C, C4′), 73.36 (1C, C2′), 70.87 (1C, C3′), 61.91 (1C, C5′).

LC-MS (*m*/*z*): negative mode 281 $[M-H]^-$, positive mode 283 $[M+H]^+$.

Purity by HPLC-UV (254 nm)-ESI-MS: 100%.

22.2. Isoguanosine (157)

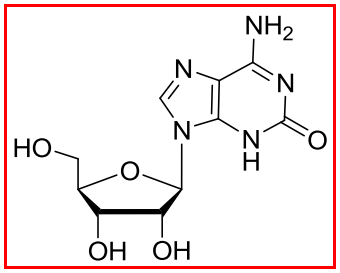

2,6-Diaminopurine riboside (**155**, 10.0 g, 35.5 mmol) was suspended in H_2O (25 mL) at 50 ^oC, then $NaNO_2$ (9.44 g, 137 mmol) in H_2O (6 mL) was added. Then AcOH (245 mmol, 14.1 mL) was added at 50 ^oC over 5 min. The resulting clear solution was stirred for 5 min and then diluted with H_2O (15 mL). The excess of acetic acid was neutralized by adding 2 mL of aq. NH_3 soln. The solution was evaporated and the remaining solid washed with H_2O to get light yellow powder.

Yield: 531 mg (98%).

Melting Point (^{o}C): 238-240 [**literature**, 237-241][162]

^{1}H NMR (500 MHz, DMSO-*d*$_6$): δ 8.25 (s, 1H, C8-H), 7.93 (bs, 1H, NH), 7.64 (bs, 2H, NH_2), 5.86 (d, *J* = 3.4 Hz, 1H, C1′-H), 5.44 (s, 1H, C2′-H), 5.19 (dd, *J* = 6.1, 3.5 Hz, 1H, C3′-H), 4.90 (dd, *J* = 6.2, 2.4 Hz, 1H, C4′-H), 4.16 (td, *J* = 4.3, 2.4 Hz, 2H, C5′-H_2), 3.64 – 3.61 (m, 1H, C5′-OH), 3.43 – 3.35 (m, 2H, C3′-OH and C2′-OH).

^{13}C NMR (126 MHz, DMSO-*d*$_6$): δ 155.10 (1C, C2), 151.32 (1C, C6), 138.01(1C, C4), 132.80 (1C, C8), 113.09 (1C, C5) , 89.35 (1C, C1′), 86.02 (1C, C4′) , 82.86 (1C, C2′), 81.38 (1C, C3′), 61.90 (1C, C5′).

LC-MS (*m*/*z*): negative mode 282 $[M-H]^-$, positive mode 284 $[M+H]^+$.

Purity by HPLC-UV (254 nm)-ESI-MS: 100%.

23.1. General procedure for the synthesis of nucleotides (151-154, 156 and 158)

A solution of methylenebis(phosphonic dichloride) (2 mmol) in trimethyl phosphate (2 mL), cooled to 0 ^{o}C was added to a suspension of corresponding nucleosides, inosine (**25**), 6-chloro-purine riboside (**28**), guanosine (**93**), 2-amino-6-chloropurine riboside (**96**), 2,6-diaminopurine riboside (**155**) and isoguanosine (**157**) (1 mmol) in trimethyl phosphate at 0 ^{o}C. The reaction mixture was stirred at 0 ^{o}C and samples were withdrawn at 10 min. interval for TLC to check the disappearance of nucleosides. After 1 h, on disappearance of nucleoside, 7 mL of cold 0.5 M aqueous TEAC solution (pH 7.4-7.6) was added. It was stirred at 0 ^{o}C for 15 min followed by stirring at room temperature for 1h. Trimethyl phosphate was extracted using (2 x 100 mL) of *tert*.butylmethyl ether and the aqueous layer was lyophilized. The mixture of nucleotide and dinucleotide was separated by ion-exchange chromatography on DEAE Sephadex (A-25, HCO^{-}_{3} form), using linear gradient of aqueous TEAC. Fractions containing the product were pooled and evaporated to dryness, with ethanol added repeatedly to remove TEAC buffer. The compound was then purified by RP-HPLC using a gradient of 50 mM ammoniumbicarbonate/ACN from 100:0 to 40:60 and suitable fraction were pooled and lyophilized to obtain final product as glassy solid.

23.2. Inosine-5'-O-[(phosphonomethyl)phosphonic acid] (151)

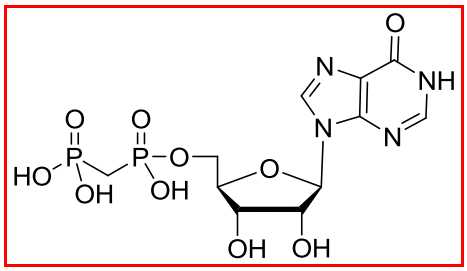

^{1}H NMR (500 MHz, D_2O): δ 8.65 (s, 1H, C8-H), 8.25 (s, 1H, C2-H), 6.17 (d, *J* = 5.0 Hz, 1H, H1′), 4.55 (t, *J* = 4.7 Hz, 1H, C2′-H), 4.40 (d, *J* = 3.7 Hz, 1H, C3′-H), 4.22 (d, *J* = 15.0 Hz, 2H, C5′-$\underline{H_2}$), 3.79 – 3.65 (m,1H, C4′-H), 2.29 (t, *J* = 19.5 Hz, 2H, P-C$\underline{H_2}$-P).

^{13}C NMR (126 MHz, D_2O): δ 160.90 (1C, C6), 151.45 (1C, C4), 149.44 (1C, C2), 142.57 (1C, C8), 124.60 (1C, C5), 90.80 (1C, C1′), 86.86 (1C, C4′), 77.23 (1C, C2′), 72.91 (1C, C3′), 66.41 (1C, C5′), 51.72 (1C, P-$\underline{C}$H$_2$-P).

^{31}P NMR (202 MHz, D_2O): δ 18.06 (**P_α**), 17.53 (**P_β**).

LC-MS (*m*/*z*): negative mode 425 $[M-H]^-$, positive mode 427 $[M+H]^+$.

Purity by HPLC-UV (254 nm)-ESI-MS: 100%.

<u>23.3. 6-Chloropurine riboside-5′-O-[(phosphonomethyl)phosphonic acid] (152)</u>

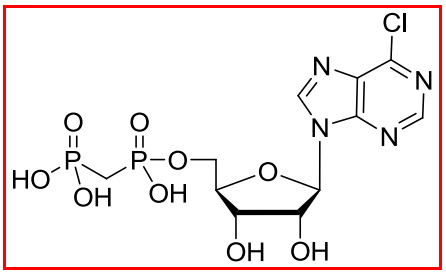

^{1}H NMR (500 MHz, D_2O): δ 8.93 (s, 1H, C8-H), 8.76 (s, 1H, C2-H), 6.26 (d, *J* = 5.0 Hz, 1H, C1′-H), 4.82 (t, *J* = 5.1 Hz, 1H, C2′-H), 4.58 (t, *J* = 4.8 Hz, 1H, C3′-H), 4.48 – 4.33 (m, 1H, C4′-H), 4.20 (d, *J* = 5.7 Hz, 2H, C5′-$\underline{H_2}$), 2.15 (t, *J* = 19.8 Hz, 2H, P-C$\underline{H_2}$-P).

^{13}C NMR (126 MHz, D_2O): δ 154.73 (1C, C6), 154.12 (1C, C4), 152.99 (1C, C2), 148.31 (1C, C8), 134.08 (1C, C5), 90.86 (1C, C1′), 86.90 (1C, C4′), 77.18 (1C, C2′), 72.90 (1C, C3′), 66.13 (1C, C5′), 49.47 (1C, P-$\underline{C}$H$_2$-P).

^{31}P NMR (202 MHz, D_2O): δ 19.76 (d, *J* = 22.6 Hz, **P_α**), 14.13 (td, *J* = 19.6, 9.6 Hz, **P_β**).

LC-MS (*m*/*z*): negative mode 443 $[M-H]^-$, positive mode 445 $[M+H]^+$.

Purity by HPLC-UV (254 nm)-ESI-MS: 100%.

23.4. Guanosine-5'-O-[(phosphonomethyl)phosphonic acid] (153)

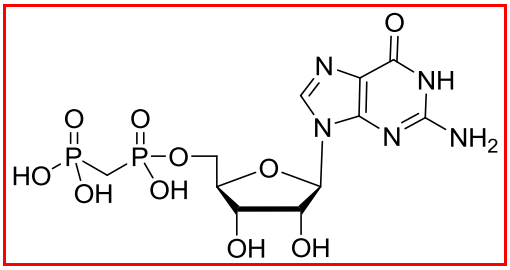

^{1}H NMR (600 MHz, D_2O): δ 8.28 (s, 1H, C8-H), 5.95 (d, *J* = 5.5 Hz, 1H, C1′-H), 4.53 (t, *J* = 4.5 Hz, 1H, C2′-H), 4.40 – 4.37 (m, 1H, C3′-H), 4.35 (t, *J* = 3.7 Hz, 1H, C4′-H), 4.25 – 4.08 (m, 2H, C5′-H_2), 2.20 (t, *J* = 19.6 Hz, 2H, P-CH_2-P).

^{13}C NMR (151 MHz, D_2O): δ 165.76 (1C, C6), 161.43 (1C, C4), 156.96 (1C, C2), 140.49 (1C, C8), 120.15 (1C, C5), 90.01 (1C, C1′), 86.76 (1C, C4′), 76.54 (1C, C2′), 73.06 (1C, C3′), 66.39 (1C, C5′), 49.52 (1C, P-CH_2-P).

^{31}P NMR (243 MHz, D_2O): δ 18.69 (**P_α**), 15.46 (**P_β**).

LC-MS (*m*/*z*): negative mode 440 $[M-H]^-$, positive mode 442 $[M+H]^+$.

Purity by HPLC-UV (254 nm)-ESI-MS: 100%.

23.5. 2-Amino-6-chloroadenosine-5'-O-[(phosphonomethyl)phosphonic acid] (154)

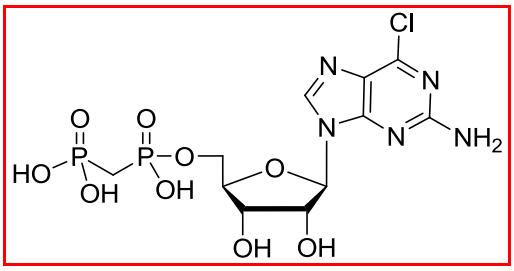

^{1}H NMR (500 MHz, D_2O): δ 8.28 (s, 1H, C8-H), 6.11 (dd, *J* = 5.7, 1.1 Hz, 1H, C1′-H), 5.22 (td, *J* = 5.8, 1.0 Hz, 1H, C2′-H), 4.67 – 4.57 (m, 1H, C3′-H), 4.30 (t, *J* = 4.8 Hz, 1H, C4′-H), 4.27 – 4.13 (m, 2H, C5′-H_2), 2.16 (t, *J* = 19.9 Hz, 2H, P-CH_2-P).

^{13}C NMR (126 MHz, D_2O): δ 155.11 (1C, C2), 153.87 – 151.33 (1C, C4), 142.82 (1C, C6), 132.05 (1C, C8), 120.37 (1C, C5), 91.59 (1C, C1′), 86.57 (1C, C4′), 74.05 (1C, C2′), 72.59 (1C, C3′), 66.39 (1C, C5′), 49.51 (1C, P-$\underline{C}H_2$-P).

^{31}P NMR (202 MHz, D_2O): δ 20.28 – 17.40 (d, $\mathbf{P_\alpha}$), 15.37 (d, J = 9.5 Hz, $\mathbf{P_\beta}$).

LC-MS (*m*/*z*): negative mode 458 $[M-H]^-$, positive mode 460 $[M+H]^+$.

Purity by HPLC-UV (254 nm)-ESI-MS: 100%.

23.6. 2,6-Diaminoadenosine-5′-O-[(phosphonomethyl)phosphonic acid] (156)

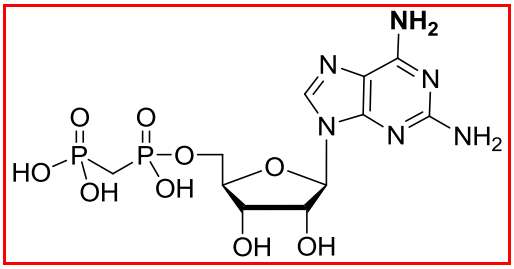

^{1}H NMR (500 MHz, D_2O): δ 8.22 (s, 1H, C8-H), 5.91 (s, 1H, C1′-H), 4.70 – 4.65 (m, 1H, C2′-H), 4.51 – 4.48 (m, 1H, C3′-H), 4.34 (s, 1H, C4′-H), 4.20 (s, 2H, C5′-$\underline{H_2}$), 2.21 – 2.15 (m, 2H, P-C$\underline{H_2}$-P).

^{13}C NMR (126 MHz, D_2O): δ 165.69 (1C, C6), 156.87 (1C, C2), 150.67 (1C, C4), 142.30 (1C, C8), 120.33 (1C, C5), 90.19 (1C, C1′), 86.73 (1C, C4′), 76.74 (1C, C2′), 72.94 (1C, C3′), 66.47 (1C, C5′), 46.67 (1C, P-$\underline{C}H_2$-P).

^{31}P NMR (202 MHz, D_2O): δ 18.36 ($\mathbf{P_\alpha}$), 16.90 ($\mathbf{P_\beta}$).

LC-MS (*m*/*z*): negative mode 439 $[M-H]^-$, positive mode 441 $[M+H]^+$.

Purity by HPLC-UV (254 nm)-ESI-MS: 100%.

23.7. Isoguanosine-5'-O-[(phosphonomethyl)phosphonic acid] (158)

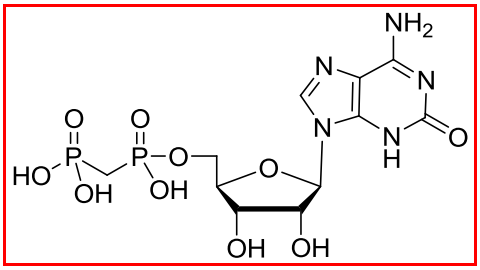

^{1}H NMR (500 MHz, D_2O): δ 8.27 (s, 1H, C8-H), 5.88 (d, *J* = 5.2 Hz, 1H, C1′-H), 4.70 – 4.68 (m, 1H, C2′-H), 4.51 – 4.47 (m, 1H, C3′-H), 4.39 – 4.31 (m, 1H, C4′-H), 4.18 – 4.11 (m, 2H, C5′-$\underline{H_2}$), 2.24 (td, 2H, P-C$\underline{H_2}$-P).

^{13}C NMR (151 MHz, D_2O): δ 165.97 (1C, C2), 154.91 (1C, C6), 152.66 (1C, C4), 141.36 (1C, C8), 120.33 (1C, C5), 90.86 (1C, C1′), 87.56 (1C, C4′), 77.10 (1C, C2′), 73.45 (1C, C3′), 66.48 (1C, C5′), 58.11 (1C, P-$\underline{C}H_2$-P).

^{31}P NMR (243 MHz, D_2O): δ 18.22 ($\mathbf{P_\alpha}$), 17.35 ($\mathbf{P_\alpha}$).

LC-MS (*m*/*z*): negative mode 440 $[M-H]^-$, positive mode 442 $[M+H]^+$.

Purity by HPLC-UV (254 nm)-ESI-MS: 100%.

24.1. 2',3'-O-Isoproylidene-adenosine (159)

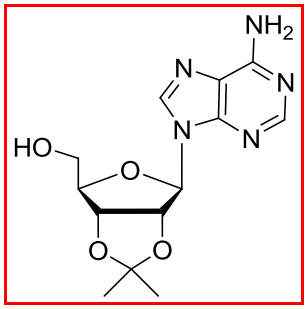

Commercial adenosine **5** (1.0 g) was dissolved in 45 mL of acetone, to it 5 mL of 2,2-dimethoxypropane and 0.5 mL of sulfuric acid was added. It was stirred at room temperature for

30 min. Then 5 mL of Et_3N was added and the resulting solution was evaporated in vacuo and subjected to the column chromatography separation to yield compound **159** as white solid.

Yield: 531 mg (98%).

Melting Point (^oC): 218-220 [**literature**, 220][196]

^1H NMR (500 MHz, DMSO-d_6): δ 8.52 (s, 1H, C8-H), 8.35 (s, 1H, C2-H), 7.35 (bs, 2H, $N\underline{H_2}$), 6.27 (d, *J* = 3.4 Hz, 1H, C1′-H), 5.45 – 5.41 (m, 1H, C2′-H), 5.33 – 5.29 (m, 1H, C3′-H), 4.25 (dd, 1H, C4′-H), 4.19 (td, 2H, C5′-$\underline{H_2}$), 1.68 (s, 6H, 3xCH_3).

^{13}C NMR (126 MHz, DMSO-d_6): δ 158.05 (1C, C6), 152.65 (1C, C2), 148.82 (1C, C4), 141.35 (1C, C8), 135.18 (1C, Ar), 121.43 (1C, CH_3-$\underline{C}$-CH_3), 118.42 (1C, C5), 88.23 (1C, C1′), 84.03 (1C, C2′) , 83.58 (1C, C3′), 71.34 (1C, C4′), 66.65 (1C, C5′), 27.72 (2C, 2xCH_3).

LC-MS (*m*/*z*): negative mode 306 $[M-H]^-$, positive mode 308 $[M+H]^+$.

Purity by HPLC-UV (254 nm)-ESI-MS: 100%.

<u>24.2. 2',3'-O-Isopropylidene-5'-tosyladenosine (160)</u>

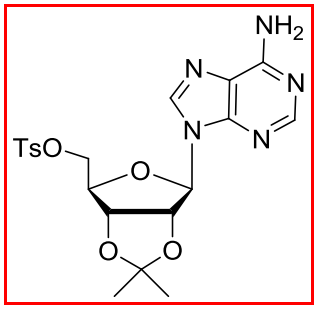

Compound **159** (1.0 g) was dissolved in 5 mL of pyridine, to it 200 mg of DMAP and 600 mg of *p*-toluenesulphonyl chloride in an air tight flask was added. It was stirred under argon atmosphere at room temperature for 14 h. After completion of reaction, it was evaporated in vacuo. Resulting precipitate which was formed on stirring with water and ethylacetate (1: 1) was

removed by filtration, and the filtrate was purified by extraction with 1N HCl and brine, and subsequent crystallization with methanol. The final product was obtained as white solid.

Yield: 531 mg (98%).

Melting Point (^{o}C): 179-181.

^{1}H NMR (500 MHz, DMSO-d_6): δ 8.53 (s, 1H, C8-H), 8.39 (s, 1H, C2-H), 7.80 – 7.75 (m, 2H, Ar), 7.64 (bs, 2H, N$\underline{H}_2$), 7.23 – 7.01 (m, 2H, Ar), 6.21 (d, *J* = 3.4 Hz, 1H, C1′-H), 5.53 – 7.45 (m, 1H, C2′-H), 5.27 – 5.20 (m, 1H, C3′-H), 4.27 (dd, 1H, C4′-H), 4.21 (td, 2H, C5′-$\underline{H}_2$), 1.64 (s, 6H, 3xC$\underline{H}_3$).

^{13}C NMR (126 MHz, DMSO-d_6): δ 156.60 (1C, C6), 154.42 (1C, Ar), 151.71 (1C, C2), 146.18 (1C, C4), 140.34 (1C, C8), 133.41 (1C, Ar), 130.54 (2C, Ar), 126.46 (2C, Ar), 124.84 (1C, CH_3-$\underline{C}$-CH_3), 119.49 (1C, C5), 89.10 (1C, C1′), 85.02 (1C, C2′) , 83.88 (1C, C3′), 70.78 (1C, C4′), 68.22 (1C, C5′), 26.45 (2C, 2x$\underline{C}H_3$), 21.41 (1C, $\underline{C}H_3$-Ar).

LC-MS (*m*/*z*): negative mode 476 $[M-H]^-$, positive mode 478 $[M+H]^+$.

Purity by HPLC-UV (254 nm)-ESI-MS: 100%.

24.3. Procedure for the synthesis of nucleotides (161, 162)

Phosphorylating reagents, tris(tetra-*n*-butylammonium) dichloromethylenebis(phosphonic acid) and tris(tetra-*n*-butylammonium)1-hydroxyethane-1,1-diphosphonic acid was prepared by adding clodronic acid and etidronic acid (5 mmol) to 25 mL of methanol and 10 mL of tetra-*n*-butylammonium hydroxide solution in water, followed by evaporation of methanol and lyophilization of resuting solution. Lyophilized product was kept in air-tight container till use. Tris(tetra-*n*-butylammonium) dichloromethylenebis(phosphonic acid) or tris(tetra-*n*-butylammonium) 1-hydroxyethane-1,1-diphosphonic acid (5 mmol) dissolved in DMF (5 mL) in

air tight flash was added slowly to the 2′,3′-*O*-isopropylidene-5′-tosyladenosine (1 mmol). After stirring the mixture for 36 h under argon atmosphere, the reaction was lyophilized by adding water (25 mL). It was purified by ion-exchange chromatography to give intermediates. Intermediates were deprotected by 6-8% triflouroacetic acid for 3 h to remove 2′,3′-*O*-isopropylidene-group, followed by purification with C-18 HPLC to obtained desired products, adenosine-5′-dichloromethylenediphosphonic acid and adenosine-5′-(1-hydroxy)ethane-1,1-diphosphonic acid as white solids.

24.4. Adenosine-5'-dichloromethylenediphosphonic acid (161)

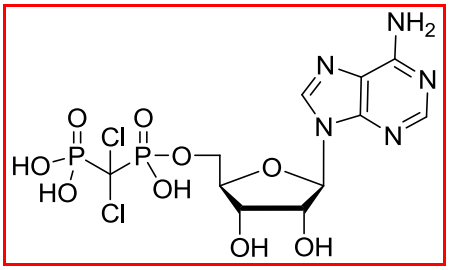

^{1}H NMR (600 MHz, D_2O): δ 8.47 (s, 1H, C8-H), 8.20 (s, 1H, C2-H), 6.16 (d, *J* = 5.0 Hz, 1H, C1′-H), 4.75 (t, *J* = 4.3 Hz, 1H, C2′-H), 4.51 (t, *J* = 4.4 Hz, 1H, C3′-H), 4.40 (t, *J* = 4.4, 2H, C5′-H_2), 4.28 – 4.19 (m, 1H, C4′-H).

^{13}C NMR (126 MHz, D_2O): δ 156.17 (1C, C6), 152.47 (1C, C4), 149.83 (1C, C2), 140.33 (1C, C8), 119.41 (1C, C5), 97.01 (1C, C1′), 96.46 (1C, C4′), 86.74 (1C, C2′), 73.42 (1C, C3′), 70.39 (1C, C5′), 60.68 (1C, P-C-P).

^{31}P NMR (243 MHz, D_2O): δ 19.75 (P_α), 17.27 (P_β).

LC-MS (*m*/*z*): negative mode 443 $[M-H]^-$, positive mode 445 $[M+H]^+$.

Purity by HPLC-UV (254 nm)-ESI-MS: 100%.

24.5. Adenosine-5'-(1-hydroxy)ethane-1,1-diphosphonic acid (162)

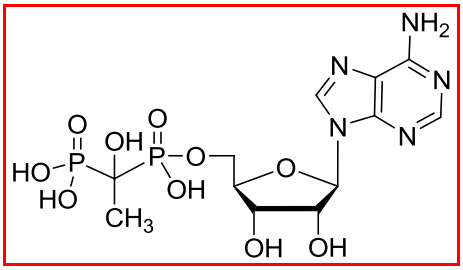

^{1}H NMR (600 MHz, D_2O): δ 8.71 (s, 1H, C8-H), 8.44 (s, 1H, C2-H), 6.15 (d, *J* = 5.6 Hz, 1H, C1′-H), 4.88 – 4.81 (m, 1H, C2′-H), 4.70 – 4.68 (m, 1H, C3′-H), 4.60 – 4.51 (m, 1H, C4′-H), 4.45 – 4.29 (m, 2H, C5′-H_2), 1.60 (d, *J* = 20.4 Hz, 3H).

^{13}C NMR (126 MHz, D_2O): δ 152.67 (1C, C6), 151.07 (1C, C4), 147.73 (1C, C2), 145.53 (1C, C8), 121.21 (1C, C5), 90.61 (1C, C1′), 87.16 (1C, C4′), 77.44 (1C, C2′), 72.92 (1C, C3′), 67.99 (1C, C5′), 22.68 (1C, P-C-P), 22.10 (1C, CH_3).

^{31}P NMR (243 MHz, D_2O): δ 21.08 (**P_α**), 19.19 (**P_β**).

LC-MS (*m*/*z*): negative mode 454 $[M-H]^-$, positive mode 456 $[M+H]^+$.

Purity by HPLC-UV (254 nm)-ESI-MS: 100%.

25.1. Biological experiments

25.1.1. Radiometric *e*N assay (Assay performed by Marianne Freundlieb)

The compounds were tested in a radioactive assay using [^{3}H]AMP as a substrate. Purified recombinant rat *ecto*-5′-NT was used which was prepared as described in the literatures.[67, 112, 118] Assays were carried out with a substrate concentration of 5 μM. Compounds were initially tested at 10 μM concentration and for the potent compounds, full concentration−response curves were obtained. Data were analyzed using GraphPad Prism 5.0 (GraphPad Software Inc., San Diego, CA, USA). Curves were fitted by nonlinear regression using the Marquardt method as

implemented in GraphPad Prism. Reactions were carried out in assay buffer consisting of 25 mM TRIS, 140 mM sodium chloride and 50 mM sodium phosphate with a pH adjusted to 7.4. [^{3}H]Adenosine-5′-monophosphate diluted to a specific activity of 100 mCi/mmol was used as a substrate. 10 µL of the substrate solution (final concentration of 5 µM) were added to 80 µL of assay buffer and the mixture was preincubated for 5 min at 37 °C. The reaction was then initiated by adding 10 µL of enzyme solution (final concentration of 0.3µg/mL in enzyme buffer containing 40 mM HEPES and 4 mM iodacetamide with a pH of 7.4) to each tube. The mixture was incubated for 25 min at 37 °C. To stop the reaction 500 µL of precipitation buffer containing 100 mM lanthanum chloride and 100 mM sodium acetate, pH 4.0, was added. After 30 minutes the precipitation was completed and the reaction mixture was filtered through GF/B glass fiber filters using an M24 Brandell cell harvester (Brandell M-24, Gaitherburg, MD, USA) equipped with an individual box for collecting the filtrates. After washing three times with 1 mL each of the precipitation buffer the filtrates were poured into scintillation vials containing 6 mL of the scintillation cocktail ULTIMA Gold XR, and were quantified by scintillation counting (TRICARB 2900 TR, Packard/Perkin-Elmer) at an efficiency of 34%.[112, 118]

25.1.2. NPP 1-3 colorimetric assay (Assay performed by Sang-Yong Lee)

The human *e*NPP 2 gene (Genbank accession no. NM-006209; full length) and the human *e*NPP 1and 3 genes (Genbank accession no. NM-006208 and NM-005021, respectively; partial without a transmembrane domain) were subcloned in the expression vector pAcG2T baculovirus (BD BaculoGold). Stable transfection into Sf9 insect cells was performed using Cellfectin (Invitrogen). After multiple infections into insect cells, the culture supernatants of Sf9 cells containing the recombinant enzymes were collected and further concentrated by Amicon (50 kDa cutoff). Subsequently, it was transferred into the buffer containing 50 mM Tris (pH 7.5), 10 mM

NaCl and 5% glycerol by Amicon (50 kDa cutoff). Finally, samples were kept at –80 °C till use.[106, 116]

25.1.2.1. Assay condition for NPP 1 and NPP 3

The test compounds were screened at a concentration of 10 µM. They were prepared in the reaction buffer (1 mM $CaCl_2$, 200 µM $ZnCl_2$, 50 mM TRIS, pH 9.0) together with the substrate *p*-Nitrophenyl-5′-thymidine monophosphate (400 µM). The reaction was initiated by adding 20 µL of human recombinant NPP 1 (0.9 µg) or NPP 3 (0.4 µg) and was incubated at 37 °C for 30 min. Finally, the enzymatic reaction was stopped by adding 1.0 N NaOH. The amounts of *p*-nitrophenolate liberated were measured at 400 nm.[116]

25.1.2.2. Assay condition for NPP 2

The screenings were carried out at the inhibitor concentration of 10 µM. The enzyme inhibition assays were carried out at 37 °C in a final volume of 50 µL. The reaction mixture contained 5 mM $MgCl_2$, 5 mM $CaCl_2$, 100 mM Tris, pH 9.0, and 400 µM lysophosphatidiylcholine (18:1). The reaction was started with the addition of 10 µL of NPP 2 (44 µg). The mixture was incubated for 60 min and subsequently, the released choline was quantified colorimetrically at 555 nm after incubation at 37 °C for 10 min with 50 µL of each the peroxidase reagent (50 mM Tris at pH 9.0, 2 mM TOOS, 5 U/mL peroxidase) and the choline-oxidase reagent (50 mM Tris at pH 9.0, 2 mM aminoantipyrine, 5 U/mL choline-oxidase).[116]

25.1.3. Human NTPDases 1-3 malachite green assay (Assay performed by Amelie Fiene)

COS-7 cells were transiently transfected with a plasmid encoding hNTPDase 1, 2 and 3 respectively. Cell membranes were prepared as described in the literature.[116, 117] Substrate ATP

(20 µL) was added to a well of a 96-well plate containing 10 µL 10% aq. DMSO or test compound in 10% aq. DMSO and the reaction was initiated by the addition of 20 µL NTPDase protein extract to give a final concentration of 70 µM ATP for NTPDase 1, and 100 µM of ATP for NTPDase 2 and 3. Then the reaction was started by adding 4 ng/µL enzyme for NTPDase 1 and 3, and 3 ng/µL enzyme for NTPDase 2. After 10 min of incubation at 37°C the reaction was stopped with 17.2 µL of ammonium molybdate solution and 12.8 µL of malachite green reagent.[117] After 20 min incubation at room temperature, absorbance measurements were made at 623 nm on a BMG PheraStar FS plate reader (BMG Labtech GmbH, Ortenberg, Germany) and the percent inhibition was calculated. The test compounds were screened at a concentration of 10 µM.[116]

25.1.4. $P2Y_1$ Calcium assay (Assay performed by Dr. Aliaa Abdelrahman)

Measurement of intracellular calcium mobilisation (G_q signaling pathway)

Calcium assays were performed according to the published procedures.[197] 1321N1 Human astrocytoma cells expressing the human $P2Y_1$ were harvested with 0.05% trypsin / 0.02% EDTA and rinsed with culture medium. The cells were kept under 5% CO_2 at 37°C for 45 min and then centrifuged at 200 x g at 4°C for 5 min. After that the cells were incubated for 1 h at 25 °C in Krebs-Ringer-HEPES buffer, pH 7.4 containing 3 µM Oregon Green BAPTA-1/AM and 1 % Pluronic®F127. The cells were rinsed 3 times with KRH buffer, diluted and plated into 96-well plates at a density of approximately 16,000 cells/well and left for 20 min. Fluorescence intensity was measured at 520 nm for 30 s at 0.4 s intervals. Measurements were performed using a Novostar®microplate reader. At least three independent experiments were performed in duplicates.

25.1.5. $P2Y_{12}$ *β*-arrestin assay (Assay performed by Dr. Aliaa Abdelrahman)

For the preparation of $P2Y_{12}$ cell line, the *h*$P2Y_{12}$ sequences were cloned into pCMV- ProLink-1vector and were subsequently expressed into CHO cell lines. The cells were selected for 2 weeks in order to produce the desired stable cell line. The cells were kept growing in F12 medium (Gibco – life technologies). One day before the assay, cells were detached from flask using dissociations buffer and were seeded into 96-well plates at a density of 30000 cells/well and to each well 90 µL of optimum medium was added. Compounds dilutions were diluted in Optimum medium without supplements, 10 µL of diluted compounds were added to each well. After 90 min of incubation at 37 °C, 50 µL of detection reagent (DiscoverX, Fremont, CA) per well were added and then the plate incubated for further 60 min at room temperature. After that, Luminescence was determined using a Topcount NXT plate reader (Perkin-Elmer, Meriden, CT). Three to four independent experiments were performed, each in duplicate. GraphPadPrism, Version 4.02 (GraphPad Inc., La Jolla, CA) were used to analyze Data.[107, 170, 198]

25.2. Metabolic stability studies on rat liver

25.2.1. Preparation of Rat Liver Microsomes

Rat liver microsomes were prepared from fresh rat liver (6.5 g) which was homogenized in 30 mL of freshly prepared Dulbecco's phosphate buffered saline (DPBS) consisting of 132.5 mg of $CaCl_2 \cdot 2H_2O$, 100 mg of $MgCl_2 \cdot 6H_2O$, 200 mg of KCl, 200 mg of KH_2PO_4, 8000 mg of NaCl, and 1500 mg of Na_2HPO_4 in a total volume of 1000mL, pH 7.2, and centrifuged at 9000*g* for 30 min at 4 °C. The supernatant, which contained the soluble microsomes, was carefully decanted and stored at -80 °C until used. The protein concentration was 5 mg/mL as determined by the method of Bradford.[133]

25.2.2. LC-MS Analyses

HPLC was performed on a C18 column (50 mm × 2 mm, particle size 3 μm, Phenomenex Luna) using a mixture of H_2O (solvent A) and MeOH (solvent B) containing 20 mM of NH_4OAc as eluent at a flow rate of 250 μL/min. Mass spectra were recorded on an API 2000 mass spectrometer (electron spray ion source, Applied Biosystems, Darmstadt, Germany) coupled with an HPLC system (Agilent 1100, Böblingen, Germany). Data were collected and analyzed by Analyst Software, version 1.3.1. The separation was carried out at room temperature by gradient elution. The elution was started with a mixture of solvent A and solvent B (90:10, to 0:100 v/v) up to 20 min. The limit of detection (LOD), defined as the lowest analyte concentration with a signal-to-noise (S/N) ratio of 3, was determined for compounds to be approximately 0.1 μg/mL.[133]

25.2.3. Metabolism by rat Liver Microsomes

Compounds were incubated with rat liver microsomes (2 mg of protein per vial) at a concentration of 100 μM in a final volume of 1 mL tris-HCl buffer solution with or without NADPH regenerating system. NADPH regenerative system consists of NADP (0.57 mM), NADH (0.57 mM), isocitrate (6.4 mM), isocitrate dehydrogenase (0.57 mM), and $MgCl_2$ (23.4 mM) (pH 7.2). The samples were incubated for different time intervals at 37 °C in a water bath and ice-cooled acetonitrile was added to stop the enzymatic reaction. After centrifugation at 14000*g*, the supernatant was analyzed by LC-MS.[133]

25.2.4. Plasma stability studies

Blood from healthy donors was obtained from the blood bank, University Clinic Bonn. The blood (100 mL) had been mixed with 70 mL of a stabilizing solution, which contained (per 100

mL): citric acid monohydrate (327 mg), sodium citrate (2.63 g), sodium dihydrogenphosphate (251 mg), and dextrose monohydrate (2.55 g) in water (aqua ad injectabilia). For every reaction, a solution of compounds in water was added to give final concentration of 100 μM. The obtained solution was pipetted into vials (1 mL per vial) and incubated at 37 ºC. At different time points (1, 5, 10, 30, 60,120 and 300 min), 100 μL of sample was taken to it 300 μL of ice-cooled acetonitrile (LCMS quality from sigma aldrich) was added to stop the reaction. The samples were sonicated in an ultrasonic bath for 5 min followed by centrifugation at 4000 rpm for 10 min. The supernatants were transferred to LC-MS sample vials and quantified. Experiments were performed in triplicate.[75]

VI. Summary

This thesis consists of five parts. The first part contains a general introduction about purinergic signalling and *ecto*-nucleotidases including our enzyme of interest *ecto*-5′-nucleotidase (*e*N, CD73, EC 3.1.3.5). The second part constitutes an introduction into the medicinal chemistry of *e*N inhibitors and the different high-throughput *e*N assay methods used for the evaluation of inhibitors. The third part presents the aims of the project including the design of the target compounds. The fourth part describes the results and their discussion including synthetic chemistry, pharmacological investigations and liver stability studies in microsomes as well as in blood plasma. The final part contains detailed experimental procedures for the syntheses, the pharmacological evaluation and the metabolic stability studies.

Project I and II: Design and synthesis of adenine base-modified and methylene bisphosphate chain-modified derivatives and analoguesof AOPCP

The *e*N belongs to a group of enzymes, the *ecto*-nucleotidases which dephosphorylate extracellular nucleotides, mainly AMP. Other membrane-bound *ecto*-nucleotidases include nucleoside triphosphate diphosphohydrolases (NTPDases; subtypes 1, 2, 3 and 8), nucleotide pyrophosphatases (NPPs 1-4) and alkaline phosphatases (APs; tissue non-specific, intestinal, placental and germ cell). NTPDases and NPPs lead to an increase in the extracellular concentrations of nucleotides resulting in P2 receptor activation whereas *e*N increases adenosine concentrations resulting in a stimulation of P1 (adenosine) receptors. *e*N inhibitors therefore reduce extracellular adenosine levels, resulting in an indirect blockade of adenosine (P1) receptor activation. They possess potential as novel drugs, e.g. for cancer therapy or for the treatment of neurodegenerative diseases. AOPCP, an analogue of ADP, is currently one of the most potent competitive inhibitors of *e*N.

In part I of the current project a series of 2-, 6- and 8-substituted derivatives of AOPCP was synthesized with the goals to study structure-activity relationships, and to obtain more potent and stable *e*N inhibitors which cannot be metabolized to adenosine or adenosine receptor ligands. Also in this part the best individual substitutions at the 2-and 6-position were combined in order to obtain more potent and selective di-substituted derivatives. Simultaneously, we also enhanced the metabolic stability and selectivity by synthesizing N^6-disubstituted AOPCP derivatives as well as 6-O- and 6-S-substituted analogues. For the preparation of the target compounds with 2-, 6- or 8-substitution, or 2,6-disubstitution, respectively, a convergent synthetic strategy was applied which involves first the synthesis of the intermediate nucleosides followed by phosphorylation to provide the nucleotides- AOPCP derivatives and analogs. For project II, methylene bisphosphate chain-modified derivatives of AOPCP were synthesized. The side chain was replaced by commercially available substituted bis(phosphonic acid) derivatives, in which the methylene group of the 5′-methylene diphosphate group was substituted.

A library of 55 purine nucleosides was initially synthesized, out of which 24 are novel not previously described in the literature. They were obtained in high yields. The nucleosides were subsequently phosphorylated to provide AOPCP derivatives and analogues in good isolated yields of 30-75% by using an optimized phosphorylation method. This was achieved by a large excess of phosphorylating reagent, which reduced the formation of side-products and thereby facilitated the purification process. The compounds were purified by ion exchange chromatography or by preparative HPLC depending on the type of by-products formed in each reaction. Altogether 60 AOPCP derivatives and analogs were synthesized, out of which 58 are novel, not previously described compounds. The developed synthetic strategy is straightforward and allows for broad structural modifications. The structures of the synthesized compounds were

confirmed by ^{1}H-, ^{13}C-NMR, DEPT-135 and ^{31}P-NMR (for AOPCP analogues) spectroscopy, in addition to HPLC analysis coupled to electrospray ionization mass spectrometry (LC/ESI-MS), which was also used to determine the compounds' purity.

Enzyme inhibition was determined in radiometric *e*N assay using [^{3}H]AMP as substrate.[118] We were able to obtain many potent compounds. Selected inhibitors were further investigated at other *ecto*-nucleotidases including *e*NTPDase 1-3 and *e*NPP 1-3. The lead compound AOPCP showed some inhibitory potency at *e*NPP 1 with a K_i value of **16.5** μM (human enzyme). Most of the newly developed compounds were inactive at those enzymes, which showed that they were selective inhibitors of *e*N. Selected compounds were further investigated at the ADP-activated P2Y receptor subtypes $P2Y_1$ and $P2Y_{12}$. The tested nucleotide derivative did not show any affinity for the investigated P2Y receptor subtypes and can therefore be regarded as highly selective for *e*N.

The most potent nucleotides of the present series were 2-chloro-N^6-(2-chlorobenzyl)purine riboside-5′-*O*-[(phosphonomethyl)phosphonic acid] (**144**, K_i= 0.34 nM) and 2-chloro-N^6-benzyl-N^6-methylpurine riboside-5′-*O*-[(phosphonomethyl)phosphonic acid] (**149,** K_i= 0.88 nM). Compared to a K_i value of 197 nM for the lead structure AOPCP tested under the same conditions, up to 580-fold improvement in potency was achieved. The structures of AOPCP derivatives **144** and **149** are depicted in Figure 31. Compound **149** being N^6-disubstituted is not expected to yield adenosine receptor activating metabolites.

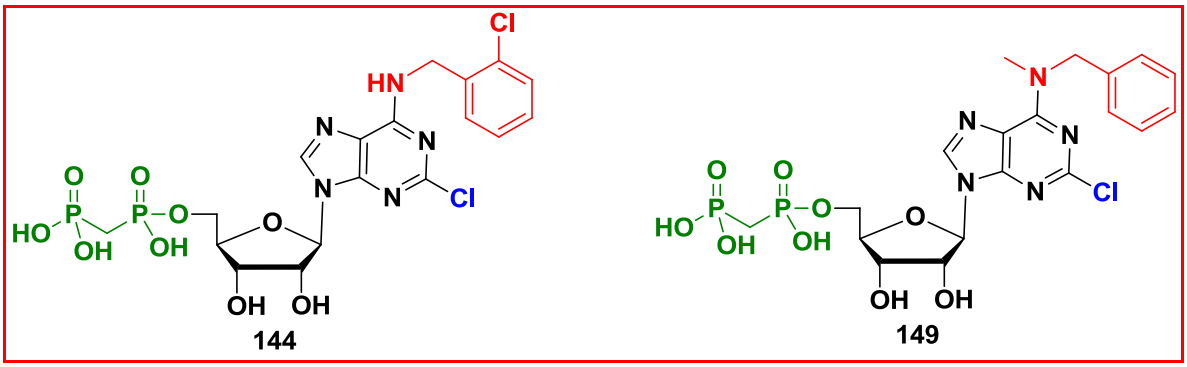

Figure 31. Structure of the most potent *e*N inhibitors

Structure-activity relationships of 6-and 8-substituted AOPCP derivatives

N^6-Substitution of AOPCP generally increased potency. N^6-Mono-substitution indicated that large, hydrophobic N^6-substituents were beneficial for high inhibitory potency of *e*N. N^6-Di-substituted derivatives with one large N^6-substituent, but not with two voluminous residues at the exocyclic N atom, were also well tolerated. Analysis of structure-activity relationships allowed structural optimization and thus the development of highly potent inhibitors. Aromatic substitutions were better than alkyl-substitution at N^6. Corresponding 2′,3′-*O*-isopropylidene analogs were less potent. We also investigated compounds with various substitutions of the N^6-benzyl residue (one of the potent compound in the series). Electron-withdrawing groups (e.g. Cl) of the phenyl ring appeared to be better tolerated than electron-donating functions (NH_2). Especially, N^6-benzyl-, N^6-(2-phenylethyl)-, N^6-(4-chlorobenzyl)-, N^6-(3-chlorobenzyl)-, N^6-(2-chlorobenzyl)-, N^6-(4-methoxybenzyl)-, N^6-(1-phenylethyl)- and N^6-methyl,N^6-benzyl-substituents at the 6-position of the core structure had major impacts on the compounds' inhibitory potency yielding very potent inhibitors. When the 6-(aryl)alkylamino group was substituted with 6-(aryl)thio and 6-(aryl)alkyloxy groups comparable potency was observed. The synthesis of 6-O- and 6-S-substituted analogues offers the possibility to move away from

adenine nucleotide derivatives, which might be metabolized to (N^6-substituted) adenosine derivatives after hydrolysis which may activate adenosine A_1 receptors and thereby inducing negative inotropic and chronotropic effects, eventually leading to cardiac arrest.

At the 8-position smaller substituent like 8-chloro-substitution was tolerated whereas larger 8-substituents like 8-bromo, 8-thioethyl and 8-aminomethyl resulted in a drastic reduction in activity. A reason for this may be that larger 8-substituents can induce a conformational change from the *anti*- to the *syn*-conformation around the nucleosidic bond, which is unfavourable for binding to the enzyme. Compounds were inactive at purinergic targets including ADP-activated P2Y receptor subtypes ($P2Y_1$ and $P2Y_{12}$), *e*NTPDase 1-3 and *e*NPP 1-3.

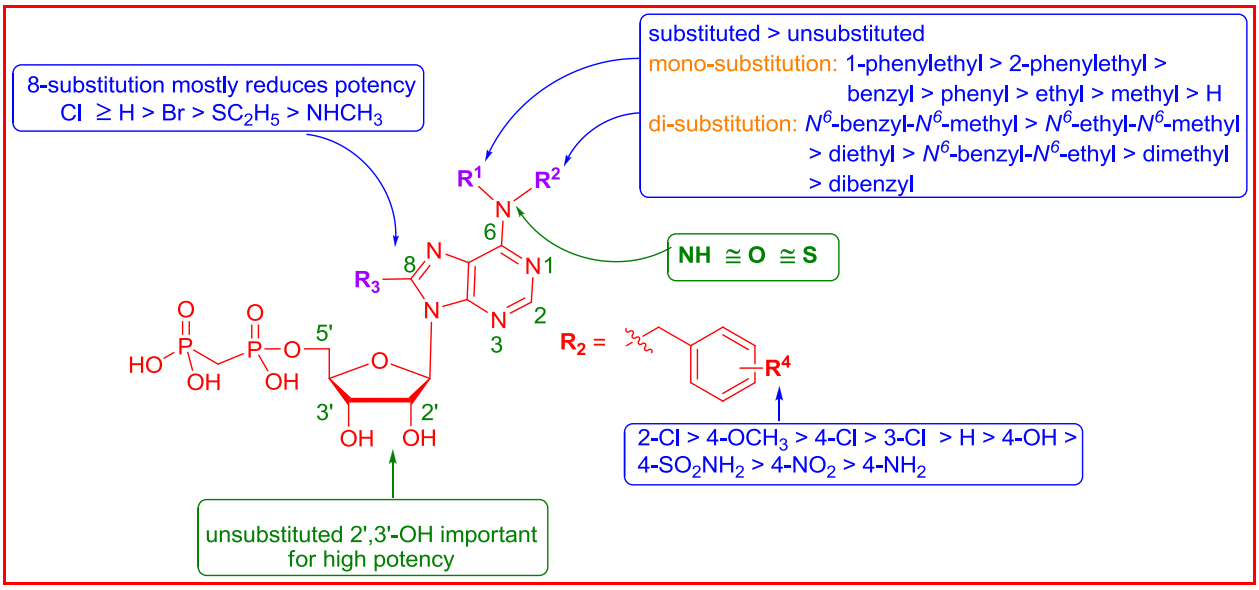

Figure 32. Structure-activity relationships of 6-and 8-substituted AOPCP derivatives and analogs

Structure-activity relationships of 2-mono-, 2,6-disubstituted and side-chain-modified AOPCP derivatives

Several substitutions at the 2-position of AOPCP improved potency. The order of potency for 2-substituted compounds was 2-iodo > 2-chloro > 2-amino > 2-hydrazinyl > 2-oxo >> piperazinyl, suggesting that polar and electron-withdrawing groups (e.g. Cl or I) appeared to be particularly well tolerated. The 2-thio-substituted derivatives, e.g. 2-cyclohexylethylthio- and 2-allylthio-substituted compounds were also very potent. The best 2-substituents amino, chloro and iodo were combined with the best 6-alkyl and 6-aryl substitutents to give 2,6-disubstituted derivatives. Several combinations tremendously improved activity to the sub nanomolar range. Combination of 2-chlorobenzyl at the N^6-position with chloro at the 2-position produced the most potent derivative **144** (K_i = 0.34 nM). Combination of N^6-benzyl-N^6-methyl at the 6-position with chloro at the 2-position gave another very potent derivative **149** (K_i = 0.88 nM). The compounds with combinations of beneficial N^6-groups with chloro at the 2-position were more potent than those with 2-iodo substitution, although iodo was the best 2-substituent without an N^6-substituent. This suggests that for di-substituted derivatives smaller groups like chloro are better tolerated at the 2-position as compared to larger residues like iodo.

Further derivatives with substitution of the methylenebis(phosphate) side-chain of AOPCP were also synthesized. But the substitution resulted in a decrease or loss of potency. The structure-activity relationships are depicted in Figure 33.

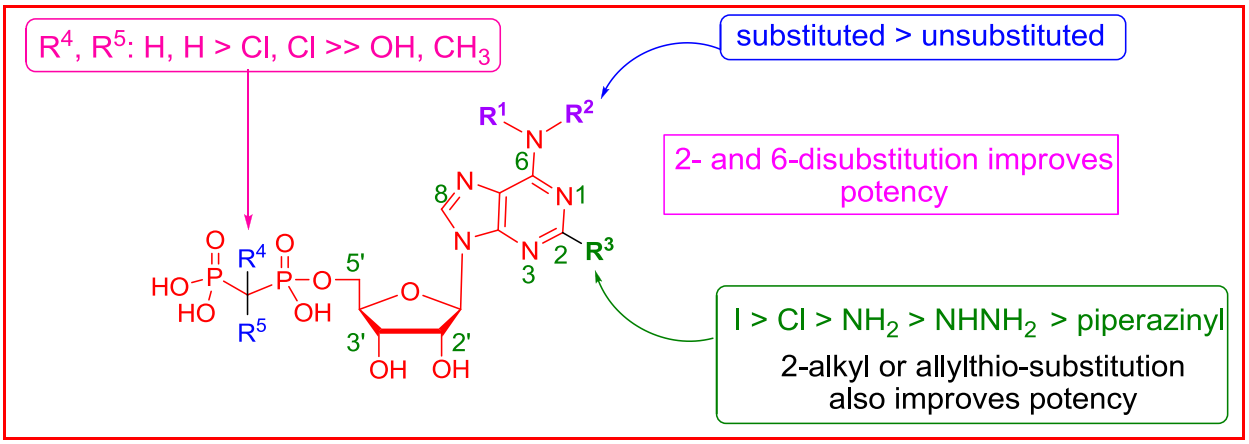

Figure 33. Structure-activity relationships of 2-mono-, 2,6-disubstituted and methylene bis(phosphate) side chain-modified AOPCP

Project III: Metabolic stability studies of selected potent AOPCP derivatives and analogues

Selected potent inhibitors were further investigated for their metabolic stability, (i) in rat liver microsomes in order to investigate potential metabolic degradation by liver enzymes, and (ii) in human blood, in order to determine plasma stability. This was done in order to be able to select stable inhibitors for subsequent extended pharmacological experiments. The studies involved incubation of inhibitors with microsomes or plasma at 37 °C and subsequent analysis of the samples by LC-MS. The compounds used for the studies are depicted in Figure 34.

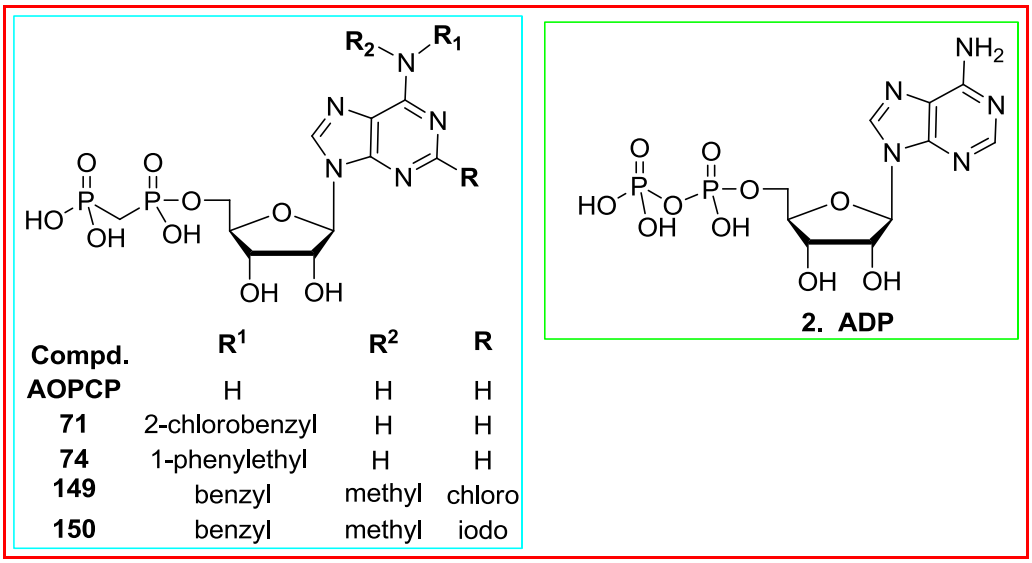

Compd.	R^1	R^2	R
AOPCP	H	H	H
71	2-chlorobenzyl	H	H
74	1-phenylethyl	H	H
149	benzyl	methyl	chloro
150	benzyl	methyl	iodo

2. ADP

Figure 34. Compounds investigated in metabolic studies

For stability studies in liver microsomes all compounds depicted in Figure 22 were investigated, while for plasma stability studies **74** was left out owing to its low microsomal stability as compared to other compounds. Incubation with rat liver microsomes showed that the inhibitors were relatively stable towards liver enzymes, but low stability was observed for both, ADP and AOPCP. The order of stability was **149** > **150** > **71** > **74** >>> **AOPCP** > **ADP**. The identified metabolites were the corresponding nucleosides, the nucleobases and methylenebis(phosphonic acid). The hydrolyses are presumably catalyzed by hydrolytic enzymes present in rat liver. Incubation with human blood showed that only **ADP** was unstable, but the other compounds were stable. After 5 hours of incubation the order of stability was determined to be **149** > **71** > **150** > **AOPCP >>> ADP**.

Concluding remarks

Potent inhibitors for *e*N have been identified with potencies in the low nanomolar to sub-nanomolar range. Selected potent *e*N inhibitors were found to be stable upon incubation with rat liver microsomes and in human blood serum. These compounds are the most potent *e*N inhibitors known to date and may serve as valuable pharmacological tools to further elucidate the enzyme's (patho)physiological roles and help to validate it as a new drug target.

VII. References

1. Abbracchio, M. P.; Burnstock, G. Purinergic signalling: Pathophysiological roles. *Jpn. J. Pharmacol.* **1998**, *78*, 113−145.

2. Burnstock, G. Purinergic signalling. *Br. J. Pharmacol.* **2006**, *147*, 172−181.

3. Burnstock, G. Purinergic nerves. *Pharmacol. Rev.* **1972**, *24*, 509−581.

4. Burnstock, G. Physiology and pathophysiology of purinergic neurotransmission. *Physiol. Rev.* **2007**, *87*, 659–797.

5. Zimmermann, H. 5′-Nucleotidase: molecular structure and functional aspects. *Biochem. J.* **1992**, *285*, 345−365.

6. Zimmermann, H. *Ecto*-nucleotidases: some recent developments and a note on nomenclature. *Drug Dev. Res.* **2001**, *52*, 44–56.

7. Burnstock, G. Introduction: P2 Receptors. *Curr. Top. Med. Chem.* **2004**, *4*, 793−803.

8. Jacobson, K. A.; Jarvis, M. F.; Williams, M. Purine and pyrimidine (P2) receptors as drug targets. *J. Med. Chem.* **2002**, *45*, 4057–4093.

9. Müller, C. E. P2-Pyrimidinergic receptors and their ligands. *Curr. Pharm. Des.* **2002**, *8*, 2353−2369.

10. Thimm, D.; Knospe, M.; Abdelrahman, A.; Moutinho, M.; Alsdorf, B. A. A.; von Kügelgen, I.; Schiedel, A.; C. Müller, C. E. Characterization of new G protein-coupled adenine receptors in mouse and hamster. *Purinergic Signalling* **2013**, *9*, 415−426.

11. Jacobson, K. A.; Gao, Z. G. Adenosine receptors as therapeutic targets. *Nat. Rev. Drug Discovery* **2006**, *5*, 247–264.

12. Cristalli, G.; Lambertucci, C.; Taffi, S.; Vittori, S.; Volpini, R. Medicinal chemistry of adenosine A_{2A} receptor agonists. *Curr. Top. Med. Chem.* **2003**, *3*, 387−401.

13. Fredholm, B. B.; Ijzerman, A. P.; Jacobson, K. A.; Klotz, K. N.; Linden, J. International union of pharmacology. XXV. Nomenclature and classification of adenosine receptors. *Pharmacol. Rev.* **2001**, *53*, 527–552.

14. Ralevic, V.; Burnstock, G. Receptors for purines and pyrimidines. *Pharmacol. Rev.* **1998**, *50*, 413−492.

15. Abbracchio, M. P.; Burnstock, G.; Boeynaems, J. M.; Barnard, E. A.; Boyer, J. L.; Kennedy, C.; Knight, G. E.; Fumagalli, M.; Gachet, C.; Jacobson, K. A.; Weisman, G. A. International union of pharmacology LVIII: update on the P2Y G protein-coupled nucleotide receptors: from molecular mechanisms and pathophysiology to therapy. *Pharmacol. Rev.* **2006**, *58*, 281−341.

16. Ingall, A. H.; Dixon, J.; Bailey, A.; Coombs, M. E.; Cox, D.; McInally, J. I.; Hunt, S. F.; Kindon, N. D.; Teobald, B. J.; Willis, P. A.; Humphries, R. G.; Leff, P.; Clegg, J. A.; Smith, J. A.; Tomlinson, W. Antagonists of the platelet P2T receptor: A novel approach to antithrombotic therapy. *J. Med. Chem.* **1999**, *42*, 213−220.

17. Yegutkin, G. G. Nucleotide- and nucleoside-converting ectoenzymes: important modulators of purinergic signalling cascade. *Biochim. Biophys. Acta.* **2008**, *1783*, 673–694.

18. Hoyle, C. H. V.; Hilderman, R. H.; Pintor, J. J.; Schuelter, H.; King, B. F. Diadenosine polyphosphates as extracellular signal molecules. *Drug Dev. Res.* **2001**, *52*, 260−273.

19. Burnstock, G.; Williams, M. P2 Purinergic receptors: modulation of cell function and therapeutic potential. *J. Pharmacol. Exp. Ther.* **2000**, *295*, 862−869.

20. Burnstock, G. Potential therapeutic targets in the rapidly expanding field of purinergic signalling. *Clin. Med.* **2002**, *2*, 45–53.

21. Zimmermann, H. Extracellular metabolism of ATP and other nucleotides. *Naunyn−Schmiedeberg's Arch. Pharmacol.* **2000**, *362*, 299−309.

22. Zimmermann, H. Two novel families of *ecto*-nucleotidases: molecular structures, catalytic properties and a search for function. *Trends Pharmacol. Sci.* **1999**, *20*, 231–236.

23. Zimmermann, H.; Zebisch, M.; Sträter, N. Cellular function and molecular structure of *ecto*-nucleotidases. *Purinergic Signalling* **2012**, *8*, 437−502.

24. Shirley, D. G.; Vekaria, R.; Sévigny, J. *Ecto*-nucleotidases in the kidney. *Purinergic Signalling* **2009**, *5*, 501–511.

25. Kirley, T. L.; Crawford, P. A.; Smith, T. M. The structure of the nucleoside triphosphate diphosphohydrolases (NTPDases) as revealed by mutagenic and computational modeling analyses. *Purinergic signalling* **2006**, *2*, 379−389.

26. Iqbal, J.; Vollmayer, P.; Braun, N.; Zimmermann, H.; Müller, C. E. A capillary electrophoresis method for the characterization of *ecto*-nucleoside triphosphate diphosphohydrolases (NTPDases) and the analysis of inhibitors by in-capillary enzymatic microreaction. *Purinergic Signalling* **2005**, *1*, 349−358.

27. Zebisch, M.; Krauss, M.; Schäfer, P.; Lauble, P.; Sträter, N. Crystallographic snapshots along the reaction pathway of nucleoside triphosphate diphosphohydrolases. *Structure* **2013**, *21*, 1460−1475.

28. Zebisch, M.; Krauss, M.; Schäfer, P.; Sträter, N. Crystallographic evidence for a domain motion in rat nucleoside triphosphate diphosphohydrolase (NTPDase) 1. *J. Mol. Biol.* **2012**, *415*, 288−306.

29. Kukulski, F.; Levesque, S. A.; Lavoie, E. G.; Lecka, J.; Bigonnesse, F.; Knowles, A. F.; Robson, S.; Kirley, T. L.; Sévigny, J. Comparative hydrolysis of P2 receptor agonists by NTPDases 1, 2, 3 and 8. *Purinergic Signalling* **2005**, *1*, 193−204.

30. Knowles, A. F. The GDA1_CD39 superfamily: NTPDases with diverse functions. *Purinergic Signalling* **2011**, *7*, 21–45.

31. Langer, D.; Ikehara, Y.; Takebayashi, H.; Hawkes, R.; Zimmermann, H. The *ecto*-nucleotidases alkaline phosphatase and nucleoside triphosphate diphosphohydrolase 2 are associated with subsets of progenitor cell populations in the mouse embryonic, postnatal and adult neurogenic zones *Neuroscience* **2007**, *150*, 863–879.

32. Lazarowski, E. R.; Boucher, R. C.; Harden, T. K. Mechanisms of release of nucleotides and integration of their action as P2X- and P2Y-receptor activating molecules. *Mol. Pharmacol.* **2003**, *64*, 785−795.

33. Gendron, F. P.; Benrezzak, O.; Krugh, B. W.; Kong, Q.; Weisman, G. A.; Beaudoin, A. R. Purine signalling and potential new therapeutic approach: possible outcomes of NTPDase inhibition. *Curr. Drug Targets* **2002**, *3*, 229−245.

34. Gendron, F. P.; Halbfinger, E.; Fischer, B.; Beaudoin, A. R. Inhibitors of NTPDase: key players in the metabolism of extracellular purines. *Adv. Exp. Med. Biol.* **2000**, *486*, 119−123.

35. Martín-Satué, M.; Lavoie, E. G.; Pelletier, J.; Fausther, M.; Csizmadia, E.; Guckelberger, O.; Robson, S. C.; Sévigny, J. Localization of plasma membrane bound NTPDases in the murine reproductive tract. *Histochem. Cell. Biol.* **2009**, *131*, 615–628.

36. Robson, S. C.; Sévigny, J.; Zimmermann, H. The *E*-NTPDase family of *ecto*-nucleotidases: Structure-function relationships and pathophysiological significance. *Purinergic Signalling* **2006**, *2*, 409–430.

37. Bastid, J.; Cottalorda-Regairaz, A.; Alberici, G.; Bonnefoy, N.; Eliaou, J.-F.; Bensussan, A. *E*-NTPD1/CD39 is a promising therapeutic target in oncology. *Oncogene* **2013**, *32*, 1743–1751.

38. Baqi, Y.; Weyler, S.; Iqbal, J.; Zimmermann, H.; Müller, C. E. Structure-activity relationships of anthraquinone derivatives derived from bromaminic acid as inhibitors of *ecto*-nucleoside triphosphate diphosphohydrolases (*E*-NTPDases). *Purinergic Signalling* **2009**, *5*, 91–106.

39. Sévigny, J.; Levesque, F. R.; Grondin, G.; Beaudoin, A. R. Purification of the blood vessel ATP diphosphohydrolase, identification and localization by immunological techniques. *Biochim. Biophys. Acta* **1997**, *1334*, 73−88.

40. Belcher, S. M.; Zsarnovszky, A.; Crawford, P. A.; Hemani, H.; Spurling, L.; Kirley, T. L. Immunolocalization of *ecto*-nucleoside triphosphate diphosphohydrolase 3 in rat brain: implications for modulation of multiple homeostatic systems including feeding and sleep-wake behaviors. *Neurosci.* **2006**, *137*, 1331−1346.

41. Bigonnesse, F.; Levesque, S. A.; Kukulski, F.; Lecka, J.; Robson, S. C.; Fernandes, M. J. G.; Sévigny, J. Cloning and characterization of mouse nucleoside triphosphate diphosphohydrolase-8. *Biochemistry* **2004**, *43*, 5511−5519.

42. Zebisch, M.; Baqi, Y.; Schäfer, P.; Müller, C. E.; Sträter, N. Crystal structure of NTPDase 2 in complex with the sulfoanthraquinone inhibitor PSB-071. *J. Struct. Biol.* **2014**, *185*, 336−341.

43. Wang, C. J.; Vlajkovic, S. M.; Housley, G. D.; Braun, N.; Zimmermann, H.; Robson, S. C.; Sévigny, J.; Soeller, C.; Thorne, P. R. C-terminal splicing of NTPDase 2 provides distinctive catalytic properties, cellular distribution and enzyme regulation. *Biochem. J.* **2005**, *385*, 729−736.

44. Stefan, C.; Jansen, S.; Bollen, M. NPP-type *ecto*-phosphodiesterases: unity in diversity. *Trends Biochem. Sci.* **2005**, *30*, 542–550.

45. Harmey, D.; Hessle, L.; Narisawa, S.; Johnson, K. A.; Terkeltaub, R.; Millán, J. L. Concerted regulation of inorganic pyrophosphate and osteopontin by akp2, *e*npp1 and ank: an integrated model of the pathogenesis of mineralization disorders. *Am. J. Pathol.* **2004**, *164*, 1199–1209.

46. Cimpean, A.; Stefan, C.; Gijsbers, R.; Stalmans, W.; Bollen, M. Substrate-specifying determinants of the nucleotide pyrophosphatases/phosphodiesterases NPP 1 and NPP 2. *Biochem. J.* **2004**, *381*, 71–77.

47. Lee, S.-Y.; Levesque, S. A.; Sévigny, J.; Müller, C. E. A highly sensitive capillary electrophoresis method using *p*-nitrophenyl 5'-thymidine monophosphate as a substrate for the monitoring of nucleotide pyrophosphatase/phosphodiesterase activities. *J.Chromatogr. B* **2012**, *911*, 162−169.

48. Gijsbers, R.; Aoki, J.; Arai, H.; Bollen, M. The hydrolysis of lysophospholipids and nucleotides by autotaxin (NPP 2) involves a single catalytic site. *FEBS Lett.* **2003**, *538*, 60–64.

49. Sakagami, H.; Aoki, J.; Natori, Y.; Nishikawa, K.; Kakehi, Y.; Natori, Y.; Arai, H. Biochemical and molecular characterization of a novel choline-specific glycerophosphodiester phosphodiesterase belonging to the nucleotide pyrophosphatase/phosphodiesterase family. *J. Biol. Chem.* **2005**, *280*, 23084–23093.

50. Asensio, A. C.; Rodriguez-Ferrer, C. R.; Castaneyra-Perdomo, A.; Oaknin, S.; Rotllan, P. Biochemical analysis of *ecto*-nucleotide pyrophosphatase phosphodiesterase activity in brain membranes indicates involvement of NPP 1 isoenzyme in extracellular hydrolysis of diadenosine polyphosphates in central nervous system. *Neurochem. Int.* **2007**, *50*, 581–590.

51. Vollmayer, P.; Clair, T.; Goding, J. W.; Sano, K.; Servos, J. Hydrolysis of diadenosine polyphosphates by nucleotide pyrophosphatases/phosphodiesterases. *Eur. J. Biochem.* **2003**, *270*, 2971−2978.

52. Terkeltaub, R. Physiologic and pathologic functions of the NPP (nucleotide pyrophosphatase/phosphodiesterase) family focusing on NPP 1 in calcification. *Purinergic Signalling* **2006**, *2*, 371−377.

53. Goding, J. W.; Grobben, B.; Slegers, H. Physiological and pathophysiological functions of the *ecto*-nucleotide pyrophosphatase/phosphodiesterase family *Biochim. Biophys. Acta* **2003**, *1638*, 1−19.

54. Aerts, I.; Martin, J. J.; De Deyn, P. P.; Van Ginniken, C.; Van Ostade, X.; Kockx, M.; Dua, G.; Slegers, H. The expression of *ecto*-nucleotide pyrophosphatase/phosphodiesterase 1 (*E*-NPP 1) is correlated with astrocytic tumor grade. *Clin. Neurol. Neurosurg.* **2011**, *113*, 224–229.

55. Kato, K.; Nishimasu, H.; Okudaira, S.; Mihara, E.; Ishitani, R.; Takagi, J.; Aoki, J.; Nureki, O. Crystal structure of Enpp1, an extracellular glycoprotein involved in bone mineralization and insulin signaling. *Proc. Natl. Acad. Sci. U.S.A.* **2012**, *109*, 16876–16881.

56. Gijsbers, R.; Ceulemans, H.; Stalmans, W.; Bollen, M. Structural and catalytic similarities between nucleotide pyrophosphatases/phosphodiesterases and alkaline phosphatases. *J. Biol. Chem.* **2001**, *276*, 1361–1368.

57. Millán, J. L. Alkaline phosphatases. Structure, substrate specificity and functional relatedness to other members of a large superfamily of enzymes. *Purinergic signalling* **2006**, *2*, 335−341.

58. Narisawa, S.; Harmey, D.; Yadav, M. C.; O'Neill, W. C.; Hoylaerts, M. F.; Millán, J. L. Novel inhibitors of alkaline phosphatase suppress vascular smooth muscle cell calcification *J. Bone Miner. Res.* **2007**, *22*, 1700–1710.

59. Whyte, M. P. Physiological role of alkaline phosphatase explored in hypophosphatasia. *Ann. N. Y. Acad. Sci.* **2010**, *1192*, 190−200.

60. Hessle, L.; Johnson, K. A.; Anderson, H. C.; Narisawa, S.; Sali, A.; Goding, J. W.; Terkeltaub, R.; Millán, J. L. Tissue-nonspecific alkaline phosphatase and plasma cell membrane glycoprotein-1 are central antagonistic regulators of bone mineralization. *Proc. Natl. Acad. Sci. U.S.A.* **2002**, *99*, 9445–9449.

61. Bobyr, E.; Lassila, J. K.; Wiersma-Koch, H. I.; Fenn, T. D.; Lee, J. J.; Nikolic-Hughes, I.; Hodgson, K. O.; Rees, D. C.; Hedman, B.; Herschlag, D. High-resolution analysis of Zn^{2+} coordination in the alkaline phosphatase superfamily by EXAFS and X-ray crystallography. *J. Mol. Biol.* **2012**, *415*, 102–117.

62. Etten, R. L. V. Human prostatic acid phosphatase: A histidine phosphatase. *Ann. N. Y. Acad. Sci.* **1982**, *390*, 27−51.

63. Ek-Rylander, B.; Flores, M.; Wendel, M.; Heinegaerd, D.; Andersson, G. Dephosphorylation of osteopontin and bone sialoprotein by osteoclastic tartrate-resistant acid phosphatase. Modulation of osteoclast adhesion in vitro. *J. Biol. Chem.* **1994**, *269*, 14853−14856.

64. Oddie, G. W.; Schenk, G.; Angel, N. Z.; Walsh, N.; Guddat, L. W.; de Jersey, J.; Cassady, A. I.; Hamilton, S. E.; Hume, D. A. Structure, function, and regulation of tartrate-resistant acid phosphatase. *Bone* **2000**, *27*, 575−584.

65. Smith, T. M.; Hicks-Berger, C. A.; Kim, S.; Kirley, T. L. Cloning, expression, and characterization of a soluble calcium-activated nucleotidase, a human enzyme belonging to a new family of extracellular nucleotidases. *Arch. Biochem. Biophys.* **2002**, *406*, 105−115.

66. El-Tayeb, A.; Iqbal, J.; Behrenswerth, A.; Romio, M.; Schneider, M.; Zimmermann, H.; Schrader, J.; Müller, C. E. Nucleoside-5′-monophosphates as prodrugs of adenosine A_{2A} receptor agonists activated by *ecto*-5′-nucleotidase. *J. Med. Chem.* **2009**, *52*, 7669−7677.

67. Servos, J.; Reiländer, H.; Zimmermann, H. Catalytically active soluble *ecto*-5′-nucleotidase purified after heterologous expression as a tool for drug screening. *Drug Dev. Res.* **1998**, *45*, 269−276.

68. Alam, M. S.; Kurtz, C. C.; Rowlett, R. M.; Reuter, B. K.; Wiznerowicz, E.; Das, S.; Linden, J.; Crowe, S. E.; Ernst, P. B. CD73 is expressed by human regulatory T-helper cells and suppresses proinflammatory cytokine production and Helicobacter felis-induced gastritis in mice. *J. Infect. Dis.* **2009**, *199*, 494–504.

69. Sadej, R.; Spychala, J.; Skladanowski, A. C. Expression of *ecto*-5′-nucleotidase (*e*N, CD73) in cell lines from various stages of human melanoma. *Melanoma Res.* **2006**, *16*, 213–222.

70. Grondal, E. J. M.; Zimmermann, H. Purification, characterization and cellular localization of 5′-nucleotidase from Torpedo electric organ. *Biochem.J.* **1987**, *245*, 805−810.

71. Knapp, K.; Zebisch, M.; Pippel, J.; El-Tayeb, A.; Müller, C. E.; Sträter, N. Crystal structure of the human *ecto*-5′-nucleotidase (CD73): insights into the regulation of purinergic signalling. *Structure* **2012**, *20*, 2161−2173.

72. Furtmann, N.; J. Bajorath, J. Evaluation of molecular model-based discovery of *ecto*-5′-nucleotidase inhibitors on the basis of X-ray structures. *Bioorg. Med. Chem.* **2013**, *21*, 6616−6622.

73. Sträter, N. *Ecto*-5′-nucleotidase: structure-function relationships. *Purinergic Signalling* **2006**, *2*, 343−350.

74. Knöfel, T.; Sträter, N. Mechanism of hydrolysis of phosphate esters by the dimetal center of 5′-nucleotidase based on crystal structures. *J. Mol. Biol.* **2001**, *309*, 239−254.

75. Flögel, U.; Burghoff, S.; van Lent, P. L.; Temme, S.; Galbarz, S. L.; Ding, Z.; El-Tayeb, A.; Huels, S.; Bönner, F.; Borg, N.; Jacoby, C.; Müller, C. E.; Berg, W. B.; Schrader, J. Selective

activation of adenosine A_{2A} receptors on immune cells by a CD73-dependent prodrug suppresses joint inflammtion in experimental rheumatoid arthritis. *Sci. Transl. Med.* **2012**, *4*, 146ra108.

76. Naito, Y.; Lowenstein, J. 5′-Nucleotidase from rat heart. *Biochemistry* **1981**, *20*, 5188–5194.

77. Ujházy, P.; Berleth, E. S.; Pietkiewicz, J. M.; Kitano, H.; Skaar, J. R.; Ehrke, M. J.; Mihich, E. Evidence for the involvement of *ecto*-5′-nucleotidase (CD73) in drug resistance. *Int. J. Cancer* **1996**, *68*, 493–500.

78. Colgan, S. P.; Eltzschig, H. K.; Eckle, T.; Thompson, L. F. Physiological roles for *ecto*-5′-nucleotidase (CD73). *Purinergic Signalling* **2006**, *2*, 351–360.

79. Resta, R.; Yamashita, Y.; Thompson, L. F. *Ecto*-enzyme and signaling functions of lymphocyte CD73. *Immunol. Rev.* **1998**, *161*, 95–109.

80. Ohtsuka, T.; Changelian, P. S.; Bouis, D.; Noon, K.; Harada, H.; Lama, V. N.; Pinsky, D. J. *Ecto*-5′-nucleotidase (CD73) attenuates allograft airway rejection through adenosine 2A receptor stimulation. *J. Immunol.* **2010**, *185*, 1321–1329.

81. Li, X.; Zhou, T.; Zhi, X.; Zhao, F.; Yin, L.; Zhou, P. Effect of hypoxia/reoxygenation on CD73 (*ecto*-5′-nucleotidase) in mouse microvessel endothelial cell lines. *Microvasc. Res.* **2006**, *72*, 48–53.

82. Picher, M.; Burch, L. H.; Boucher, R. C. Metabolism of P2 receptor agonists in human airways: implications for mucociliary clearance and cystic fibrosis. *J. Biol. Chem.* **2004**, *279*, 20234−20241.

83. Deaglio, S.; Robson, S. C. *Ecto*-nucleotidases as regulators of purinergic signalling in thrombosis, inflammation, and immunity. *Adv. Pharmacol.* **2011**, *61*, 301−332.

84. Buchheiser, A.; Ebner, A.; Burghoff, S.; Ding, Z.; Romio, M.; Viethen, C.; Lindecke, A.; Köhrer, K.; Fischer, J. W.; Schrader, J. Inactivation of CD73 promotes atherogenesis in apolipoprotein-E deficient mice. *Cardiovasc. Res.* **2011**, *92*, 338−347.

85. Clayton, A.; Al-Taei, S.; Webber, J.; Mason, M. D.; Tabi, Z. Cancer exosomes express CD39 and CD73, which suppress T-cells through adenosine production. *J. Immunol.* **2011**, *187*, 676–683.

86. Jin, D.; Fan, J.; Wang , L.; Thompson, L.; Liu, A.; Daniel, B.; Shin, T.; Curiel, T.; Zhang, B. CD73 on tumor cells impairs antitumor T-cell responses: a novel mechanism of tumor-induced immune suppression. *Cancer Res.* **2010**, *70*, 2245–2255.

87. Koszalka, P.; Özüyaman, B.; Huo, Y. Z., A.; Flögel, U.; Braun, N.; Buchheiser, A.; Decking, U. K. M.; Smith, M. L.; Sévigny, J.; Gear, A.; Weber, A.-A.; Molojavyi, A.; Ding, Z.; Weber, C.; Ley, K.; Zimmermann, H.; Gödecke, A.; Schrader, J. Targeted disruption of CD73/*ecto*-5′-nucleotidase alters thromboregulation and augments vascular inflammatory response. *Circ. Res.* **2004**, *95*, 814–821.

88. Kawashima, Y.; Nagasawa, T.; Ninomiya, H. Contribution of *ecto*-5′-nucleotidase to the inhibition of platelet aggregation by human endothelial cells. *Blood* **2000**, *96*, 2157–2162.

89. Atkinson, B.; Dwyer, K.; Enjyoji, K.; Robson, S. C. *Ecto*-nucleotidases of the CD39/NTPDase family modulate platelet activation and thrombus formation: potential as therapeutic targets. *Blood Cells Mol. Dis.* **2006**, *36*, 217−222.

90. Kobie, J. J.; Shah, P. R.; Yang, L.; Rebhahn, J. A.; Fowell, D. J.; Mosmann, T. R. T regulatory and primed uncommitted CD4 T Cells express CD73, which suppresses effector CD4 T cells by converting 5′-adenosine monophosphate to adenosine. *J. immunol.* **2006**, *177*, 6780−6786.

91. Sowa, N. A.; Voss, M. K.; Zylka, M. Recombinant *ecto*-5′-nucleotidase (CD73) has long lasting antinociceptive effects that are dependent on adenosine A_1 receptor activation. *J. Mol. Pain* **2010**, *6*, 20.

92. Stagg, J. The double-edge sword effect of anti-CD73 cancer therapy. *OncoImmunology* **2012**, *1*, 217–218.

93. Wang, L.; Fan, J.; Thompson, L. F.; Zhang, Y.; Shin, T.; Curiel, T. J.; Zhang, B. CD73 has distinct roles in nonhematopoietic and hematopoietic cells to promote tumor growth in mice. *J. Clin. Invest.* **2011**, *121*, 2371–2382.

94. Mikhailov, A.; Sokolovskaya, A.; Yegutkin, G. G.; Amdahl, H.; West, A.; Yagita, H.; Lahesmaa, R.; Thompson, L. F.; Jalkanen, S.; Blokhin, D.; Eriksson, J. E. CD73 participates in cellular multiresistance program and protects against TRAIL-induced apoptosis. *J. Immunol.* **2008**, *181*, 464–475.

95. Navarro, J.; Olmo, N.; Turnay, J.; López-Conejo, M.; Lizarbe, M. *Ecto*-5′-nucleotidase from a human colon adenocarcinoma cell line. Correlation between enzyme activity and levels in intact cells. *Mol. Cell Biochem.* **1998**, *187*, 121–131.

96. Zhou, X.; Zhi, X.; Zhou, P.; Chen, S.; Zhao, F.; Shao, Z.; Ou, Z.; Yin, L. Effects of *ecto*-5′-nucleotidase on human breast cancer cell growth in vitro and in vivo. *Oncol. Rep.* **2007**, 17, 1341–1346.

97. Loi, S.; Pommey, S.; Haibe-Kains, B.; Beavis, P. A.; Darcy, P. K.; Smyth, M. J.; Stagg, J. CD73 promotes anthracycline resistance and poor prognosis in triple negative breast cancer. *Proc. Natl. Acad. Sci.* **2013**, *110*, 11091−11096.

98. Zalatan, J. G.; Fenn, T. D.; Brunger, A. T.; Herschlag, D. Structural and functional comparisons of nucleotide pyrophosphatase/phosphodiesterase and alkaline phosphatase: Implications for mechanism and evolution. *Biochemistry* **2006**, *45*, 9788–9803.

99. Stagg, J.; Smyth, M. J. Extracellular adenosine triphosphate and adenosine in cancer. *Oncogene* **2010**, *29*, 5346–5358.

100. Stagg, J.; Beavis, P. A.; Divisekera, U.; Liu, M. C. P.; Möller, A.; Darcy, P. K.; Smyth, M. J. CD73-deficient mice are resistant to carcinogenesis. *Cancer Res.* **2012**, *72*, 2190–2196.

101. Stagg, J.; Divisekera, U.; Duret, H.; Sparwasser, T.; Teng, M. W.; Darcy, P. K.; Smyth, M. J. CD73-deficient mice have increased antitumor immunity and are resistant to experimental metastasis. *Cancer Res.* **2011**, *71*, 2892–2900.

102. Zhi, X.; Chen, S.; Zhou, P.; Shao, Z.; Wang, L.; Ou, Z.; Yin, L. RNA interference of *ecto*-5′-nucleotidase (CD73) inhibits human breast cancer cell growth and invasion. *Clin. Exp. Metastasis* **2007**, *24*, 439–448.

103. Garcia-Ayllon, M.; Campoy, F.; Vidal, C.; Muñoz-Delgado, E. Identification of inactive *ecto*-5′-nucleotidase in normal mouse muscle and its increased activity in dystrophic Lama2^{dy} mice. *J. Neurosci. Res.* **2001**, *66*, 656–665.

104. Stagg, J.; Divisekera, U.; McLaughlin, N.; Sharkey, J.; Pommey, S.; Denoyer, D.; Dwyer, K. M.; Smyth, M. J. Anti-CD73 antibody therapy inhibits breast tumor growth and metastasis. *Proc. Natl. Acad. Sci.* **2010**, *107*, 1547–1552.

105. Joseph, S. M.; Pifer, M. A.; Przybylski, R. J.; Dubyak, G. R. Methylene ATP analogs as modulators of extracellular ATP metabolism and accumulation. *Br. J. Pharmacol.* **2004**, *142*, 1002−1014.

106. Lee, S.-Y.; Müller, C. E. Large-volume sample stacking with polarity switching for monitoring of nucleotide pyrophosphatase/phosphodiesterase 1 (NPP 1) reactions by capillary electrophoresis. *Electrophoresis* **2014**, *35*, 855–863.

107. Ohlmann, P.; Lecchi, A.; El-Tayeb, A.; Müller, C. E.; Cattaneo, M.; Gachet, C. The platelet $P2Y_{12}$ receptor under normal and pathological conditions. Assessment with the radiolabeled selective antagonist [^{3}H]PSB-0413. *Purinergic Signalling* **2013**, *9*, 59–66.

108. Iqbal, J.; Jirovsky, D.; Lee, S.-Y.; Zimmermann, H.; Müller, C. E. Capillary electrophoresis-based nanoscale assays for monitoring *ecto*-5′-nucleotidase activity and inhibition in preparations of recombinant enzyme and melanoma cell membranes. *Anal. Biochem.* **2008**, *373*, 129−140.

109. Brunschweiger, A. Darstellung und charakterisierung von uracil- und adeninnucleotid-mimetika als selektive ectonucleotidase-inhibitoren. Dissertation Universität Bonn, Bonn, 2007.

110. Li, W. Therapeutically important enzymes with polar substrates or products: characterization by capillary electrophoresis and identification of inhibitors. Dissertation Universität Bonn, Bonn, 2014.

111. Baqi, Y.; Lee, S.-Y.; Iqbal, J.; Ripphausen, P.; Lehr, A.; Scheiff, A.; Zimmermann, H.; Bajorath, J.; Müller, C. Development of potent and selective inhibitors of *ecto*-5′-nucleotidase based on an anthraquinone scaffold. *J. Med. Chem.* **2010**, *53*, 2076−2086.

112. Ripphausen, P.; Freundlieb, M.; Brunschweiger, A.; Zimmermann, H.; Müller, C. E.; Bajorath, J. Virtual screening identifies novel sulfonamide inhibitors of *ecto*-5′-nucleotidase. *J. Med. Chem.* **2012**, *55*, 6576–6581.

113. Iqbal, J.; Saeed, A.; Raza, R.; Matin, A.; Hameed, A.; Furtmann, N.; Lecka, J.; Sévigny, J.; Bajorath, J. Identification of sulfonic acids as efficient *ecto*-5'-nucleotidase inhibitors. *Eur. J. Med. Chem.* **2013**, *70*, 685−691.

114. Uchino, K.; Matsuo, T.; Iwamoto, M.; Tonosaki, Y.; Fukuchi, A. New 5′-nucleotidase inhibitors, NPF-86IA, NPF-86IB, NPF-86IIA, and NPF-86IIB from Areca catechu; Part I. Isolation and biological properties. *Planta Med.* **1988**, *54*, 419–422.

115. Braganhol, E.; Tamajusuku, A. S.; Bernardi, A.; Wink, M. R.; Battastini, A. M. *Ecto*-5′-nucleotidase/CD73 inhibition by quercetin in the human U138MG glioma cell line. *Biochim. Biophys. Acta* **2007**, *1770*, 1352–1359.

116. Lee, S.-Y.; Fiene, A.; Li, W.; Hanck, T.; Brylev, K. A.; Fedovrov, V. E.; Lecka, J.; Haider, A.; Pietzsch, H.-J.; Zimmermann, H.; Sévigny, J.; Kortz, U.; Stephan, H.; Müller, C. E. Polyoxometalates - potent and selective *ecto*-nucleotidase inhibitors. *Biochem. Pharmacol.* **2015**, *93*, 171–181.

117. Fiene, A.; Baqi, Y.; Lecka, J.; Sévigny, J.; Müller, C. E. Fluorescence polarization immunoassays for monitoring nucleoside triphosphate diphosphohydrolase (NTPDase) activity. *Analyst* **2015**, *140*, 140–148.

118. Freundlieb, M.; Zimmermann, H.; Müller, C. E. A new, sensitive *ecto*-5′-nucleotidase assay for compound screening. *Anal. Biochem.* **2014**, *446*, 53−58.

119. Lecka, J.; Gillerman, I.; Fausther, M.; Salem, M.; Munkonda, M. N.; Brosseau, J.-P.; Cadot, C.; Martín-Satué, M.; D'Orléans-Juste, P.; Rousseau, E.; Poirier, D.; Künzli, B.; Fischer, B.; Sévigny, J. 8-BuS-ATP derivatives as specific NTPDase1 inhibitors. *Br. J. Pharmacol.* **2013**, *169*, 179−196.

120. Cogan, E. B.; Birrell, G. B.; Griffith, O. H. A robotics-based automated assay for inorganic and organic phosphates. *Anal. Biochem.* **1999**, *271*, 29−35.

121. Baykov, A. A.; Evtushenko, O. A.; Avaeva, S. M. A malachite green procedure for orthophosphate determination and its use in alkaline phosphatase-based enzyme immunoassay. *Anal. Biochem.* **1988**, *171*, 266–270.

122. Sachsenmeier, K. F.; Hay, C.; Brand, E.; Clarke, L.; Rosenthal, K.; Guillard, S.; Rust, S.; Minter, R.; Hollingsworth, R. Development of a novel *ecto*-nucleotidase assay suitable for high-throughput screening. *J. Biomol. Screen.* **2012**, *17*, 993−998.

123. Bookser, B. C.; Raffaele, N. B. High-throughput five minute microwave accelerated glycosylation approach to the synthesis of nucleoside libraries. *J. Org. Chem.* **2006**, *72*, 173−179.

124. Kohyama, N.; Yamamoto, Y. A facile synthesis of AICAR from inosine. *Synthesis* **2003**, 2639−2642.

125. Gerster, J. F.; Jones, J. W.; Robins, R. K. Purine nucleosides. IV. The synthesis of 6-halogenated 9-*β*-D-ribofuranosylpurines from inosine and guanosine. *J. Org. Chem.* **1963**, *28*, 945−948.

126. Mathew, S. C.; Ghosh, N.; By, Y.; Berthault, A.; Virolleaud, M.-A.; Carrega, L.; Chouraqui, G.; Commeiras, L.; Condo, J.; Attolini, M.; Gaudel-Siri, A.; Ruf, J.; Parrain, J.-L.; Rodriguez, J.; Guieu, R. Design, synthesis and biological evaluation of a bivalent μ opiate and adenosine A_1 receptor antagonist. *Bioorg. Med. Chem. lett.* **2009**, *19*, 6736−6739.

127. Middleton, R. J.; Briddon, S. J.; Cordeaux, Y.; Yates, A. S.; Dale, C. L.; George, M. W.; Baker, J. G.; Hill, S. J.; Kellam, B. New fluorescent adenosine A_1-receptor agonists that allow

quantification of ligand-receptor interactions in microdomains of single living cells. *J. Med. Chem.* **2007**, *50*, 782–793.

128. Korboukh, I.; Hull-Ryde, E. A.; Rittiner, J. E.; Randhawa, A. S.; Coleman, J.; Fitzpatrick, B. J.; Setola, V.; Janzen, W. P.; Frye, S. V.; Zylka, M. J.; Jin, J. Orally active adenosine A_1 receptor agonists with antinociceptive effects in mice. *J. Med. Chem.* **2012**, *55*, 6467–6477.

129. Kolyachkina, S. V.; Tararov, V. I.; Alexeev, C. S.; Krivosheev, D. M.; Romanov, G. A.; Stepanova, E. V.; Solomko, E. S.; Inshakov, A. N.; Mikhailov, S. N. N^6-substituted adenosines. Cytokinin and antitumor activities. *Collect. Czech. Chem. Commun.* **2011**, *76*, 1361–1378.

130. Doležal, K.; Popa, I.; Hauserová, E.; Spíchal, L.; Chakrabarty, K.; Novák, O.; Kryštof, V.; Holub, J. V.; Strnad, M. Preparation, biological activity and endogenous occurrence of N^6-benzyladenosines. *Bioorg. Med. Chem.* **2007**, *15*, 3737–3747.

131. Golisade, A.; Wiesner, J.; Herforth, C.; Jomaa, H.; Link, A. Anti-malarial activity of N^6-substituted adenosine derivatives. Part 1. *Bioorg. Med. Chem.* **2002**, *10*, 769–777.

132. Jacobson, K. A.; Nikodijevic, O.; Ji, X. D.; Berkich, D. A.; Eveleth, D.; Dean, R. L.; Hiramatsu, K. I.; Kassell, N. F.; van Galen, P. J. M.; Lee, K. S.; Bartus, R. T.; Daly, J. W.; LaNoue, K. F.; Maillard, M. Synthesis and biological activity of N^6-(*p*-sulphonyl)alkyl and N^6-sulfoalkyl derivatives of adenosine: water-soluble and peripherally selective adenosine agonists. *J. Med. Chem.* **1992**, *35*, 4143–4149.

133. Brunschweiger, A.; Iqbal, J.; Umbach, F.; Scheiff, A. B.; Munkonda, M. N.; Sévigny, J.; Knowles, A. F.; Müller, C. E. Selective nucleoside triphosphate diphosphohydrolase-2 (NTPDase 2) inhibitors: nucleotide mimetics derived from uridine-5-carboxamide. *J. Med. Chem.* **2008**, *51*, 4518–4528.

134. Xu, Y.; Jin, H.; Yang, Z.; Zhang, L.; Zhang, L. Synthesis and biological evaluation of novel neamine-nucleoside conjugates potentially targeting to RNAs. *Tetrahedron* **2009**, *65*, 5228–5239.

135. Lesiak, K.; Watanabe, K. A.; George, J.; Pankiewicz, K. W. 2-(4-Nitrophenyl)ethyl methylenebis (phosphonate): a versatile reagent for the synthesis of nucleoside 5′-methylenebis-(phosphonate)s. *J. Org. Chem.* **1998**, *63*, 1906–1909.

136. Pankiewicz, K. W.; Lesiak, K.; Watanabe, K. A. Efficient synthesis of methylenebis(phosphonate) analogues of P^1, P^2-disubstituted pyrophosphates of biological interest. A novel plausible mechanism. *J. Am. Chem. Soc.* **1997**, *119*, 3691–3695.

137. Dixit, V. M.; Poulter, C. D. Convenient syntheses of adenosine 5'-diphosphate, adenosine 5'-methylenediphosphonate, and adenosine 5'-triphosphate. *Tetrahedron Lett.* **1984**, *25*, 4055–4058.

138. Davisson, V. J.; Davis, D. R.; Dixit, V. M.; Poulter, C. D. Synthesis of nucleotide 5'-diphosphates from 5'-*O*-tosyl nucleosides. *J. Org. Chem.* **1987**, *52*, 1794–1801.

139. Myers, T. C.; Nakamura, K.; Danielzadeh, A. B. Phosphonic acid analogs of nucleoside phosphates. III. The synthesis of adenosine-5'-methylenediphosphonate, a phosphonic acid analog of adenosine-5'-diphosphate. *J. Org. Chem.* **1965**, *30*, 1517–1520.

140. Kalek, M.; Jemielity, J.; Stepinski, J.; Stolarski, R.; Darzynkiewicz, E. A direct method for the synthesis of nucleoside 5′-methylenebis(phosphonate)s from nucleosides. *Tetrahedron Lett.* **2005**, *46*, 2417–2412.

141. Shipitsyn, A. V.; Tarussova, N. B.; Shirokova, E. A.; Krayevsky, A. A. Synthesis of [bis(inosine-5′)]-tetraphosphate and [bis-(inosine-5′)]-pentaphosphate analogues bearing the

residues of methylenediphosphonic acid. *Nucleosides, Nucleotides Nucleic Acids* **2000**, *19*, 881–889.

142. Yoshikawa, M.; Kato, T.; Takenishi, T. Studies of phosphorylation. III. Selective phosphorylation of unprotected nucleosides. *Bull. Chem. Soc. Jpn.* **1969**, *42*, 3505–3508.

143. Ludwig, J. A new route to nucleoside 5'-triphosphates. *Acta Biochim. Biophys. Acad. Sci. Hung.* **1981**, *16*, 131–133.

144. Baker, B. R.; Hewson, K.; Thomas, H. J.; Johnson, J. A. Synthesis of potential anticancer agents. VI.[2] Use of *O*-benzoyl blocking group for synthesis of 6-chloropurine nucleosides. *J. Org. Chem.* **1957**, *22*, 954–959.

145. Fox, J. J.; Wempen, I.; Hampton, A.; Doerr, I. L. Thiation of nucleosides. I. Synthesis of 2-amino-6-mercapto-9-*β*-D-ribofuranosylpurine ('thioguanosine') and related purine nucleosides. *J. Am. Chem. Soc.* **1958**, *80*, 1669–1675.

146. Niu, H.; Xia, C.; Qu, G.; Wu, S.; Jiang, Y.; Jin, X.; Guo, H. Microwave-promoted "one-pot" synthesis of 4-nitrobenzylthioinosine analogues using thiourea as a sulfur precursor. *Chem.-Asian J.* **2012**, *7*, 45–49.

147. Jamison, M. T.; Boddy, C. N.; Molinski, T. F. Salvadenosine, a 5'-Deoxy-5'-(methylthio) nucleoside from the Bahamian Tunicate *Didemnum* sp. *J. Org. Chem.* **2014**, *79*, 9992–9997.

148. Hwu, J. R.; Lin, S.-Y.; Tsay, S.-C.; De Clercq, E.; Leyssen, P.; Neyts, J. Coumarin-purine ribofuranoside conjugates as new agents against Hepatitis C virus. *J. Med. Chem.* **2011**, *54*, 2114–2126.

149. Ghanty, U.; Fostvedt, E.; Valenzuela, R.; Beal, P. A.; Burrows, C. J. Promiscuous 8-alkoxyadenosine in the guide strand of an siRNA: modulation of silencing efficacy and off-pathway protein binding. *J. Am. Chem. Soc.* **2012**, *134*, 17643–17652.

150. Müller, C. E. Adenosine receptor ligands – recent developments. Part I. Agonists. *Curr. Med. Chem.* **2000**, *7*, 1269–1288.

151. Uesugi, S.; Ikehara, M. Carbon-13 magnetic resonance spectra of 8-substituted purine nucleosides. Characteristic shifts for the syn conformation. *J. Am. Chem. Soc.* **1977**, *99*, 3250–3253.

152. Bressi, J. C.; Choe, J.; Hough, M. T.; Buckner, F. S.; Van Voorhis, W. C.; Verlinde, C. L. M. J.; Hol, W. G. J.; Gelb, M. H. Adenosine analogues as inhibitors of *Trypanosoma brucei* phosphoglycerate kinase: elucidation of a novel binding mode for a 2-amino-N^6-substituted adenosine. *J. Med. Chem.* **2000**, *43*, 4135–4150.

153. Francom, P.; Robins, M. J. Nucleic acid realted compounds. 118. Nonaqueous diazotization of aminopurine derivatives. Convalent access to 6-halo and 2,6-dihalopurine nucleosides and 2´-deoxynucleosides with acyl or silyl halides *J. Org. Chem.* **2003**, *68*, 666–669.

154. Gerster, J. F.; Robins, R. K. Purine Nucleosides. XIII. The Synthesis of 2-fluoro- and 2-chloroinosine and certain derived purine nucleosides[1]. *J. Org. Chem.* **1966**, *31*, 3258–3262.

155. Heisig, F. Synthese neuer, funktionalisierter BODIPY fluorophore zur fluoreszenz markierung von membranrezeptor-liganden. Dissertation Universität Bonn, Bonn, 2007.

156. Grünewald, C.; Kwon, T.; Piton, N.; Förster, U.; Wachtveitl, J.; Engels, J. W. RNA as scaffold for pyrene excited complexes. *Bioorg. Med. Chem.* **2008**, *16*, 19–26.

157. El-Tayeb, A.; Gollos, S. Synthesis and structure-activity relationships of 2-hydrazinyladenosine derivatives as A_{2A} adenosine receptor ligands. *Bioorg. Med. Chem.* **2013**, *21*, 436–447.

158. Niiya, K.; Olsson, R. A.; Thompson, R. D.; Silvia, S. K.; Ueeda, M. 2-(*N'*-alkylidenehydrazino)adenosines: potent and selective coronary vasodilators. *J. Med. Chem.* **1992**, *35*, 4557–4561.

159. Abiru, T.; Miyashita, T.; Watanabe, Y.; Yamaguchi, T.; Machida, H.; Matsuda, A. Nucleosides and nucleotides. 107. 2-(Cycloalkylalkynyl)adenosines: adenosine A_2 receptor agonists with potent antihypertensive effects. *J. Med. Chem.* **1992**, *35*, 2253–2260.

160. Kikugawa, K.; Suehiro, H.; Yanase, R. Platelet aggregation inhibitors IX. Chemical transformation of adenosine into 2-thioadenosine derivatives. *Chem. Pharm. Bull.* **1977**, *25*, 1959–1969.

161. Kikugawa, K.; Suehiro, H.; Aoki, A. Platelet aggregation inhibitors. X. S-Substituted 2-thioadenosines and their derivatives. *Chem. Pharm. Bull*. **1977**, *25*, 2624–2637.

162. Nair, V.; Young, D. A. A new synthesis of isoguanosine. *J. Org. Chem.* **1985**, *50*, 406–408.

163. McClung, M.; Harris, S. T.; Miller, P. D.; Bauer, D. C.; Davison, K. S.; Dian, L.; Hanley, D. A.; Kendler, D. L.; Yuen, C. K.; Lewiecki, E. M. Bisphosphonate therapy for osteoporosis: benefits, risks, and drug holiday. *Am. J. Med.* **2013**, *126*, 13–20.

164. Cheng, Y.-C.; Prusoff, W. H. Relationship between the inhibition constant (K_i) and the concentration of inhibitor which causes 50% inhibition (IC_{50}) of an enzymatic reaction. *Biochem. Pharmacol* **1973**, *22*, 3099−3108.

165. Marquardt, D. W. An algorithm for least squares estimation of non-linear parameters. *J. Soc. Indust. Appl. Math.* **1963**, *11*, 431−441.

166. Yan, L.; Burbiel, J. C.; Maaß, A.; Müller, C. E. Adenosine receptor agonists: from basic medicinal chemistry to clinical development. *Expert Opin. on Emerging Drugs* **2003**, *8*, 537−576.

167. Verzijl, D.; IJzerman, A. P. Functional selectivity of adenosine receptor ligands. *Purinergic Signalling* **2011**, *7*, 171−192.

168. Stolarski, R.; Hagberg, C.-E.; Shugar, D. Studies on the dynamic *syn-anti* equilibrium in purine nucleosides and nucleotides with the aid of ^{1}H and ^{13}C NMR spectroscopy. *Eur. J. Biochem.* **1984**, *138*, 187−192.

169. Cogan, E. B.; Birrell, G. B.; Griffith, O. H. A robotics-based automated assay for inorganic and organic phosphates. *Anal. Biochem.* **1999**, *271*, 29−35.

170. Högberg, C.; Gidlöf, O.; Deflorian, F.; Jacobson, K. A.; Abdelrahman, A.; Müller, C. E.; Olde, B.; Erlinge, D. Farnesyl pyrophosphate is an endogenous antagonist to ADP-stimulated $P2Y_{12}$ receptor-mediated platelet aggregation. *Thromb. Haemost.* **2012**, *108*, 119−132.

171. Umbach, F. Stabilitäts- und metabolismusuntersuchungen neuer purinerger wirkstoffe und *ecto*-nucleotidase-inhibitoren mittels HPLC-DADMS(/MS). Dissertation Universität Bonn, Bonn, 2012.

172. Kerns, E. H.; Di, L. Chapter 11- Metabolic stability. In *drug-like properties: concepts, structure design and methods*. Academic press: San Diego, 2008, pp 137−165.

173. Jia, L.; Liu, X. The Conduct of drug metabolism studies considered good practice (II): In vitro experiments. *Curr. Drug Metab.* **2007**, *8*, 822−829.

174. Azran, S.; Förster, D.; Danino, O.; Nadel, Y.; Reiser, G.; Fischer, B. Highly efficient biocompatible neuroprotectants with dual activity as antioxidants and P2Y receptor agonists. *J. Med. Chem.* **2013**, *56*, 4938−4952.

175. Meltzer, D.; Nadel, Y.; Lecka, J.; Amir, A.; Sévigny, J.; Fischer, B. Nucleoside-(5′→P) methylenebisphosphonodithioate analogues: Synthesis and chemical properties. *J. Org. Chem.* **2013**, *78*, 8320−8329.

176. Kerns, E. H.; Di, L. Chapter 12 - Plasma stability. *In drug-like properties: concepts, structure design and methods*. Academic press: San Diego, 2008, pp. 169−177.

177. Yadav, V.; Chu, C. K.; Rais, R. H.; Al Safarjalani, O. N.; Guarcello, V.; Naguib, F. N. M. Synthesis, biological activity and molecular modeling of 6-benzylthioinosine analogues as subversive substrates of *Toxoplasma gondii* adenosine kinase. *J. Med. Chem.* **2004**, *47*, 1987−1996.

178. Tararov, V. I.; Kolyachkina, S. V.; Alexeev, C. S.; Mikhailov, S. N. N^6-Acetyl-2,3,5-tri-*O*-acetyladenosine; a convenient, missed out substrate for regioselective N^6-alkylations. *Synthesis* **2011**, *15*, 2483−2489.

179. Kissman, H. M.; Pidacks, C.; Baker, B. R. Puromycin. Synthetic studies. XI. D-Ribofuranosyl derivatives of 6-dimethylaminopurine. *J. Am. Chem. Soc.* **1955**, *77*, 18−24.

180. Wan, Z.-K.; Binnun, E.; Wilson, D. P.; Lee, J. A highly facile and efficient one-step synthesis of N^6-adenosine and N^6-2'-Deoxyadenosine derivatives. *Org. Lett.* **2005**, *7*, 5877−5880.

181. Ottria, R.; Casati, S.; Baldoli, E.; Maier, J. A. M.; Ciuffreda, P. N^6-Alkyladenosines: Synthesis and evaluation of in vitro anticancer activity. *Bioorg. Med. Chem.* **2010**, *18*, 8396−8402.

182. Huang, N.-K.; Chern, Y.; Fang, J.-M.; Lin, C.-I.; Chen, W.-P.; Lin, Y.-L. Neuroprotective principles from *Gastrodia elata*. *J. Nat. Prod.* **2007**, *70*, 571−574.

183. Chen, J.-B.; Liu, E. M.; Chern, T.-R.; Yang, C.-W.; Lin, C.-I.; Huang, N.-K.; Lin, Y.-L.; Chern, Y.; Lin, J.-H.; Fang, J.-M. Design and synthesis of novel dual-action compounds targeting the adenosine A_{2A} receptor and adenosine transporter for neuroprotection. *Chem. Med. Chem.* **2011**, *6*, 1390−1400.

184. Neres, J.; Labello, N. P.; Somu, R. V.; Boshoff, H. I.; Wilson, D. J.; Vannada, J.; Chen, L.; Barry, C. E.; Bennett, E. M.; Aldrich, C. C. Inhibition of siderophore biosynthesis in Mycobacterium tuberculosis with nucleoside bisubstrate analogues: Structure-activity relationships of the nucleobase domain of 5'-O-[*N*-(salicyl)sulfamoyl]adenosine. *J. Med. Chem.* **2008**, *51*, 5349−5370.

185. Chen, L. S.; Sheppard, T. L. Synthesis and hybridization properties of RNA containing 8-chloroadenosine. *Nucleosides, Nucleotides and Nucleic Acids* **2002**, *21*, 599−617.

186. Gendron, F.-P.; Halbfinger, E.; Fischer, B.; Duval, M.; D'Orléans-Juste, P.; Beaudoin, A. R. Novel inhibitors of nucleoside triphosphate diphosphohydrolases: chemical synthesis and biochemical and pharmacological characterizations. *J. Med. Chem.* **2000**, *43*, 2239−2247.

187. Torii, T.; Shiragami, H.; Yamashita, K.; Suzuki, Y.; Hijiya, T.; Kashiwagi, T.; Izawa, K. Practical syntheses of penciclovir and famciclovir from N2-acetyl-7-benzylguanine. *Tetrahedron* **2006**, *62*, 5709−5716.

188. Ohno, M.; Gao, Z.-G.; Van Rompaey, P.; Tchilibon, S.; Kim, S.-K.; Harris, B. A.; Gross, A. S.; Duong, H. T.; Van Calenbergh, S.; Jacobson, K. A. Modulation of adenosine receptor affinity and intrinsic efficacy in adenine nucleosides substituted at the 2-position. *Bioorg. Med. Chem.* **2004**, *12*, 2995−3007.

189. Tchilibon, S.; Joshi, B. V.; Kim, S.-K.; Duong, H. T.; Gao, Z.-G.; Jacobson, K. A. (*N*)-Methanocarba 2,N^6-disubstituted adenine nucleosides as highly potent and selective A_3 adenosine receptor agonists. *J. Med. Chem.* **2004**, *48*, 1745−1758.

190. Robins, R. K. A New synthesis of chloropurine ribonucleosides[1]. *J. Am. Chem. Soc.* **1960**, *82*, 2654−2655.

191. Ishido, Y.; Tanaka, H.; Yoshino, T.; Sekiya, M.; Iwabuchi, K.; Sato, T. Acid-catalyzed and autocatalytic reactions of acetylated sugars with purine derivatives in organic solvents (1, 2). *Tetrahedron Lett.* **1967**, *8*, 5245−5248.

192. Schaeffer, H. J.; Thomas, H. J. Synthesis of potential anticancer agents. XIV. Ribosides of 2,6-disubstituted purines. *J. Am. Chem. Soc.* **1958**, *80*, 3738−3742.

193. van Tilburg, E. W.; von Frijtag Drabbe Künzel, J.; de Groote, M.; Ijzerman, A. P. 2,5'-Disubstituted adenosine derivatives: evaluation of selectivity and efficacy for the adenosine A_1, A_{2A}, and A_3 receptor. *J. Med. Chem.* **2001**, *45*, 420−429.

194. Janebaa, Z.; Lina, X.; Robinsa, M. J. Functionalization of guanosine and 2′-deoxyguanosine at C6: A modified appel process and SNAr displacement of imidazole. *Nucleosides, Nucleotides and Nucleic Acids* **2004,** *23*, 137−147.

195. Davoll, J.; Lowy, B. A. A new synthesis of purine nucleosides. The synthesis of adenosine, guanosine and 2,6-diamino-9-*β*-D-ribofuranosylpurine[1]. *J. Am. Chem. Soc.* **1951**, *73*, 1650−1655.

196. Bayryamov, S. G.; Vassilev, N. G.; Rangelov, M. A.; Mladjova, A. P.; Petkov, D. D. Design and synthesis of substrates for model ribosomal reactions. *Protein Pept. Lett.* **2009**, *16*, 392−401.

197. Hechler, B.; Léon, C.; Vial, C.; Vigne, P.; Frelin, C.; Cazenave, J.-P.; Gachet, C. The $P2Y_1$ receptor is necessary for adenosine 5'-diphosphate-induced platelet aggregation. *blood* **1998**, *92*, 152−159.

198. Foster, H. R.; Fuerst, E.; Lee, T. H.; Cousins, D. J.; Woszczek, G. Characterisation of $P2Y_{12}$ receptor responsiveness to cysteinyl leukotrienes. *PLoS ONE* **2013**, *8*, e58305.

VIII. Abbreviations

ABC	ATP-binding cassette
ACRs	Apyrase-conserved regions
ADA	Adenosine deaminase
Ado	Adenosine
ADP	Adenosine diphosphate
AMP	Adenosine monophosphate
AOPCP	*α*,*β*-methylene-ADP
AP	Alkaline phosphatase
AP_4P	Diadenosine 5',5'''-P^1,P^4-tetraphosphate
ATP	Adenosine triphosphate
BETA	Benzyltriethylammonium
*c*AMP	cyclic AMP
CAN	Calcium-activated nucleotidase
CE	Capillary electrophoresis
CFTR	Cystic fibrosis transmembrane conductance regulator
CL	Clearance
CPPD	Calcium pyrophosphate dihydrate disease
DEAE	Diethylaminoethyl
DEPT	Distortionless enhancement by polarization transfer
DMAP	4-Dimethylaminopyridine
DMF	*N*,*N*-dimethylformamide
DMSO	Dimethyl sulfoxide
EDMA	*N*-Ethyldimethylamine
*e*N	*Ecto*-5'-nucleotidase

ER	Estrogen receptor
*E*NPPs	*Ecto*-nucleotide pyrophosphatases/ phosphodiesterases
*E*NTPDase	*Ecto*-nucleoside triphosphate diphosphohydrolases
FAD	Flavin adenine dinucleotide
FDA	Food and drug administration
FMO	Flavine monooxygenase
FPLC	Fast protein liquid chromatography
GCAP	Germ cell AP
GPCR	G protein-coupled receptor
GPI	Glycosylphosphatidylinositol
Hyp	Hypoxanthine
HPLC	High performance liquid chromatography
Ino	Inosine
IAP	Intestinal AP
LC-MS	Liquid chromatography-mass spectrometry
L-DOPA	*L*-3,4-dihydroxyphenylalanine
LGIC	Ligand-gated ion channel
LOD	Limit of detection
NAD^+	Nicotinamide adenine dinucleotide
NANC	Nonadrenergic noncholinergic
NCAM	Neural cell adhesion molecule
NLD	Nuclease like domain
OPLL	Ossification of posterior longitudinal ligament
PAP	Prostatic acid phosphatase
PDB	Protein data bank

PLAP	Placental AP
PLP	Pyridoxal 5'-phosphate
PM	Plasma membrane
PNP	Purine nucleoside phosphorylase
POMs	Polyoxometalates
PSB	Pharmaceutical Sciences Bonn
RP-HPLC	Reversed-phase high performance liquid chromatography
SARs	Structure-activity relationships
TEAC	Triethyl ammonium bicarbonate buffer
TFA	Trifluoroacetic acid
THF	Tetrahydrofuran
TFN-α	Tumor necrosis factor alpha
IFN-γ	Interferon gamma
Thpp	Uncommitted primed precursors Th
TMDs	Transmembrane domains
TNAP	Tissue-nonspecific AP
TNBC	Triple-negative breast cancers
TRAMP	Transgenic adenocarcinoma of the mouse prostate
TRAP	Tartrate resistant acid phosphatase
Treg	T regulatory cells
UDP	Uridine diphosphate
UMP	Uridine monophosphate
UTP	Uridine triphosphate
UGTs	Uridine 5'-diphospho-glucuronosyltransferases
V_d	Volume of distribution